UNIVERSITÀ DEGLI STUDI DI TRIESTE

e

UNIVERSITÀ CA' FOSCARI DI VENEZIA

XXXI CICLO DEL DOTTORATO DI RICERCA IN

CHIMICA

Half-Sandwich Complexes with Azo Ligand: Preparation and Reactivity

Settore scientifico-disciplinare: **CHIM/03**

DOTTORANDA
FRANCESCA SIBILLA

Ph.D. student
Francesca Sibilla

COORDINATORE
PROF. BARBARA MILANI

Ph.D. program Coordinator
Prof. Barbara Milani

SUPERVISORE DI TESI
PROF. GABRIELE ALBERTIN

Thesis Supervisor
Prof. Gabriele Albertin

CO-SUPERVISORE DI TESI
PROF. STEFANO ANTONIUTTI

Thesis Co-Supervisor
Prof. Stefano Antoniutti

ANNO ACCADEMICO 2017/2018

ABSTRACT

English Version

Aldazine complexes of the type [RuCl(η^6-*p*-cymene){κ^1-[N=C(H)R1]-N=C(H)R1}L]BPh_4 and [Ru(η^5-C_5H_5){κ^1-[N=C(H)R1]-N=C(H)R1}(PPh_3){$P(OMe)_3$}]BPh_4 [L= $P(OMe)_3$, $P(OEt)_3$, $PPh(OEt)_2$, P^iPr_3; R1= Ph, 4-$CH_3C_6H_4$, 4-$CH_3OC_6H_4$, Et] were prepared by allowing the chloro compounds to react with the azine R1(H)C=N-N=C(H)R1. Depending on the nature of the phosphine ligand, the reaction of ketazine $(CH_3)_2C$=N-N=$C(CH_3)_2$ with chloro compounds $RuCl_2$(η^6-*p*-cymene)L yielded either hydrazone derivatives [RuCl(η^6-*p*-cymene){NH_2N=$C(CH_3)_2$}L]BPh_4 [L=$P(OMe)_3$, $P(OEt)_3$] or κ^1-azine complex [RuCl(η^6-*p*-cymene){κ^1-[N=$C(CH_3)_2$]N=$C(CH_3)_2$}(P^iPr_3)]BPh_4, while the reaction of the acetoneazine with the cyclopentadienyl complexes Ru(η^5-C_5H_5)(PPh_3)[$P(OR)_3$] (R= Me, Et) led to the formation of [Ru(η^5-C_5H_5){NH_2N=$C(CH_3)_2$}(PPh_3){$P(OMe)_3$}]BPh_4 [R1= Ph, 4-$CH_3C_6H_4$, C_2H_5]. Oxidation of these hydrazone derivative with HgO gave dimethyldiazoalkane complex [Ru(η^5-C_5H_5){$N_2C(CH_3)_2$}(PPh_3){$P(OMe)_3$}]BPh_4.

Half-sandwich azine complexes [OsCl(η^6-*p*-cymene){κ^1-[N=C(H)C_6H_4R1]N=C(H)C_6H_4R1}{$P(OR)_3$}]-BPh_4 and [OsCl(η^6-*p*-cymene){κ^1-[N=$C(CH_3)_2$]N=$C(CH_3)_2$}{$P(OR)_3$}]BPh_4 [R = Me, Et; R1 = H , 4-CH_3, 2,6-$(CH_3)_2$] were prepared by allowing chloro compounds [$OsCl_2$(η^6-*p*-cymene){$P(OR)_3$}] to react first with one equivalent of AgOTf and then with azine. Interestingly in solution κ^1-azine complexes undergo metalation reaction, giving chelate derivatives [Os{κ^2-R1C_6H_3C(H)=N-N=C(H)C_6H_4R1}(η^6-*p*-cymene){$P(OR)_3$}]BPh_4 [R = Me, Et; R1 = H, 4-CH_3].

Using the same synthetic route were prepared the analogues azine complexes of rhodium, [RhCl(η^5-C_5Me_5){κ^1-[N=C(H)Ph]–N=C(H)Ph}L]BPh_4 and [Rh{κ^2-R1C_6H_3C(H)=N-N=C(H)C_6H_4R1}(η^5-C_5Me_5)-{$P(OR)_3$}]BPh_4, and iridium, [IrCl(η^5-C_5Me_5){κ^1-[N=C(H)Ph]–N=C(H)Ph}L]BPh_4 and [Ir{κ^2-R1C_6H_3-C(H)=N-N=C(H)C_6H_4R1}(η^5-C_5Me_5){$P(OR)_3$}]BPh_4. Interestingly, most of the κ^2-arylazine derivatives of iridium showed photoluminescence properties upon excitation with near-UV and violet light, with emission peaks at around 650 nm. The photoluminescence features were rationalised according to DFT calculations.

Diazoalkane complexes of the type Os(η^5-C_5Me_5)(N_2CAr1Ar2(PPh_3){$P(OR)_3$}]BPh_4 were prepared by allowing the chloro compounds to react with the diazoalkanes N_2=CAr1Ar2 (Ar1=Ar2= Ph; Ar1 = Ph, Ar2 = *p*-tolyl; Ar1Ar2 = $C_{12}H_8$). Among the properties shown by these complexes, interesting is

the dipolar (3+2) cycloaddition with acetylene HC≡CH affording 3-H pyrazole derivatives. Substitution of the diazoalkane ligand also occurs with dioxygen, yielding the κ^2-O_2 derivatives, with terminal alkynes R1C≡CH yielding vinylidene derivatives and with propargylic alcohols [HC≡CC(OH)R1R2] yielding allenylidene and hydroxyvinylidene derivatives.

Half-sandwich fragment $[Os(\eta^5\text{-}C_5H_5)(PPh_3)\{P(OR)_3\}]^+$ can stabilise organic azide complexes $[Os(\eta^5\text{-}C_5H_5)(\kappa^1\text{-}N_3R)(PPh_3)\{P(OR1)_3\}]BPh_4$ and imine derivatives $[Os(\eta^5\text{-}C_5H_5)\{\kappa^1\text{-}NH{=}C(R1)Ar\}(PPh_3)\{P(OR)_3\}]BPh_4$ (R1 = H, CH_3). The binuclear dinitrogen derivative $[Os(\eta^5\text{-}C_5H_5)(PPh_3)\{P(OMe)_3\}_2(\mu\text{-}N_2)](BPh_4)_2$ was prepared from phenylazide PhN_3 complexes.

The reaction between azides and half-sandwich fragment of the type $[IrCl(\eta^5\text{-}C_5Me_5)\{P(OR1)_3\}]^+$ leads to the formation of imino $[IrCl(\eta^5\text{-}C_5Me_5)\{\kappa^1\text{-}NH{=}C(R1)Ar\}(PPh_3)\{P(OR)_3\}]BPh_4$ (R1= H, CH_3; Ar=C_6H_5, *p*-tolyl) and amino $[IrCl(\eta^5\text{-}C_5Me_5)(NH_2Ph)\{P(OR)_3\}]BPh_4$ derivatives. Moreover, changing the reaction condition, the reaction between azides and the dimeric compound $[IrCl(\mu\text{-}Cl)(\eta^5\text{-}C_5Me_5)]_2$ leads to the formation of both mono- $[IrCl_2(\eta^5\text{-}C_5Me_5)(\kappa^1\text{-}NH{=}C(R1)Ar)]$ and di-imine complexes $[IrCl(\eta^5\text{-}C_5Me_5)(\kappa^1\text{-}NH{=}C(R1)Ar)_2]BPh_4$ (R1= H, CH_3; Ar=C_6H_5, *p*-tolyl). Treatment of the fragment $[Ir(\kappa^1\text{-}Otf)_2(\eta^5\text{-}C_5Me_5)\{P(OR1)_3\}]^+$ with azides yield the bis-imine derivatives $[Ir(\eta^5\text{-}C_5Me_5)(\kappa^1\text{-}NH{=}C(R1)Ar)_2\{P(OR)_3\}](BPh_4)_2$.

Versione Italiana

Complessi azinici del tipo $RuCl(\eta^6\text{-}p\text{-cymene})\{\kappa^1\text{-}[N{=}C(H)R1]\text{-}N{=}C(H)R1\}L]BPh_4$ and $[Ru(\eta^5\text{-}C_5H_5)\{\kappa^1\text{-}[N{=}C(H)R1]\text{-}N{=}C(H)R1\}(PPh_3)\{P(OMe)_3\}]BPh_4$ [L= $P(OMe)_3$, $P(OEt)_3$, $PPh(OEt)_2$, P^iPr_3; R1= Ph, 4-$CH_3C_6H_4$, 4-$CH_3OC_6H_4$, Et] sono stati preparati lasciando reagire i cloro complessi precursori con le azine libere R1(H)C=N-N=C(H)R1. A seconda del legante fosfinico utilizzato la reazione tra i complessi precursori stabilizzati da *p*-cimene $RuCl_2(\eta^6\text{-}p\text{-cymene})L$ con acetone azina, $(CH_3)_2C{=}N\text{-}N{=}C(CH_3)_2$, portava alla formazione degli idrazoni complessi $[RuCl(\eta^6\text{-}p\text{-cymene})\text{-}\{NH_2N{=}C(CH_3)_2\}L]BPh_4$ [L=$P(OMe)_3$, $P(OEt)_3$] o con la chetazina coordinata κ^1- $[RuCl(\eta^6\text{-}p\text{-cymene})\text{-}\{\kappa^1\text{-}[N{=}C(CH_3)_2]N{=}C(CH_3)_2\}(P^iPr_3)]BPh_4$. La reazione della stessa chetazina con il complesso precursore stabilizzato da ciclopentadiene $RuCl(\eta^5\text{-}C_5H_5)(PPh_3)[P(OR)_3]$ (R= Me, Et) portava invece alla sola formazione degli idrazoni complessi $[Ru(\eta^5\text{-}C_5H_5)\{NH_2N{=}C(CH_3)_2\}(PPh_3)\{P(OMe)_3\}]BPh_4$ [R1= Ph, 4-$CH_3C_6H_4$, C_2H_5]. Particolarmente interessante di questi ultimi complessi è la reazione di ossidazione con HgO che porta alla formazione del diazoalcano complesso derivato $[Ru(\eta^5\text{-}C_5H_5)\{N_2C(CH_3)_2\}(PPh_3)\{P(OMe)_3\}]BPh_4$.

Complessi azinici del tipo $[OsCl(\eta^6\text{-}p\text{-cymene})\{\kappa^1\text{-}[N{=}C(H)C_6H_4R1]N{=}C(H)C_6H_4R1\}\{P(OR)_3\}]BPh_4$ e $[OsCl(\eta^6\text{-}p\text{-cymene})\{\kappa^1\text{-}[N{=}C(CH_3)_2]N{=}C(CH_3)_2\}\{P(OR)_3\}]BPh_4$ [R = Me, Et; R1 = H , 4-CH_3, 2,6-$(CH_3)_2$] sono stati preparati facendo reagire i cloro complessi precursori prima con un equivalente di AgOTf e successivamente con le diverse azine. Curiosamente, in questo caso, i complessi con coordinate le azine κ^1- spontaneamente davano in soluzione reazione di ciclizzazione intramolecolare con la formazione dei derivati chelati $[Os\{\kappa^2\text{-}R1C_6H_3C(H){=}N\text{-}N{=}C(H)C_6H_4R1\}(\eta^6\text{-}p\text{-cymene})\{P(OR)_3\}]BPh_4$ [R = Me, Et; R1 = H, 4-CH_3].

Utilizzando lo stesso metodo sintetico sono stati preparati anche i complessi azinici di rodio, $[RhCl(\eta^5\text{-}C_5Me_5)\{\kappa^1\text{-}[N{=}C(H)Ph]\text{–}N{=}C(H)Ph\}L]BPh_4$ e $[Rh\{\kappa^2\text{-}R1C_6H_3C(H){=}N\text{-}N{=}C(H)C_6H_4R1\}(\eta^5\text{-}C_5Me_5)\{P(OR)_3\}]BPh_4$, and iridio, $[IrCl(\eta^5\text{-}C_5Me_5)\{\kappa^1\text{-}[N{=}C(H)Ph]\text{–}N{=}C(H)Ph\}L]BPh_4$ e $[Ir\{\kappa^2\text{-}R1C_6H_3\text{-}C(H){=}N\text{-}N{=}C(H)C_6H_4R1\}(\eta^5\text{-}C_5Me_5)\{P(OR)_3\}]BPh_4$. Curiosamente, molti dei complessi di iridio con le azine coordinate κ^2- hanno mosrtrato intressanti proprietà di fotoluminescenza: l'eccitazione con *near-UV* e la luce nel violetto portava infatti all'emissione di picchi intorno a 650 nm.

Diazoalcani complessi del tipo $[Os(\eta^5\text{-}C_5Me_5)(N_2CAr1Ar2(PPh_3)\{P(OR)_3\}]BPh_4$ sono stati preparati lasciando reagire in soluzione i cloro complessi precursori con i diversi diazoalcani $N_2{=}CAr1Ar2$

(Ar1=Ar2= Ph; Ar1 = Ph, Ar2 = *p*-tolyl; Ar1Ar2 = $C_{12}H_8$). Tra le proprietà studiate da questi nuovi diazoalcano complessi è particolarmente interessante la reazione di ciclizzazione dipolare (3+2) con l'acetilene, HC≡CH, che porta alla formazione dei 3H-pirazoli derivati. Importanti anche le reazioni di sostituzione con ossigeno, con formazione degli ossigeno complessi derivati in cui l'O_2 si coordina *side-one*, la sostituzione con alchini terminali R1C≡CH, con formazione dei corrispondenti vinilideni complessi, e infine la sostituzione con alcoli propargilici [HC≡CC(OH)R1R2], che porta alla formazione dei corrispondenti idrossi-vinilideni e allenilideni complessi.

Le azidi organiche possono coordinarsi a centri metallici in complessi del tipo [Os(η^5-C_5H_5)(κ^1-N_3R)-(PPh_3){$P(OR1)_3$}]BPh_4. A seconda del gruppo funzionale legato al gruppo N_3 dell'azide tuttavia è possibile ottenere anche altri complessi, dovuti alla decomposizione dell'azide, come ad esempio i complessi imminici derivati [Os(η^5-C_5H_5){κ^1-NH=C(R1)Ar}(PPh_3){$P(OR)_3$}]BPh_4 (R1 = H, CH_3) o i complessi binucleari di azoto [Os(η^5-C_5H_5)(PPh_3){$P(OMe)_3$}$_2$(μ-N_2)]$(BPh_4)_2$. Quest'ultimo in particolare è stato preparato facendo reagire il bromo complesso precursore con fenilazide PhN_3.

Risultati simili sono stati ottenuti anche dalla reazione delle azidi organiche con frammenti *half-sandwich* di iridio in cui si è andati a osservare la formazione dei corrispondenti immino [IrCl(η^5-C_5Me_5){κ^1-NH=C(R1)Ar}(PPh_3){$P(OR)_3$}]BPh_4 (R1= H, CH_3; Ar=C_6H_5, *p*-tolyl) e ammino [IrCl(η^5-C_5Me_5)(NH_2Ph){$P(OR)_3$}]BPh_4 complessi. Di particolare interesse il fatto che, dalla reazione tra complessi dimeri di iridio e le azidi organiche, a seconda delle condizioni di reazione utilizzate, è possibile andare a ottenere sia il mono- [$IrCl_2$(η^5-C_5Me_5)(κ^1-NH=C(R1)Ar)] che il bis-immino derivato [IrCl(η^5-C_5Me_5)(κ^1-NH=C(R1)Ar)$_2$]BPh_4 (R1= H, CH_3; Ar=C_6H_5, *p*-tolyl). Infine, la reazione del clorocomplesso precursore, prima con due equivalenti di argento triflato, e successivamente con le azidi organiche portava alla formazione del bis-imine complesso [Ir(η^5-C_5Me_5)(κ^1-NH=C(R1)Ar)$_2${$P(OR)_3$}]$(BPh_4)_2$.

INDEX

METALS

Together iron, ruthenium, osmium, cobalt, rhodium, iridium, nickel, palladium and platinum form the Group VIII of Mendeleev's periodic table. As in other triads of the transition metals, owing to their different reactivity, the three the elements of the first period are distinguished from the other six, being these commonly known as the "platinum" metals. In particular, in this thesis the attention has been focused on the study of four of these peculiar metals: ruthenium, osmium, rhodium and iridium.

Usually, when one thinks about the chemistry of the transition metals, a key and most important role is attributed to iron, with its extensive chemistry both in water that in apolar solvents thanks to the remarkably wide range of oxidation states.

However, even if the two heavier metals of the triad, ruthenium and osmium, are more stable than iron, they too show a wide and fascinating chemistry and a considerable amount of stable oxidation states, the most common being +2 and +3 for ruthenium, and +2 and +4 for osmium. Also, interesting and with increasingly possible uses in industrial catalysed processes are the "platinum" metals of the cobalt group: their chemistry has been developed in the last few years industrial catalysis, where these metals show remarkable properties and applications. The most common oxidation state of both rhodium and iridium is +3 owing to a greater CFSE. However, with π-acceptor ligands coordinated to the metals, also their +1 oxidation state chemistry is rich and various.

Within the field of organometallic chemistry, iron has long held a dominant position, but the last decades have seen an explosive growth in the organometallic chemistry of ruthenium and osmium, in particular carbonyls and metallocenes occupy leading positions in this research field. Metallocenes, compounds of the general formula $[M(\eta^5\text{-}C_5H_5)_2]$, constitute a fundamental class of organometallic complexes in which a transition metal is sandwiched between the two pentahaptocoordinated cyclopentadienyl ligands[1,2]. Since the landmark discovery of the ferrocene, iron(II) bis(η^5-cyclopentadienyl) $[Fe(\eta^5\text{-}C_5H_5)_2]$, by Kealy and Pauson in 1951[3] (followed by its independent structural characterization by Wilkinson[4] and Fischer[5]) and following synthesis of ruthenocene $[Ru(\eta^5\text{-}C_5H_5)_2]$ by Wilkinson in 1952[6], a huge number of metallocenes with a variety of transition metals have been prepared[1,2]. Rhodocene, $[Rh(\eta^5\text{-}C_5H_5)_2]$, is also known but it is

unstable to oxidation and tends to form dimeric species. Claims for the existence of iridocene probably refer to Ir^{III} complexes. However, the yellow rhodicenium and iridicenium cations are better known.

Nowadays metallocenes, both arene and cyclopentadienyl substituted, are among the most important coordination compounds, being widely used in the development of organometallic chemistry and their synthesis, general properties[7] and application in different field of material science (such as asymmetric catalysis, olefin polymerization, supramolecular chemistry, nonlinear optics, luminescent and fluorescent materials, medicine, etc.[8]) are described in numerous books and journal articles[7]. Interestingly, less attention has been paid to the corresponding half-sandwich, or "piano-stool" complexes, $M(\eta^6\text{-}C_6R_6)L^1L^2L^3$ and $M(\eta^5\text{-}C_5R_5)L^1L^2L^3$. These species somewhat represent a conceptual link between classical Werner complexes and organometallic molecules, since they combine the two prototypical coordinative environments within one single mononuclear unit that merge and modulate the chemical characteristics of both species.

Nowadays half-sandwich compounds have been shown to be efficient starting reagents for synthetic work and they are used in different field. For example (*p*-cymene)Ru(II) complexes can be used as catalysts for hydrogen transfer reactions[9], for the oligomerization of α-amino acid esters[10], for olefin cyclopropanations[11] and for isomerization reactions[12], while Cp*Rh and Cp*Ir (Cp*= C_5Me_5) complexes are utilized as catalysts for Diels–Alder[13] and hydrogenation reactions[14].

AZINES

2.1 Introduction

In chemistry with the term “azine” it is possible to indicate two different types of molecules according to their structure: in heterocyclic chemistry, azines are aromatic six-membered rings containing at least one N atom; while in alicyclic chemistry, azines are the final product of the reaction between hydrazine and two identical molecules of a carbonyl compounds. Symmetrical azines, or with two different ones, unsymmetrical azines[15] (Figure 2.1). The molecules are named aldazines or ketazines depending on whether the carbonyl compound used is respectively an aldehyde or a ketone.

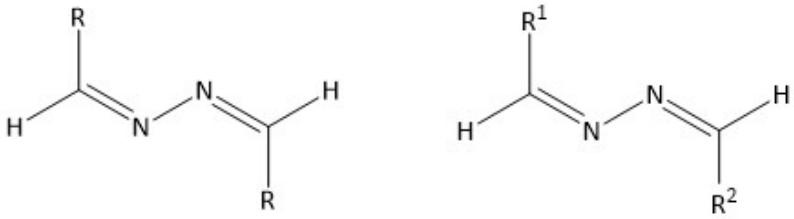

Figure 2.1 Structure of symmetrical and unsymmetrical aldazines.

It can be said that azines are really similar to 1,3-butadiene, the only difference being the presence of the N-N bond between the conjugated double bonds. Glaser, at the beginning of the 21st century, examined the bond lengths attempting to find evidence of electronic delocalization within azines structure: however, different crystallographic data on conformational properties of the N–N and R–C bonds, bond length analysis, spectroscopic studies, and theoretical calculations have shown no evidence of electronic conjugation within the azine backbone. It has been concluded that an azine bridge, now identified as a “conjugation stopper”[16,17], prevents the delocalization (at least in the solid state), although theoretically, the C=N–N=C spacer could have the necessary structural elements to function as a good conjugation bridge[18,19] (Figure 2.2).

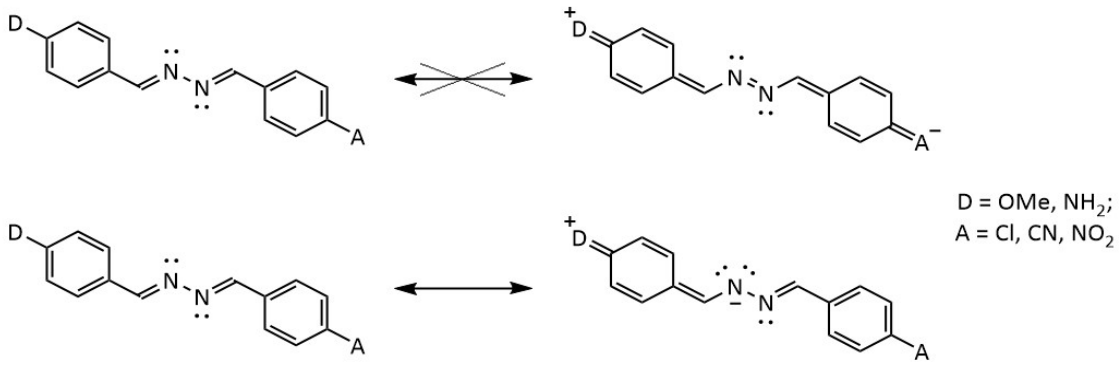

Figure 2.2 Even if it is possible to theorize the existence of electron delocalization in the structure of the azine, the presence of the N-N bond acts as a "conjugation stopper".

Formaldehyde azine, the simplest azine, was prepared in 1959 by Neureiter[20]. While in general all azines are readily synthesized, directly or indirectly, by the reaction of hydrazine with excess aldehyde or ketone[21] the mechanisms of addition of hydrazine to carbonyl compounds can turn out to be more problematic than expected because of the bifunctionality of hydrazine. It's known that hydrazine can behave both as nucleophile and as a base, so it can exist in three different forms: not protonated, monoprotonated and diprotonated.

Whereas the diprotonated form does not possess a nitrogen atom with a free electron pair, which is necessary for the nucleophilic attack on the carbonyl group, the mono-protonated and unprotonated forms of hydrazine can behave as nucleophiles. However, while both of them can form the hydrazone reacting with one molecule of carbonyl compound, only the unprotonated hydrazine can react with another molecule of the carbonyl compound to obtain the final azine of the type R(R')C=N-N=C(R')R[22] (Scheme 2.1).

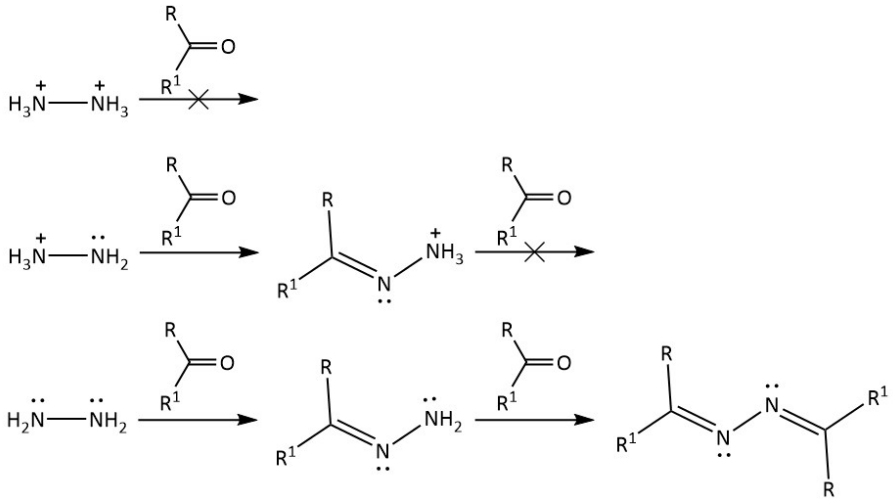

Scheme 2.1 Reaction scheme of the different mechanisms of addition of hydrazine to carbonyl compounds depending on the azine protonation.

Also, it can be said that the reaction's rate of hydrazine with various carbonyl compounds decrease with the increase of steric hindrance according to the following order: aldehyde > dialkyl ketone > alkaryl ketone > diaryl ketone. So, in general, aldazines form more quickly than ketazines. Moreover, the reaction of aldehyde hydrazones with a second molecule of aldehyde is faster than the reaction with hydrazine itself, thus aldazine is the normal final product. On the other hand, for the more hindered ketazines, the presence of excess ketone together with a catalyst is required, usually acetic or formic acid[23].

However, some in-depth studies on the formation of the azines have shown that their mechanisms of formation are neither simple nor straightforward. In some reported cases the main reaction is not a plain nucleophilic addition-elimination: it could be hypotised that an electron-transfer process is operating. Such processes are usually not sensitive to steric hindrance and also show a different electronic demand than simple nucleophilic substitutions[24].

The conformation of azines is controlled by the four atoms chain C=N–N=C. Though in general aldazines and ketazines may occur as three configurational isomers, (E,E), (E,Z), and (Z,Z)[25], almost all studied on aromatic azines showed that they exist in the preferred (E,E) configuration: with the large groups attached to the C=N bonds on the opposite sides of the C=N–N=C chain (trans isomerisation)[26]. However, azines can undergo photochemical E/Z isomerisation of the C=N bonds to produce (E/Z) and (Z/Z) isomers from the thermodynamically most stable (E/E) form[27].

Over the past few years, one of the active areas of organic e inorganic chemistry has been the study of systems containing two connected nitrogens in their structure. Within this general classification of compounds, the three types of molecules that have attracted the most attention are imines, hydrazines and hydrazones. As for the azides, while their coordination chemistry is still relatively unexplored, their organic chemistry has been well studied and they have been evaluated for their possible use in analytical and synthetic chemistry. Lately, azines have attracted a lot of attention because of their versatility in different fields of application.

As a matter of fact, azines are useful for the isolation, purification, and characterization of carbonyl compounds. They have several advantages as protective agents: economic, easy to isolate because of their symmetrical structure, easy to identify due to colourful structures and with high melting points[18,28]. Unsymmetrical azines are particularly appealing for this kind of application because of their ability to link two dissimilar groups.

Some azines were also studied to be used as Liquid Crystal (LC) compounds[27,29–31] and, more recently, azines have attracted interest because the two imine bonds making up their backbone can be considered polar acceptor groups oriented in opposite directions. This characteristic, combined with the possibility of using two aryl rings containing a donor and an acceptor group, makes them ideal candidates for organic Non-Linear Optics (NLO) materials[32–34].

Conjugated polyazines may be doped with iodine to give conducting materials[35]; substituted aromatic azines, such as *ortho*-hydroxyacetophenone azine, have gained considerable attention for their useful applications in colouring and dyeing processes. Some unsymmetrical azines are used as organic luminophores, and others are used to synthesize unsymmetrical diarylethylenes. Azines can also have an significant role in supramolecular chemistry[36,37].

Finally azines constitute an important class of significant nitrogen donor ligands in organometallic complexes and their ability to act as binding molecules or modulators of biological receptors makes them suitable candidates for drug development[38]: recently their antibacterial activities against several germs[39], as well as their antifungal activities[40] were evaluated. Azines were also studied for their use as antimalarial[41], opioid antagonists[24], anticonvulsant, antidepressant, anti-inflammatory, antiviral[42] and antitumor agents[43].

2.2 Organic Chemistry

Azines are a class of compounds with interesting chemical properties and undergo a wide variety of chemical processes[24] and their use as starting materials in organic synthesis is well documented. For example, they can undergo oxidation and reduction reactions. In 1967, Gillis and Lamontagne reported the oxidation of aldazines and ketazines with lead tetraacetate[44] (Scheme 2.2).

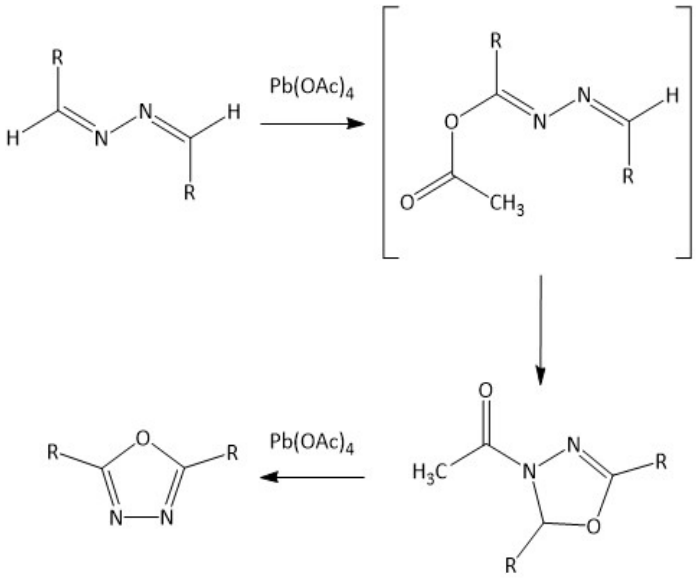

Scheme 2.2 Oxidation of aldazines and ketazines with lead tetraacetate.

The reduction of an azine over palladium or platinum catalyst affords the corresponding hydrazine compound. This compound then could be readily oxidized to the respective azohydrocarbon by using cupric salts, oxygen[45], or hydrogen peroxide.

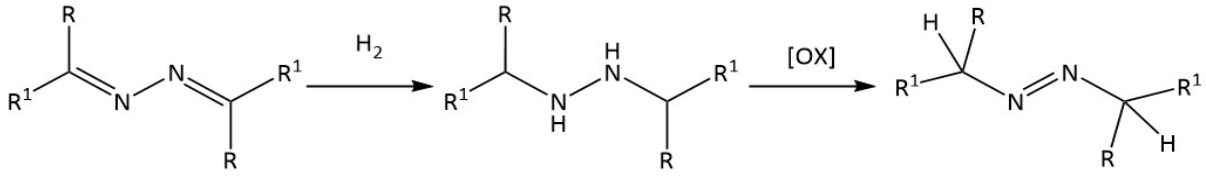

Scheme 2.3 Reduction of azines with subsequent oxidation.

Azines have also been widely used as substrates in the synthesis of substituted hydrazones and heterocyclic compounds such as pyrazoles, purines, and pyrimidines. They show unusual 1,3-dipolar cycloaddition reaction with dienophiles, providing a convenient route to five-membered rings. A first example of this kind of chemistry was given in 1971 by Hartzler who suggested that acetone azine reacts to give 1,3-dipolar cycloaddition by diazomethane extrusion[22] and some years later, in 1976, Satsumabayashi reported a cycloaddition reactions of 2,2-diphenylethenone

with aldehyde azines[46]. Moreover, azines participate in (3+2) cycloaddition reactions as ene fragments (Scheme 2.4 and Scheme 2.5).

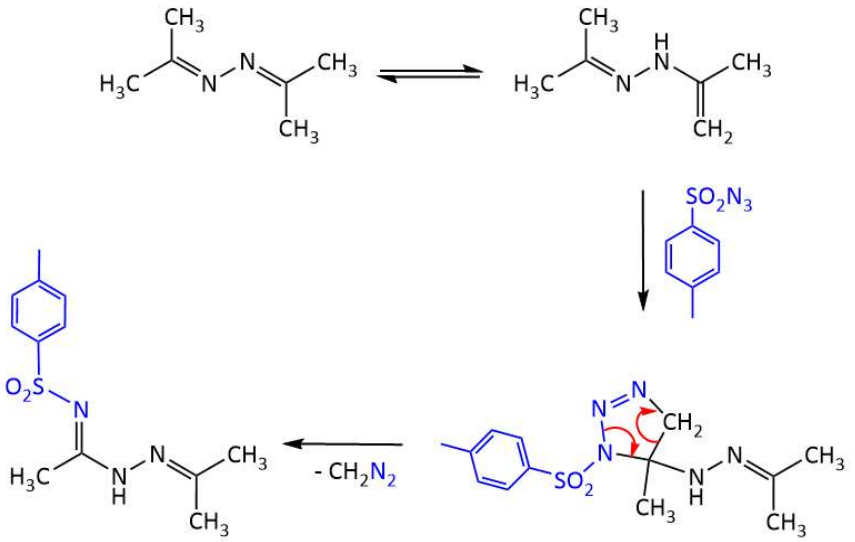

Scheme 2.4 Hartzler reaction.

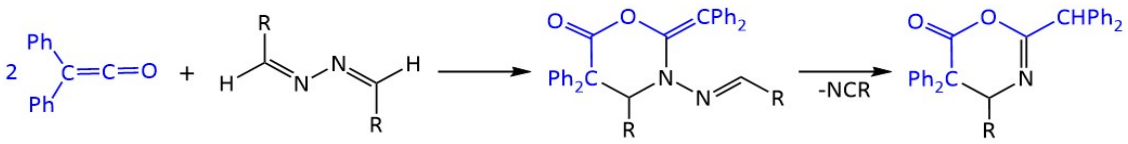

Scheme 2.5 Satsumabayashi reaction.

As it was previously pointed out, one of the most remarkable features of azines is that, thanks to their different proprieties, they can be used in a wide variety of fields and, one of these is as photochemicals. Particularly interesting are the studies on this subject reported by Binkley and co-workers in 1972 about the unique photochemical characteristics of benzophenone azine[47]. This ketazine occupies a place by itself in azine photochemistry because it gives no evidence of participation in the nitrogen-nitrogen bond homolysis cleavage process, the major reaction process experienced by other acyclic azines. Moreover, while normally for this kind of reduction process it has been possible to isolate the intermediates and then irradiate them too, the intermediate products of the conversion of benzophenone azine are themselves extremely unstable, and they quickly decompose to yield many different final compounds. After many studies on the subject it has been found that the results from the photolysis of benzophenone azine may be summarized by saying that, in general, it participates in two photochemical processes: the first of these is a photoreduction, the second is a rearrangement.

Another interesting reaction of azine was studied by Hashidzume et al. in 2006. In this work on the reactivity and polymerizability of alkyl aldehyde azines they observed that acetaldehyde azine (AcAz) underwent crisscross addition with 1,4-phenylene diisocyanate ($Ph(IC)_2$) under mild conditions. Using crisscross addition of AcAz, they obtained a polymeric product[48] (Scheme 2.6).

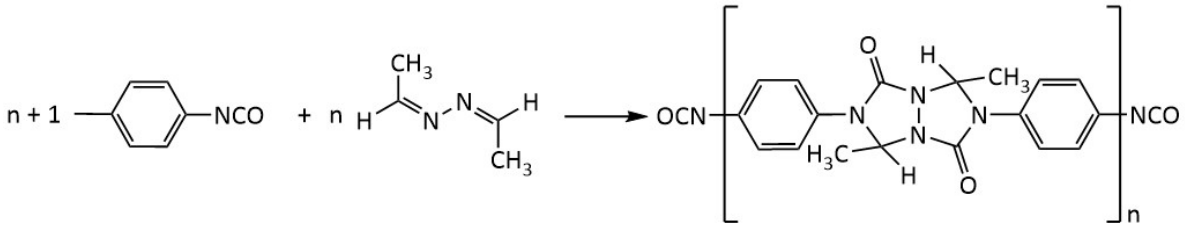

Scheme 2.6 Crisscross addition of acetaldehyde azine with 1,4-phenylene diisocyanate.

2.3 Inorganic Chemistry

In addition to the intriguing properties studied in organic chemistry it is necessary to underline azines show some interesting reactivity also with transition metals. First of all, because of their ability to donate both via lone pairs of the N atom and the C=N π-orbital electrons, azines have versatile properties of coordination binding to metal centres[49]. Furthermore, N–N bond activation is important in catalysis and in organic synthesis in general[50–53]. However, despite the remarkable potential it is difficult to find in literature more than a few examples of azine complexes.

Stapfer and D'Andrea described in 1971 novel complexes of cobalt(II) halides with azine and some of their chemical properties[54]. For example, a benzophenone azino complex of cobalt(II) bromide was obtained by refluxing a suspension of the bis-hydrazinate in 2 equiv. of benzophenone. It is interesting to know that the authors underline that this compound could not be obtained by direct reaction of benzophenoneazine with cobalt(II) bromide (Scheme 2.7).

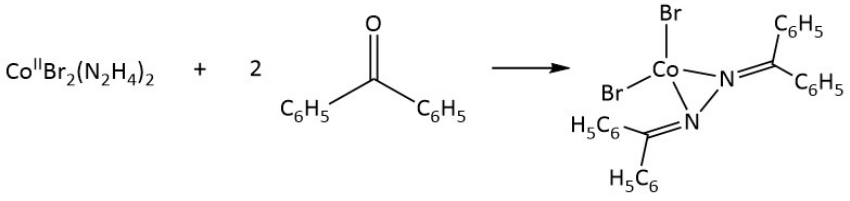

Scheme 2.7 Formation of benzophenone azino complex of cobalt(II).

In 1996, Singh and Srivastav prepared a novel unsymmetrical tetradentate azine, 2-acetylpyridinesalicylaldazine (Haps), by condensing salicylhydrazone with 2-acetylpyridine. This ligand reacted with Mn, Co, Ni, Cu, and Zn acetates to yield deprotonated $M(aps)_2(H_2O)_2$ complexes as shown in Figure 2.3.

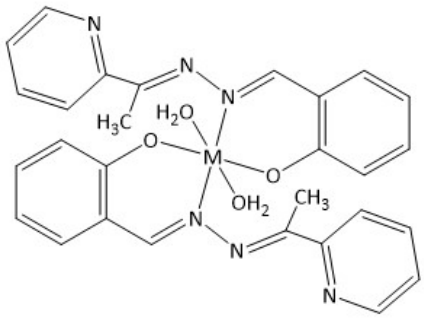

Figure 2.3 Unsymmetrical tetradentate azine of Mn, Co, Ni, Cu and Zn.

Nickel(II) complexes of azine diphosphine ligands were prepared by Cermak for the first time in 2002 by reactions with anhydrous NiX_2 (X = Cl, Br, I). The azine is coordinated as a tetradentate ligand in E,Z configuration and form a bicyclic ligand frame[45] (Scheme 2.8).

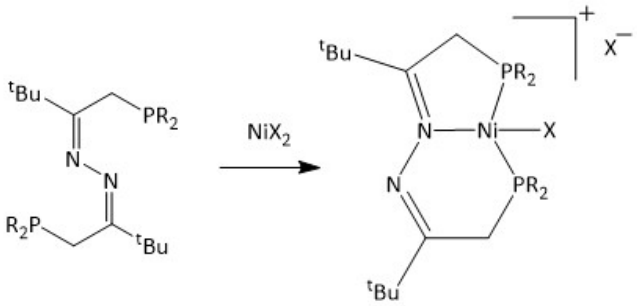

Scheme 2.8 Tetraded coordination of an azine diphosphine to Nickel(II).

In 2004, Dönnecke reported that upon treatment with $Fe_2(CO)_9$, azine ligands bearing halogen substituents in the ortho position undergo two typical reactions: one is the symmetrical cleavage of the N–N bond of azine to yield either binuclear or trinuclear iron carbonyl compounds, the other is the formation of the trinuclear iron carbonyl cluster compound exhibiting a tetrahedral Fe_3N cluster core[55]. It is interesting to note that among all the different halogens investigated by the authors the compound with the fluoro in the ortho position turned out to be much more reactive when treated with $Fe_2(CO)_9$, so much that it wasn't possible to isolate and identify all the different clusters formed, but only five (Scheme 2.9).

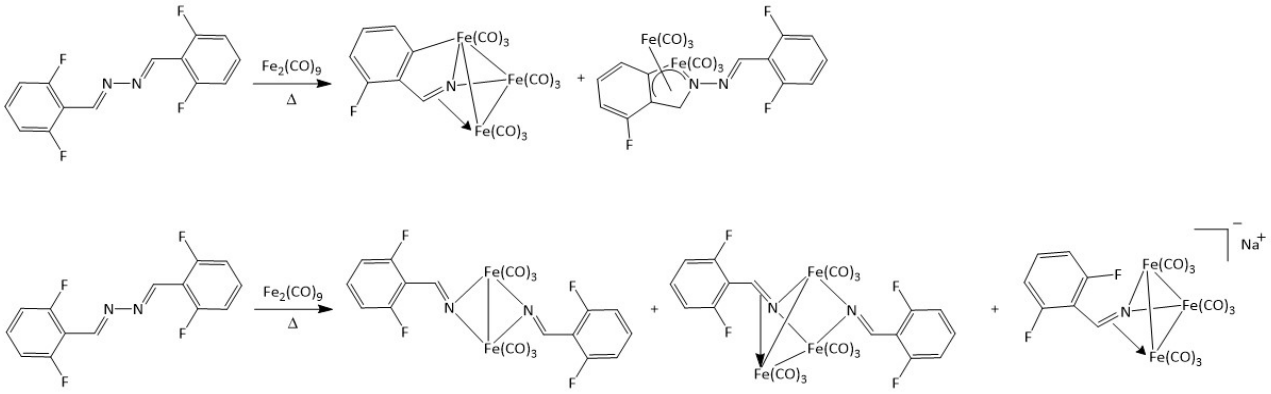

Scheme 2.9 Identified products of the reaction between $Fe_2(CO)_9$ and azine ligands bearing fluorine substituents in the ortho position.

As previously said, azine and its derivatives are well known and are a useful class of organic compounds for supramolecular studies. So, the design of metal–azine coordination polymers of supramolecular architecture is an important subject to be explored. In 2008 Hwang reported his studies on the extended structure of silver complexes with azine ligand[56]. The choice to use silver as metal centre is because, as a soft acid, the Ag(I) ion helps a lot the formation of supramolecular assemblies, and it favours stable coordination to soft bases like unsaturated nitrogen. As it is known, the development of supramolecules is also largely affected by the nature of the counter ions. Hwang observed that, with a di-2-pyridyl ketone azine both the coordination environment and the packing of the crystals were different using different anions. In particular, three coordination complexes builded up by self-assembly of the azine and Ag ions have been structurally characterized: nitrate and trifluoroacetate complexes are both tetranuclear but with dissimilar coordination structure to the Ag(I) centres, whereas the perchlorate complex has a polynuclear chain structure (Scheme 2.10). Such variation in the environment of a complex molecule is termed as “Chemical Frustration”.

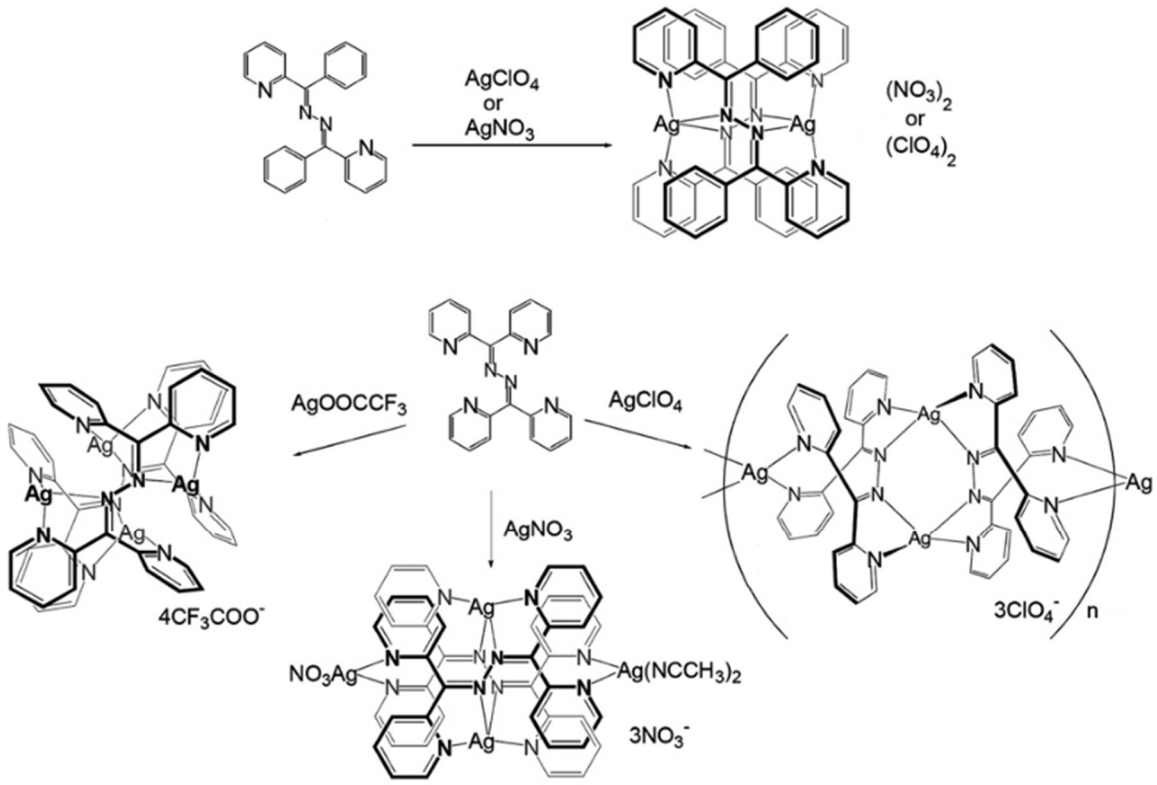

Scheme 2.10 Azine complexes of silver.

However, a glance through the literature show that azine complexes of iron and cobalt triad are very rare: indeed, apart from some studies on iron cluster, no example of azine complex has been reported for these metals.

DIAZOALKANES

3.1 Introduction

Molecules comparable to azines are diazoalkanes, RR'CNN. Beyond the similar structure due to the presence of the nitrogen-nitrogen bond inside the molecular backbone, as consequence of the fact that both organic compounds are produced by the reaction of a molecule of hydrazone respectively with an azine or with mercury oxide, the main characteristic that binds diazoalkanes to azines is that the decomposition of diazoalkanes, catalysed by metal complexes, often leads to the formation of azines as a primary product.

Diazoalkanes (R_2CN_2), like azines, have been useful intermediates in organic chemistry from the beginning of the twentieth century and, consequently, many reactions of these molecules have been fully investigated. In all these years there has been a tremendous growth of interest in diazoalkanes from both synthetic and mechanistic viewpoints. Despite the notorious toxicity by inhalation or by contact with the skin or eyes, the main role as the prototype compound for many of the studies on diazoalkanes' chemistry was the simplest diazoalkane, the diazomethane H_2CN_2, discovered by German chemist Hans von Pechmann in 1894. The classical methods for preparation of diazomethane involved the treatment of a nitroso-compound, either N-nitroso-N-methylurethane or N-nitroso-N-methylurea, with a suitable base, generally an alkali like potassium hydroxide. For the preparation of disubstituted diazoalkanes the oxidation of a ketohydrazone is normally used.

Much of the interest in diazoalkane chemistry derives from worldwide studies of the reactivity and structure of carbenes (R_2C:). The latter are now recognized as the most common intermediates in photolysis and thermolysis of diazoalkanes and were widely characterized during the early nineteen fifties, largely as a result of pioneering studies by Doering[57], Skell[58], Herzberg[59] and their collaborators. Other major developments in diazoalkane chemistry during the years include cycloaddition and catalysed alkylation, homologation, and polymerization processes.

3.2 Organic Chemistry

Despite the instability of many diazo compounds, it was discovered that under the appropriate conditions diazoalkanes will behave as an acid or a base, as an electrophile or a nucleophile, as a 1,3-dipole, or as a carbene source[60,61].

These many possible applications of diazoalkanes can be quite easily explained considering the structure of diazoalkanes. During the first fifty years of the twentieth century, many groups centred their research on the description of the structure of diazomethane: initially a linear, planar structure was established by electron diffraction, microwave spectroscopic techniques[62], molecular orbital calculation (HMO)[63], calculation of the lengths of the C-N bond (1.300 Å) and the N-N bond (1.139 Å). However, while a complete analysis[64] of the vibrational spectrum of gaseous and solid CH_2N_2 confirmed the linear, planar structure with sp^2 hybridized carbon, it also indicated the presence of a bent structure.

Following this discovery, it was quite easy to rationalize the different reactions of diazoalkanes considering the electron distribution based on the different conformations (linear or bent) of the molecule, represented in the following scheme by resonance forms A-D (Figure 3.1).

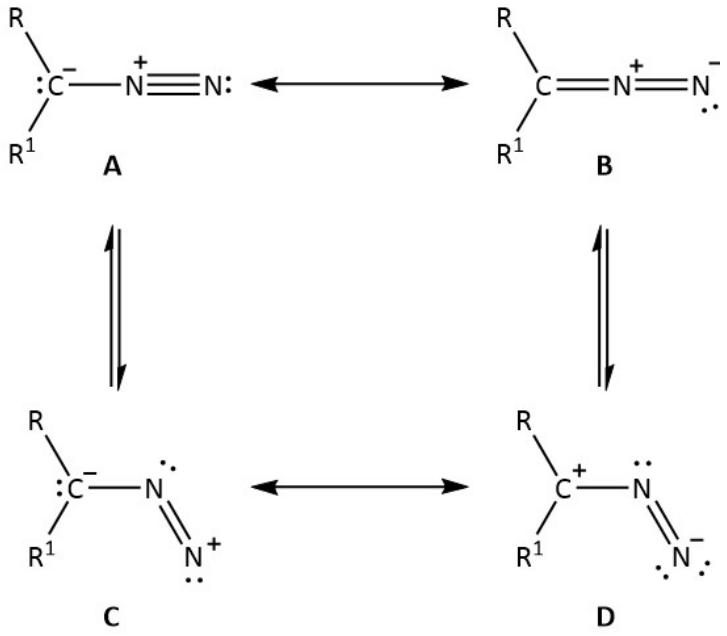

Figure 3.1 Resonance forms of diazoalkanes.

Forms **A** and **C** dictate the reactivity of diazoalkanes towards acids and electrophiles, with forms B and D playing a minor role. Proton abstraction by bases is governed by form B whereas reactions with nucleophiles are best rationalized by consideration of forms A and C. Two are the

potentially basic sites in simple diazoalkanes, the carbon in structures A-C and the nitrogen of structures B-D. The reaction with the former leads to the usually observed products of reactions with acids[65]. The alternative site is not apparently involved.

Obviously, the conformation of diazoalkanes is not the only feature that influences their reactivity, other issues can also impact on the final results of the different reactions.

For example, the acid strength and reaction conditions necessary to protonate diazoalkanes vary largely with the substituents. Whereas diazomethane reacts readily and smoothly with carboxylic acids and phenols to give the substrates' methylated derivatives, the reactions between diazoesters and diazoketones require gentle warming. On the other end, diazoethane reacts with alcohols at room temperature. However, the efficiency and rapidity of reaction increase with substitution of electron-withdrawing groups in the latter. Moreover, reduction of the already feeble acidity of the hydroxyl group by solvation may completely prevent the reaction: thus, trichloroethanol is methylated in heptane but not in ether. On the other hand, intensification of the proton acidity by prior complexation of the hydroxyl oxygen with an electrophilic species dramatically improves the efficiency of the process (Scheme 3.1).

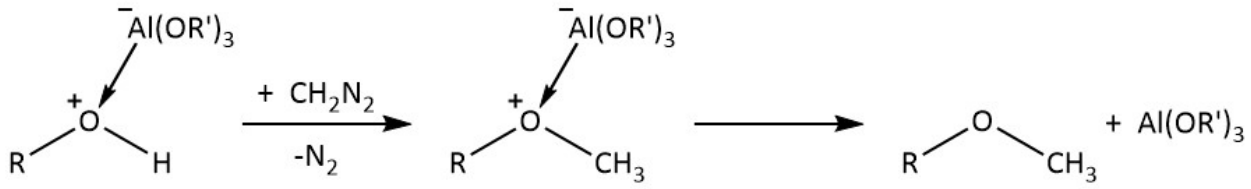

Scheme 3.1 Reaction between diazomethane and a generic alcohol catalyzed by a nucleophile.

As already noted above, in all studied cases, only carbon acts as a basic site, however it is reported in literature an unequivocal examples of electrophilic attack at the terminal nitrogen of diazoalkanes and it involves a carbene species[66,67] (Scheme 3.2).

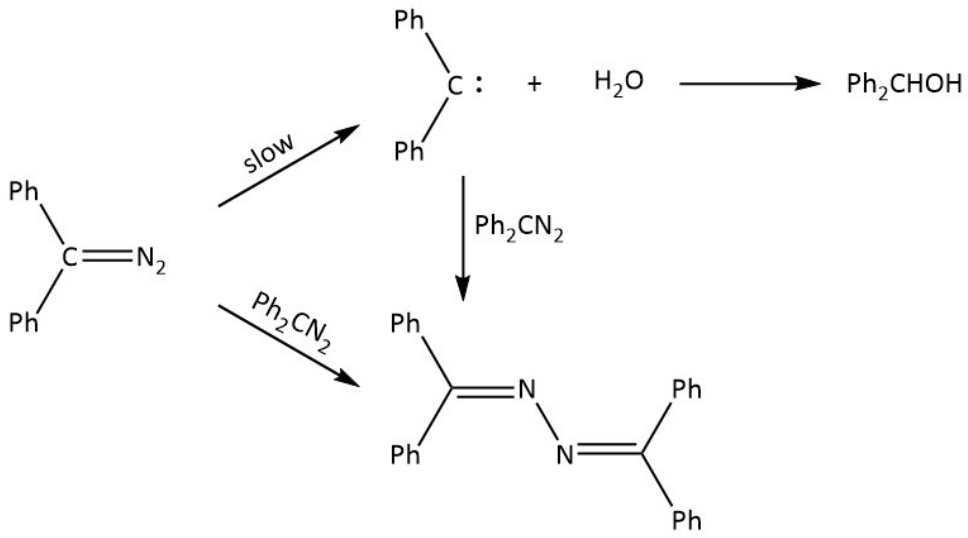

Scheme 3.2 Electrophilic attack on the terminal nitrogen of diazoalkanes.

Another interesting feature of diazoalkanes is their thermal reactivity with aldehydes and ketones to give mixtures of homologous carbonyl compounds and epoxides[68] as reported in Scheme 3.3.

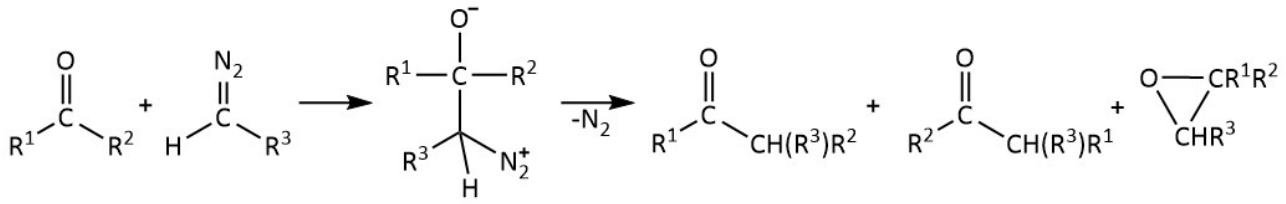

Scheme 3.3 Reaction between diazoalkanes and ketones.

Epoxide formation is favoured by electron-withdrawing substituents in the carbonyl compound and the reactions are catalysed by protic agents, particularly alcohols.

However, despite all possible kind of reactivity shown by diazoalkanes, their most interesting and studied reaction is the 1,3 dipolar cycloaddition.

Cycloadducts of diazoalkanes have been known since many years but it was not until the early 1960s that the classification of the reaction as a 1,3-dipolar cycloaddition became generally accepted[61]. This followed a series of outstanding studies by Huisgen and coworkers[69] (Scheme 3.4).

1,3-Dipolar cycloadditions exhibit common mechanistic features: they are not markedly influenced in rate or stereochemistry by solvent polarity; they show low enthalpies of activation

and large negative entropies of activation and produce five-membered cyclic compounds in which the stereochemistry of the reacting olefin (dipolarophile) is maintained.

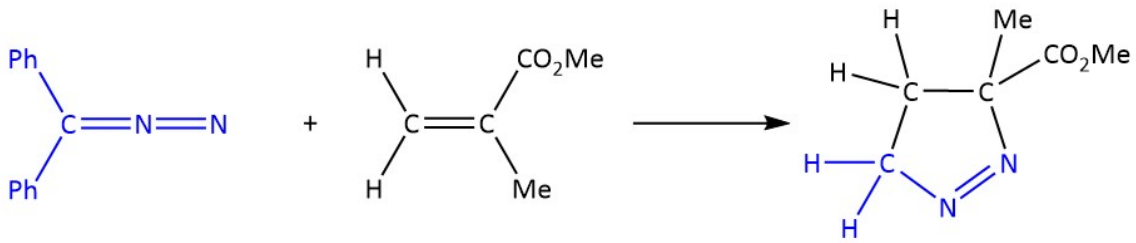

Scheme 3.4 Example of 1,3-dipolar cycloaddition reaction with diazoalkane.

Reactivity of diazoalkanes in cycloaddition is markedly reduced by conjugating substituents, but increased by alkyl groups: reactivity falls in the sequence[69,70]: $MeCHN_2$ > CH_2N_2 >> Ph_2CN_2 > N_2CHCO_2Et, indicating dominance of electronic effects. On the other hand, ring strain or polarizing influence of conjugating substituents strongly promotes dipolarophile reactivity and all types of substituent exert a retarding steric effect.

Finally, this type of reaction can be also obtained and improved by the coordination of the diazoalkane to a metal centre.

3.3 Inorganic Chemistry

Some of the complexes that have raised a remarkable interest in the past decade are those containing diazoalkanes in their coordination sphere. Diazoalkanes are heterocumulene ligands because they possess unsaturated bonds and lone electron pairs. Owing to the well-established view that compounds containing metal-diazo bonds are unstable, diazoalkanes were long believed to be catalytically decomposed into carbenes by transition metals. The synthesis of N-bonded diazoalkane complexes has been initially developed to study the mechanistic aspects of their catalytic decomposition or nitrogen activation. The diazoalkanes used for these studies were those stabilized either by resonance, like diazotetrachlorocyclopentadiene, diazofluorene and diazophenylmethane, or by strongly electron-withdrawing groups, such as CN, CF_3, CO_2R, C(O)R.

Nowadays plentiful studies show that the formation of a stable bond between diazoalkanes and metal centres is possible, and they form numerous kinds of complexes. Indeed, neutral diazoalkanes possess free electron pairs located on the two N atoms and π electrons in the double or triple bonds, so diazoalkanes can act as two-, four- or six-electron donor ligand and they may

coordinate to transition metal centres with different geometry: the four possible structural models are illustrated in the Figure 3.2.

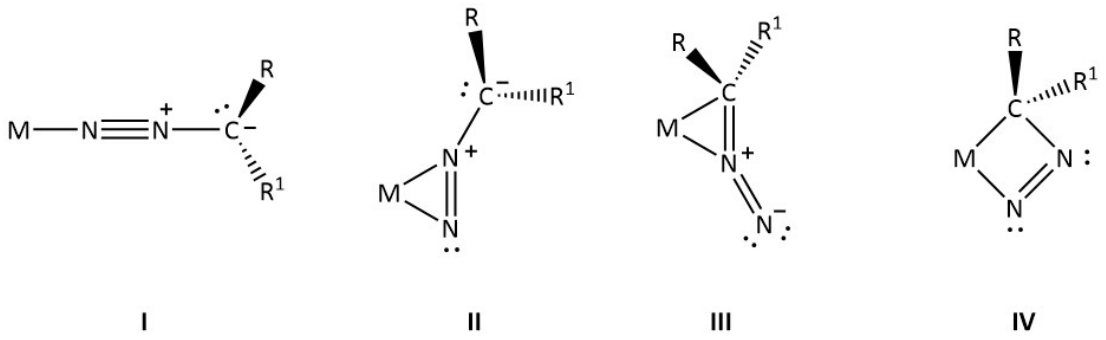

Figure 3.2 Diazoalkane coordination models.

The diazoalkanes can form a σ-bond with the metal through the terminal N atom (type **I**, η^1 end-on N coordination); or, via the π function of N=N and C=N bonds, diazoalkanes can coordinate side-on respectively η^2 (N,N) (types **II**) and η^2 (N,C) (type **III**), finally the coordination model type **IV** is an η^2 metallacycle. Unfortunately, until now, only the coordination modes **I** and **II** have been experimentally observed. The structural geometry **III** and **IV** have been only proposed as intermediates in the mechanisms of decomposition of diazoalkanes but have not yet been isolated.

The end-on η^1 coordination mode of the diazo moiety may cover different electronic configurations as shown in Figure 3.3:

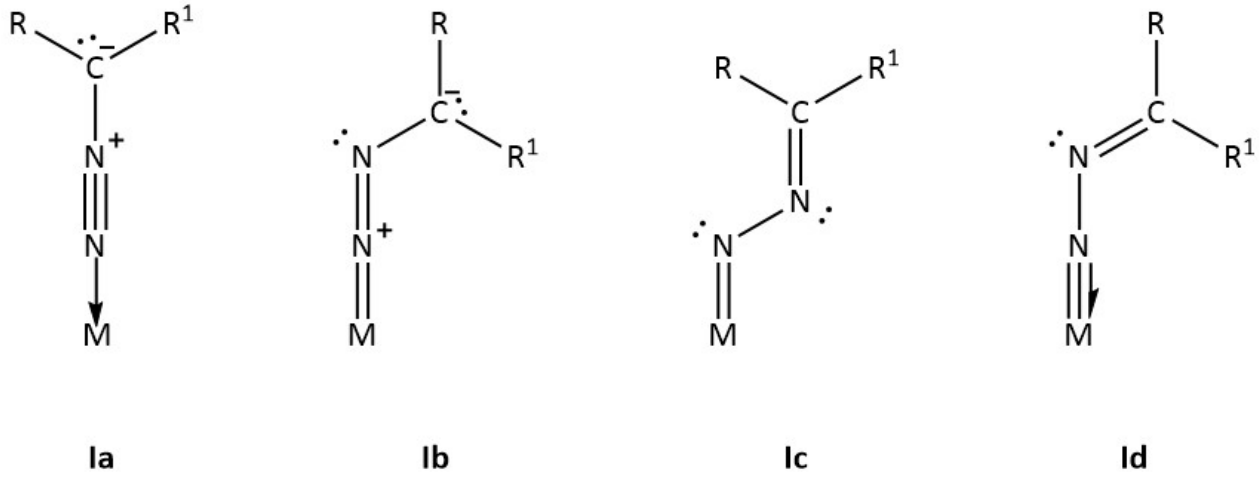

Figure 3.3 End-on η^1 coordination mode for diazoalkanes bonded to single metal fragments

R_2CN_2 may act as a two (**Ia**, **Ib** and **Ic**) or a four-electron donor (**Id**) making one to three bonds to a metal. In type **Ia** complexes, the terminal N atom acts as a $2e^-$ donor, forming a dative bond with the metal centre, thus behaving as a neutral diazo ligand. This totally linear coordination has been first observed by Dartiguenave and coworkers[71] in chromium and tungsten complexes of the type $[M\{N_2C(SiMe_3)_2\}(CO)_5]$ (M=Cr, W) and $[W\{N_2C(SiMe_3)_2\}(CO)_4(PPh_3)]$.

In type **Ib** (single bent) and **Ic** (double bent) species, the terminal nitrogen has two covalent (σ+π) bonds with the metal. Most of these compounds have been prepared through ligand substitution reacting diazoalkanes on late transition metal complexes under mild conditions. They were described, respectively, by Herrmann[72] in complexes of $[CpMn(CO)_2\{N_2CH(CO_2Me)\}]$, whereas the diazoalkane complexes of iridium $[IrCl(N_2CR'_2)(PR_3)_2]$ (R'=C_5Cl_4, Ph, *p*-tol, *p*-FC_6H_4) were obtained by Schramm and Ibers[73–75] and Werner and coworkers[76]. This η^1 end-on coordination is illustrated by the X-ray structural characterization of $[IrCl(N_2C_5Cl_4)(PPh_3)_2]$, Figure 3.4. The diazoalkane group is single bent at the central N_2 atom, giving the molecule a non-linear geometry.

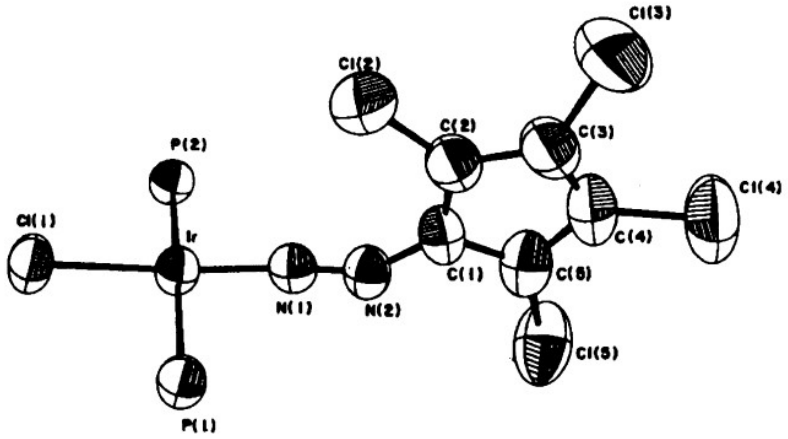

Figure 3.4 ORTEP drawing of $[IrCl(N_2C_5Cl_4)(PPh_3)_2]$, example of Ic coordination.

It is interesting to note that this is one of the few characterized by X-ray structure complexes where it is clear the **Ic** coordination of the diazoalkane to the metal centre. Generally, type **Ib** and **Ic** complexes involved in equilibrium with **Ia** or **Id**[71], so they are more difficult to isolate and characterize.

Finally, diazoalkanes of the type **Id** are $4e^-$ donor with two covalent bonds and one dative bond. Consequently, the diazo ligand, in the ionic formalism of electron count, may be considered reduced by the metal centre into the hydrazido(−2) derivative: this type of coordination can be

described as an oxidative addition, which increases the formal oxidation state of the metal centre by +2 units. There are several examples of **Id**-type coordination mode, where the terminal nitrogen atom N^1 acts as a 4e− donor. Monometallic and bimetallic complexes have been described, but, in all cases, only middle transition metals (Mo and W) are involved with oxidation states ranging from IV to VI. Interestingly, none of the first complexes showing **Id** coordination mode were produced from free diazoalkane, but rather were prepared by oxidative addition of dibromocarbene on Mo(0) complexes or by condensation of a coordinated hydrazido ligand with a carbonyl compound. This is an important type of coordination because the four-electron donating singly bent diazoalkanes show some interesting reactivity: they are susceptible to attack by nucleophiles such as $LiAlH_4$, and Grignard reagents at the C atom adjacent to the diazo group and they also have a tendency to be deprotonated by a strong base, like NaOH, to give alkenyldiazenido ligand (N=N-C(R)=CR'R'')[77].

Type **II** complexes are characterized by an η^2(N,N) coordination mode (Figure 3.2) and it is possible to find in the literature several examples of this type of coordination mode, including early to late transition metals. An example is illustrated in the X-ray structure of [Ni(^{t}BuNC)$_2$(9-diazofluorene)] (Fig. 3.5) which shows a diazofluorene molecule singly bent, η^2-bonded to the Ni atom through the N1–N2 multiple bond.

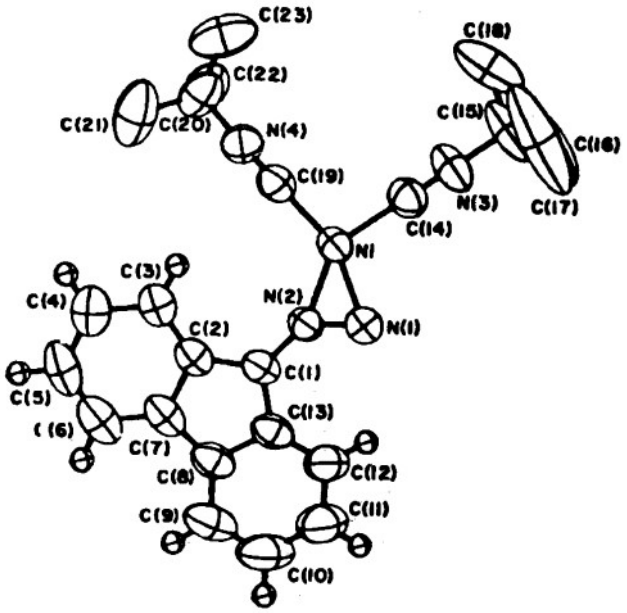

Figure 3.5 ORTEP drawing of [Ni(^{t}BuNC)$_2$(9-diazofluorene)], example of η^2(N,N) coordination.

This coordination mode is a consequence of the electronic configuration of the metal. In these electron-rich systems, the diazo molecule acts as a *π-acid* ligand.

The number of diazoalkane coordination modes increases considerably in the presence of bimetallic complexes or clusters. Besides the modes (**I** to **IV**) reported with single metal centres, four new modes (types **V** to **VIII**; Figure 3.6) may be proposed in the valence bond formalism.

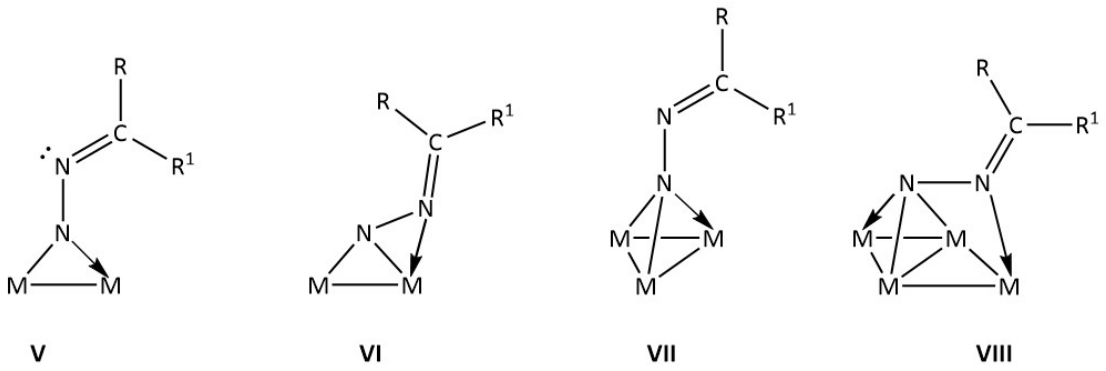

Figure 3.6 Possible structural model for diazoalkanes N-bonded to bimetallic metal complexes and clusters.

In types **V** and **VII**, the former coordination model described for the first time by Messerle and Curtis[78], the diazoalkane is bonded via its terminal nitrogen atom to bimetallic or trimetallic fragments and acts as a $4e^-$ donor giving two covalent bonds and a dative bond. In type **VI**, first discovered by Herrmann, both N atoms are involved in the coordination ($4e^-$). Coordination mode **VIII,** described by Carty, presents a diazoalkane bonded to four metal centres through two dative and two covalent bonds acting as a six-electron donor ligand. As in the case of monometallic complexes, the ionic formalism can be used for counting electrons. Then, these coordination modes are best described as a $2e^-$ oxidative addition of diazoalkane on the metallic fragment. The diazoalkane behaves as an hydrazido ligand: $(N_2CR_2)^{2-}$ and the metallic fragment or cluster increases its formal oxidation state by two units.

Interestingly, the maximum coordination mode possible for a diazoalkane ligand, i.e. $8e^-$ donor, has not been observed yet.

In general, when studying the coordination of diazoalkanes to different metal centre, for their characterization is suitable the observation of the infrared stretching frequency of the diazoalkane ligand ν(C=N=N). Free diazoalkanes generally have the $\nu(CN_2)$ vibrations in the 2100–2200 cm^{-1} range. When they are coordinated to metals, this band shifts to lower frequencies, as expected from the disappearance of the triple N≡N bond and formation of N=N and N=C double bonds. However, caution must be exercised in using these numerical values because the

vibrational coupling is strongly dependent on the diazo substituent, on the metal and on the number of ligands in the metal coordination sphere.

As previously described, reactions of diazoalkanes with metal complexes often result in the formation of carbene complexes[71,77,79–83] concurrent with the loss of N_2. This is a key process in catalytic reactions such as the cyclopropanation of olefins and carbene insertion into C-H bonds, which are largely used in organic synthesis. However, in addition to N_2 extrusion on metal complexes, diazoalkane ligands are expected to exhibit various reactivities depending on their coordination mode and the electronic state of the central metals. Indeed, the metal-mediated reactions of diazoalkane ligands are remarkably different from those of free diazoalkanes, from which a variety of nitrogen-containing species have been obtained, as the azines.

In literature has been reported that, in some cases, diazoalkanes complexes can decompose to give, instead of carbene, dinitrogen [M]−N_2 derivatives. Diazoalkane coordinated to ruthenium complexes of the type [Ru(η^5-C_5Me_5)(N_2CAr1Ar2)(PPh_3){$P(OR)_3$}]BPh_4 can undergo hydrolysis reaction to afford 1,2-diazene derivatives [Ru(η^5-C_5Me_5)(η^2-NH=NH)(PPh_3){$P(OR)_3$}]BPh_4[84,85]. The formation of a diazene species is rather surprising but can be explained on the basis of a nucleophilic attack of H_2O on the carbon atom of the coordinated diazoalkane, followed by hydrogen shift, giving a hydrazido intermediate. This species is quite unstable and give intramolecular hydrogen transfer from the acidic OH group to the hydrazido N_α group with concurrent cleavage of the C−N_β bond, affording free ketone Ar1Ar2C=O and the 1,2-diazene molecule, which acts as a π-bonded ligand (Scheme 3.5).

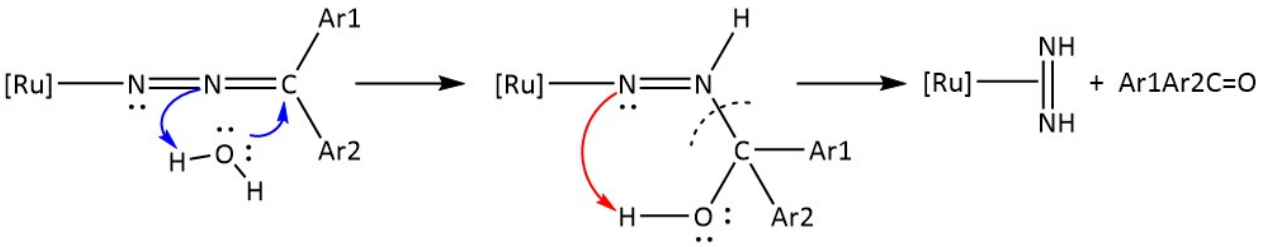

Scheme 3.5 Formation of diazene complex from a diazoalkane complex.

Diazoalkanes are also known to insert into metal-hydrogen bonds without extrusion of N_2. Examples involve both 1,1-insertion (at N-N) which give the hydrazido(1-) derivative, and 1,3-insertion (at N-C) which lead to the formation of the alkyldiazenido(1-) complex. Also the N−N bond cleavage[86], as well as the reduction of the coordinated N_2CAr1Ar2 ligand[80,87] has been reported.

An important reaction for the coordinated diazoalkanes in metal complexes is the cycloaddition, reaction which has been extensively studied, for both fundamental and synthetic reasons[69]. In literature reported that diazoalkane complexes can undergo [3+2] cycloaddition reaction[88,89] with alkenes and alkyne affording 3H-pyrazole derivatives. The research group of this PhD thesis published in 2014 a systematic study on the cyclization reaction of coordinated diazoalkane[90], where was shown that, depending on the type of substrate, it was possible to modulate the reactivity of the diazoalkane complexes. Indeed, treatment under mild conditions of diazoalkane complexes of the type $Ru(\eta^5\text{-}C_5H_5)(N_2CAr1Ar2)(PPh_3)(L)]BPh_4$ with ethylene ($CH_2{=}CH_2$) led to dipolar [3+2] cycloaddition reaction, affording the 4,5-dihydro-3H-pyrazole derivatives $[Ru(\eta^5\text{-}C_5H_5)\{\eta^1\text{-}N{=}NC(Ar1Ar2)CH_2CH_2\}(PPh_3)(L)]BPh_4$. Conversely, acrylonitrile [$CH_2{=}C(H)CN$] instead reacted with the same diazoalkane complexes to give the 1H-pyrazoline derivatives $[Ru(\eta^5\text{-}C_5H_5)\{\eta^1\text{-}N{=}C(CN)CH_2C(Ar1Ar2)NH\}(PPh_3)(L)]BPh_4$. Finally, the treatment of the diazoalkane complexes with acetylene CH≡CH under mild conditions led to dipolar cycloaddition, affording the 3H-pyrazole complexes $[Ru(\eta^5\text{-}C_5H_5)\{\eta^1\text{-}N{=}NC(Ar1Ar2)CH{=}CH\}(PPh_3)\{P(OMe)_3\}]BPh_4$. All these reactions are reported in Scheme 3.6.

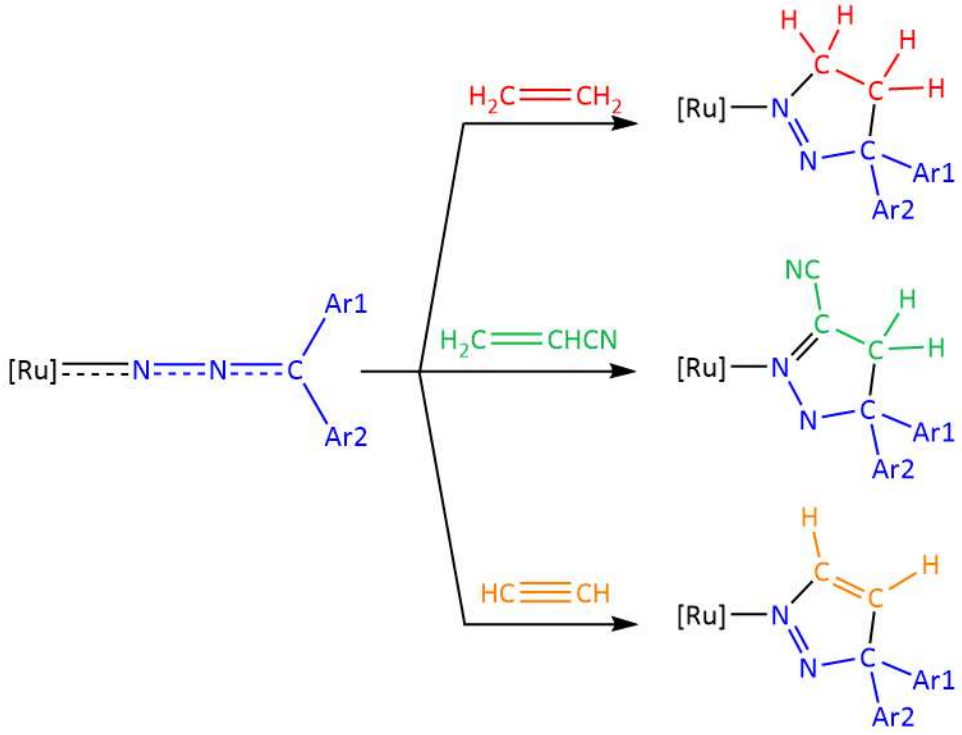

Scheme 3.6 Cycloaddition reaction of diazoalkanes complex of ruthenium with alkenes and alkyne.

In the same paper, the authors stressed the influence of the steric and electronic factors of the substituents on the organic substrate in leading to cycloaddition versus a substitution process.

AZIDES

4.1 Introduction

The term "azides" refers to the molecules having a functional group -N_3. They derive from the hydrazoic acid, HN_3, a weak acid, liquid at room temperature, with high vapour pressure and with toxicity comparable to that of hydrocyanic acid[91]. It is indeed known that all the azides species are noxious to human organism: for example, the oral LD_{50} on rat for sodium azide is 27 mg/kg. The pharmacology, toxicity and mutagenic properties of azides have been extensively investigated[92,93] and nowadays it is know that the main reason of the azides toxicity is the inhabiting activity of N_3^- group toward the "IV complex", or “cytochrome C oxidase”, the last enzyme in the respiratory electron transport chain: the inhibited protein can’t work anymore and this lead to the chemical asphyxiation of cell. Moreover, compounds such as sodium azide can be decomposed via enzymatic catalysis by red blood cells into nitrogen monoxide, a powerful vasodilator, thus bringing to a poisoning process and, furthermore, some inorganic azides are known as mutagen and neurotoxic agents[94]. So, in general, it can be said that azides are rather harmful to humans and must be handled with care.

Azides compounds can be formally divided into organic and inorganic azides. Because of the increasing interest, a rapidly growing number of publications on both categories, has been published in literature.

The inorganic azides are the derived salts of the hydrazoic acid, and two of the most known are lead azide, $Pb(N_3)_2$, and silver azide, AgN_3. One of the most acknowledged feature of heavy metal azides is that they run very easily into detonation and this specific property has established the use of both silver azide and lead azide as primary explosives in detonators[95]. There are also alkali metal azides, like LiN_3 and NaN_3, that are remarkably safer since they can hardly explode due to impact or friction and, indeed, for most laboratory conditions, alkali metal azides are not considered explosives[96]. However, if ignited or exposed to strong heat (300 °C), alkali metal azides decompose rapidly with the evolution of large volumes of nitrogen gas[97] (Scheme 4.1).

$$2\ NaN_3(s) \rightarrow 2Na(l) + 3N_2(g)$$

Scheme 4.1 Thermodecomposition reaction of sodium azide.

The beginnings of azide chemistry date back more than 150 years. During all these years, the preparation, properties, synthetic uses and applications options and limits of azide have been examined in great detail by many authors and the results have been summarized in numerous articles and books that can be easily found in literature[96,98–103]. Particularly, in the last twenty years, azide chemistry has undergone a huge development thanks to the discovery of its applications in medicine: it is worthwhile to mention the international interest on azidonucleosides as an effective drug for the treatment of acquired immune deficiency syndrome (AIDS)[94] and their application for the preparation of bioconjugates via Staudinger ligation[104]. Also, azides play an important role in biology and materials sciences and, on top of that, azides have received renewed interest in synthetic chemistry and are becoming established as an important and versatile class of chemical compounds. Among others organic compounds organic azides are currently considered as optimal precursors for reactive species such as nitrenes, aziridines, azirines, triazoles, triazolines and triazenes. Moreover, organic azides can be easily transformed into amines, isocyanates and other functional molecules. Lastly azides have more recently received an increasing interest as valuable and versatile reagents within the concept of "Click Chemistry". However, alongside their huge utility in organic synthesis the potential hazardous properties of organic azides must be always carefully taken into account. As previously said, the safety risk involved in the handling of azides refers to their toxicity, sometimes to their thermal instability, but also to their possible sensitivity to shock and friction that can lead to explosion: organic and inorganic azides are indeed very energy-rich molecules. This is because the azido group is a highly energetic functional group: the N_3 π-bond can be easily polarized which consequently results in strong exothermic dissociation reactions with release of molecular nitrogen and reactive nitrene groups. So, many organic compounds containing azido groups have not found wide application as practical energetic materials because of their high sensitivity. Another particular risk is found where the formation of free, extremely shock-sensitive hydrazoic acid (HN_3) must be reckoned with. The explosion of a few tenths of a millilitre of free, liquid HN_3 can destroy a complete laboratory-scale production unit[95]. The explosion-like decomposition can be triggered by the slightest thing, exposure to extremely small friction or shock energies and/or flowing over rough surfaces.

The chemistry of azides begins with the preparation of the first organic azide, phenyl azide, by Peter Griess in 1864[103] and with the discovery of hydrogen azide and the rearrangement of acyl azides to the corresponding isocyanate reported by Curtius in 1890 (Curtius rearrangement)[105].

However, only in the 1950s and 1960s did organic azides receive considerable attention pushed by the reviews of Smith[105] and Boyer[106] on the chemistry of the acyl, aryl, and alkyl azides. Since then numerous syntheses of organic azides have been developed. In the following are shown two of the more historically relevant synthetic methods for the preparation of azides.

The more common method for the preparation of sodium azide starts from ammonia and occurs in two stages developed by Wislicenus in 1892: in the first step NH_3 reacts with molten metallic Na to give sodium amide, while in the second reaction the sodium amide reacts with nitrous oxide to afford sodium azide, ammonia and sodium hydroxide[97,107] (Scheme 4.2).

$$2\ Na + 2\ NH_3 \rightarrow 2\ NaNH_2 + H_2$$
$$2\ NaNH_2 + N_2O \rightarrow NaN_3 + NaOH + NH_3$$

Scheme 4.2 Wislicenus sodium azide synthesis.

The gas composition and the extreme reactivity of sodium and sodium amide with traces of water represent a particular safety risk of this synthesis method. Some variations of this process were described by Bretschneider and Abe fifty years later[95].

At the beginning of the twentieth century Curtius and Thiele developed another production process where a nitrite ester is converted to sodium azide using hydrazine[95] (Scheme 4.3).

$$2\ NaNO_2 + 2\ C_2H_5OH + H_2SO_4 \rightarrow 2\ C_2H_5ONO + Na_2SO_4 + 2\ H_2O$$
$$C_2H_5ONO + N_2H_4{\cdot}H_2O + NaOH \rightarrow NaN_3 + C_2H_5OH + 3\ H_2O$$

Scheme 4.3 Curtius synthesis of sodium azide.

4.2 Organic Chemistry

If the hydrogen atom of the hydrazoic acid is replaced with an alkyl or aryl substituent, the organic azides (R-N_3) are obtained. Organic azides are also called covalent azides, given the bond formed between the terminal nitrogen atom and the carbon atom of the alkyl or aryl group. Azidomethanes, CH_3N_3, the easiest organic azide, was prepared by O. Dimroth in 1905 by simple methylation of sodium azide with dimethyl sulfate[108]. So, among the various possibilities for preparing alkyl azides, classic nucleophilic substitution is one of the more favourite ways. In this synthetic method alkali metal azides, mainly sodium azide, are commonly used as the azide ions source while substrates bearing leaving groups such as halides or sulfonates offer a simple, safe and high yield method to access to alkyl azides[103,109–111] (Scheme 4.4).

Scheme 4.4 Classic nucleophilic substitution to synthesize alkyl azides.

Using the same synthetic steps, but starting from substituted organic substrates, primary, secondary and even some tertiary alkyl azides can be prepared by the reaction with azide ion[112].

Aromatic azides, on the other hand, are prepared starting from phenylhydrazine, sodium nitrite and hydrochloric acid[113] (Scheme 4.5).

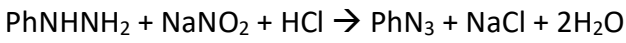

Scheme 4.5 Synthesis of phenyl azide.

The organic azides have been extremely studied in organic chemistry because the -N_3 group can be easily converted into other functional groups: the dipolar character and relative instability of the azide group can activate it towards different reactions path, in relation to the molecular structure, the reagents and the experimental conditions. Some of the most important types of reactions of organic azides are described in the following[114].

Organic azides can undergo either electrophilic attack on the α-nitrogen atom or nucleophilic attack on the terminal nitrogen atom (Scheme 4.6).

Scheme 4.6 On the left electrophilic attack on the azide's α-nitrogen atom, on the right nucleophilic attack on the azide's terminal nitrogen atom.

Also organic azides can be subjected to redox reaction. The reduction of the –N_3 group can be conducted catalytically, usually with H_2/Pd, but it is preferable to use alternative reagents, like lithium aluminium hydride ($LiAlH_4$) which is highly selective for the reduction of the azidic group[106] as shown in Scheme 4.7:

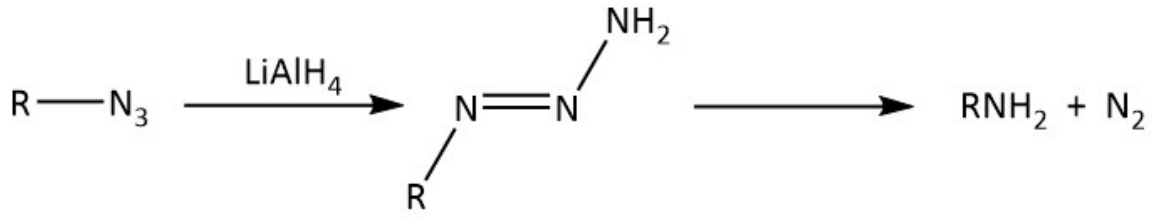

Scheme 4.7 Azide undergo a redox reaction.

Another deeply studied reaction in organic chemistry is the decomposition of azides with formation of a nitrene species. An example of this kind of reactions is that studied by Curtius[115] in 1980 that involves the final formation of a primary amine by decomposition, rearrangement and subsequent hydration of carboxylic azides. A general scheme of the reaction is described in Scheme 4.8:

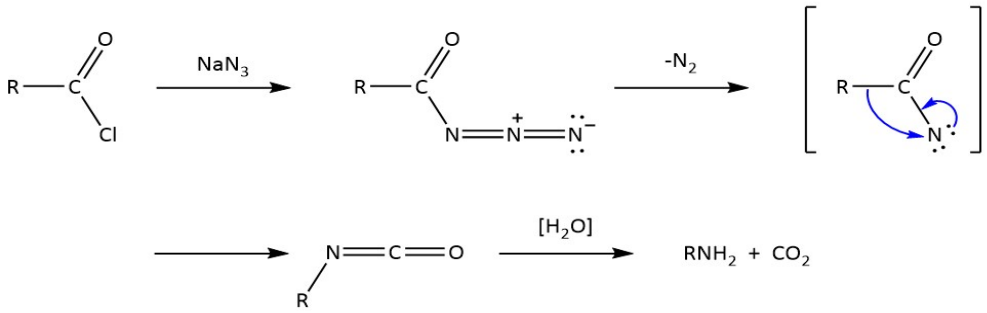

Scheme 4.8 Curtius rearrangement.

It is also possible to obtain amides with a similar mechanism through the reaction of Schmidt[116], but using hydrogen azide as starting material and acid condition, according to the following Scheme 4.9:

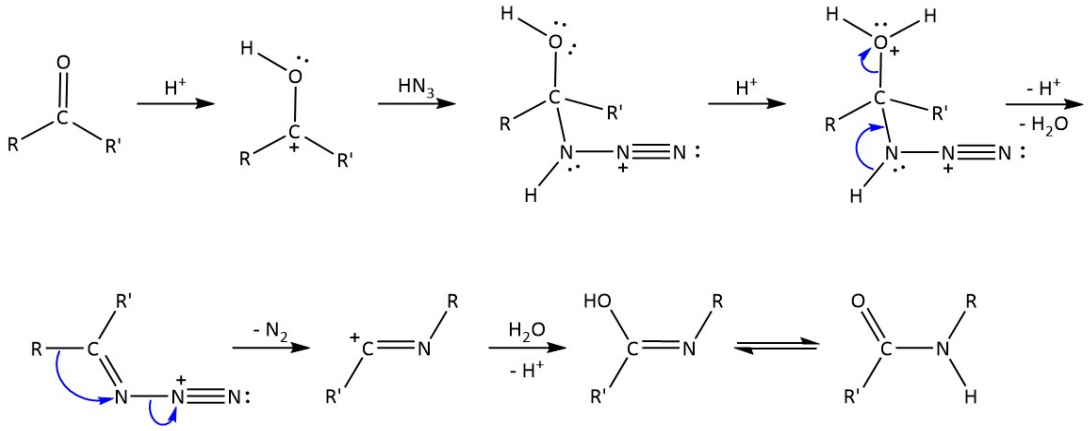

Scheme 4.9 Schmidt reaction.

The azide group can also be used to synthesize imines. This can occur, for example, thanks to the action of strong acids on aliphatic azides, causing the migration of either a hydrogen or an alkyl group on nitrogen, giving the corresponding aldimines or ketimines, Scheme 4.10.

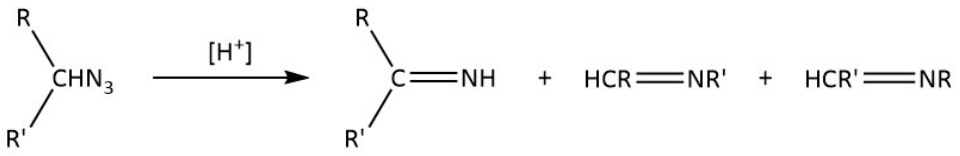

Scheme 4.10 Formation of imines from azides.

4.3 Inorganic Chemistry

In coordination chemistry, azido complexes wherein azide ions are coordinated to metal sites have been known since long time[117]. The azide ion was found in terminal as well as in bridging coordination geometries. It is well established in the literature that the stability of such compounds decreases with an increase of the covalence of the M-N_3 bond and with an increasing M/N_3 ratio. Systems of the type $M(N_3)_x$ usually decompose under formation of dinitrogen and elemental M.

The terminal nitrogen atom of organic azides (RN_3) provide a more directed electron pair for the coordination of the Lewis acid (Figure 4.1).

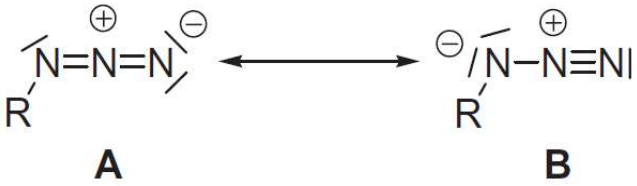

Figure 4.1 Lewis's structure for azide.

However, transition metal sites not only possess Lewis acidic properties, they are often redox active too. Metal compounds in low and middle oxidation states can deliver electrons to substrates like organoazides. By a formal two electron reduction, $[RN_3]^{2-}$ dianions are generated, which again can be described by at least two mesomeric forms (Figure 4.2) and which should be stabilized due to the presence of electronegative nitrogen atoms.

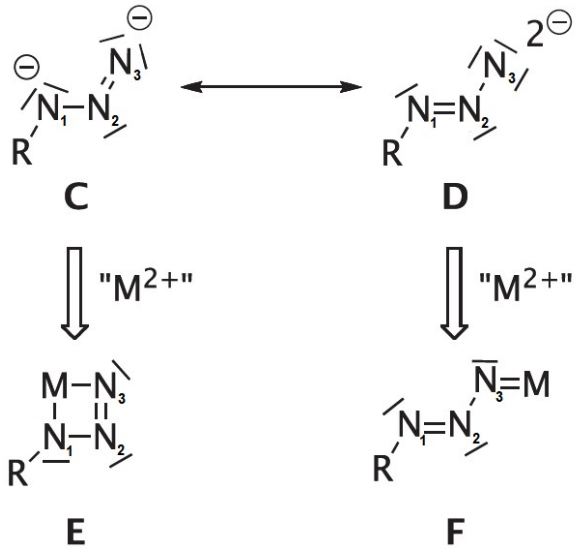

Figure 4.2 Coordination mode for organoazides.

Obviously, such species can act either as bidentate ligands including the nitrogen atoms N_1 and N_3 as two electron donor sites (structures **C** and **E**) in a triazametallacyclobutene type structure, or as a monodentate ligand (structures **D** and **F**) wherein the terminal nitrogen atom N_3 acts as a four-electron donating site. The latter coordination mode is preferentially realized with high valent transition metal centres. The triazametallacyclobutene type structure **E** will have a destabilizing effect on the N_1- N_2 bond and can also be considered as a transition state in the description of the metal mediated decomposition of organoazides by dinitrogen elimination. In the case of high valent transition metal sites, this would lead to the formation of a stable imido complex, being this reaction strongly exothermic due to the formation of highly stable dinitrogen. Therefore, if the η^2-coordination of the organoazide (structure **E**) is of relevance on the reaction pathway of the azide decomposition. Examples of this kind of chemistry were reported by Cummins and Floriani. The former in 1995 published a vanadium(III) precursor and mesityl azide leading to a vanadium(V) diazenylimido complex, which loses dinitrogen already at room temperature[118], while the latter, just a few years later, described the reaction between a tungsten(IV) calixarene system and phenyl azide giving under oxidation to tungsten(VI) the corresponding diazenylimido complex, which again loses dinitrogen[119].

In literature are reported some studies where is pointed out that in most cases the best way to prevent the decomposition of the azide in the presence of a transition metal is to avoid a free coordination site on the metal centre. However, while inhibiting a metal mediated decomposition of an organoazide can be realized by hindering any interaction between the N_3 unit and the metal site, it also know that the coordination of the organoazide will not necessary lead to decomposition of the ligand: in 1995 Bergman[120,121] described the first structurally characterized bent organoazide complex of tantalum(III), $Cp_2Ta(CH_3)(PMe_3)(N_3R)$, while in 1998 Thiel[122] published the firsts structurally characterized linear organoazides coordinated to palladium(II) and copper(II). In this last two complexes both elements are known among others to be efficient catalysts for the decomposition of organoazides[123–125]. The solid-state structures of these compounds are shown in Figure 4.3.

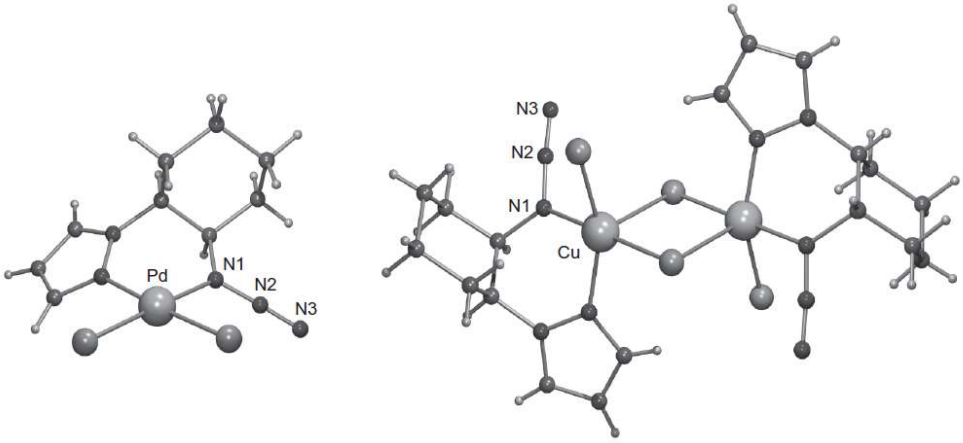

Figure 4.3 Solid state structures of (cis -2 azidopyrazol -1- ylcyclohexane)dichloridopalladium(II) and di(cis-2 -azidopyrazol-1-ylcyclohexane)(chlorido)(μ-chlorido)copper(II).

While the copper(II) complex is completely stable in the solid state and in solution, the palladium(II) compound decomposes slowly in dichloromethane solution to give the corresponding complex with an amine -NH_2 function. The azide unit of the palladium complex is still capable of undergoing slow [2+3]-cycloaddition with EtOOC-C≡C-COOEt to yield the corresponding triazole. However, it is not yet clear whether this is due to decoordination of the azide ligand in solution or if the reaction takes place while the ligand is still coordinated.

Due to the reactive nature of organoazides, a series of reactions concerning an attack at a metal coordinated ligand are known. Especially carbonyl complexes have been investigated for their reactivity with compounds of the type R-N_3. In most of these cases, a transfer of two electrons from the metal site to the organoazide will not lead to a stable diazenylimido complex but subsequent transformations will occur. One of the main routes of reactivity is the evolution of dinitrogen under primary formation of a coordinated nitrene species. For low valent transition metal sites such systems are instable in most cases, which may result in the typical nitrene type of reactivity. However, if the transition metal site has the chance to reach a stable oxidation state, carbonyl ligands can be included into the organoazide attack.

However the most important and studied reactions with azides, catalysed by transition metals, are the cycloaddition reactions that leads to a remarkably wide variety of five-membered heterocyclic compounds[69], like triazoles and tetrazoles. The history of 1,3-dipoles began in the nineteenth century: in 1963, Huisgen published a systematic study on the concerted 1,3-dipolar cycloaddition as well as kinetic studies on the mechanism[126]. The Huisgen reaction, also known as Copper-Catalysed Azide-Alkyne Cycloaddition (CuAAC)[103,127], produces only 1,4-and can be performed in aqueous systems. The proposed mechanism of the CuAAC[128] reaction outlined in

Scheme 4.11 is based on several investigations, but has not yet been fully tested. Some details, especially those concerning the complexation of the Cu(I) species and the origin of the selectivity of the cycloaddition, are still unknown.

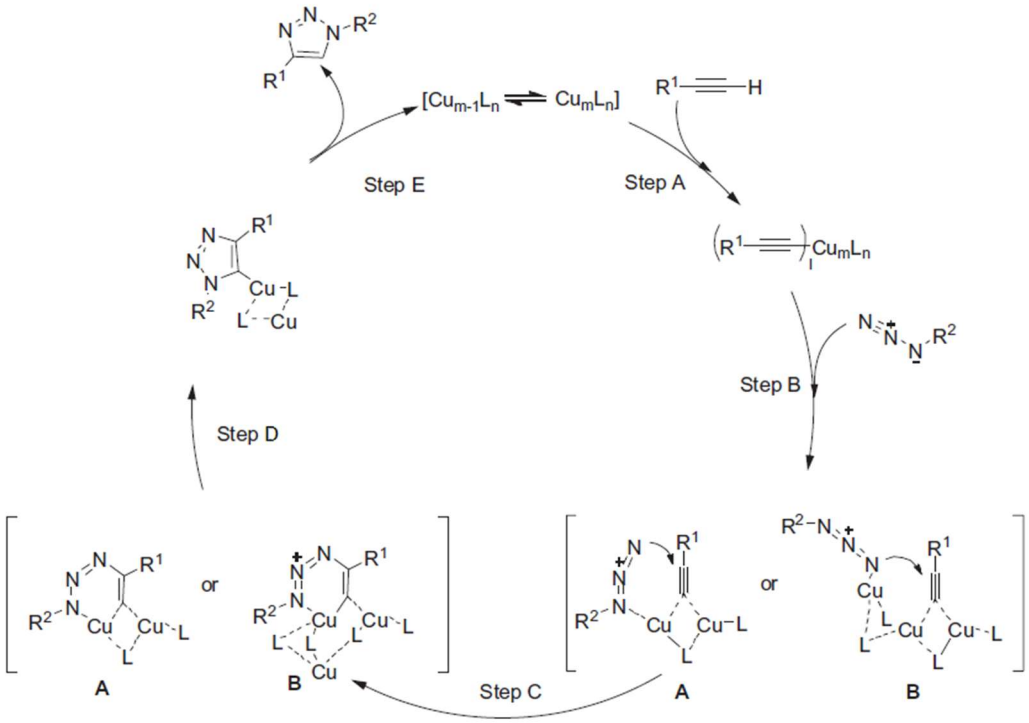

Scheme 4.11 Proposed mechanism for CuAAC reaction.

The azide-alkyne cycloaddition is highly relevant for biological applications. However, in vivo applications are limited by the toxicity of copper ions for living organisms.

The great demand of metal-free Click reactions for in vivo studies has been an immense challenge. Thus, though metal-free strategies have been developed, the reactions are not regioselective, very slow and require higher temperatures in the absence of transition metals. Another way studied to eliminate the copper ion for Click reaction in vivo application is the use of ruthenium complexes as catalytic agent. The Ruthenium-Catalysed Azide-Alkyne Cycloaddition (RuAAC) complements the well-established CuAAC reaction, as the formation of 1,5-substituted triazoles can be achieved with high regioselectivity. In contrast to the CuAAC reaction, triazoles that are synthesized via RuAAC reaction can be formed from terminal as well as internal alkynes. This offers the possibility of the formation of fully-substituted triazoles.

There are other characteristic properties that must be considered concerning the RuAAC reaction. For example, many aprotic solvents like THF or toluene can be used for RuAAC, but protic

solvents such as MeOH result in reduced yields and the formation of side products. To current knowledge, the RuAAC is not sensible to the presence of atmospheric oxygen and reactions can be carried out between room temperature and 110 °C.

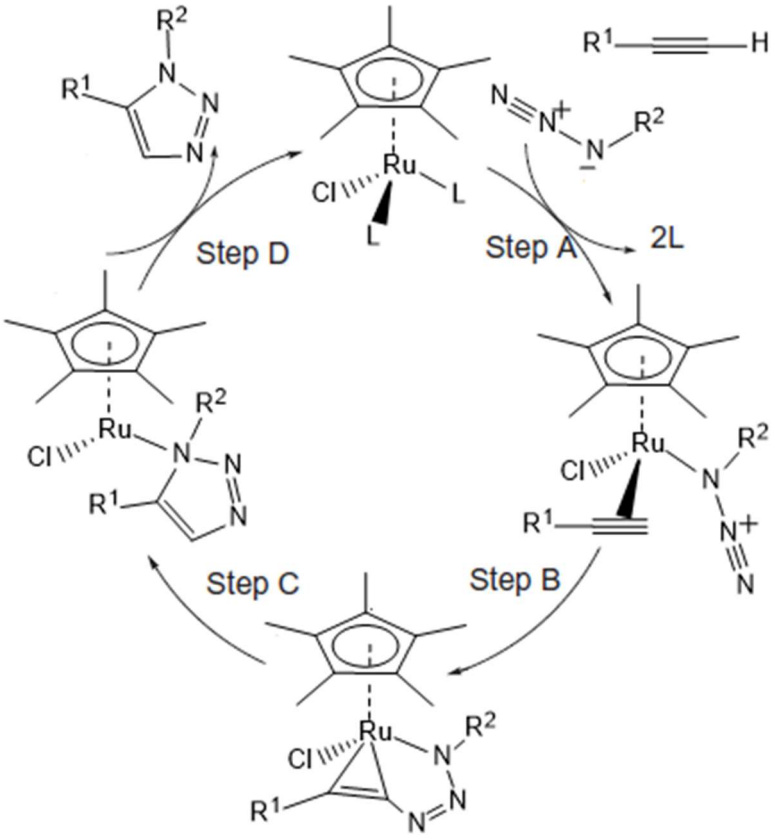

Scheme 4.12 Proposed mechanism for the RuAAC-reaction

The mechanism of the RuAAC reaction has been investigated by several groups and is summarized in Scheme 4.12 [129–132]. The proposed catalytic cycle includes the formation of the catalytically active species [Cp*RuCl] and the formal substitution of the spectator ligands by both the alkyne and the azide (Step A). After oxidative coupling of the alkyne and the azide (Step B), the intermediate species undergoes reductive elimination (Step C) and releases the aromatic triazole product (Step D).

The choice of Ru(II) catalyst is of crucial importance for the success of the RuAAC reaction. Up until now, Ru(II) catalysts bearing a η^5-pentamethylcyclopentadienyl ligand are the only catalytic systems that show high selectivity as well as excellent yields. It has been suggested that the presence of the electron rich Cp* ligand is irreplaceable within the ruthenium catalyst. This high activity of the Cp*RuCl catalysts may also depend on the lability of the bystander ligands in those complexes that enable the formation of the intermediate where both the alkyne and the

azide are coordinated to the metal centre and on the sterically-demanding nature of Cp*, facilitating the reductive elimination in the catalytic cycle.

An interesting feature of RuAAC reactions is that the success and reaction rate are nearly unaffected by the substituents of the alkyne, but strongly dependent on the nature of the azides. Cycloadditions of primary azides result in high yields, whereas secondary azides react more slowly and produce lower yields and tertiary azides are hardly clickable. The RuAAC reaction has been applied to the synthesis of a variety of other substrates.

To date, there is only one investigation concerning metals beyond ruthenium and copper that may catalyse triazole formation through an AAC reaction with palladium, platinum and nickel.

AIM OF THE PHD THESIS

The research group in which I held my doctoral thesis has a long-standing interest in the chemistry of azo-complexes of transition metals and has reported in the last years the synthesis and reactivity of hydrazine, diazene aryldiazenido and diazoalkane complexes of manganese and iron triad with several π-acceptor ligands. The interesting results obtained in these studies prompted us to extend our research to pentamethylcyclopentadienyl derivatives of various metals and, on the other hand, new "azo" ligand such as azines and organic azides.

The aim of these studies was to deepen the coordination chemistry of these ligands, the results of which are rather scarce in the literature, and to understand how the nature of the metal fragment could change the proprieties of the organic "azo" group.

In particular, the aim of my PhD research was to choose appropriate metal fragments of Ru, Os, Rh and Ir able to allow the preparation of azine, diazoalkane and organic azide complexes and then study their reactivity with the perspective of highlighting novel chemical proprieties.

The full characterization (spectroscopic and crystallographic) of all the prepared compounds completes my thesis work.

SYNTHESIS OF COMPLEXES

6.1 Materials and Physical Measurements.

All synthetic work was carried out in appropriate atmosphere (Ar, N_2) using standard Schlenk techniques or in an inert atmosphere dry-box. Once isolated, the complexes were relatively stable in air, but even so, they were stored under nitrogen at −25 °C. All solvents were dried over appropriate drying agents, degassed on a vacuum line, and distilled into vacuum-tight storage flasks. $RuCl_3 \bullet 3H_2O$, OsO_4, $RhCl_3 \bullet 3H_2O$ and $IrCl_3 \bullet 3H_2O$ were a Pressure Chemical Co. (USA) product, used as received. Phosphites $P(OMe)_3$ and $P(OEt)_3$ were Aldrich products, purified by distillation under argon; phenyldiethoxyphosphine $PPh(OEt)_2$ was prepared by the method reported in literature by Rabinowitz and Pellon[133]; azines[134–137], diazoalkanes[138,139], benzyl[111] and phenyl[113] azides were prepared following methods reported in literature. The labelled benzylazides 4-$CH_3C_6H_4CH_2{}^{15}N_3$ and $C_6H_5CH(CH_3){}^{15}N_3$ were prepared[140] by reacting Na[^{15}NNN] (98% enriched, CIL) with either 4-methylbenzylbromide 4-$CH_3C_6H_4CH_2Br$ or 1-bromoethyl)benzene $C_6H_5CH(CH_3)Br$. Equimolar mixtures of both 4-$CH_3C_6H_4$-$CH_2{}^{15}$NNN and 4-$CH_3C_6H_4CH_2NN{}^{15}N$ and of both $C_6H_5CH(CH_3){}^{15}$NNN and $C_6H_5CH(CH_3)NN{}^{15}N$ were obtained. Other reagents were purchased from commercial sources in the highest available purity and used as received. Infrared spectra were recorded on a Perkin-Elmer Spectrum-One FT-IR spectrophotometer. NMR spectra (^{1}H, ^{13}C, ^{31}P) were obtained on AVANCE 300 Bruker or AVANCE III 400 spectrometers at temperatures between -90 and +25 °C, unless otherwise noted. ^{1}H and ^{13}C spectra are referred to internal tetramethylsilane. $^{31}P\{^1H\}$ chemical shifts are reported with respect to 85% H_3PO_4 whereas ^{15}N shifts with respect to $CH_3{}^{15}NO_2$; in both cases, downfield, shifts are considered positive. COSY, HMQC and HMBC NMR experiments were performed with standard programs. The *i*NMR software package (G. Balacco, http://www.inmr.net/) was used to treat NMR data. Absorption spectra were collected for CH_2Cl_2 solutions of the complexes using a Perkin-Elmer Lambda 40 spectrophotometer. Emission (PL) spectra of solid samples and dichloromethane solutions were recorded at room temperature in the range 420–1035 nm with an OceanOptics Flame-T spectrometer coupled with an optical fiber, a collimating lens and a longpass filter, using UV led (280–375 nm) and laser (405 nm) sources for excitation. Quantum yields (FP) were estimated using $[Ru(bpy)_3]Cl_2$ as standard (ϕ_P = 9.4 ± 0.3%)[141]. Emission lifetime measurements were carried out on solid samples at room temperature, using the third harmonic of a pulsed Nd:YAG laser (355 nm) as excitation source. Emitted photons were detected with a photomultiplier tube

(Hamamatsu R928) coupled to a Cinel 25 monochromator. Emission decay curves were recorded using a Tektronix TDS3032 oscilloscope. The conductivity of 10^{-3} mol·dm^{-3} solutions of the complexes in CH_3NO_2 at 25 °C was measured on a Radiometer CDM 83. Elemental analyses were determined in the Microanalytical Laboratory of the Dipartimento di Scienze del Farmaco, University of Padova (Italy) and in the Departamento de Química Inorgánica, Universidade de Vigo (Spain). All crystallographic data were collected at CACTI (University of Vigo) at 100 K (CryoStream 800) using a Bruker D8 Venture Photon 100 CMOS detector and Mo-Kα radiation (λ = 0.71073 Å) generated by an Incoatec high brilliance IμS microsource. The software APEX3 was used for collecting frames of data, indexing reflections, and the determination of lattice parameters, SAINT for integration of intensity of reflections, and SADABS for scaling and empirical absorption correction. Further crystallographic treatment was performed with the Oscail program[142]. The structure was solved by using the SHELXT program[143] and refined by a full-matrix least-squares based on F^2, SHELXL program[144]. Non-hydrogen atoms were refined with anisotropic displacement parameters. Hydrogen atoms were included in idealized positions and refined with isotropic displacement parameters.

6.2 Preparation of Precursors of Ruthenium

Dimeric $[RuCl_2(\eta^6\text{-}p\text{-cymene})]_2$ and monomeric complexes $RuCl_2(\eta^6\text{-}p\text{-cymene})L$ [L = $P(OMe)_3$, $P(OEt)_3$, $PPh(OEt)_2$, P^iPr_3], and $[RuCl(\eta^5\text{-}C_5H_5)(PPh_3)\{P(OR)_3\}]$ were prepared following the methods previously reported in literature[145–147].

- **$RuCl_2(\eta^6\text{-}p\text{-cymene})L$**

In a 50 mL one-necked round-bottomed flask an excess of the appropriate phosphite or phosphine (3.5 mmol) was added to a solution of the dimeric complex $[RuCl(\mu\text{-}Cl)(\eta^6\text{-}p\text{-cymene})]_2$ (0.7 mmol) in CH_2Cl_2 (10 mL) and the reaction mixture was stirred at room temperature for 3 h. The solvent was removed under reduced pressure to give an oil which was triturated with *n*-hexane (10 mL). A yellow solid slowly separated out which was filtered and crystallized from dichloromethane and hexane. Yield: 90%.

- **[RuCl(η^5-C_5H_5)(PPh_3)$_2$]**

The reaction was carried out in a 2 L, two-neck, round-bottom flask equipped with a 500 mL dropping funnel and a reflux condenser topped with a nitrogen bypass. Triphenylphosphine (21.00 g, 80 mmol) was dissolved in 1 L of ethanol by heating. Hydrated ruthenium trichloride (5.0 g, 20 mmol) is dissolved in ethanol (100 mL), the dissolution was favoured by heating the mixture, and then allowing the solution to cool. Freshly distilled cyclopentadiene (10 mL, 8.0 g, 120 mmol) was added to the ruthenium trichloride solution, and the mixture is transferred to the dropping funnel. The dark-brown solution was then added to the triphenylphosphine solution over a period of 10 minutes while maintaining the temperature at the reflux point. After the ruthenium trichloride/cyclopentadiene solution has been added, the mixture has a dark-brown colour, which after 1 hour has lightened to a dark red-orange. The orange crystals were filtered and dried under vacuum. Yield: 90-95%.

- **[RuCl(η^5-C_5H_5)(PPh_3){$P(OR)_3$}]**

In a 100 mL three-necked round-bottomed flask equipped with a reflux condenser and nitrogen bypass were placed 1.7 g [RuCl(η^5-C_5H_5)(PPh_3)$_2$] (2.34 mmol), an excess of the appropriate phosphite (14 mmol) and 50 mL of benzene. The reaction mixture was stirred at reflux temperature for 3 h. The solvent was then removed under reduced pressure to give an oil which was triturated with EtOH (3 mL). A yellow solid slowly separated out which was filtered and washed with EtOH. Yield: 85%.

6.3 Preparation of New Complexes: Azines of Ruthenium.

[RuCl(η^6-*p*-cymene){κ^1-[N=C(H)R]–N=C(H)R}L]BPh_4 (1–3)
[L = $P(OMe)_3$ (1), $P(OEt)_3$ (2), $PPh(OEt)_2$ (3); R = Ph (a), C_2H_5 (d)].

In a 25 mL three-necked round-bottomed flask were placed solid samples of the appropriate chloro complex $RuCl_2$(η^6-*p*-cymene)L (0.2 mmol), an excess of azine R(H)C=N–N=C(H)R (0.8 mmol), an excess of $NaBPh_4$ (0.4 mmol, 137 mg), 5 mL of ethanol and 5 of dichloromethane. The reaction mixture was stirred at room temperature for 24 h and then the solvent was removed under reduced pressure to give an oil, which was triturated with 1 mL of ethanol. A yellow solid slowly separated out, which was filtered and crystallised from CH_2Cl_2 and EtOH. Yield ≥65%.

1a: ^{1}H NMR (CD_2Cl_2, 20 °C) δ: 8.54 (s, 1H, =CH), 7.92 (s, 1H, κ^1 =CH), 7.71–6.80 (m, 30H, Ph), 5.82, 5.69, 5.44, 5.39 (d, 4H, Ph *p*-cym), 3.75 (d, 9H, CH_3 phos), 2.83 (m, 1H, CH ^{i}Pr), 2.05 (s, 3H, *p*-CH_3 *p*-cym), 1.27, 1.24 (d, 6H, CH_3 ^{i}Pr); ^{31}P{^{1}H} NMR (CD_2Cl_2, 20 °C) δ: A, 118.2 (s); Anal. Calcd. for $C_{51}H_{55}BClN_2O_3PRu$ (922.30): C, 66.41; H, 6.01; Cl, 3.84; N, 3.04; Found: C, 66.27; H, 6.13; Cl, 3.70; N, 3.12%; Λ_M = 52.9 $\Omega^{-1}mol^{-1}cm^2$.

1d: IR (KBr, cm^{-1}) $\nu_{C=N}$ 1630 (m); ^{1}H NMR (CD_2Cl_2, 20 °C) δ: 7.71 (t, 1H, =CH), 7.33–6.85 (m, 20H, Ph), 7.15 (t, 1H, κ^1 =CH), 5.74, 5.61, 5.33 (d, 4H, Ph *p*-cym), 3.74 (d, 9H, CH_3 phos), 2.77 (m, 1H, CH ^{i}Pr), 2.40 (m, 4H, CH_2), 2.06 (s, 3H, *p*-CH_3 *p*-cym), 1.25 (d, 6H, CH_3 ^{i}Pr), 1.17, 1.08 (t, 6H, CH_3 EtC=); ^{31}P{^{1}H} NMR (CD_2Cl_2, 20 °C) δ: A, 117.8 (s); Anal. Calcd. for $C_{43}H_{55}BClN_2O_3PRu$ (826.22): C, 62.51; H, 6.71; Cl, 4.29; N, 3.39; Found: C, 62.35; H, 6.62; Cl, 4.40; N, 3.28%; Λ_M =51.6 $\Omega^{-1}mol^{-1}cm^2$.

2a: IR (KBr, cm^{-1}) $\nu_{C=N}$ 1603 (m); ^{1}H NMR (CD_2Cl_2, 20 °C) δ: 8.54 (s, 1H, =CH), 7.98 (s, 1H, κ^1 =CH), 7.78–6.86 (m, 30H, Ph), 5.83, 5.69, 5.41, 5.28 (d, 4H, Ph *p*-cym), 4.12 (m, 6H, CH_2), 2.85 (m, 1H, CH ^{i}Pr), 2.06 (s, 3H, *p*-CH_3 *p*-cym), 1.27 (t, 9H, CH_3 phos), 1.27, 1.25 (d, 6H, CH_3 ^{i}Pr); ^{31}P{^{1}H} NMR (CD_2Cl_2, 20 °C) δ: A, 113.7 (s); ^{13}C{^{1}H} NMR (CD_2Cl_2, 20 °C) δ: 165–121 (m, Ph), 164.49 (s, C=N), 160.62 (s, κ^1-N=C), 121.1 (d, C4 *p*-cym), 103.41 (s, C1 *p*-cym), 91.24, 91.03 (d), 89.92, 84.75 (s) (Ph *p*-cym), 64.72 (d, CH_2), 31.43 (s, CH ^{i}Pr), 22.49, 21.49 (s, CH_3 ^{i}Pr), 18.64 (s, *p*-CH_3 *p*-cym), 16.36 (d, CH_3 phos); Anal. Calcd. for $C_{54}H_{61}BClN_2O_3PRu$ (964.38): C, 67.25; H, 6.38; Cl, 3.68; N, 2.90; Found: C, 67.07; H, 6.25; Cl, 3.81; N, 2.83%; Λ_M = 52.4 $\Omega^{-1}mol^{-1}cm^2$.

2d: IR (KBr, cm^{-1}) $\nu_{C=N}$ 1630 (m); ^{1}H NMR (CD_2Cl_2, 20 °C) δ: 7.73 (t, 1H, =CH), 7.31–6.89 (m, 20H, Ph), 7.24 (s, 1H, κ^1 =CH), 5.74, 5.62, 5.31, 5.27 (d, 4H, Ph *p*-cym), 4.08 (m, 6H, CH_2 phos), 2.80 (m, 1H, CH ^{i}Pr), 2.41 (m, 4H, CH_2 EtC=), 2.08 (s, 3H, *p*-CH_3 *p*-cym), 1.32 (d, 6H, CH_3 ^{i}Pr), 1.30 (t, 9H, CH_3 phos), 1.19 (t, 6H, CH_3 EtC=); ^{31}P{^{1}H} NMR (CD_2Cl_2, 20 °C) δ: A, 113.4 (s); Anal. Calcd. for $C_{46}H_{61}BClN_2O_3PRu$ (868.30): C, 63.63; H, 7.08; Cl, 4.08; N, 3.23; Found: C, 63.44; H, 7.17; Cl, 3.95; N, 3.32%; Λ_M = 52.1 $\Omega^{-1}mol^{-1}cm^2$.

3a: IR (KBr, cm^{-1}) $\nu_{C=N}$ 1602 (m); ^{1}H NMR (CD_2Cl_2, 20 °C) δ: 8.21 (s, 1H, =CH), 7.77 (s, 1H, κ^1 =CH), 7.75–6.85 (m, 35H, Ph), 5.76, 5.58, 5.17, 5.11 (d, 4H, Ph *p*-cym), 4.09 (m, 4H, CH_2 phos), 2.79 (m, 1H, CH ^{i}Pr), 2.01 (s, 3H, *p*-CH_3 *p*-cym), 1.37 (t, 6H, CH_3 phos), 1.25, 1.19 (d, 6H, CH_3 ^{i}Pr); ^{31}P{^{1}H} NMR (CD_2Cl_2, 20 °C) δ: A, 142.23 (s); Anal. Calcd. for $C_{58}H_{61}BClN_2O_2PRu$ (996.42): C, 69.91; H, 6.17; Cl, 3.56; N, 2.81; Found: C, 69.72; H, 6.26; Cl, 3.44; N, 2.87%; Λ_M = 51.8 $\Omega^{-1}mol^{-1}cm^2$.

[RuCl(η^6-*p*-cymene){κ^1-[N=C(H)4-$CH_3C_6H_4$]–N=C(H)4-$CH_3C_6H_4$}{P(OMe)$_3$}]BPh$_4$ (1b)
[RuCl(η^6-*p*-cymene){κ^1-[N=C(H)4-$CH_3OC_6H_4$]–N=C(H)4-$CH_3OC_6H_4$}{P(OEt)$_3$}]BPh$_4$ (2c)

In a 25 mL three-necked round-bottomed flask were placed solid samples of the appropriate chloro complex $RuCl_2$(η^6-*p*-cymene)L (0.2 mmol), an excess of azine R(H)C=N–N=C(H)R (0.6 mmol), an excess of $NaBPh_4$ (0.4 mmol, 137 mg), 5 mL of ethanol and 10 of dichloromethane. The reaction mixture was stirred at room temperature for 48 h and then the solvent was removed under reduced pressure. The complex was extracted from the obtained solid with three 5 mL portions of ethanol. The extracts were evaporated to dryness to leave an oil, which was triturated with 1 mL of ethanol. The yellow solid which slowly separated out was filtered and crystallised from CH_2Cl_2 and EtOH. Yield ≥ 55%.

1b: ^{1}H NMR (CD_2Cl_2, 20 °C) δ: 8.47 (s, 1H, =CH), 7.91 (s, 1H, κ^1 =CH), 7.75–6.87 (m, 28H, Ph), 5.84, 5.71, 5.47, 5.38 (d, 4H, Ph *p*-cym), 3.76 (d, 9H, CH_3 phos), 2.84 (m, 1H, CH ^{i}Pr), 2.48 (s, 3H, CH_3 *p*-tolyl), 2.07 (s, 3H, *p*-CH_3 *p*-cym), 1.27 (d, 6H, CH_3 ^{i}Pr); ^{31}P{^{1}H} NMR (CD_2Cl_2, 20 °C) δ: A, 117.2 (s); Anal. Calcd. for $C_{53}H_{59}BClN_2O_3PRu$ (950.35): C, 66.98; H, 6.26; Cl, 3.73; N, 2.95; Found: C, 66.76; H, 6.35; Cl, 3.60; N, 3.03%; Λ_M = 53.3 $\Omega^{-1}mol^{-1}cm^2$.

2c: ^{1}H NMR (CD_2Cl_2, 20 °C) δ: 8.44 (s, 1H, =CH), 8.03 (s, 1H, κ^1 =CH), 7.81–6.87 (m, 28H, Ph), 5.82, 5.70, 5.41, 5.30 (d, 4H, Ph *p*-cym), 4.10 (m, 6H, CH_2), 3.90, 3.84 (s, 3H, *p*-CH_3O), 2.85 (m, 1H, CH ^{i}Pr), 2.09 (s, 3H, *p*-CH_3 *p*-cym), 1.28, 1.26 (d, 6H, CH_3 ^{i}Pr), 1.24 (t, 9H, CH_3 phos); ^{31}P{^{1}H} NMR (CD_2Cl_2, 20 °C) δ: A, 113.4 (s); Anal. Calcd. for $C_{56}H_{65}BClN_2O_5PRu$ (1024.43): C, 65.66; H, 6.40; Cl, 3.46; N, 2.73; Found: C, 65.79; H, 6.32; Cl, 3.57; N, 2.66%; Λ_M = 52.5 $\Omega^{-1}mol^{-1}cm^2$.

[RuCl(η^6-*p*-cymene){η^1-[N=C(H)Ph]–N=C(H)Ph}(P^{i}Pr$_3$)]BPh$_4$ (4a)

This complex was prepared like the phosphite compounds **1–3** starting from $RuCl_2$(η^6-*p*-cymene)(P^{i}Pr$_3$), using the azine Ph(H)C=N–N=C(H)Ph as a reagent and a reaction time of 24 h. Yield ≥65%.

^{1}H NMR (CD_2Cl_2, 20 °C) δ: 8.45 (s, 1H, =CH), 7.87–6.86 (m, 30H, Ph), 7.73 (s, 1H, κ^1 =CH), 5.50, 5.46, 5.42, 5.33 (d, 4H, Ph *p*-cym), 2.84 (m, 1H, CH ^{i}Pr *p*-cym), 2.33 (s, 3H, *p*-CH_3 *p*-cym), 2.18 (m, 3H, CH ^{i}Pr phos), 1.28, 1.26 (d, 6H, CH_3 ^{i}Pr *p*-cym), 1.22, 1.16 (d, 18H, CH_3 phos); ^{31}P{^{1}H} NMR (CD_2Cl_2, 20 °C) δ: A, 50.48 (s); Anal. Calcd. for $C_{57}H_{67}BClN_2PRu$ (958.46): C, 71.43; H, 7.05; Cl, 3.70; N, 2.92; Found: C, 71.25; H, 6.97; Cl, 3.82; N, 2.84%; Λ_M = 53.5 $\Omega^{-1}mol^{-1}cm^2$.

[RuCl(η^6-*p*-cymene){$NH_2N=C(CH_3)_2$}L]BPh_4 (5, 6)
[L = $P(OMe)_3$ (5), $P(OEt)_3$ (6)].

An excess of acetone azine $(CH_3)_2C=N–N=C(CH_3)_2$ (0.8 mmol, 107 μL) was added to a solution of the appropriate chloro complex $RuCl_2$(η^6-*p*-cymene)L (0.2 mmol) in 5 mL of ethanol and 5 of dichloromethane containing an excess of $NaBPh_4$ (0.4 mmol, 137 mg). The reaction mixture was stirred at room temperature for 24 h and then the solvent was removed under reduced pressure to give an oil, which was triturated with ethanol (2 mL). A yellow solid slowly separated out, which was filtered and crystallised from CH_2Cl_2 and EtOH. Yield ≥ 75%.

5: IR (KBr, cm^{-1}) ν_{NH} 3278, 3222 (m); δ_{NH2} 1651 (m); ^{1}H NMR (CD_2Cl_2, 20 °C) δ: 7.36–6.89 (m, 20H, Ph), 5.74 (br, 2H, NH_2), 5.62, 5.55, 5.38, 5.15 (d, 4H, Ph *p*-cym), 3.79 (d, 9H, CH_3 phos), 2.77 (m, 1H, CH ^{i}Pr), 2.07 (s, 3H, *p*-CH_3 *p*-cym), 2.06, 1.89 (s, 6H, CH_3C=), 1.27 (d, 6H, CH_3 ^{i}Pr); ^{31}P{^{1}H} NMR (CD_2Cl_2, 20 °C) δ: A, 119.2 (s); ^{13}C{^{1}H} NMR (CD_2Cl_2, 20 °C) δ: 166.10 (s, C=N), 165–122 (m, Ph), 114.42 (d, C1 *p*-cym), 106.41 (s, C4), 91.70 (d), 87.45 (s) (C3/C5), 89.17 (d), 88.42 (s) (C2/C6), 55.49 (d, CH_3 phos), 31.17 (s, CH ^{i}Pr), 25.57, 17.04 (s, *C*H_3C=), 22.26 (d, CH_3 ^{i}Pr), 18.78 (s, *p*-CH_3 *p*-cym); Anal. Calcd. for $C_{40}H_{51}BClN_2O_3PRu$ (786.15): C, 61.11; H, 6.54; Cl, 4.51; N, 3.56; Found: C, 61.32; H, 6.46; Cl, 4.39; N, 3.64%; Λ_M = 51.6 $\Omega^{-1}mol^{-1}cm^2$.

6: IR (KBr, cm^{-1}) ν_{NH} 3350, 3261 (w); δ_{NH2} 1651 (m); ^{1}H NMR (CD_2Cl_2, 20 °C) δ: 7.32–6.88 (m, 20H, Ph), 5.96, 5.85 (br, 2H, NH_2), 5.62, 5.56, 5.36, 5.11 (d, 4H, Ph *p*-cym), 4.15 (qnt, 6H, CH_2), 2.80 (m, 1H, CH ^{i}Pr), 2.08 (s, 3H, *p*-CH_3 *p*-cym), 2.08, 1.92 (s, 6H, CH_3C=), 1.35 (t, 9H, CH_3 phos), 1.24, 1.22 (d, 6H, CH_3 ^{i}Pr); ^{31}P{^{1}H} NMR (CD_2Cl_2, 20 °C) δ: A, 114.7 (s); ^{13}C{^{1}H} NMR (CD_2Cl_2, 20 °C) δ: 166.06 (s, C=N), 165–122 (m, Ph), 113.98 (d, C1 *p*-cym), 106.65 (s, C4), 91.90, 88.83 (d, C3/C5), 88.43, 86.02 (d, C2/C6), 65.12 (d, CH_2), 31.28 (s, CH ^{i}Pr), 25.60, 18.80 (s, *C*H_3C=), 22.34 (d, CH_3 ^{i}Pr), 18.83 (s, *p*-CH_3 *p*-cym), 16.33 (d, CH_3 phos); Anal. Calcd. for $C_{43}H_{57}BClN_2O_5PRu$ (828.23): C, 62.36; H, 6.94; Cl, 4.28; N, 3.38; Found: C, 62.15; H, 7.01; Cl, 4.16; N, 3.44%; Λ_M = 52.1 $\Omega^{-1}mol^{-1}cm^2$.

[RuCl(η^6-*p*-cymene){κ^1-[$N=C(CH_3)_2$]–$N=C(CH_3)_2$}(P^iPr_3)]BPh_4 (7)

This complex was prepared exactly like the related phosphite compounds **5**, **6** by reacting the chloro compound $RuCl_2$(η^6-*p*-cymene)(P^iPr_3) with an excess of acetone azine $(CH_3)_2C=N–N=C(CH_3)_2$, using a reaction time of 24 h. Yield ≥73%.

^{1}H NMR (CD_2Cl_2, 20 °C) δ: 7.39–6.88 (m, 20H, Ph), 5.19, 5.13, 5.05, 4.59 (d, 4H, Ph *p*-cym), 2.81 (m, 1H, CH *p*-cym), 2.61, 2.59 (s, 6H, CH_3C=), 2.20 (m, 3H, CH phos), 1.99 (s, 3H, *p*-CH_3 *p*-cym), 1.70, 1.58 (s, 6H, CH_3C=), 2.18 (m, 3H, CH phos), 1.20 (m, 24H, CH_3 ^{i}Pr); $^{31}P\{^{1}H\}$ NMR (CD_2Cl_2, 20 °C) δ: A, 68.0 (s); Anal. Calcd. for $C_{49}H_{67}BClN_2PRu$ (862.38): C, 68.24; H, 7.83; Cl, 4.11; N, 3.25; Found: C, 68.17; H, 7.90; Cl, 4.02; N, 3.31%; Λ_M = 51.3 $\Omega^{-1}mol^{-1}cm^2$.

[RuCl(η^6-*p*-cymene){κ^1-[N=C(CH_3)Ph]–N=C(H)Ph}L]BPh_4 (8, 9)
[L = $P(OMe)_3$ (8), $P(OEt)_3$ (9)].

In a 25 mL three-necked round-bottomed flask were placed solid samples of the appropriate chloro complex $RuCl_2$(η^6-*p*-cymene)L (0.2 mmol), an excess of azine Ph(CH_3)C=N–N=C(H)Ph (0.6 mmol, 133 mg), an excess of $NaBPh_4$ (0.4 mmol, 137 mg), 5 mL of ethanol and 10 of dichloromethane. The reaction mixture was stirred at room temperature for 24 h and then the solvent was removed under reduced pressure to give an oil from which the complex was extracted with three 5 mL portions of ethanol. The extracts were evaporated to dryness to leave an oil, which was triturated with 2 mL of ethanol. The yellow solid which slowly separated out was filtered and crystallised from CH_2Cl_2 and EtOH. Yield ≥65%.

8: ^{1}H NMR (CD_2Cl_2, 20 °C) δ: 8.40 (s, 1H, =CH), 7.94–6.87 (m, 30H, Ph), 5.89, 5.41 (d, 4H, Ph *p*-cym), 3.75 (d, 9H, CH_3 phos), 2.80 (m, 1H, CH ^{i}Pr), 2.59 (s, 3H, CH_3C=), 2.13 (s, 3H, *p*-CH_3 *p*-cym), 1.25 (d, 6H, CH_3 ^{i}Pr); $^{31}P\{^{1}H\}$ NMR (CD_2Cl_2, 20 °C) δ: A, 118.5 (s); Anal. Calcd. for $C_{52}H_{57}BClN_2O_3PRu$ (936.33): C, 66.70; H, 6.14; Cl, 3.79; N, 2.99; Found: C, 66.61; H, 6.18; Cl, 3.73; N, 3.05%; Λ_M = 52.1 $\Omega^{-1}mol^{-1}cm^2$.

9: ^{1}H NMR (CD_2Cl_2, 20 °C) δ: 8.40 (s, 1H, =CH), 7.45–6.87 (m, 30H, Ph), 5.54, 5.39 (d, 4H, Ph *p*-cym), 4.11 (m, 6H, CH_2), 2.84 (m, 1H, CH ^{i}Pr), 2.50 (s, 3H, CH_3C=), 2.10 (s, 3H, *p*-CH_3 *p*-cym), 1.30 (t, 9H, CH_3 phos), 1.23 (d, 6H, CH_3 ^{i}Pr); $^{31}P\{^{1}H\}$ NMR (CD_2Cl_2, 20 °C) δ: A, 112.7 (s); $^{13}C\{^{1}H\}$ NMR (CD_2Cl_2, 20 °C) δ: 158.06 (s, C=N), 142.62 (s, κ^1-N=C), 137–118 (m, Ph), 108.77, 101.03, 89.71, 89.22 (d, Ph *p*-cym), 63.19 (d, CH_2), 30.77 (s, *C*H_3C=), 30.08 (s, CH ^{i}Pr), 22.11 (s, CH_3 ^{i}Pr), 18.37 (s, *p*-CH_3 *p*-cym), 16.30 (d, CH_3 phos); Anal. Calcd. for $C_{55}H_{63}BClN_2O_3PRu$ (978.41): C, 67.52; H, 6.49; Cl, 3.62; N, 2.86; Found: C, 67.37; H, 6.40; Cl, 3.73; N, 2.74%; Λ_M = 52.8 $\Omega^{-1}mol^{-1}cm^2$.

[Ru(η^5-C_5H_5){κ^1-[N=C(H)R]–N=C(H)R}(PPh_3){$P(OMe)_3$}]BPh_4 (10)
[R = Ph (a), *p*-tolyl (b), C_2H_5 (d)].

In a 25 mL three-necked round-bottomed flask covered with an aluminium foil were placed 103 mg (0.175 mmol) of the chloro complex RuCl(η^5-C_5H_5)(PPh_3)[$P(OMe)_3$], 45 mg (0.175 mmol) of AgOTf and 4 mL of dichloromethane. The reaction mixture was stirred for 24 h and then filtered on paper to remove the AgCl which formed. An excess of the appropriate azine R(H)C=N–N=C(H)R (0.2 mmol) was added to the resulting solution and the mixture stirred for 24 h. The solvent was removed under reduced pressure to give an oil, which was triturated with 2 mL of ethanol containing an excess of $NaBPh_4$ (0.35 mmol, 120 mg). A yellow solid slowly separated out, which was filtered and crystallised from CH_2Cl_2 and EtOH. Yield ≥75%.

10a: IR (KBr, cm^{-1}) $\nu_{C=N}$ 1602 (m); ^{1}H NMR (CD_2Cl_2, 20 °C) δ: 8.66 (s, 1H, =CH), 7.86–6.86 (m, 45H, Ph), 7.47 (s, 1H, κ1 =CH), 4.72 (s, 5H, C_5H_5), 3.59 (d, 9H, CH_3); ^{31}P{^{1}H} NMR (CD_2Cl_2, 20 °C) δ: AB, δ_A 147.12, δ_B 51.85, J_{AB} = 66.8 Hz; ^{13}C{^{1}H} NMR (CD_2Cl_2, 20 °C) δ: 162.2 (s, C=N), 156.03 (s, κ^1-C=N), 136–127 (m, Ph), 83.59 (s, C_5H_5), 53.58 (br, CH_3); Anal. Calcd. for $C_{64}H_{61}BN_2O_3P_2Ru$ (1080.01): C, 71.17; H, 5.69; N, 2.59; Found: C, 71.02; H, 5.77; N, 2.46%; Λ_M = 53.4 $\Omega^{-1}mol^{-1}cm^2$.

10b: IR (KBr, cm^{-1}) $\nu_{C=N}$ 1605 (m); ^{1}H NMR (CD_2Cl_2, 20 °C) δ: 8.60 (s, 1H, =CH), 7.72–6.87 (m, 43H, Ph), 7.45 (s, 1H, κ1 =CH), 4.70 (s, 5H, C_5H_5), 3.58 (d, 9H, CH_3 phos), 2.47 (s, 6H, CH_3 *p*-tolyl); ^{31}P{^{1}H} NMR (CD_2Cl_2, 20 °C) δ: AB, δ_A 147.31, δ_B 51.82, J_{AB} = 68.0 Hz; Anal. Calcd. for $C_{66}H_{65}BN_2O_3P_2Ru$ (1108.06): C, 71.54; H, 5.91; N, 2.53; Found: C, 71.36; H, 6.00; N, 2.44%; Λ_M = 51.6 $\Omega^{-1}mol^{-1}cm^2$.

10d: IR (KBr, cm^{-1}) $\nu_{C=N}$ 1625 (m); ^{1}H NMR (CD_2Cl_2, 20 °C) δ: 6.63 (t, 1H, =CH), 7.42–6.87 (m, 35H, Ph + 1H, κ1 =CH), 4.60 (s, 5H, C_5H_5), 3.55 (d, 9H, CH_3 phos), 2.36 (m, 4H, CH_2), 1.21, 1.20 (t, 6H, CH_3 C_2H_5); ^{31}P{^{1}H} NMR (CD_2Cl_2, 20 °C) δ: AB, δ_A 147.89, δ_B 50.43, J_{AB} = 67.7 Hz; Anal. Calcd. for $C_{56}H_{61}BN_2O_3P_2Ru$ (983.92): C, 68.36; H, 6.25; N, 2.85; Found: C, 68.31; H, 6.34; N, 2.76%; Λ_M = 51.0 $\Omega^{-1}mol^{-1}cm^2$.

[Ru(η^5-C_5H_5){$NH_2N=C(CH_3)_2$}(PPh_3){$P(OMe)_3$}]BPh_4 (11)

In a 25 mL three-necked round-bottomed flask were placed 162 mg (0.28 mmol) of the chloro complex RuCl(η^5-C_5H_5)(PPh_3)[$P(OMe)_3$], an excess of $NaBPh_4$ (0.6 mmol, 205 mg), 5 mL of ethanol, 5 mL of dichloromethane and an excess of acetone azine (0.9 mmol, 120 μL). The reaction mixture

was stirred for 24 h and then the solvent was removed under reduced pressure to give an oil, which was triturated with 2 mL of ethanol. A yellow solid slowly separated out, which was filtered and crystallised from CH_2Cl_2 and EtOH. Yield ≥80%.

IR (KBr, cm^{-1}) ν_{NH} 3300, 3244 (m); δ_{NH2} 1653 (m); ^1H NMR (CD_2Cl_2, 20 °C) δ: 7.55–6.87 (m, 35H, Ph), 5.59, 4.89 (d br, 2H, NH_2), 4.59 (s, 5H, C_5H_5), 3.51 (d, 9H, CH_3 phos), 1.91, 1.64 [s, 6H, $=C(CH_3)_2$]; $^{31}P\{^1H\}$ NMR (CD_2Cl_2, 20 °C) δ: AB, δ_A 148.26, δ_B 55.75, J_{AB} = 65.0 Hz; Anal. Calcd. for $C_{53}H_{57}BN_2O_3P_2Ru$ (943.86): C, 67.44; H, 6.09; N, 2.97; Found: C, 67.26; H, 6.18; N, 2.90%; Λ_M = 51.5 $\Omega^{-1}mol^{-1}cm^2$.

[RuCl(η⁶-*p*-cymene){P(OEt)₃}{P(OMe)₃}]BPh₄ **(12)**

An excess of $P(OMe)_3$ (0.3 mmol, 37 μL) was added to a solution of [RuCl(η⁶-*p*-cymene){κ¹-[N=C(H)Ph]–N=C(H)Ph}{P(OEt)₃}]BPh_4 (**2a**) (0.2 mmol, 193 mg) in 7 mL of dichloromethane, and the reaction mixture was stirred for 24 h. The solvent was removed under reduced pressure giving an oil, which was triturated with 2 mL of ethanol containing $NaBPh_4$ (0.1 mmol, 68 mg). A yellow solid slowly separated out, which was filtered and crystallised from CH_2Cl_2 and EtOH. Yield ≥80%.

^1H NMR (CD_2Cl_2, 20 °C) δ: 7.50–6.87 (m, 20H, Ph), 5.86, 5.84, 5.80 (d, 4H, Ph *p*-cym), 4.16 (qnt, 6H, CH_2), 3.80 [d, 9H, CH_3 $P(OMe)_3$], 2.66 (m, 1H, CH ^{i}Pr), 2.00 (s, 3H, *p*-CH_3 *p*-cym), 1.34 [t, 9H, CH_3 $P(OEt)_3$], 1.21 (d, 6H, CH_3 ^{i}Pr); $^{31}P\{^1H\}$ NMR (CD_2Cl_2, 20 °C) δ: AB, δ_A 123.68, δ_B 117.00, J_{AB} = 121.5 Hz; Anal. Calcd. for $C_{43}H_{58}BClO_6P_2Ru$ (880.20): C, 58.68; H, 6.64; Cl, 4.03; Found: C, 58.81; H, 6.52; Cl, 4.17%; Λ_M = 51.4 $\Omega^{-1}mol^{-1}cm^2$.

[Ru(η⁵-C₅H₅){N₂C(CH₃)₂}(PPh₃){P(OMe)₃}]BPh₄ **(13)**

In a 25 mL three-necked round-bottomed flask were placed solid samples of the hydrazone complex [Ru(η⁵-C_5H_5){$NH_2N=C(CH_3)_2$}(PPh_3){$P(OMe)_3$}]BPh_4 (**11**) (100 mg, 0.11 mmol), an excess of HgO yellow (46 mg, 0.21 mmol), 40 mL of diethylether and 0.2 mL of a saturated solution of KOH in ethanol. The reaction mixture was stirred for 24 h, filtered and then the solvent removed under reduced pressure. The oil obtained was triturated with 1 mL of ethanol giving a yellow solid, which was filtered and crystallised from CH_2Cl_2 and EtOH. Yield ≥55%.

IR (KBr, cm^{-1}) ν_{N2} 1958 (m); ^1H NMR (CD_2Cl_2, 20 °C) δ: 7.58–6.87 (m, 35H, Ph), 4.43 (d, 5H, C_5H_5), 3.46 (d, 9H, CH_3 phos), 1.80, 1.57 (s, 6H, $=CCH_3$); $^{31}P\{^1H\}$ NMR (CD_2Cl_2, 20 °C) δ: AB, δ_A 151.19, δ_B

48.29, J_{AB} = 76.56 Hz; Anal. Calcd. for $C_{53}H_{55}BN_2O_3P_2Ru$ (941.84): C, 67.59; H, 5.89; N, 2.97; Found: C, 67.42; H, 5.97; N, 2.90%; Λ_M = 51.9 $\Omega^{-1}mol^{-1}cm^2$.

6.4 Preparation of Precursors of Osmium.

Compounds $[OsCl_2(\eta^6\text{-}p\text{-cymene})]_2$ and $[OsCl_2(\eta^6\text{-}p\text{-cymene})\{P(OR)_3\}]$ were prepared following the reported methods[38,145,148].

- **$[OsCl_2(\eta^6\text{-}p\text{-cymene})]_2$**

In a 100 mL round-bottomed flask equipped with a reflux condenser were placed 2.00 g of $Na_2[OsCl_6]$ (4.46 mmol), α-phellandrene (10 mL), and absolute ethanol (20 mL). The reaction mixture was stirred at reflux temperature under argon for 100 h. The resulting yellow-orange suspension was vacuum-concentrated to 8 mL and cooled at 0 °C overnight. The solid was filtered off, washed with cold ethanol and diethyl ether, and crystallized from dichloromethane-hexane to give orange-yellow crystals. Yield: 70%.

- **$[OsCl_2(\eta^6\text{-}p\text{-cymene})\{P(OR)_3\}]$**
  [R= Me, Et]

An excess amount of the appropriate phosphite (3.5 mmol) was added to a solution of the dimeric complex $[OsCl_2(\eta^6\text{-}p\text{-cymene})]_2$ (0.7 mmol) in CH_2Cl_2 (10 mL), and the reaction mixture was stirred at room temperature for 3 h. The solvent was removed under reduced pressure to give an oil, which was triturated with *n*-hexane (10 mL). A yellow solid slowly separated out, which was filtered and crystallized from dichloromethane and hexane. Yield: 90 %

6.5 Preparation of New Complexes: Azines of Osmium.

$[OsCl(\eta^6\text{-}p\text{-cymene})\{\kappa^1\text{-}[N=C(H)R1]\text{–}N=C(H)R1\}\{P(OR)_3\}]BPh_4$ (14, 15)
[R = Me (14), Et (15); R1 = Ph (a), 4-$CH_3C_6H_4$ (b), 2,6-$(CH_3)_2C_6H_3$ (f)]

In a 25 mL three-necked round-bottomed flask covered with an aluminium foil were placed 0.18 mmol of the appropriate complex $[OsCl_2(\eta^6\text{-}p\text{-cymene})\{P(OR)_3\}]$, an equimolar amount of AgOTf (0.18 mmol, 46.3 mg) and 5 mL of CH_2Cl_2. The reaction[145,148,149] mixture was stirred for 24 h and then filtered on paper to remove the AgCl formed. A slight excess of the appropriate azine R1C(H)=N–N=C(H)R1 (0.20 mmol) in 3 mL of CH_2Cl_2 was added and the reaction mixture stirred for 4 h. The solvent was removed under reduced pressure to give an oil, which was triturated with

ethanol (1 mL) containing an excess of $NaBPh_4$ (0.36 mmol, 123 mg). A yellow solid slowly separated out, which was filtered and crystallised from CH_2Cl_2 and EtOH. Yield: 80%.

14a: IR (KBr pellet): $\nu_{C=N}$ 1603 (m) cm^{-1}. ^1H NMR (CD_2Cl_2, 25 °C) δ: 8.63 (s, 1H, NN=CH), 7.83 (s, 1H, OsN=CH), 7.76–6.87 (m, 30H, Ph), 5.80, 5.76, 5.58, 5.56 (d, 4H, Ph *p*-cym), 3.72 (d, J_{PH} = 11.2 Hz, 9H, CH_3 phos), 2.76 (m, 1H, CH ^{i}Pr), 2.17 (s, 3H, *p*-CH_3 *p*-cym), 1.27, 1.25 (d, J_{HH} = 6.9 Hz, 6H, CH_3 ^{i}Pr). $^{31}P\{^1H\}$ NMR (CD_2Cl_2, 25 °C) δ: 71.53 (s). Anal. Calcd. for $C_{51}H_{55}BClN_2O_3OsP$ (1011.46): C, 60.56; H, 5.48; Cl, 3.51; N, 2.77; Found: C, 60.38; H, 5.55; Cl, 3.38; N, 2.84%. Λ_M = 52.6 $\Omega^{-1}mol^{-1}cm^2$

15a: IR (KBr pellet): $\nu_{C=N}$ 1618 (m) cm^{-1}. ^1H NMR (CD_2Cl_2, 25 °C) δ: 8.65 (s, 1H, NN=CH), 7.88 (s, 1H, OsN=CH), 7.76–6.86 (m, 30H, Ph), 5.82, 5.79, 5.60, 5.53 (d, 4H, Ph *p*-cym), 4.08 (qnt, 6H, CH_2), 2.77 (m, 1H, CH ^{i}Pr), 2.18 (s, 3H, *p*-CH_3 *p*-cym), 1.28 (d, J_{HH} = 7.0 Hz, 6H, CH_3 ^{i}Pr), 1.25 (t, J_{HH} = 7.0 Hz, 9H, CH_3 phos). $^{31}P\{^1H\}$ NMR (CD_2Cl_2, 25 °C) δ: 67.40 (s). $^{13}C\{^1H\}$ NMR (CD_2Cl_2, 25 °C) δ: 164.21 (s, NN=CH), 161.22 (s, OsN=CH), 165–122 (m, Ph), 114.83 (d, C1 *p*-cym), 97.40 (d, C4 *p*-cym), 83.11, 82.51 (d, C3/C5 *p*-cym), 82.03, 76.15 (d, C2/C6 *p*-cym), 64.40 (d, CH_2), 31.08 (s, CH ^{i}Pr), 22.56, 21.56 (s, CH_3 ^{i}Pr), 18.48 (s, *p*-CH_3 *p*-cym), 16.32 (d, CH_3 phos) ppm. Anal. Calcd. for $C_{54}H_{61}BClN_2O_3OsP$ (1053.54): C, 61.56; H, 5.84; Cl, 3.37; N, 2.66; Found: C, 61.34; H, 5.92; Cl, 3.26; N, 2.73%. Λ_M = 51.4 $\Omega^{-1}mol^{-1}cm^2$.

15b: IR (KBr pellet): $\nu_{C=N}$ 1619 (m) cm^{-1}. ^1H NMR (CD_2Cl_2, 25 °C) δ: 8.58 (s, 1H, NN=CH), 7.87 (s, 1H, OsN=CH), 7.71–6.87 (m, 28H, Ph), 5.80, 5.78, 5.57, 5.52 (d, 4H, Ph *p*-cym), 4.08 (qnt, 6H, CH_2), 2.75 (m, 1H, CH ^{i}Pr), 2.47, 2.40 (s, 6H, CH_3 *p*-tol), 2.19 (s, 3H, *p*-CH_3 *p*-cym), 1.27 (d, J_{HH} = 6.8 Hz, 6H, CH_3 ^{i}Pr), 1.25 (t, J_{HH} = 7.0 Hz, 9H, CH_3 phos). $^{31}P\{^1H\}$ NMR (CD_2Cl_2, 25 °C) δ: 67.21 (s). Anal. Calcd. for $C_{56}H_{65}BClN_2O_3OsP$ (1081.59): C, 62.19; H, 6.06; Cl, 3.28; N, 2.59; Found: C, 62.01; H, 6.13; Cl, 3.17; N, 2.68%. Λ_M = 53.0 $\Omega^{-1}mol^{-1}cm^2$.

15f: IR (KBr pellet): $\nu_{C=N}$ 1615 (m) cm^{-1}. ^1H NMR (CD_2Cl_2, 25 °C) δ: 8.96 (s, 1H, NN=CH), 7.83 (s, 1H, OsN=CH), 7.32–6.87 (m, 26H, Ph), 5.90, 5.76, 5.63, 5.54 (d, 4H, Ph *p*-cym), 4.16 (m, 6H, CH_2), 2.83 (m, 1H, CH ^{i}Pr), 2.54, 2.30, 2.24 (s, 12H, CH_3 *o*-Me_2), 2.21 (s, 3H, *p*-CH_3 *p*-cym), 1.30 (t, J_{HH} = 7.0 Hz, 9H, CH_3 phos), 1.29, 1.24 (d, J_{HH} = 6.9 Hz, 6H, CH_3 ^{i}Pr). $^{31}P\{^1H\}$ NMR (CD_2Cl_2, 25 °C) δ: 65.20 (s). $^{13}C\{^1H\}$ NMR (CD_2Cl_2, 25 °C) δ: 166.90 (s, NN=CH), 158.41 (s, OsN=CH), 165–122 (m, Ph), 115.01 (d, C1 *p*-cym), 98.33 (d, C4 *p*-cym), 82.89, 82.64 (d, C3/C5 *p*-cym), 81.36, 76.42 (d, C2/C6 *p*-cym), 65.04 (d, CH_2), 31.08 (s, CH ^{i}Pr), 22.60, 20.44 (s, CH_3 ^{i}Pr), 21.60, 21.48, 20.44 (s, CH_3 *o*-Me_2), 18.61

(s, *p*-CH_3 *p*-cym), 16.37 (d, CH_3 phos) ppm. Anal. Calcd. for $C_{54}H_{61}BClN_2O_3OsP$ (1053.54): C, 62.78; H, 6.27; Cl, 3.19; N, 2.52; Found: C, 62.54; H, 6.36; Cl, 3.10; N, 2.61%. Λ_M = 51.4 $\Omega^{-1}mol^{-1}cm^2$.

[OsCl(η^6-*p*-cymene){κ^1-[N=C(CH$_3$)$_2$]–N=C(CH$_3$)$_2$}{P(OR)$_3$}]BPh$_4$ (16, 17)
[R = Me (16), Et (17)]

These complexes were prepared exactly like the related aldazine complexes **14**, **15**, using acetone azine $(CH_3)_2C=N–N=C(CH_3)_2$ as a reagent. Yield: 77%.

16: IR (KBr pellet): $\nu_{C=N}$ 1635 (m) cm^{-1}. ^1H NMR (CD_2Cl_2, 25 °C) δ: 7.75–6.87 (m, 20H, Ph), 5.65, 5.63, 5.52, 5.50 (d, 4H, Ph *p*-cym), 3.73 (d, J_{PH} = 11.2 Hz, 9H, CH_3 phos), 2.78 (m, 1H, CH ^{i}Pr), 2.37, 2.30 (s, 6H, N=CCH_3), 2.21 (s, 3H, *p*-CH_3 *p*-cym), 2.06 (s, 6H, free N=CCH_3), 1.23 (d, J_{HH} = 6.9 Hz, 6H, CH_3 ^{i}Pr). $^{31}P\{^1H\}$ NMR (CD_2Cl_2, 25 °C) δ: 73.84 (s). Anal. Calcd. for $C_{43}H_{55}BClN_2O_3OsP$ (915.38): C, 56.42; H, 6.06; Cl, 3.87; N, 3.06; Found: C, 56.27; H, 6.13; Cl, 3.99; N, 3.01%. Λ_M = 52.4 $\Omega^{-1}mol^{-1}cm^2$.

17: IR (KBr pellet): $\nu_{C=N}$ 1639 (m) cm^{-1}. ^1H NMR (CD_2Cl_2, 25 °C) δ: 7.31–6.86 (m, 20H, Ph), 5.83, 5.62, 5.27, 5.25 (d, 4H, Ph *p*-cym), 4.08 (m, 6H, CH_2), 2.73 (m, 1H, CH ^{i}Pr), 2.30, 2.23 (s, 6H, N=CCH_3), 2.10 (s, 3H, *p*-CH_3 *p*-cym), 2.07 (s, 6H, free N=CCH_3), 1.32, 1.23 (d, 6H, CH_3 ^{i}Pr), 1.30 (t, J_{HH} = 7.0 Hz, 9H, CH_3 phos). $^{31}P\{^1H\}$ NMR (CD_2Cl_2, 25 °C) δ: 63.35 (s). Anal. Calcd. for $C_{46}H_{61}BClN_2O_3OsP$ (957.46): C, 57.70; H, 6.42; Cl, 3.70; N, 2.93; Found: C, 57.53; H, 6.29; Cl, 3.58; N, 3.00%. Λ_M = 52.5 $\Omega^{-1}mol^{-1}cm^2$.

[OsCl(η^6-*p*-cymene){NH$_2$N=C(CH$_3$)$_2$}{P(OR)$_3$}]BPh$_4$ (18, 19)
[R = Me (18), Et (19)]

In a 25 mL three-necked round-bottomed flask were placed 0.1 mmol of the appropriate complex [$OsCl_2$(η^6-*p*-cymene){$P(OR)_3$}], an excess of $NaBPh_4$ (0.36 mmol, 123 mg), 10 mL of EtOH and 5 mL of CH_2Cl_2. An excess of acetone azine $(CH_3)_2C=N–N=C(CH_3)_2$ (0.54 mmol, 72 μL) was added to the resulting solution, which was stirred for 24 h. The solvent was removed under reduced pressure to give an oil, which was triturated with ethanol (2 mL). A yellow solid slowly separated out, which was filtered and crystallised from CH_2Cl_2 and EtOH. Yield: 60%.

18: IR (KBr pellet): ν_{NH} 3263, 3206 (m); δ_{NH2} 1647 (m) cm^{-1}. ^1H NMR (CD_2Cl_2, 25 °C) δ: 6.66, 6.23 (d br, 2H, NH_2), 7.35–6.87 (m, 20H, Ph), 5.82, 5.54, 5.30, 4.99 (d, 4H, Ph *p*-cym), 3.53 (d, J_{PH} = 11.2 Hz, 9H, CH_3 phos), 2.46 (m, 1H, CH ^{i}Pr), 2.23, 1.98 [s, 6H, =C$(CH_3)_2$], 2.20 (s, 3H, *p*-CH_3 *p*-cym),

1.14, 1.08 (d, J_{HH} = 6.9 Hz, 6H, CH_3 ^{i}Pr). $^{31}P\{^1H\}$ NMR (CD_2Cl_2, 25 °C) δ: 79.40 (s). Anal. Calcd. for $C_{40}H_{51}BClN_2O_3OsP$ (875.31): C, 54.89; H, 5.87; Cl, 4.05; N, 3.20; Found: C, 54.66; H, 5.82; Cl, 4.14; N, 3.07%. Λ_M = 54.7 $\Omega^{-1}mol^{-1}cm^2$.

19: IR (KBr pellet): ν_{NH} 3255, 3201 (m); $\delta_{C=N}$ 1643 (m) cm^{-1}. ^1H NMR (CD_2Cl_2, 25 °C) δ: 6.69, 6.37 (d br, 2H, NH_2), 7.33–6.87 (m, 20H, Ph), 5.62, 5.59, 5.53, 5.35 (d, 4H, Ph *p*-cym), 4.11 (m, 6H, CH_2), 2.73 (m, 1H, CH ^{i}Pr), 2.15 (s, 3H, *p*-CH_3 *p*-cym), 2.10, 1.92 [s, 6H, =C(CH_3)$_2$], 1.33 (t, J_{HH} = 7.0 Hz, 9H, CH_3 phos), 1.28, 1.22 (d, J_{HH} = 6.9 Hz, 6H, CH_3 ^{i}Pr). $^{31}P\{^1H\}$ NMR (CD_2Cl_2, 25 °C) δ: 68.92 (s). $^{13}C\{^1H\}$ NMR (CD_2Cl_2, 25 °C) δ: 166.93 (s, N=C), 165–122 (m, Ph), 107.16 (d, C1 *p*-cym), 101.71 (d, C4 *p*-cym), 83.94, 80.91 (d, C3/C5 *p*-cym), 79.34, 76.33 (d, C2/C6 *p*-cym), 64.85 (d, CH_2), 30.96 (s, CH ^{i}Pr), 25.33, 18.58 (s, =C(CH_3)$_2$), 22.63, 22.43 (s, CH_3 ^{i}Pr), 17.22 (s, *p*-CH_3 *p*-cym), 16.22 (d, CH_3 phos) ppm. Anal. Calcd. for $C_{43}H_{57}BClN_2O_3OsP$ (917.39): C, 56.30; H, 6.26; Cl, 3.86; N, 3.05; Found: C, 56.14; H, 6.19; Cl, 3.98; N, 2.94%. Λ_M = 53.5 $\Omega^{-1}mol^{-1}cm^2$.

[Os{κ^2-R1C_6H_3C(H)=N-N=C(H)C_6H_4R1}(η^6-*p*-cymene){P(OR)$_3$}]BPh_4 (20, 21)
[R = Me (20), Et (21); R1 = H (a), 4-CH_3 (b)]

In a 25 mL three-necked round-bottomed flask covered with an aluminium foil were placed 0.18 mmol of the appropriate complex [$OsCl_2$(η^6-*p*-cymene){P(OR)$_3$}], two equivalents of AgOTf (0.36 mmol, 93 mg) and 10 mL of CH_2Cl_2, and the resulting solution was stirred for 24 h. After filtration on paper to remove the AgCl formed, an excess of the appropriate azine R1C_6H_4C(H)=N–N=C(H)C_6H_4R1 (0.36 mmol) in 5 mL of CH_2Cl_2 was added and the resulting solution was stirred for 20 h. The solvent was removed under reduced pressure to give an oil, which was triturated with ethanol (2 mL) containing an excess of $NaBPh_4$ (0.36 mmol, 123 mg). A yellow solid slowly separated out, which was filtered and crystallised from CH_2Cl_2 and EtOH. Yield: 75%.

20a: IR (KBr pellet): $\nu_{C=N}$ 1614 (m) cm^{-1}. ^1H NMR (CD_2Cl_2, 25°C) δ: 8.88 (d, J_{PH} = 2.65 Hz, 1H, OsN=CH ring), 8.58 (s, 1H, NN=CH), 7.88–6.88 (m, 29H, Ph), 5.63, 5.53, 5.49, 5.27 (d, 4H, Ph *p*-cym), 3.33 (d, J_{PH} = 11.2 Hz, 9H, CH_3 phos), 2.48 (m, 1H, CH ^{i}Pr), 2.45 (s, 3H, *p*-CH_3 *p*-cym), 1.16, 0.57 (d, J_{HH} = 6.9 Hz, 6H, CH_3 ^{i}Pr). $^{31}P\{^1H\}$ NMR (CD_2Cl_2, 25°C) δ: 76.70 (s). $^{13}C\{^1H\}$ NMR (CD_2Cl_2, 25°C) δ: 174.89 (s, OsN=CH), 162.07 (s, NN=CH), 165–122 (m, Ph), 140.80 (d, Os–C), 117.65 (d, C1 *p*-cym), 103.74 (d, C4 *p*-cym), 89.49, 82.39 (d, C3/C5 *p*-cym), 80.74, 78.47 (d, C2/C6 *p*-cym), 54.43 (d, CH_3 phos), 31.30 (s, CH ^{i}Pr), 24.03, 19.76 (s, CH_3 ^{i}Pr), 19.21 (s, *p*-CH_3 *p*-cym) ppm. Anal. Calcd.

for $C_{51}H_{54}BN_2O_3OsP$ (975.00): C, 62.83; H, 5.58; N, 2.87; Found: C, 62.55; H, 5.67; N; 2.81%. Λ_M = 51.4 $\Omega^{-1}mol^{-1}cm^2$.

21a: IR (KBr pellet): $\nu_{C=N}$ 1614 (m) cm^{-1}. ^1H NMR (CD_2Cl_2, 25 °C) δ: 8.83 (d, J_{PH} = 2.65 Hz, 1H, OsN=CH ring), 8.60 (s, 1H, NN=CH), 7.89–6.87 (m, 29H, Ph), 5.60, 5.51, 5.46, 5.25 (d, 4H, Ph *p*-cym), 3.63 (m, 6H, CH_2), 2.77 (m, 1H, CH ^{i}Pr), 2.48 (s, 3H, *p*-CH_3 *p*-cym), 1.14, 0.51 (d, J_{HH} = 6.9 Hz, 6H, CH_3 ^{i}Pr), 1.10 (t, J_{HH} = 7.0 Hz, 9H, CH_3 phos). $^{31}P\{^1H\}$ NMR (CD_2Cl_2, 25 °C) δ: 72.47 (s). $^{13}C\{^1H\}$ NMR (CD_2Cl_2, 25 °C) δ: 174.70 (s, OsN=CH), 162.00 (s, NN=CH), 165–122 (m, Ph), 140.50 (d, Os–C), 118.20 (d, C1 *p*-cym), 103.09 (d, C4 *p*-cym), 89.65, 81.95 (d, C3/C5 *p*-cym), 80.37, 77.30 (d, C2/C6 *p*-cym), 64.37 (d, CH_2), 31.06 (s, CH ^{i}Pr), 24.16 (s, CH_3 ^{i}Pr), 19.44 (s, *p*-CH_3 *p*-cym), 16.06 (d, CH_3 phos) ppm. Anal. Calcd. for $C_{54}H_{60}BN_2O_3OsP$ (1017.08): C, 63.77; H, 5.95; N, 2.75; Found: C, 63.56; H, 6.03; N, 2.67%. Λ_M = 53.0 $\Omega^{-1}mol^{-1}cm^2$.

21b: IR (KBr pellet): $\nu_{C=N}$ 1621 (m) cm^{-1}. ^1H NMR (CD_2Cl_2, 25 °C) δ: 8.76 (d, J_{PH} = 2.62 Hz, 1H, OsN=CH ring), 8.53 (s, 1H, NN=CH), 7.78–6.87 (m, 27H, Ph), 5.62, 5.48, 5.43, 5.25 (d, 4H, Ph *p*-cym), 3.62 (m, 6H, CH_2), 2.52 (m, 1H, CH ^{i}Pr), 2.48, 2.46 (s, 6H, CH_3 *p*-tol), 2.42 (s, 3H, *p*-CH_3 *p*-cym), 1.15, 0.54 (d, J_{HH} = 6.9 Hz, 6H, CH_3 ^{i}Pr), 1.09 (t, J_{HH} = 7.0 Hz, 9H, CH_3 phos). $^{31}P\{^1H\}$ NMR (CD_2Cl_2, 25 °C) d: 73.16 (s) ppm. δ_M = 52.2 $\Omega^{-1}mol^{-1}cm^2$. Anal. Calcd. for $C_{56}H_{64}BN_2O_3OsP$ (1045.13): C, 64.36; H, 6.17; N, 2.68; Found: C, 64.18; H, 6.02; N 2.77%.

6.6 Preparation of Precursors of Rhodium.

Precursor complexes $[RhCl(\mu\text{-}Cl)(\eta^5\text{-}C_5Me_5)]_2$ and $RhCl_2(\eta^5\text{-}C_5Me_5)[P(OR)_3]$ (R = Me, Et) were prepared following the methods previously reported.[150–152]

- **$[RhCl(\mu\text{-}Cl)(\eta^5\text{-}C_5Me_5)]_2$**

The reaction is carried out in a 100 mL round-bottom flask equipped a reflux condenser topped with a nitrogen bypass. Inside the flask were placed 2.00 g of $RhCl_3{\cdot}3H_2O$ (7.60 mmol) pentamethylcyclopentadiene (1.4 mL, 8.00 mol), methanol (50 mL). The mixture was then refluxed gently under nitrogen for 48h with stirring. The reaction mixture was allowed to cool to room temperature and the red precipitate was filtered off in air through a glass sinter. The filtrate was reduced in to give more red crystals. Yield: 75%.

- **$RhCl_2(\eta^5\text{-}C_5Me_5)[P(OR)_3]$**
  [R = Me, Et]

In a three-necked round-bottom flask equipped a reflux condenser an excess amount of the appropriate phosphite (1.8 mmol) was added to a solution of the dimeric complex $[RhCl(\mu\text{-}Cl)(\eta^5\text{-}C_5Me_5)]_2$ (500 mg, 0.81 mmol) in ROH (30 mL, R= Me or Et), and the reaction mixture was stirred at reflux temperature for 2 h. The solvent was removed under reduced pressure to give an oil, which was triturated with ROH (1 mL). A yellow solid slowly separated out, which was filtered and crystallized from dichloromethane and ROH. Yield: 80 %

6.7 Preparation of New Complexes: Azines of Rhodium

$[RhCl(\eta^5\text{-}C_5Me_5)\{\kappa^1\text{-}[N=C(H)R1]\text{–}N=C(H)R1\}\{P(OEt)_3\}]BPh_4$ (22)
[R1 = Ph (a), 4-$CH_3C_6H_4$ (b)].

In a 25 mL three-necked round-bottomed flask covered with an aluminium foil were placed 0.2 mmol of the appropriate chloro complex $RhCl_2(\eta^5\text{-}C_5Me_5)[P(OEt)_3]$, one equivalent of AgOTf (0.2 mmol, 51.4 mg) and 7 mL of CH_2Cl_2 and the reaction mixture was stirred at room temperature for 24 h. After filtration on paper to remove AgCl, a slight excess (0.22 mmol) of the appropriate azine R1(H)=N–N=C(H)R1 was added and the reaction mixture was stirred at room temperature for 24 h. The solvent was removed under reduced pressure to give an oil, which was triturated with ethanol (2 mL) containing an excess of $NaBPh_4$ (0.3 mmol, 103 mg). An orange solid slowly separated out, which was filtered and crystallized from CH_2Cl_2 and EtOH. Yield: 56%.

22a: IR (KBr, cm^{-1}) $\nu_{C=N}$ 1616 (m); ^1H NMR (CD_2Cl_2, 20 °C) δ: 8.58 (s, 1H, CH=N–N), 8.14 (s, 1H, CH=N–Ir), 7.85–6.87 (m, 30H, Ph), 4.17 (d qnt, 6H, CH_2 phos), 1.66 (d, 15H, CH_3 Cp*), 1.28 (t, 9H, CH_3 phos); $^{31}P\{^1H\}$ NMR (CD_2Cl_2, 20 °C) δ: AX spin syst, δ_A 111.3, J_{AX}= 215.6. Anal. Calcd. for $C_{44}H_{47}BClN_2O_3PRh$ (967.24): C, 63.52; H, 5.69; Cl, 4.26; N, 3.37; Found: C, 63.22; H, 5.87; Cl, 4.25; N, 3.56%; Λ_M = 52.8 $\Omega^{-1}mol^{-1}cm^2$; m.p.

22b: IR (KBr, cm^{-1}) $\nu_{C=N}$ 1619 (m); ^1H NMR [$(CD_3)_2CO$, 20 °C] δ: 8.57 (s, 1H, CH=N–N), 8.20 (s, 1H, CH=.N–Ir), 7.80–6.82 (m, 28H, Ph), 4.20 (qnt, 6H, CH_2 phos), 2.39 (s, 6H, CH_3 *p*-tolyl), 1.67 (d, 15H, CH_3 Cp*), 1.25 (t, 9H, CH_3 phos); $^{31}P\{^1H\}$ NMR [$(CD_3)_2CO$, 20 °C] δ: AX spin syst, δ_A 112.2, J_{AX}= 216.3. Anal. Calcd. for $C_{46}H_{51}BClN_2O_3PRh$ (860.06): C, 64.24; H, 5.98; Cl, 4.12; N, 3.26; Found: C, 64.04; H, 6.11; Cl, 3.98; N, 3.46%; Λ_M = 53.1 $\Omega^{-1}mol^{-1}$ cm^2; m.p.

[RhCl(η^5-C$_5$Me$_5$){κ^1-[N=C(CH$_3$)$_2$]–N=C(CH$_3$)$_2$}{P(OEt)$_3$}]BPh$_4$) **(23)**

This complex was prepared exactly like the related aldazine derivatives **22** using ketazine (CH$_3$)$_2$C=N–N=C(CH$_3$)$_2$ as a reagent. Yield: 30%.

IR (KBr, cm^{-1}) $\nu_{C=N}$ 1601 (m); ^{1}H NMR [(CD$_3$)$_2$CO, 20 °C] δ: 7.33–6.82 (m, 20H, Ph), 4.02 (qnt, 6H, CH$_2$ phos), 2.35, 2.22 (s, 12H, CH$_3$C=N), 1.59 (d, 15H, CH$_3$ Cp*), 1.29 (t, 9H, CH$_3$ phos); ^{31}P{^{1}H} NMR [(CD$_3$)$_2$CO, 20 °C] δ: AX spin syst, δ_A 111.6, J_{AX}= 208.7. Anal. Calcd. for C$_{36}$H$_{47}$BClN$_2$O$_3$PRh (735.92): C, 58.76; H, 6.44; Cl, 4.82; N, 3.81; Found: C, 58.83; H, 6.31; Cl, 4.77; N, 3.85%; Λ_M = 51.5 Ω^{-1}mol^{-1}cm^2.

[Rh{κ^2-C$_6$H$_4$(H)C=N–N=C(H)(C$_6$H$_5$)}(η^5-C$_5$Me$_5$){P(OEt)$_3$}]BPh$_4$ **(24)**

In a 25 mL three-necked round-bottomed flask covered with an aluminium foil were placed solid samples of the appropriate chloro complex RhCl$_2$(η^5-C$_5$Me$_5$)[P(OEt)$_3$] (0.2 mmol), two equivalents of AgOTf (0.2 mmol, 51 mg) and 7 mL of CH$_2$Cl$_2$ and the reaction mixture was stirred at room temperature for 24 h. After filtration on paper to remove AgCl, a slight excess of the appropriate aldazine Ph(H)C=N–N=C(H)Ph (0.22 mmol) was added and the reaction mixture was stirred at room temperature for 24 h. The solvent was then removed under reduced pressure to give an oil, which was triturated with ethanol (2 mL) containing an excess of NaBPh$_4$ (0.3 mmol, 103 mg). An orange solid slowly separated out, which was filtered and crystallized from CH$_2$Cl$_2$ and EtOH. Yield: 48%.

IR (KBr, cm^{-1}) $\nu_{C=N}$ 1616 (m); ^{1}H NMR (CD$_2$Cl$_2$, 20 °C) δ: 8.71 (t, 1H, N=CH ring), 8.52 (s, 1H, CH=N–N), 7.91–6.87 (m, 29H, Ph), 3.70 (m, 6H, CH$_2$ phos), 1.67 (d, 15H, CH$_3$ Cp*), 1.15 (t, 9H, CH$_3$ phos); ^{13}C{^{1}H} NMR (CD$_2$Cl$_2$, 20 °C) δ: 172.26 [s, N=CH ring], 162.45 (s, CH=N–N), 143.13 [d, Rh–C, J_{CP} = 18.0 Hz], 165–122 (m, Ph), 102.77 (d, J_{CP} = 3.5, C$_5$ Cp*), 64.26 (d, J_{CP} = 9.3, CH$_2$ phos), 16.25 (d, J_{CP} = 6.8, CH$_3$ phos), 9.80 (s, CH$_3$ Cp*); ^{31}P{^{1}H} NMR (CD$_2$Cl$_2$, 20 °C) δ: AX spin syst, δ_A 114.63, J_{AX}= 238.1. Anal. Calcd. for C$_{54}$H$_{61}$BN$_2$O$_3$PRh (930.78): C, 69.68; H, 6.61; N, 3.01; Found: C, 69.71; H, 6.90; N, 2.89%; Λ_M = 52.1 Ω^{-1}mol^{-1}cm.

6.8 Preparation of Precursors of Iridium

Precursor complexes [IrCl(μ-Cl)(η^5-C$_5$Me$_5$)]$_2$ and IrCl$_2$(η^5-C$_5$Me$_5$)[P(OR)$_3$] (R = Me, Et) were prepared following the methods previously reported.[150–152]

- **$[IrCl(\mu\text{-}Cl)(\eta^5\text{-}C_5Me_5)]_2$**

The reaction is carried out in a 100 mL round-bottom flask equipped a reflux condenser topped with a nitrogen bypass. Inside the flask were placed 2.00 g of $IrCl_3 \cdot 3H_2O$ (5.67 mmol) pentamethylcyclopentadiene (1.5 mL, 9.64 mol) and methanol (50 mL). The mixture was then refluxed gently under nitrogen for 36h with stirring. The reaction mixture is allowed to cool to room temperature and the dark orange precipitate is filtered off in air through a glass sinter. The filtrate is reduced in to give more crystals. Yield: 85%.

- **$IrCl_2(\eta^5\text{-}C_5Me_5)[P(OR)_3]$**
  [R = Me, Et]

In a three-necked round-bottom flask equipped a reflux condenser an slight excess amount of the appropriate phosphite (1.4 mmol) was added to a solution of the dimeric complex $[IrCl(\mu\text{-}Cl)(\eta^5\text{-}C_5Me_5)]_2$ (500 mg, 0.63 mmol) in ROH (10 mL, R= Me or Et), and the reaction mixture was stirred at reflux temperature for 3 h. The solvent was removed under reduced pressure to give an oil, which was triturated with ROH (1 mL). A yellow solid slowly separated out, which was filtered and crystallized from dichloromethane and ROH. Yield: 80 %.

6.9 Preparation of New Complexes: Azines of Iridium.

$[IrCl(\eta^5\text{-}C_5Me_5)\{\kappa^1\text{-}[N=C(H)R1]\text{–}N=C(H)R1\}\{P(OR)_3\}]BPh_4$ (25, 26)
[R = Me (25), Et (26); R1 = Ph (a), 4-$CH_3C_6H_4$ (b), 2,6-$(CH_3)_2C_6H_3$ (f)].

In a 25 mL three-necked round-bottomed flask covered with an aluminium foil were placed 0.2 mmol of the appropriate chloro complex $IrCl_2(\eta^5\text{-}C_5Me_5)[P(OR)_3]$, one equivalent of AgOTf (0.2 mmol, 51.4 mg) and 7 mL of CH_2Cl_2 and the reaction mixture was stirred at room temperature for 24 h. After filtration on paper to remove AgCl, a slight excess (0.22 mmol) of the appropriate azine R1(H)=N–N=C(H)R1 was added and the reaction mixture was stirred at room temperature for about 3 h. The solvent was removed under reduced pressure to give an oil, which was triturated with ethanol (2 mL) containing an excess of $NaBPh_4$ (0.3 mmol, 103 mg). An orange solid slowly separated out, which was filtered and crystallized from CH_2Cl_2 and EtOH. Yield: 86%.

25a: IR (KBr, cm^{-1}) $\nu_{C=N}$ 1619 (m); ^1H NMR (CD_2Cl_2, 20 °C) δ: 8.68 (s, 1H, CH=N–N), 8.02 (s, 1H, CH=N–Ir), 7.85–6.84 (m, 30H, Ph), 3.77 (d, 9H, CH_3 phos), 1.69 (d, 15H, CH_3 Cp*); $^{31}P\{^1H\}$ NMR (CD_2Cl_2, 20 °C) δ: 79.58 (s); $^{13}C\{^1H\}$ NMR (CD_2Cl_2,20 °C) δ: 164.78 (s, CH=N–Ir), 161.16 (s, CH=N–N),

165–122 (m, Ph), 94.89 (s br, C_5 Cp*), 55.28 (d, J_{CP} = 9.3, CH_3 phos), 9.59 (d, J_{CP} = 9.3, CH_3 Cp*). Anal. Calcd. for $C_{51}H_{56}BClIrN_2O_3P$ (1014.46): C, 60.38; H, 5.56; Cl, 3.49; N, 2.76; Found: C, 60.13; H, 5.44; Cl, 3.31; N, 2.83%; Λ_M = 52.7 $\Omega^{-1}mol^{-1}cm^2$; m.p. (dec) 132–134 °C.

26a: IR (KBr, cm^{-1}) $\nu_{C=N}$ 1616 (m); ^1H NMR (CD_2Cl_2, 20 °C) δ: 8.71 (s, 1H, CH=N–N), 8.07 (s, 1H, CH=N–Ir), 7.87–6.86 (m, 30H, Ph), 4.11 (d qnt, 6H, CH_2 phos), 1.68 (d, 15H, CH_3 Cp*), 1.26 (t, 9H, CH_3 phos); $^{31}P\{^1H\}$ NMR (CD_2Cl_2, 20 °C) δ: 75.19 (s); $^{13}C\{^1H\}$ NMR (CD_2Cl_2, 20 °C) d: 165.80 (s, CH=N–Ir), 162.84 (s, CH=N–N), 165–122 (m, Ph), 96.85 (d, J_{CP} = 4.4, C_5 Cp*), 64.69 (d, J_{CP} = 8.5, CH_2 phos), 16.32 (d, J_{CP} = 7.3, CH_3 phos), 9.23 (s, CH_3 Cp*). Anal. Calcd. for $C_{54}H_{62}BClIrN_2O_3P$ (1056.54): C, 61.39; H, 5.91; Cl, 3.36; N, 2.65; Found: C, 61.22; H, 6.00; Cl, 3.25; N, 2.56%; Λ_M = 51.8 $\Omega^{-1}mol^{-1}cm^2$; m.p. (dec) 115–117 °C.

26b: IR (KBr, cm^{-1}) $\nu_{C=N}$ 1619 (m); ^1H NMR (CD_2Cl_2, 20 °C) δ: 8.64 (s, 1H, CH=N–N), 8.04 (s, 1H, CH=N–Ir), 7.75–6.86 (m, 28H, Ph), 4.16 (qnt, 6H, CH_2 phos), 2.47, 2.41 (s, 6H, CH_3 *p*-tolyl), 1.67 (d, 15H, CH_3 Cp*), 1.28 (t, 9H, CH_3 phos); $^{31}P\{^1H\}$ NMR (CD_2Cl_2, 20 °C) δ: 77.71 (s); $^{13}C\{^1H\}$ NMR (CD_2Cl_2, 20 °C) δ: 163.43 (s, CH=N–Ir), 161.95 (s, CH=N–N), 165–122 (m, Ph), 96.21 (d, J_{CP} = 4.4, C_5 Cp*), 64.02 (d, J_{CP} = 8.4, CH_2 phos), 21.80, 20.07 (s, CH_3 *p*-tolyl), 16.26 (d, J_{CP} = 7.0, CH_3 phos), 8.97 (s, CH_3 Cp*). Anal. Calcd. for $C_{56}H_{66}BClIrN_2O_3P$ (1084.59): C, 62.01; H, 6.13; Cl, 3.27; N, 2.58; Found: C, 61.84; H, 6.21; Cl, 3.18; N, 2.66%; Λ_M = 53.1 $\Omega^{-1}mol^{-1}$ cm^2; m.p. (dec) 107–117 °C.

26f: IR (KBr, cm^{-1}) $\nu_{C=N}$ 1615 (m); ^1H NMR (CD_2Cl_2, 20 °C) δ: 8.96 (s, 1H, CH=N–N), 8.62 (s, 1H, CH=N–Ir), 7.63–6.87 (m, 26H, Ph), 3.96 (qnt, 6H, CH_2 phos), 2.59 (s, 6H, 2,6-$(CH_3)_2C_6H_3C$=N–N), 2.55, 2.44 (s, 6H, 2,6-$(CH_3)_2C_6H_3C$=N–Ir), 1.54 (d, 15H, CH_3 Cp*), 1.27 (t, 9H, CH_3 phos); $^{31}P\{^1H\}$ NMR (CD_2Cl_2, 20 °C) δ: 72.68 (s); $^{13}C\{^1H\}$ NMR (CD_2Cl_2, 20 °C) δ: 162.95 (s, CH=N–Ir), 161.80 (s, CH=N–N), 165–122 (m, Ph), 96.06 (d, J_{CP} = 4.4, C_5 Cp*), 63.35 (d, J_{CP} = 8.4, CH_2 phos), 22.41, 19.43 {s, 2,6-$(CH_3)_2$}, 16.20 (d, J_{CP} = 7.22, CH_3 phos), 8.87 (s, CH_3 Cp*). Anal. Calcd. for $C_{58}H_{70}BClIrN_2O_3P$ (1112.64): C, 62.61; H, 6.34; Cl, 3.19; N, 2.52; Found: C, 62.42; H, 6.27; Cl, 3.31; N, 2.43%; Λ_M = 52.0 $\Omega^{-1}mol^{-1}cm^2$; m.p. (dec) 121–123 °C.

[IrCl(η^5-C_5Me_5){κ^1-[N=C$(CH_3)_2$]–N=C$(CH_3)_2$}{P$(OR)_3$}]BPh_4 (27, 28) [R = Me (27), Et (28)].

These complexes were prepared exactly like the related aldazine derivatives **25** and **26** using ketazine $(CH_3)_2C$=N–N=C$(CH_3)_2$ as a reagent. Yield: 84%.

27: IR (KBr, cm^{-1}) $\nu_{C=N}$ 1597 (m); ^{1}H NMR (CD_2Cl_2, 20 °C) d: 7.33–6.88 (20, 20H, Ph), 3.77 (d, 15H, CH_3 Cp*), 2.19, 2.14 (s, 12H, CH_3C=N), 1.63 (d, 9H, CH_3 phos); $^{31}P\{^{1}H\}$ NMR (CD_2Cl_2, 20 °C) δ: 82.65 (s); $^{13}C\{^{1}H\}$ NMR (CD_2Cl_2, 20 °C) δ: 165–122 (m, Ph), 96.76 (d, J_{CP} = 3.0, C5 Cp*), 61.46 [s, free $C(CH_3)_2$], 58.13 [s, $C(CH_3)_2$], 55.14 (d, J_{CP} = 9.3, CH_3 phos), 18.80, 18.25 [s, $C(CH_3)_2$], 8.96 (s br, CH_3 Cp*). Anal. Calcd. for $C_{43}H_{56}BClIrN_2O_3P$ (918.37): C, 56.24; H, 6.15; Cl, 3.86; N, 3.05; Found: C, 56.02; H, 6.07; Cl, 3.99; N, 3.13%; Λ_M = 51.6 $\Omega^{-1}mol^{-1}cm^2$; m.p. (dec) 132–134 °C.

28: IR (KBr, cm^{-1}) $\nu_{C=N}$ 1601 (m); ^{1}H NMR (CD_2Cl_2, 20 °C) δ: 7.33–6.82 (m, 20H, Ph), 4.02 (qnt, 6H, CH_2 phos), 2.35, 2.22 (s, 12H, CH_3C=N), 1.59 (d, 15H, CH_3 Cp*), 1.29 (t, 9H, CH_3 phos); $^{31}P\{^{1}H\}$ NMR (CD_2Cl_2, 20 °C) δ: 78.96 (s); $^{13}C\{^{1}H\}$ NMR (CD_2Cl_2, 20 °C) δ: 165–122 (m, Ph), 96.51 (d br, C_5 Cp*), 64.15 (d, J_{CP} = 9.3, CH_2 phos), 62.04 (s, free C(CH3)2), 57.62 (s, $C(CH_3)_2$), 19.05, 18.37 (s, $C(CH_3)_2$), 16.20 (d br, CH_3 phos), 9.12 (s br, CH_3 Cp*). Anal. Calcd. for $C_{46}H_{62}BClIrN_2O_3P$ (960.45): C, 57.52; H, 6.51; Cl, 3.69; N, 2.92; Found: C, 57.30; H, 6.59; Cl, 3.57; N, 2.85%; Λ_M = 52.5 $\Omega^{-1}mol^{-1}cm^2$; m.p. (dec) 138–140 1C.

$[Ir\{\kappa^2\text{-}R1C_6H_3(H)C{=}N{-}N{=}C(H)(R1C_6H_4)\}(\eta^5\text{-}C_5Me_5)\{P(OR)_3\}]BPh_4$ (29, 30)
[R = Me (29), Et (30); R1 = H (a), 4-CH_3 (b), 4-CH_3O (c), 4-F (d), 4-NO_2 (e)]

Method A. In a 25 mL three-necked round-bottomed flask covered with an aluminium foil were placed solid samples of the appropriate chloro complex $IrCl_2(\eta^5\text{-}C_5Me_5)[P(OR)_3]$ (0.2 mmol), one equivalent of AgOTf (0.2 mmol, 51 mg) and 7 mL of CH_2Cl_2 and the reaction mixture was stirred at room temperature for 24 h. After filtration on paper to remove AgCl, a slight excess of the appropriate aldazine $R1C_6H_4(H)C{=}N{-}N{=}C(H)R1C_6H_4$ (0.22 mmol) was added and the reaction mixture was stirred at room temperature for about 30 h. After this time another equivalent of AgOTf was added to the reaction mixture and the resulting solution was stirred in the dark for another 24 h. The solvent was then removed under reduced pressure to give an oil, which was triturated with ethanol (2 mL) containing an excess of $NaBPh_4$ (0.3 mmol, 103 mg). An orange solid slowly separated out, which was filtered and crystallized from CH_2Cl_2 and EtOH. Yield: 67%.

Method B. In a 25 mL three-necked round-bottomed flask covered with an aluminium foil were placed solid samples of $IrCl_2(\eta^5\text{-}C_5Me_5)[P(OR)_3]$ (0.2 mmol), two equivalents of AgOTf (0.4 mmol, 102 mg) and 7 mL of CH_2Cl_2 and the reaction mixture was stirred at room temperature for 24 h. After filtration on paper to remove AgCl, an excess of the appropriate aldazine (0.3 mmol) was added and the reaction mixture was stirred at room temperature for 15 h. The solvent was

removed under reduced pressure and the oil obtained was treated with ethanol (2 mL) containing an excess of $NaBPh_4$ (0.3 mmol, 103 mg). An orange solid slowly separated out, which was filtered and crystallized from CH_2Cl_2 and EtOH. Yield: 78%.

29a: IR (KBr, cm^{-1}) $\nu_{C=N}$ 1619 (m); ^1H NMR (CD_2Cl_2, 20 °C) δ: 8.81 (d, 1H, N=CH ring), 8.54 (s, 1H, CH=N–N), 7.85–6.84 (m, 29H, Ph), 3.42 (d, 9H, CH_3 phos), 1.74 (d, 15H, CH_3 Cp*); $^{31}P\{^1H\}$ NMR (CD_2Cl_2, 20 °C) δ: 71.95 (s); $^{13}C\{^1H\}$ NMR (CD_2Cl_2, 20 °C) δ: 174.62 [s, N=CH ring (C11)], 165–120 (m, Ph), 162.13 [s, C(H)=N–N], 158.44 [d, J_{CP} = 18.0, Ir–C (C13)], 143.60 [s br, Ir–C–C (C12)], 98.18 (s br, C5 Cp*), 55.27 (d, JCP = 9.3, CH3 phos), 9.35 (d, J_{CP} = 1.5, CH_3 Cp*); UV-VIS (CH_2Cl_2, r.t., nm): < 480, 267 sh (ε = 21 400 $M^{-1}cm^{-1}$), 323 max (ε = 18 600 $M^{-1}cm^{-1}$), 383 sh (ε = 4900 $M^{-1}cm^{-1}$). PL (solid sample, $\lambda_{excitation}$ = 405 nm, r.t., nm): 531–830, max 654 (FWHM = 3400 cm ^{1}). τ (solid sample, $\lambda_{excitation}$ = 355 nm, $\lambda_{emission}$ = 650 nm, r.t.): 0.41 ms. ϕ_p (r.t.) = 1%. Anal. Calcd. for $C_{51}H_{55}BIrN_2O_3P$ (978.00): C, 62.63; H, 5.67; N, 2.86; Found: C, 62.40; H, 5.75; N, 2.73%; Λ_M = 52.4 $\Omega^{-1}mol^{-1}cm^2$; m.p. (dec) 136–138 °C.

29d: IR (KBr, cm^{-1}) $\nu_{C=N}$ 1618 (m); ^1H NMR (CD_2Cl_2, 20 °C) δ: 8.71 (d, 1H, N=CH ring), 8.42 (s, 1H, CH=N–N), 7.88–6.86 (m, 27H, Ph), 3.45 (d, 9H, CH_3 phos), 1.74 (d, 15H, CH_3 Cp*); $^{31}P\{^1H\}$ NMR (CD_2Cl_2, 20 °C) δ: 71.45 (s); $^{13}C\{^1H\}$ NMR (CD_2Cl_2, 20 °C) δ: 174.19 [s, N=CH ring (C11)], 166–122 (m, Ph), 161.58 [s, C(H)=N–N], 159.47 [d, J_{CP} = 18.2, J_{CF} = 7.1, Ir–C (C13)], 141.05 [s br, Ir–C–C (C12)], 98.03 (s br, JCP = 3.9, C5 Cp*), 55.12 (d, J_{CP} = 9.3, CH3 phos), 9.44 (d, J_{CP} = 1.5, CH_3 Cp*); UV-VIS (CH_2Cl_2, r.t., nm): <485, 270 sh (ε = 23 000 $M^{-1}cm^{-1}$), 314 max (ε = 24 900 $M^{-1}cm^{-1}$), 370 sh (ε = 7500 $M^{-1}cm^{-1}$) 411 sh (ε = 3500 $M^{-1}cm^{-1}$). PL (solid sample, $\lambda_{excitation}$ = 405 nm, r.t., nm): 540–818, max 648 (FWHM = 3200 cm^{-1}). Anal. Calcd. for $C_{51}H_{53}BF_2IrN_2O_3P$ (1013.98): C, 60.41; H, 5.27; N, 2.76; Found: C, 60.19; H, 5.14; N, 2.63%; Λ_M = 51.9 $\Omega^{-1}mol^{-1}cm^2$; m.p. (dec) 164–166 °C.

29e: IR (KBr, cm^{-1}) $\nu_{C=N}$ 1597 (m); ^1H NMR (CD_2Cl_2, 20 °C) δ: 8.45 (d, 1H, N=CH ring), 8.03 (s, 1H, CH=N–N),7.81–6.84 (m, 27H, Ph), 3.47 (d, 9H, CH_3 phos), 1.76 (d, 15H, CH_3 Cp*); $^{31}P\{^1H\}$ NMR (CD_2Cl_2, 20 °C) δ: 70.19 (s); $^{13}C\{^1H\}$ NMR (CD_2Cl_2, 20 °C) δ: 173.74 [s, N=CH ring (C11)], 164–120 (m, Ph), 161.19 [s, C(H)=N–N], 157.85 [d, J_{CP} = 18.2, Ir–C (C13)], 148.94 [s, Ir–C–C(C12)], 98.44 (d, J_{CP} = 3.4, C_5 Cp*), 55.35 (d, J_{CP} = 9.2, CH_3 phos), 9.47 (d, J_{CP} = 1.4, CH_3 Cp*); UV-VIS (CH_2Cl_2, r.t., nm): <700, 343 max (ε = 18 000 $M^{-1}cm^{-1}$), 414 sh (ε = 6200 $M^{-1}cm^{-1}$), 570 sh (ε = 1200 $M^{-1}cm^{-1}$). Anal. Calcd. for $C_{51}H_{53}BIrN_4O_7P$ (1067.99): C, 57.35; H, 5.00; N, 5.25; Found: C, 57.17; H, 5.14; N, 5.41%; Λ_M = 52.3 $\Omega^{-1}mol^{-1}cm^2$; m.p. (dec) 140–143 °C.

30a: IR (KBr, cm^{-1}) $\nu_{C=N}$ 1616 (m); ^{1}H NMR (CD_2Cl_2, 20 °C) δ: 8.84 (d, 1H, N=CH ring), 8.60 (s, 1H, CH=N–N), 7.92–6.86 (m, 29H, Ph), 3.71 (qnt, 6H, CH_2 phos), 1.74 (d, 15H, CH_3 Cp*), 1.13 (t, 9H, CH_3 phos); $^{13}C\{^{1}H\}$ NMR (CD_2Cl_2, 20 °C) δ: 175.76 [s, N=CH ring (C11)], 163.19 (s, CH=N–N), 156.76 [d, Ir–C (C13), J_{CP} = 18.0 Hz], 144.58 [s, Ir–C–C (C12)], 165–122 (m, Ph), 97.53 (d, J_{CP} = 3.5, C_5 Cp*), 64.05 (d, J_{CP} = 9.3, CH_2 phos), 16.15 (d, J_{CP} = 6.8, CH_3 phos), 9.41 (s, CH_3 Cp*); $^{31}P\{^{1}H\}$ NMR (CD_2Cl_2, 20 °C) δ: 67.41 (s); UV-VIS (CH_2Cl_2, r.t., nm): <480, 303 max (ε = 19 600 $M^{-1}cm^{-1}$), 328 sh (ε = 13 900 $M^{-1}cm^{-1}$), 385 sh (ε = 2700 $M^{-1}cm^{-1}$). PL (solid sample, $\lambda_{excitation}$ = 405 nm, r.t., nm): 540–890, max 653 (FWHM = 3100 cm^{-1}). τ (solid sample, $\lambda_{excitation}$ = 355 nm, $\lambda_{emission}$ = 650 nm, r.t.): 0.36 ms. ϕ_P (r.t.) = 1%. Anal. Calcd. for $C_{54}H_{61}BIrN_2O_3P$ (1020.08): C, 63.58; H, 6.03; N, 2.75; Found: C, 63.71; H, 5.90; N, 2.62%; Λ_M = 51.0 $\Omega^{-1}mol^{-1}cm^2$; m.p. (dec) 150–152 °C.

30b: IR (KBr, cm^{-1}) $\nu_{C=N}$ 1619 (m); ^{1}H NMR (CD_2Cl_2, 20 °C) δ: 8.78 (d, 1H, N=CH ring), 8.51 (s, 1H, CH=N–N), 7.82–6.86 (m, 27H, Ph), 3.70 (qnt, 6H, CH_2 phos), 2.49, 2.46 (s, 6H, CH_3 *p*-tolyl), 1.74 (d, 15H, CH_3 Cp*), 1.13 (t, 9H, CH_3 phos); $^{31}P\{^{1}H\}$ NMR (CD_2Cl_2, 20 °C) δ: 68.40 (s); $^{13}C\{^{1}H\}$ NMR (CD_2Cl_2, 20 °C) δ: 174.19 [d, J_{CP} = 3.5, N=CH ring (C11)], 165–122 (m, Ph), 162.29 [s, C(H)=N–N], 156.21 [d, J_{CP} = 18.0, Ir–C (C13)], 141.66 [s, Ir–C–C (C12)], 97.02 (d, J_{CP} = 3.5, C5 Cp*), 63.51 (d, J_{CP} = 9.3, CH_2 phos), 21.71, 21.50 (s, CH_3 *p*-tolyl), 15.73 (d, J_{CP} = 6.8, CH_3 phos), 9.00 (d, J_{CP} = 1.3, CH_3 Cp*); UV-VIS (CH_2Cl_2, r.t., nm): <485, 326 max (ε = 26 800 $M^{-1}cm^{-1}$), 337 sh (ε = 25 500 $M^{-1}cm^{-1}$), 423 sh (ε = 4600 $M^{-1}cm^{-1}$). PL (solid sample, $\lambda_{excitation}$ = 405 nm, r.t., nm): 553–814, max 663 (FWHM = 2900 cm^{-1}). Anal. Calcd. for $C_{56}H_{65}BIrN_2O_3P$ (1048.13): C, 64.17; H, 6.25; N, 2.67; Found: C, 64.00; H, 6.18; N, 2.78%; Λ_M = 51.6 $\Omega^{-1}mol^{-1}cm^2$; m.p. (dec) 132–134 °C.

30c: IR (KBr, cm^{-1}) $\nu_{C=N}$ 1614 (m); ^{1}H NMR (CD_2Cl_2, 20 °C) δ: 8.72 (d, 1H, N=CH ring), 8.43 (s, 1H, CH=N–N), 7.84–6.87 (m, 27H, Ph), 3.91, 3.89 (s, 6H, CH_3O), 3.73 (m, 6H, CH_2 phos), 1.75 (d, 15H, CH_3 Cp*), 1.15 (t, 9H, CH_3 phos); $^{31}P\{^{1}H\}$ NMR (CD_2Cl_2, 20 °C) δ: 68.24 (s); $^{13}C\{^{1}H\}$ NMR (CD_2Cl_2, 20 °C) δ: 175.08 [s, N=CH ring (C11)], 165–122 (m, Ph), 163.02 [s, C(H)=N–N], 157.34 [d, J_{CP} = 18.0, Ir–C (C13)], 143.55 [s, Ir–C–C (C12)], 97.73 (d, J_{CP} = 3.5, C_5 Cp*), 67.13, 66.60 (s, CH_3O), 63.91 (d, J_{CP} = 9.3, CH_2 phos), 16.02 (d, J_{CP} = 6.8, CH_3 phos), 9.22 (s br, CH_3 Cp*); UV-VIS (CH_2Cl_2, r.t., nm): <480, 264 sh (ε = 20 200 $M^{-1}cm^{-1}$), 663 max (ε = 23 000 $M^{-1}cm^{-1}$), 383 sh (ε = 22 400 $M^{-1}cm^{-1}$). PL (solid sample, $\lambda_{excitation}$ = 405 nm, r.t., nm): 569–795, max 625, 663 (FWHM = 2900 cm^{-1}). Anal. Calcd. for $C_{56}H_{65}BIrN_2O_5P$ (1080.13): C, 62.27; H, 6.07; N, 2.59; Found: C, 62.09; H, 5.96; N, 2.47%; Λ_M = 52.2 $\Omega^{-1}mol^{-1}cm^2$; m.p. (dec) 142–144 °C.

Ir{κ²-CH₂(CH₃)C=N–N=C(CH₃)₂}(η⁵-C₅Me₅){P(OR)₃}]BPh₄ (31, 32)
[R = Me (31), Et (32)]

These complexes were prepared exactly like the related κ²-benzaldehydeazine derivatives **29** and **30** with both methods A and B, using acetoneazine $(CH_3)_2C=N–N=C(CH_3)_2$ as a reagent. Yield: 73%**.**

31: IR (KBr, cm^{-1}) $\nu_{C=N}$ 1579 (m); ^1H NMR (CD_2Cl_2, 20 °C) δ: 7.33–6.85 (m, 20H, Ph), 3.77 (d, 9H, CH_3 phos), ABC_3X spin 1.0, J_{BC} = 0.7, J_{BX} = 0.9, J_{CX} = 1.0 (2H, $–CH_2$), 2.07 (s, 3H, $CH_3C=$), 1.65 (d, 15H, CH_3 Cp*), 1.32, 1.12 [s, 6H, $(CH_3)_2C=$]; $^{31}P\{^1H\}$ NMR (CD_2Cl_2, 20 °C) δ: 80.9 (s); $^{13}C\{^1H\}$ NMR (CD_2Cl_2, 20 °C) δ: 165–122 (m, Ph), 164.61 [s, $=C(CH_3)$], 96.79 (d, J_{CP} = 4.4, C5 Cp*), 61.54 [s,$=C(CH_3)_2$], 55.32 (d, J_{CP} = 9.0, CH_3 phos), 52.81 (s, Ir–CH_2), 27.17, 26.92 [s,$=C(CH_3)_2$], 18.89 [s,$=C(CH_3)$], 9.08 (s, CH_3 Cp*). Anal. Calcd. for $C_{43}H_{55}BIrN_2O_3P$ (881.91): C, 58.56; H, 6.29; N, 3.18; Found: C, 58.37; H, 6.35; N, 3.08%; Λ_M = 51.8 $\Omega^{-1}mol^{-1}cm^2$; m.p. (dec) 147–149 °C.

32: IR (KBr, cm^{-1}) $\nu_{C=N}$ 1590 (m); ^1H NMR (CD_2Cl_2, 20 °C) δ: 7.34–6.69 (m, 20H, Ph), 4.09 (qnt, 6H, CH_2 phos), ABC_3X spin syst (X = ^{31}P), δ_A 2.92, d_B 2.86, δ_C 2.09, J_{AB} = 18.1, J_{AC} = 1.5, J_{AX} = 1.0, J_{BC} = 0.7, J_{BX} = 0.9, J_{CX} = 0.5 (2H, $–CH_2$), 2.09 (s, 3H, $CH_3C=$), 1.64 (d, 15H, CH_3 Cp*), 1.34, 1.11 [s, 6H, $(CH_3)_2C=$], 1.32 (t, 9H, CH_3 phos); $^{31}P\{^1H\}$ NMR (CD_2Cl_2, 20 °C) δ: 76.54 (br); $^{13}C\{^1H\}$ NMR (CD_2Cl_2, 20 °C) δ: 165–120 (m, Ph), 163.5 [s,$=C(CH_3)$], 96.23 (d, J_{CP} = 4.3, C_5 Cp*), 64.43 (d, J_{CP} = 9.4, CH_2 phos), 61.31 [s, $=C(CH_3)_2$], 52.70 (s, Ir–CH_2), 27.26, 26.91 [s, $=C(CH_3)_2$], 18.93 [s, $=C(CH_3)$], 16.35 (d, J_{CP} = 6.8, CH_3 phos), 8.91 (s, CH_3 Cp*). Anal. Calcd. for $C_{46}H_{61}BIrN_2O_3P$ (923.99): C, 59.79; H, 6.65; N, 3.03; Found: C, 59.61; H, 6.53; N, 2.91%; Λ_M = 51.5 $\Omega^{-1}mol^{-1}cm^2$; m.p. (dec) 142–144 °C.

6.10 Preparation of Precursors of Osmium

The complexes $[OsBr(\eta^5\text{-}C_5Me_5)(PPh_3)_2]$ and $[OsBr(\eta^5\text{-}C_5Me_5)(PPh_3)\{P(OR)_3\}]$ were prepared following the methods previously reported[153,154].

- **$[OsBr(\mu\text{-}Br)(\eta^5\text{-}C_5Me_5)]_2$**

A solution of OsO_4 (2.0 g, 7.9 mmol) in concentrated HBr (80 mL) was heated to reflux for 2 h. The dark red solution was promptly taken to dryness on a rotary evaporator, keeping the bath temperature no higher than 50° C. The dried solid was further dried under vacuum at room temperature overnight. The bromo-osmic acid obtained was then dissolved in degassed tert-butyl alcohol (80 mL) and treated with pentamethylcyclopentadiene (1.80 mL, 11.8 mmol). The red solution was put under nitrogen and then heated to reflux temperature for 45 min, during which

time a brown microcrystalline solid precipitate. The precipitate was filtered, dried under vacuum and stored in argon atmosphere at -20 °C. Yield: 80%.

- **[OsBr(η^5-C_5Me_5)(PPh_3)$_2$]**

To a mixture of [OsBr(μ-Br)(η^5-C_5Me_5)]$_2$ (0.62 g, 0.64 mmol) and PPh_3(1.2 g, 4.6 mmol) was added ethanol (50 mL). The resulting solution was refluxed for 8. h; and over the course of the reaction an orange-yellow micro-crystalline precipitate formed. The orange-yellow microcrystals were isolated by filtration and then stored under argon at -20 °C. Yield: 56%.

- **[OsBr(η^5-C_5Me_5)(PPh_3){$P(OR)_3$}]**
  [R = Me, Et].

An excess of the appropriate phosphite $P(OR)_3$ (2.1 mmol) was added to a solution of [OsBr(η^5-C_5Me_5)(PPh_3)$_2$] (1.0 g, 1.07 mmol) in 50 mL of benzene and the reaction mixture was refluxed for 1 h. The solvent was removed under reduced pressure to give an oil, which was dissolved in diethylether and chromatographed on a silica gel column (80·5 cm) using diethylether as eluent. The yellow fraction was collected and evaporated to dryness and the oil obtained was triturated with alcohol (2 mL). A yellow solid slowly separated out, which was filtered and dried under vacuum. Yield ≥80%.

R = Me: ^{1}H NMR (CD_2Cl_2, 20 °C) δ: 7.60–7.25 (m, 15H, Ph), 3.39 (d, 9H, CH_3 phos), 1.41 (dd, 15H, CH_3 Cp*); $^{31}P\{^1H\}$ NMR (CD_2Cl_2, 20 °C) δ: AX spin syst, δ_A 92.92, δ_X 7.57, J_{AX}= 38.89. Anal. Calcd. for $C_{31}H_{39}BrO_3OsP_2$ (791.73): C, 47.03; H, 4.97; Br, 10.09; Found: C, 47.17; H, 5.00; Br, 9.93%.

R = Et: ^{1}H NMR (CD_2Cl_2, 20 °C) δ: 7.58-7.24 (m, 15H, Ph), 3.80 (m, 6H, CH_2 phos), 1.40 (s, 15H, CH_3 Cp*), 1.01 (t, 9H, CH_3 phos); $^{31}P\{^1H\}$ NMR (CD_2Cl_2, 20 °C) δ: AX spin syst, δ_A 89.19, δ_X 8.45, J_{AX}=41.44. Anal. Calcd. for $C_{34}H_{45}BrO_3OsP_2$ (833.81): C, 48.98; H, 5.44; Br, 9.58; Found: C, 49.03; H, 5.35; Br, 9.54%.

6.11 Preparation of New Complexes: Diazoalkanes of Osmium.

[Os(η^5-C_5Me_5)($N_2CAr1Ar2$)(PPh_3){$P(OR)_3$}]BPh_4 (33, 34)
[R = Me (33), Et (34); Ar1 = Ar2 = Ph (a); Ar1 = Ph, Ar2 = *p*-tolyl (b); Ar1Ar2 = $C_{12}H_8$ (c)]

In a 25-mL three-necked round-bottomed flask were placed 0.1 mmol of the appropriate bromo-compound [OsBr(η^5-C_5Me_5)(PPh_3){$P(OR)_3$}], an excess of the appropriate diazoalkane (0.3 mmol),

an excess of $NaBPh_4$ (0.2 mmol, 68 mg), 5 mL of ethanol and 5 mL of dichloromethane. The reaction mixture was stirred at room temperature for 48 h and then the solvent removed under reduced pressure leaving an oil, which was triturated with ethanol (1 mL). A yellow-orange solid slowly separated out from the resulting solution, which was filtered and crystallised from CH_2Cl_2 and ethanol. Yield: 75%.

33a: IR (KBr, cm^{-1}) ν_{N2} 1941 (m); ^1H NMR (CD_2Cl_2, 20 °C) δ: 7.55-6.87 (m, 45H, Ph), 3.29 (d, 9H, CH_3 phos), 1.53 (s, 15H, CH_3 Cp*); $^{31}P\{^1H\}$ NMR (CD_2Cl_2, 20 °C) δ: AX spin syst, δ_A 85.87, δ_X 7.43, J_{AX}=41.20. Anal. Calcd. for $C_{68}H_{69}BN_2O_3OsP_2$ (1225.30): C, 66.66; H, 5.68; B, 0.88; N, 2.29; Found: C, 66.56; H, 5.60; B, 1.00; N, 2.09%; Λ_M = 52.1 $\Omega^{-1}mol^{-1}cm^2$.

33b: IR (KBr, cm^{-1}) ν_{N2} 1942 (m); ^1H NMR (CD_2Cl_2, 20 °C) δ: 7.78-6.88 (m, 41H, Ph), 3.29 (d, 9H, CH_3 phos), 2.43 (s, 3H, CH_3 *p*-tolyl), 1.39 (dd, 15H, CH_3 Cp*); $^{31}P\{^1H\}$ NMR (CD_2Cl_2, 20 °C) δ: AX spin syst, δ_A 85.90, δ_X 7.51, J_{AX}=40.98. Anal. Calcd. for $C_{69}H_{71}BN_2O_3OsP_2$ (1239.33): C, 66.87; H, 5.77; B, 0.87; N, 2.26; Found: C, 66.75; H, 5.68; B, 0.93; N, 2.15%; Λ_M = 51.3 $\Omega^{-1}mol^{-1}cm^2$.

33c: IR (KBr, cm^{-1}) ν_{N2} 1946 (m); ^1H NMR (CD_2Cl_2, 20 °C) δ: 7.96-6.86 (m, 43H, Ph), 3.46 (d, 9H, CH_3 phos), 1.67 (dd, 15H, CH_3 Cp*); $^{31}P\{^1H\}$ NMR (CD_2Cl_2, 20 °C) δ: AX spin syst, δ_A 82.86, δ_X 6.00, J_{AX}=41.32. $^{13}C\{^1H\}$ NMR (CD_2Cl_2, 20 °C) δ: 165-121 (m, Ph+flurenyl), 98.32 (dd, C_5 Cp*), 83.5 (br, N=C), 55.66 (d, CH_3 phos) 9.96 (s, CH_3 Cp*). Anal. Calcd. for $C_{68}H_{67}BN_2O_3OsP_2$ (1223.28): C, 66.77; H, 5.52; B, 0.88; N, 2.29; Found: C, 66.83; H, 5.36; B, 0.98; N, 2.19%; Λ_M = 51.5 $\Omega^{-1}mol^{-1}cm^2$.

34a: IR (KBr, cm^{-1}) ν_{N2} 1935 (m); ^1H NMR (CD_2Cl_2, 20 °C) δ: 7.78-6.87 (m, 45H, Ph), 3.70 (m, 6H, CH_2 phos), 1.56 (s, 15H, CH_3 Cp*), 1.08 (t, 9H, CH_3 phos); $^{31}P\{^1H\}$ NMR (CD_2Cl_2, 20 °C) δ: AX spin syst, δ_A 81.26, δ_X 7.38, J_{AX}=42.28. $^{13}C\{^1H\}$ NMR (CD_2Cl_2, 20 °C) δ: 165-122 (m, Ph), 97.06 (dd, C_5 Cp*), 85.83 (s br, N=C), 65.64 (d, CH_2 phos), 15.90 (d, CH_3 phos), 9.87 (s, CH_3 Cp*). Anal. Calcd. for $C_{71}H_{75}BN_2O_3OsP_2$ (1267.38): C, 67.29; H, 5.97; B, 0.85; N, 2.21; Found: C, 67.30; H, 5.83; B, 0.92; N, 2.17%; Λ_M = 50.9 $\Omega^{-1}mol^{-1}cm^2$.

34b: IR (KBr, cm^{-1}) ν_{N2} 1941 (m); ^1H NMR (CD_2Cl_2, 20 °C) δ: 7.75-6.87 (m, 44H, Ph), 3.70 (m, 6H, CH_2 phos), 3.43 (s, 3H, CH_3 *p*-tolyl), 1.55 (s, 15H, CH_3 Cp*), 1.05 (t, 9H, CH_3 phos); $^{31}P\{^1H\}$ NMR (CD_2Cl_2, 20 °C) δ: AX spin syst, δ_A 81.43, δ_X 7.58, J_{AX}=42.29. Anal. Calcd. for $C_{72}H_{77}BN_2O_3OsP_2$ (1281.41): C, 67.49; H, 6.06; B, 0.84; N, 2.19; Found: C, 67.37; H, 5.96; B, 0.92; N, 2.24%; Λ_M = 52.1 $\Omega^{-1}mol^{-1}cm^2$.

34c: IR (KBr, cm^{-1}) ν_{N2} 1946 (m); ^1H NMR (CD_2Cl_2, 20 °C) δ: 8.40-6.77 (m, 43H, Ph), 3.83 (qnt, 6H, CH_2 phos), 1.66 (s, 15H, CH_3 Cp*), 1.12 (t, 9H, CH_3 phos); $^{31}P\{^1H\}$ NMR (CD_2Cl_2, 20 °C) δ: AX spin syst, δ_A 77.92, δ_X 6.01, J_{AX}=41.79. Anal. Calcd. for $C_{71}H_{73}BN_2O_3OsP_2$ (1265.36): C, 67.39; H, 5.82; B, 0.85; N, 2.21; Found: C, 67.27; H, 5.96; B, 0.73; N, 2.16%; Λ_M = 50.8 $\Omega^{-1}mol^{-1}cm^2$.

$[Os(\eta^5\text{-}C_5Me_5)(\eta^2\text{-}CH_2{=}CH_2)(PPh_3)\{P(OR)_3\}]BPh_4$ (35, 36)
[R = Me (35), Et (36)]

A solution of diazoalkane complex $[Os(\eta^5\text{-}C_5Me_5)(N_2CAr1Ar2)(PPh_3)\{P(OR)_3\}]BPh_4$ (**33, 34**) (0.1 mmol) in 10 mL of dichloroethane was refluxed under an ethylene $CH_2{=}CH_2$ atmosphere (1 atm) for 1 h. The solvent was removed under reduced pressure to leave an oil, which was triturated with ethanol (1 mL) containing $NaBPh_4$ (0.1 mmol, 34 mg). A yellow solid slowly separated out, which was filtered and crystallised from CH_2Cl_2 and ethanol. Yield: 80%.

35: ^1H NMR (CD_2Cl_2, 20 °C) δ: 7.43-6.88 (m, 35H, Ph), 3.48 (d, 9H, CH_3 phos), 2.36 (br), 2.05 (t) (4H, $CH_2{=}CH_2$), 1.43 (s, 15H, CH_3 Cp*); $^{31}P\{^1H\}$ NMR (CD_2Cl_2, 20 °C) δ: AX spin syst, δ_A 78.14, δ_X 4.91, J_{AX}=34.75. $^{13}C\{^1H\}$ NMR (CD_2Cl_2, 20 °C) δ: 164-122 (m, Ph), 96.42 (t, C_5 Cp*), 55.64 (d, CH_3 phos), 26.43 (s br, $CH_2{=}CH_2$), 9.08 (s, CH_3 Cp*). Anal. Calcd. for $C_{57}H_{63}BO_3OsP_2$ (1059.12): C, 64.64; H, 6.00; Found: C, 64.57; H, 5.89%; Λ_M = 51.9 $\Omega^{-1}mol^{-1}cm^2$.

36: ^1H NMR (CD_2Cl_2, 20 °C) δ: 7.58-6.87 (m, 35H, Ph), 3.84 (m, 6H, CH_2 phos), 2.38 (br), 2.05 (m br) (4H, $CH_2{=}CH_2$), 1.42 (s, 15H, CH_3 Cp*), 1.13 (t, 9H, CH_3 phos); $^{31}P\{^1H\}$ NMR (CD_2Cl_2, 20 °C) δ: AX spin syst, δ_A 74.34, δ_X 5.03, J_{AX}=45.60. $^{13}C\{^1H\}$ NMR (CD_2Cl_2, 20 °C) δ: 165-122 (m, Ph), 96.30 (d, C_5 Cp*), 64.78 (d, CH_2 phos), 26.46 (br, $CH_2{=}CH_2$), 15.84 (d, CH_3 phos), 9.10 (s, CH_3 Cp*). Anal. Calcd. for $C_{60}H_{69}BO_3OsP_2$ (1101.20): C, 65.44; H, 6.32; Found: C, 65.37; H, 6.41%; Λ_M = 51.5 $\Omega^{-1}mol^{-1}cm^2$.

$[Os(\eta^5\text{-}C_5Me_5)\{\kappa^2\text{-}CH_2{=}C(H)CN\}(PPh_3)\{P(OMe)_3\}]BPh_4$ (37)

An excess of acrylonitrile $CH_2{=}C(H)CN$ (1.0 mmol, 53 μL) was added to a solution of the diazoalkane complex $[Os(\eta^5\text{-}C_5Me_5)(N_2CC_{12}H_8)(PPh_3)\{P(OMe)_3\}]BPh_4$ (**33c**) (0.1 mmol) in 8 mL of dichloromethane and the reaction mixture was stirred at room temperature for 48 h. The solvent was removed under reduced pressure to leave an oil, which was triturated with ethanol (1 mL) containing $NaBPh_4$ (0.1 mmol, 34 mg). An orange solid slowly separated out, which was filtered and crystallised from CH_2Cl_2 and ethanol. Yield: 75%.

IR (KBr, cm^{-1}) ν_{NC} 2207 (w); ^1H NMR (CD_2Cl_2, 20 °C) δ: 7.71-6.87 (m, 35H, Ph), A_2BCXY spin syst (ABC = ^1H, XY = ^{31}P), δ_A 6.95, δ_B 6.52, δ_C 5.33, J_{AB} = 7.1, J_{AC} = 1.4, J_{AX} = 2.1, J_{AY} = 0.2, J_{BC} = 7.6, J_{BX} = 1.7, J_{BY} = 0.1, J_{CX} = 1.0, J_{CY} = 0.1 [3H, CH_2=C(H)], 3.55 (d, 9H, CH_3 phos), 1.53 (s, 15H, CH_3 Cp*); $^{31}P\{^1H\}$ NMR (CD_2Cl_2, 20 °C) δ: AX spin syst, δ_A 88.75, δ_X 10.97, J_{AX}=40.10. Anal. Calcd. for $C_{58}H_{62}BNO_3OsP_2$ (1084.13): C, 64.26; H, 5.76; N, 1.29; Found: C, 64.15; H, 5.70; N, 1.30%; Λ_M = 52.1 $\Omega^{-1}mol^{-1}cm^2$.

$[Os(\eta^5\text{-}C_5Me_5)(\kappa^1\text{-}N{=}NC(C_{12}H_8)CH{=}CH)(PPh_3)\{P(OR)_3\}]BPh_4$ (38, 39)
[R = Me (38), Et (39)].

A solution of the appropriate diazoalkane complex $[Os(\eta^5\text{-}C_5Me_5)(N_2CC_{12}H_8)(PPh_3)\{P(OR)_3\}]BPh_4$ (**33c, 34c**) (0.1 mmol) in 10 mL of dichloromethane was stirred under acetylene HC≡CH (1 atm) for 48 h. The solvent was removed under reduce pressure to give an oil, which was triturated with ethanol (1 mL) containing an excess of NaBPh4 (0.2 mmol, 68 mg). A yellow-orange solid slowly separated out, which was filtered and crystallised from CH_2Cl_2 and ethanol. Yield ≥78%.

38: ^1H NMR (CD_2Cl_2, 20 °C) δ: 8.40-6.87 (m, 43H, Ph), 7.53 [d, 1H, CH= (C5)], 6.72 [d, 1H, CH= (C4)], 3.57 (d, 9H, CH_3 phos), 1.47 (s, 15H, CH_3 Cp*); $^{31}P\{^1H\}$ NMR (CD_2Cl_2, 20 °C) δ: AX spin syst, δ_A 89.15, δ_X 7.60, J_{AX}=40.10. $^{13}C\{^1H\}$ NMR (CD_2Cl_2, 20 °C) δ: 165-122 (m, Ph+fluorene), 158.13 (s, =C5), 139.39 (s, =C4), 105.38 (br, C3), 95.58 (s, C_5 Cp*), 54.00 (d, CH_3 phos), 9.46 (s, CH_3 Cp*). Anal. Calcd. for $C_{70}H_{69}BN_2O_3OsP_2$ (1249.32): C, 67.30; H, 5.57; N, 2.24; Found: C, 67.27; H, 5.49; N, 2.21%; Λ_M = 50.9 $\Omega^{-1}mol^{-1}cm^2$.

39: ^1H NMR (CD_2Cl_2, 20 °C) δ: 7.87 [d, 1H, CH= (C5)], 7.70-6.87 (m, 43H, Ph), 6.73 [d, 1H, CH= (C4)], 3.84 (qnt, 6H, CH_2 phos), 1.31 (s, 15H, CH_3 Cp*), 1.24 (t, 9H, CH_3 phos); $^{31}P\{^1H\}$ NMR (CD_2Cl_2, 20 °C) δ: AX spin syst, δ_A 84.83, δ_X 7.36, J_{AX}=40.83. $^{13}C\{^1H\}$ NMR (CD_2Cl_2, 20 °C) δ: 165-122 (m, Ph+fluorene), 157.47 (s, =C5), 139.50 (s, =C4), 105.31 (br, C3), 95.57 (s, C_5 Cp*), 63.01 (d, CH_2 phos), 16.01 (d, CH_3 phos), 9.39 (s, CH_3 Cp*). Anal. Calcd. for $C_{73}H_{75}BN_2O_3OsP_2$ (1291.40): C, 67.90; H, 5.85; N, 2.17; Found: C, 67.84; H, 5.92; N, 2.10%; Λ_M = 51.8 $\Omega^{-1}mol^{-1}cm^2$.

$[Os(\eta^5\text{-}C_5Me_5)(=C{=}CH_2)(PPh_3)\{P(OMe)_3\}]BPh_4$ (40a)

In a 25-mL three-necked round-bottomed flask were placed 0.1 mmol of the bromo-compound $[OsBr(\eta^5\text{-}C_5Me_5)(PPh_3)\{P(OMe)_3\}]$, a slight excess of AgOTf (0.11 mmol, 28.3 mg) and 5 mL of toluene. The reaction mixture was stirred in the dark for 1 h, filtered to remove the AgBr formed and then the solution evaporated to dryness under reduced pressure. Dichloromethane (5 mL)

was added and the resulting solution allowed to stand under an acetylene HC≡CH atmosphere (1 atm). After 17 h of stirring, the solvent removed under reduced pressure leaving an oil, which was triturated with ethanol (1 mL) containing $NaBPh_4$ (0.1 mmol, 34 mg). A solid slowly separated out from the resulting solution, which was filtered and dried under vacuum. Yield ≥65%.

IR (KBr, cm^{-1}) $\nu_{Os=C=C}$ 1633 (m); ^1H NMR (CD_2Cl_2, 20 °C) δ: 7.80-6.81 (m, 35H, Ph), 4.42 (m, 2H, $=CH_2$), 3.44 (d, 9H, CH_3 phos), 1.44 (s, 15H, CH_3 Cp*); $^{31}P\{^1H\}$ NMR (CD_2Cl_2, 20 °C) δ: AX spin syst, δ_A 79.55, δ_X 2.83, J_{AX}=33.66. Anal. Calcd. for $C_{57}H_{61}BO_3OsP_2$ (1057.10): C, 64.76; H, 5.82; Found: C, 64.76; H, 5.82%; Λ_M = 52.0 $\Omega^{-1}mol^{-1}cm^2$.

[Os(η^5-C_5Me_5){=C=C(H)R1}(PPh$_3$){P(OR)$_3$}]BPh$_4$ (40, 41)
[R = Me (40), Et (41); R1 = Ph (b), *p*-tolyl (c), COOMe (d)]

Method A: An excess of the appropriate alkyne R1C≡CH (0.3 mmol) was added to a solution of diazoalkane complex [Os(η^5-C_5Me_5)(N_2CAr1Ar2)(PPh_3){$P(OR)_3$}]BPh_4 (**33, 34**) (0.1 mmol) in 5 mL of dichloromethane and the reaction mixture was stirred for 48 h. The solvent was removed under reduced pressure to give an oil, which was triturated with ethanol (1 mL) containing $NaBPh_4$ (0.1 mmol, 34 mg). A pink solid slowly separated out, which was filtered and crystallised from CH_2Cl_2 and ethanol. Yield ≥80%.

Method B: In a 25-mL three-necked round-bottomed flask were placed 0.1 mmol of bromo-compound [OsBr(η^5-C_5Me_5)(PPh_3){$P(OR)_3$}], an excess of $NaBPh_4$ (0.2 mmol, 68 mg), an excess of the appropriate alkyne R1C≡CH (0.3 mmol), 5 mL of ethanol and 5 mL of 1,2-dichloroethane. The reaction mixture was refluxed for 4 h (6 h for **40d**) and then the solvent removed under reduced pressure leaving an oil, which was triturated with ethanol (1 mL) containing $NaBPh_4$ (0.1 mmol, 34 mg). A pink solid slowly separated out, which was filtered and crystallised from CH_2Cl_2 and ethanol. Yield ≥75%.

40b: IR (KBr, cm^{-1}) $\nu_{Os=C=C}$ 1650 (m), 1628 (m); ^1H NMR (CD_2Cl_2, 20 °C) δ: 7.75-6.86 (m, 40H, Ph), 3.44 (d, 9H, CH_3 phos), 3.15 (m, 1H, =CH), 1.66 (s, 15H, CH_3 Cp*); $^{31}P\{^1H\}$ NMR (CD_2Cl_2, 20 °C) δ: AX spin syst, δ_A 81.29, δ_X 7.35, J_{AX}=38.37. $^{13}C\{^1H\}$ NMR (CD_2Cl_2, 20 °C) δ: 316.31 (dd, J_{CP} = 12.7, J_{CP} = 9.1, $=C_\alpha$), 165-122 (m, Ph), 115.69 (s, $=C_\beta$), 102.97 (dd, J_{CP} = 1.7, J_{CP} = 1.3, C_5 Cp*), 55.38 (d, CH_3 phos), 9.84 (s, CH_3 Cp*). Anal. Calcd. for $C_{63}H_{65}BO_3OsP_2$ (1133.20): C, 66.78; H, 5.78; Found: C, 66.80; H, 5.72%; Λ_M = 52.1 $\Omega^{-1}mol^{-1}cm^2$.

40c: IR (KBr, cm^{-1}) $\nu_{Os=C=C}$ 1655 (m), 1632 (m); ^1H NMR (CD_2Cl_2, 20 °C) δ: 7.47-6.87 (m, 39H, Ph), 3.43 (d, 9H, CH_3 phos), 3.13 (m, 1H, =CH), 2.30 (s, 3H, CH_3 *p*-tolyl), 1.65 (dd, 15H, CH_3 Cp*); $^{31}P\{^1H\}$ NMR (CD_2Cl_2, 20 °C) δ: AX spin syst, δ_A 81.54, δ_X 7.56, J_{AX}=38.89. $^{13}C\{^1H\}$ NMR (CD_2Cl_2, 20 °C) δ: 317.46 (dd, J_{CP} = 9.04, J_{CP} = 3.77, $=C_\alpha$), 165-122 (m, Ph), 115.53 (s, $=C_\beta$), 102.88 (s, C_5 Cp*), 55.36 (d, CH_3 phos), 21.03 (s, CH_3 *p*-tolyl), 9.84 (s, CH_3 Cp*). Anal. Calcd. for $C_{64}H_{67}BO_3OsP_2$ (1147.22): C, 67.01; H, 5.89; Found: C, 66.96; H, 5.92%; Λ_M = 51.7 $\Omega^{-1}mol^{-1}cm^2$.

40d: IR (KBr, cm^{-1}) ν_{CO} 1699 (s), $\nu_{Os=C=C}$ 1662 (m), 1604 (m); ^1H NMR (CD_2Cl_2, 20 °C) δ: 7.82-6.90 (m, 35H, Ph), 3.55 (s, 3H, CH_3OC), 3.47 (d, 9H, CH_3 phos), 2.83 (m, 1H, =CH), 1.69 (s, 15H, CH_3 Cp*); $^{31}P\{^1H\}$ NMR (CD_2Cl_2, 20 °C) δ: AX spin syst, δ_A 80.07, δ_X 5.61, J_{AX}=39.70. $^{13}C\{^1H\}$ NMR (CD_2Cl_2, 20 °C) δ: 310.99 (dd, J_{CP} = 12.8, J_{CP} = 9.10, $=C_\alpha$), 165-122 (m, Ph), 161.50 (s, COO), 107.43 (s, $=C_\beta$), 103.63 (d, C_5 Cp*), 55.25 (d, CH_3 phos), 51.42 (d, CH_3COO), 9.61 (s, CH_3 Cp*). Anal. Calcd. for $C_{59}H_{63}BO_5OsP_2$ (1115.14): C, 63.55; H, 5.69; Found: C, 63.43; H, 5.72%; Λ_M = 52.3 $\Omega^{-1}mol^{-1}cm^2$.

41c: IR (KBr, cm^{-1}) $\nu_{Os=C=C}$ 1637 (s); ^1H NMR (CD_2Cl_2, 20 °C) δ: 7.43-6.87 (m, 39H, Ph), 3.77 (qnt, 6H, CH_2 phos), AXD spin syst (D= ^1H, AX= ^{31}P) δ_D 3.15, J_{AD} 34.0, J_{XD} 1.7 (=CH), 2.39 (s, 3H, CH_3 *p*-tolyl), 1.65 (s, 15H, CH_3 Cp*), 1.13 (t, 9H, CH_3 phos); $^{31}P\{^1H\}$ NMR (CD_2Cl_2, 20 °C) δ: AX spin syst, δ_A 77.07, δ_X 7.24, J_{AX}=37.42. $^{13}C\{^1H\}$ NMR (CD_2Cl_2, 20 °C) δ: 317.27 (dd, J_{CP} = 12.8, J_{CP} = 9.20, $=C_\alpha$), 165-122 (m, Ph), 115.42 (s, $=C_\beta$), 102.57 (s, C_5 Cp*), 64.43 (d, CH_2 phos), 20.00 (d, CH_3 *p*-tolyl), 15.93 (d, CH_3 phos), 9.78 (s, CH_3 Cp*). Anal. Calcd. for $C_{67}H_{73}BO_3OsP_2$ (1189.31): C, 67.66; H, 6.19; Found: C, 67.61; H, 6.23%; Λ_M = 51.6 $\Omega^{-1}mol^{-1}cm^2$.

[Os(η^5-C_5Me_5)(κ^2-O_2)(PPh_3){$P(OR)_3$}]BPh_4 (42, 43)
[R = Me (42), Et (43)].

Method A: A solution of diazoalkane complex [Os(η^5-C_5Me_5)(N_2CAr1Ar2)(PPh_3){$P(OR)_3$}]BPh_4 (**33, 34**) (0.1 mmol) in 5 mL of dichloromethane was stirred under/in air (1 atm) for 48 h. The solvent was removed under reduced pressure to give an oil, which was triturated with ethanol (1 mL) containing $NaBPh_4$ (0.1 mmol, 34 mg). A yellow solid slowly separated out, which was filtered and twice crystallised from CH_2Cl_2 and ethanol. Yield: 70%.

Method B: In a 25-mL three-necked round-bottomed flask were placed 0.1 mmol of bromo-compound [OsBr(η^5-C_5Me_5)(PPh_3){$P(OR)_3$}], an excess of $NaBPh_4$ (0.2 mmol, 68 mg), 5 mL of CH_2Cl_2 and 5 mL of ethanol. The solution was stirred under/in air (1 atm) for 48 h. The solvent was removed under reduced pressure to give an oil, which was triturated with ethanol (1 mL)

containing $NaBPh_4$ (0.1 mmol, 34 mg). A yellow solid slowly separated out, from the resulting solution, which was filtered and crystallised from CH_2Cl_2 and ethanol. Yield: 75%.

42: ^1H NMR (CD_2Cl_2, 20 °C) δ: 7.48-6.87 (m, 35H, Ph), 3.54 (d, 9H, CH_3 phos), 1.47 (s, 15H, CH_3 Cp*); $^{31}P\{^1H\}$ NMR (CD_2Cl_2, 20 °C) δ: AX spin syst, δ_A 52.67, δ_X –11.43, J_{AX}=53.46. Anal. Calcd. for $C_{55}H_{59}BO_5OsP_2$ (1063.06): C, 62.14; H, 5.59; Found: C, 62.11; H, 5.52%; Λ_M = 50.8 $\Omega^{-1}mol^{-1}cm^2$.

43: ^1H NMR (CD_2Cl_2, 20 °C) δ: 7.47-6.87 (m, 35H, Ph), 3.96 (m, 6H, CH_2 phos), 1.53 (s, 15H, CH_3 Cp*), 1.06 (t, 9H, CH_3 phos); $^{31}P\{^1H\}$ NMR (CD_2Cl_2, 20 °C) δ: AX spin syst, δ_A 47.18, δ_X –11.05, J_{AX}=53.71. Anal. Calcd. for $C_{58}H_{65}BO_5OsP_2$ (1105.14): C, 63.04; H, 5.93; Found: C, 62.96; H, 6.01%; Λ_M = 52.0 $\Omega^{-1}mol^{-1}cm^2$.

$[Os(\eta^5\text{-}C_5Me_5)(=C=C=CPh_2)(PPh_3)\{P(OR)_3\}]BPh_4$ (44, 45)
[R = Me (44), Et (45)].

In a 25-mL three-necked round-bottomed flask were placed 0.1 mmol of bromo-compound $[OsBr(\eta^5\text{-}C_5Me_5)(PPh_3)\{P(OR)_3\}]$, an excess of $NaBPh_4$ (0.2 mmol, 68 mg), an excess of the propargylic alcohol $HC{\equiv}CC(Ph_2)OH$ (0.4 mmol, 83 mg), 5 mL of ethanol and 5 mL of 1,2-dichloroethane. The reaction mixture was refluxed for 4 h and then the solvent was removed under reduced pressure to give an oil, which was triturated with ethanol (1 mL). A dark-red solid slowly separated out, which was filtered and crystallised from CH_2Cl_2 and ethanol. Yield: 70%.

44: IR (KBr, cm^{-1}) $\nu_{=C=C=C}$ 1925 (s); ^1H NMR (CD_2Cl_2, 20 °C) δ: 7.89-6.87 (m, 45H, Ph), 3.41 (d, 9H, CH_3 phos), 1.65 (s, 15H, CH_3 Cp*); $^{31}P\{^1H\}$ NMR (CD_2Cl_2, 20 °C) δ: AX spin syst, δ_A 82.71, δ_X 10.39, J_{AX}=40.59. $^{13}C\{^1H\}$ NMR (CD_2Cl_2, 20 °C) δ: 259.81 (dd, $=C_\alpha$), 217.10 (dd, $=C_\beta$), 165-122 (m, Ph), 146.20 (s, $=C_\gamma$), 101.94 (d, C_5 Cp*), 54.04 (d, CH_3 phos), 9.79 (s, CH_3 Cp*). Anal. Calcd. for $C_{70}H_{69}BO_3OsP_2$ (1221.31): C, 68.84; H, 5.69; Found: C, 68.90; H, 5.65%; Λ_M = 52.1 $\Omega^{-1}mol^{-1}cm^2$.

45: IR (KBr, cm^{-1}) $\nu_{=C=C=C}$ 1921 (s); ^1H NMR (CD_2Cl_2, 20 °C) δ: 7.86-6.86 (m, 45H, Ph), 3.80 (qnt, 6H, CH_2 phos), 1.63 (s, 15H, CH_3 Cp*), 1.09 (t, 9H, CH_3 phos); $^{31}P\{^1H\}$ NMR (CD_2Cl_2, 20 °C) δ: AX spin syst, δ_A 78.29, δ_X 10.57, J_{AX}=40.95. $^{13}C\{^1H\}$ NMR (CD_2Cl_2, 20 °C) δ: 259.41 (dd, J_{CP} = 10.3, J_{CP} = 5.2, $=C_\alpha$), 218.63 (dd, J_{CP} = 5.4, J_{CP} = 1.4, $=C_\beta$), 165-122 (m, Ph), 145.10 (s, $=C_\gamma$), 101.98 (d, C_5 Cp*), 63.61 (d, CH_2 phos), 15.86 (d, CH_3 phos), 9.79 (s, CH_3 Cp*). Anal. Calcd. for $C_{73}H_{75}BO_3OsP_2$ (1263.39): C, 69.40; H, 5.98; Found: C, 69.40; H, 5.98%; Λ_M = 51.3 $\Omega^{-1}mol^{-1}cm^2$.

[Os(η^5-C_5Me_5){=C=C=C(Me)Ph}(PPh_3){P($OMe)_3$}]BPh_4 (46)
[Os(η^5-C5Me_5){=C=C(H)C(Ph)=CH_2}(PPh_3){P($OMe)_3$}]BPh_4 (47)

In a 25-mL three-necked round-bottomed flask were placed 0.2 mmol (158 mg) of bromo-compound [OsBr(η^5-C_5Me_5)(PPh_3){P($OMe)_3$}], an excess of $NaBPh_4$ (0.4 mmol, 136 mg), an excess of the propargylic alcohol HC≡CC(Me)(Ph)OH (0.8 mmol, 117 mg), 5 mL of ethanol and 10 mL of 1,2-dichloroethane. The reaction mixture was refluxed for 4 h and then the solvent was removed under reduced pressure to give an oil, which was triturated with ethanol (1 mL). The reddish-brown solid that slowly separated out was filtered and fractionally crystallised from CH_2Cl_2 and ethanol. A typical crystallisation involved slow cooling up to 25 °C of a solution of the compound prepared in ethanol (4 mL) and enough dichloromethane to obtain a saturated solution at room temperature. In any case, no separation of the two compounds was observed, since the various fractions always contained the same ratio. Yield about 40%.

46: IR (KBr, cm^{-1}) $\nu_{=C=C=C}$ 1933 (s); ^{1}H NMR (CD_2Cl_2, 20 °C) δ: 8.14-6.86 (m, 40H, Ph), 3.41 (d, 9H, CH_3 phos), 1.80 (s, 3H, C=CH_3), 1.68 (s, 15H, CH_3 Cp*); ^{31}P{^{1}H} NMR (CD_2Cl_2, 20 °C) δ: AX spin syst, δ_A 81.85, δ_X 12.15, J_{AX}=38.88. ^{13}C{^{1}H} NMR (CD_2Cl_2, 20 °C) δ: 260.99 (dd, =C_α), 210.52 (dd, =C_β), 165-122 (m, Ph), 149.68 (s, =C_γ), 101.18 (d, C_5 Cp*), 54.04 (d, CH_3 phos), 10.02 (s, CH_3C=), 9.79 (s, CH_3 Cp*). Anal. Calcd. for $C_{65}H_{67}BO_3OsP_2$ (1159.24): C, 67.35; H, 5.83; Found: C, 67.42; H, 5.79%; Λ_M = 51.5 $\Omega^{-1}mol^{-1}cm^2$.

47: IR (KBr, cm^{-1}) $\nu_{Os=C=C}$ 1631 (m); ^{1}H NMR (CD_2Cl_2, 20 °C) δ: 7.82-6.87 (m, 40H, Ph), 5.15 (d, 2H, =CH_2), 3.36 (d, 9H, CH_3 phos), 2.72 (m, 1H, =CH), 1.66 (s, 15H, CH_3 Cp*); ^{31}P{^{1}H} NMR (CD_2Cl_2, 20 °C) δ: AX spin syst, δ_A 82.63, δ_X 6.98, J_{AX}=40.20. ^{13}C{^{1}H} NMR (CD_2Cl_2, 20 °C) δ: 314.29 (dd, J_{CP} = 12.6, J_{CP} = 9.3, =C_α), 165-122 (m, Ph), 146.68 (s, =C_γ), 114.04 (s, =C_β), 113.68 (s, =C_δ), 102.40 (s, C_5 Cp*), 55.06 (d, CH_3 phos), 9.79 (s, CH_3 Cp*). Anal. Calcd. for $C_{65}H_{67}BO_3OsP_2$ (1159.24): C, 67.35; H, 5.83; Found: C, 67.29; H, 5.81%; Λ_M = 51.9 $\Omega^{-1}mol^{-1}cm^2$.

[Os(η^5-C_5Me_5){=C=C(H)C(H)Ph(OH)}(PPh_3){P($OMe)_3$}]BPh_4 (48)
[Os(η^5-C_5Me_5){=C=C(H)CH_2(OH)}(PPh_3){P($OMe)_3$}]BPh_4 (49)

These complexes were prepared by refluxing [OsBr(η^5-C_5Me_5)(PPh_3){P($OMe)_3$}] with an excess of the appropriate propargylic alcohol HC≡CC(H)(Ph)OH or HC≡CC(H_2)OH (0.8 mmol, 45 μL), following the method used for **44a** and **45a**, **43b** and **44b**. Yield: 75%.

48: IR (KBr, cm^{-1}) $\nu_{Os=C=C}$ 1653 (m); ^{1}H NMR (CD_2Cl_2, 20 °C) δ: 7.55-6.87 (m, 40H, Ph), 5.10 (d, 1H, =CH(Ph)), 3.38 (d, 9H, CH_3 phos), 2.49 (m, 1H, =CH), 1.61 (s, 15H, CH_3 Cp*); $^{31}P\{^{1}H\}$ NMR (CD_2Cl_2, 20 °C) δ: AX spin syst, δ_A 83.05, δ_X 8.17, J_{AX}=40.80. $^{13}C\{^{1}H\}$ NMR (CD_2Cl_2, 20 °C) δ: ABX spin syst. δ_X 308.67 (J_{AX} = 12.5, J_{BX} = 9.10, =C_α), 165-122 (m, Ph), 115.10 (s, =C_β), 102.40 (s, C_5 Cp*), 70.64 (s, CH), 54.72 (d, CH_3 phos), 9.70 (s, CH_3 Cp*). Anal. Calcd. for $C_{58}H_{63}BO_4OsP_2$ (1087.13): C, 64.08; H, 5.84; Found: C, 64.12; H, 5.76%; Λ_M = 51.4 $\Omega^{-1}mol^{-1}cm^2$.

49: IR (KBr, cm^{-1}) $\nu_{Os=C=C}$ 1647 (m); ^{1}H NMR (CD_2Cl_2, 20 °C) δ: 7.59-6.87 (m, 35H, Ph), ABCXY spin syst (AB = CH_2, C = HC=, XY = ^{31}P) δ_A = δ_B 4.20, δ_C 2.56, J_{AB} = 7.8, J_{AC} = 7.4, J_{AX} = 2.3, J_{AY} = 0.4, J_{BC} = 8.2, J_{BX} = 2.2, J_{BY} = 1.1, J_{CX} = 2.7, J_{CY} = 1.4 (3H, =C(H)CH_2), 3.41 (d, 9H, CH_3 phos), 1.65 (s, 15H, CH_3 Cp*); $^{31}P\{^{1}H\}$ NMR (CD_2Cl_2, 20 °C) δ: AX spin syst, δ_A 83.01, δ_X 9.01, J_{AX}=40.10. $^{13}C\{^{1}H\}$ NMR (CD_2Cl_2, 20 °C) δ: 309.65 (dd, J_{CP} = 8.5, J_{CP} = 3.6, =C_α), 165-122 (m, Ph), 107.95 (s, =C_β), 102.20 (s, C_5 Cp*), 57.88 [s, CH_2(OH)], 54.76 (d, J_{CP} = 9.8, CH_3 phos), 9.58 (s, CH_3 Cp*).

[Os(η^5-C_5Me_5){κ^1-C(H)=C(H)PPh_3}(PPh_3){P($OMe)_3$}]BPh_4 (50)

In a 25-mL three-necked round-bottomed flask were placed 0.1 mmol (122 mg) of the bromo-compound [OsBr(η^5-C_5Me_5)(PPh_3){P($OMe)_3$}], a slight excess of AgOTF (0.11 mmol, 28 mg) and5 mL of toluene. The reaction mixture was stirred in the dark for 1 h, filtered to remove the AgCl formed and, after addition of 5 mL of dichloromethane, allowed to stand under acetylene HC≡CH (1 atm). After 17 h of stirring, an excess of PPh_3 (0.3 mmol, 79 mg) was added and the reaction mixture stirred for another 24 h. The solvent was removed under reduced pressure to give an oil, which was triturated with ethanol (1 mL) containing an excess of $NaBPh_4$ (0.2 mmol, 68 mg). A reddish-brown solid slowly separated out, which was filtered and crystallised from CH_2Cl_2 and ethanol. Yield: 70%.

^{1}H NMR (CD_2Cl_2, 20 °C) δ: AXYDE spin syst (DE = ^{1}H, AXY = ^{31}P) δ_D 11.20, δ_E 6.24, J_{AD} = 3.7, J_{AE} = 1.5, J_{XD} = 2.2, J_{XE} = 1.4, J_{YD} = 32.1, J_{YE} = 38.9, J_{DE} = 17.8 (2H, CH=CH), 7.71-6.86 m (m, 50H, Ph), 3.22 (d, 9H, CH_3 phos), 1.42 (s, 15H, CH_3 Cp*); $^{31}P\{^{1}H\}$ NMR (CD_2Cl_2, 20 °C) δ: AXY spin syst, δ_A 89.90, δ_X 16.06, δ_Y 10.48, J_{AX}=38.60, J_{AY} = 4.4, J_{XY} = 5.7. $^{13}C\{^{1}H\}$ NMR (CD_2Cl_2, 20 °C) δ: AXYN spin syst. δ_N 191.09 (J_{AN} = 10.0, J_{XN} = 8.7, J_{YN} = 12.6, =C_α), 165-122 (m, Ph), 98.54 (d, J_{CP} = 7.5, C_β), 93.52 (dd, C_5 Cp*), 54.61 (d, CH_3 Cp*), 9.60 (s, CH_3 Cp*). Anal. Calcd. for $C_{75}H_{76}BO_3OsP_3$ (1319.39): C, 68.28; H, 5.81; Found: C, 68.35; H, 5.72%; Λ_M = 52.2 $\Omega^{-1}mol^{-1}cm^2$.

$[Os(\eta^5\text{-}C_5Me_5)(CO)(PPh_3)\{P(OR)_3\}]BPh_4$ (51, 52)
[R = Me (51), Et (52)].

An excess of H_2O (0.4 mmol, 7.2 µL) was added to a solution of the appropriate vinylidene complex $[Os(\eta^5\text{-}C_5Me_5)\{=C=C(H)Ph\}(PPh_3)\{P(OR)_3\}]BPh_4$ (**40b, 41b**) in 5 mL of dichloromethane and the reaction mixture was stirred for 24 h. The solvent was removed under reduced pressure to give an oil, which was triturated with ethanol (1 mL) containing $NaBPh_4$ (0.1 mmol, 34 mg). A yellow solid slowly separated out, which was filtered and crystallised from CH_2Cl_2 and ethanol. Yield: 75%.

51: IR (KBr, cm^{-1}) ν_{CO} 1951 (s); ^1H NMR (CD_2Cl_2, 20 °C) δ: 7.70-6.89 (m, 35H, Ph), 3.44 (d, 9H, CH_3 phos), 1.70 (s, 15H, CH_3 Cp*); $^{31}P\{^1H\}$ NMR (CD_2Cl_2, 20 °C) δ: AX spin syst, δ_A 84.82, δ_X 9.27, J_{AX}=33.79. $^{13}C\{^1H\}$ NMR (CD_2Cl_2, 20 °C) δ: 183.65 (dd, J_{CP} = 15.7, J_{CP} = 10.7, CO), 165-122 (m, Ph), 98.69 (dd, C_5 Cp*), 54.61 (d, CH_3 phos), 9.61 (s, CH_3 Cp*). Anal. Calcd. for $C_{56}H_{59}BO_4OsP_2$ (1059.07): C, 63.51; H, 5.62; Found: C, 63.41; H, 5.57%; Λ_M = 51.7 $\Omega^{-1}mol^{-1}cm^2$.

52: IR (KBr, cm^{-1}) ν_{CO} 1944 (s); ^1H NMR (CD_2Cl_2, 20 °C) δ: 7.70-6.87 (m, 35H, Ph), 3.85 (m, 6H, CH_2 phos), 1.69 (s, 15H, CH_3 Cp*), 1.14 (t, 9H, CH_3 phos); $^{31}P\{^1H\}$ NMR (CD_2Cl_2, 20 °C) δ: AX spin syst, δ_A 80.31, δ_X 9.73, J_{AX}=34.82. Anal. Calcd. for $C_{59}H_{65}BO_4OsP_2$ (1101.15): C, 64.36; H, 5.95; Found: C, 64.43; H, 6.03%; Λ_M = 50.9 $\Omega^{-1}mol^{-1}cm^2$.

6.12 Preparation of Precursors of Osmium

The complexes $[OsBr(\eta^5\text{-}C_5H_5)(PPh_3)_2]$ and $[OsBr(\eta^5\text{-}C_5Me_5)(PPh_3)\{P(OR)_3\}]$ were prepared following the methods previouslyreported.[145,155]

- **$[OsBr(\eta^5\text{-}C_5H_5)(PPh_3)_2]$**

An ampule of OsO_4 (1.0 g, 3.93 mmol) was broken in a flask containing HBr (40 mL), and the red solution was heated at reflux for 2h in air. Water and excess HBr were removed from the mixture by distillation at 50 °C under vacuum, leaving a dark red residue. The residue was dissolved in absolute ethanol (20 mL) and added to a stirred, boiling solution of triphenylphosphine (6.30 g, 24.0 mmol) in ethanol (180 mL), followed immediately by a solution of freshly distilled cyclopentadiene (10 mL) in ethanol (20 mL). Water (25 mL) was then added to the mixture via syringe, and the crimson suspension was heated at reflux for 2 h, resulting in a colour change to orange. After the reaction mixture was cooled to room temperature, the resulting orange-yellow powder was filtered, washed with ethanol (210 mL) and hexane (210 mL), and dried under

vacuum. The orange filtrate was concentrated to 40 mL and cooled to -35 °C to obtain the remaining product. Total yield: 97%.

- **[OsBr(η^5-C_5H_5)(PPh_3){$P(OR)_3$}]**
  [R = Me, Et].

An excess of the appropriate phosphite $P(OR)_3$ (8 mmol) was added to a solution of [OsBr(η^5-C_5H_5)(PPh_3)$_2$] (1.72 g, 2 mmol) in 50 mL of toluene and the reaction mixture was refluxed for 1 h. The solvent was removed under reduced pressure to leave an oil, which was triturated at 0 °C with ethanol (2 mL). A yellow solid slowly separated out, which was filtered and dried under vacuum. Yield ≥80%.

R = Me. ^{1}H NMR (CD_2Cl_2, 20 °C) δ: 7.52, 7.32 (m, 15H, Ph),4.65 (s, 5H, Cp), 3.41 (d, 9H, CH_3); $^{31}P\{^1H\}$ NMR (CD_2Cl_2, 20 °C) δ: AX spin syst, δ_A 100.45, δ_X 6.55, J_{AX}= 41.4. Anal. Calcd. for $C_{26}H_{29}BrO_3OsP_2$ (721.59): C, 43.28; H, 4.05; Br, 11.07; Found: C, 43.41; H, 3.96; Br, 11.28%.

R = Et. ^{1}H NMR (CD_2Cl_2, 20 °C) δ: 7.54, 7.37 (m, 15H, Ph),4.64 (s, 5H, Cp), 3.87 (m, 6H, CH_2), 1.10 (t, 9H, CH_3); $^{31}P\{^1H\}$ NMR (CD_2Cl_2, 20 °C) δ: AX spin syst, δ_A 94.80, δ_X 7.96, J_{AX}= 42.4. Anal. Calcd. for $C_{29}H_{35}BrO_3OsP_2$ (763.67): C, 45.61; H, 4.62; Br, 10.46; Found: C, 45.39; H, 4.55; Br, 10.32%.

6.13 Preparation of New Complexes: Azides of Osmium.

[Os(η^5-C_5H_5)(κ^1-N_3R1)(PPh_3){$P(OR)_3$}]BPh_4 **(53, 54)**
[R = Me (53), Et (54); R1 = $CH_2C_6H_5$ (a), $CH_2C_6H_4$-4-CH_3 (b), $CH(CH_3)C_6H_5$ (c)].

In a 25 mL three-necked round-bottomed flask covered with an aluminium foil were placed 0.14 mmol of the appropriate complex [OsBr(η^5-C_5H_5)(PPh_3){$P(OR)_3$}], a slight excess of AgOTf (0.15 mmol, 39 mg) and 5 mL of toluene. The reaction mixture was stirred for 75 min and then filtered on paper to remove the AgBr formed. An excess of the appropriate azide N_3R1 (0.18 mmol) was added to the resulting solution, which was stirred at 0 °C for 3 h. The triflate complex [Os(η^5-C_5H_5)(κ^1-N_3R1)(PPh_3){$P(OR)$}]OTf slowly separated out as a dark-green gummy material. The solvent was removed under reduced pressure to give an oil, which was triturated at 0 °C with ethanol (1 mL) containing an excess of $NaBPh_4$ (0.28 mmol, 96 mg). A green solid slowly separated out, which was filtered and crystallised at 0 °C from CH_2Cl_2 and ethanol. Yield ≥80%.

53a: IR (KBr, cm^{-1}) ν_{NNN} 2147 (m); ^{1}H NMR (CD_2Cl_2, 20 °C) δ: 7.85–6.87 (m, 40H, Ph), 4.97 (s, 5H, Cp), 4.86 (s, 2H, CH_2),3.40 (d, 9H, CH_3); $^{31}P\{^1H\}$ NMR (CD_2Cl_2, 20 °C) δ: AX spin syst, δ_A 87.70, δ_X

4.43, J_{AX}= 37.25. Anal. Calcd. for $C_{57}H_{56}BN_3O_3OsP_2$ (1094.06): C, 62.58; H, 5.16; N, 3.84; Found: C, 62.34; H, 5.27; N, 3.72%; Λ_M = 52.3 $\Omega^{-1}mol^{-1}cm^2$.

53b: IR (KBr, cm^{-1}) ν_{NNN} 2164 (m); ^1H NMR (CD_2Cl_2, 20 °C)δ: 7.60–6.88 (m, 39H, Ph), 4.99 (s, 5H, Cp), 4.85 (s, 2H, CH_2), 3.47 (d, 9H, CH_3 phos), 2.37 (s, 3H, CH_3 *p*-tolyl); $^{31}P\{^1H\}$ NMR(CD_2Cl_2, 20 °C) δ: AX spin syst, δ_A 87.79, δ_X 4.69, J_{AX}= 37.79. Anal. Calcd. for $C_{58}H_{58}BN_3O_3OsP_2$ (1108.09): C, 62.87; H, 5.28; N, 3.79; Found: C, 62.66; H, 5.20; N, 3.88%; Λ_M = 52.8 $\Omega^{-1}mol^{-1}cm^2$.

53c: IR (KBr, cm^{-1}) ν_{NNN} 2146 (m); ^1H NMR [$(CD_3)_2CO$,20 °C] δ: 7.65–6.87 (m, 40H, Ph), 5.39 (s, 5H, Cp), 3.52 (q, 1H,CHN), 3.48 (d, 9H, CH_3 phos), 1.75 (d, 3H, CH_3-CHN); $^{31}P\{^1H\}$NMR [$(CD_3)_2CO$, 20 °C] δ: AX spin syst, δ_A 89.40, δ_X 5.34, J_{AX}= 37.55. Anal. Calcd. for $C_{58}H_{58}BN_3O_3OsP_2$ (1108.09): C, 62.87; H,5.28; N, 3.79; Found: C, 62.64; H, 5.38; N, 3.70%; ΛM = 53.4$\Omega^{-1}mol^{-1}cm^2$.

54a: IR (KBr, cm^{-1}) ν_{NNN} 2147 (m); ^1H NMR [$(CD_3)_2CO$,20 °C] δ: 7.55–6.77 (m, 40H, Ph), 3.57 (s, 5H, Cp), 4.97 (s, 2H,CH_2N), 3.55 (m, 6H, CH_2 phos), 1.12 (t, 9H, CH3); $^{31}P\{^1H\}$NMR [$(CD_3)_2CO$, 20 °C] δ: AX spin syst, δ_A 82.98, δ_X 5.88, J_{AX}= 37.25. Anal. Calcd. for $C_{60}H_{62}BN_3O_3OsP_2$ (1136.14): C, 63.43; H, 5.50; N, 3.70; Found: C, 63.24; H, 5.41; N, 3.79%; Λ_M = 52.8$\Omega^{-1}mol^{-1}cm^2$.

54b: IR (KBr, cm^{-1}) ν_{NNN} 2145 (m); ^1H NMR (CD_2Cl_2, 20 °C)δ: 7.60–6.87 (m, 39H, Ph), 4.96 (s, 5H, Cp), 4.80 (s, 2H, CH_2N), 3.86 (m, 6H, CH_2 phos), 2.37 (s, 3H, CH_3 *p*-tolyl), 1.16 (t, 9H, CH_3 phos); $^{31}P\{^1H\}$ NMR (CD_2Cl_2, 20 °C) δ: AX spin syst, δ_A 81.73, δ_X 5.36, J_{AX}= 37.79. Anal. Calcd. for $C_{61}H_{64}BN_3O_3OsP_2$ (1150.17): C, 63.70; H, 5.61; N, 3.65; Found: C, 63.47; H, 5.52; N, 3.76%; Λ_M = 52.5 $\Omega^{-1}mol^{-1}cm^2$.

54c: IR (KBr, cm^{-1}) ν_{NNN} 2146 (m); ^1H NMR [$(CD_3)_2CO$,20 °C] δ: 7.50–6.77 (m, 40H, Ph), 5.39 (s, 5H, Cp), 4.03 (m, 6H,CH_2 phos), 3.56 (q, 1H, CHN), 1.77 (d, 3H, CH_3-CHN), 1.18 (t,9H, CH_3 phos); $^{31}P\{^1H\}$ NMR [$(CD_3)_2CO$, 20 °C] δ: AX spin syst, δ_A 83.05, δ_X 5.98, J_{AX}= 37.90. Anal. Calcd. for $C_{61}H_{64}BN_3O_3OsP_2$ (1150.17): C, 63.70; H, 5.61; N, 3.65; Found: C, 63.51; H, 5.73; N, 6.54%; Λ_M = 53.1 $\Omega^{-1}mol^{-1}cm^2$.

$[Os(\eta^5\text{-}C_5H_5)(\kappa^1\text{-}N_3Ph)(PPh_3)\{P(OMe)_3\}]BPh_4$ **(53d)**

In a 25 mL three-necked round-bottomed flask covered with an aluminium foil were placed $[OsBr(\eta^5\text{-}C_5H_5)(PPh_3)\{P(OMe)_3\}]$ (0.14 mmol, 100 mg), a slight excess of AgOTf (0.15 mmol, 39 mg) and 5 mL of toluene. The reaction mixture was stirred for 75 min and then filtered on paper to

remove the AgBr formed. An excess of phenylazide $C_6H_5N_3$ (0.18 mmol, 21.5 μL) was added to the resulting solution, cooled to −196 °C. The reaction mixture was left to reach 0 °C and then stirred at this temperature for 1 h. The azidecomplex $[Os(\eta^5\text{-}C_5H_5)(\kappa^1\text{-}N_3C_6H_5)(PPh_3)\{P(OMe)_3\}]OTf$ separate out from the solution as an oil. The solvent was removed under reduced pressure leaving an oil, which was triturated at 0 °C with ethanol (1 mL) containing an excess of $NaBPh_4$ (0.28 mmol, 95 mg). A green solid slowly separated out, which was filtered and crystallised at 0 °C from CH_2Cl_2 and ethanol. Yield ≥65%.

IR (KBr, cm^{-1}) ν_{NNN} 2164 (m); ^1H NMR (CD_2Cl_2,20 °C) δ: 7.70–6.88 (m, 40H, Ph), 4.98 (s, 5H, Cp), 3.48 (d, 9H, CH_3); $^{31}P\{^1H\}$ NMR (CD_2Cl_2, 20 °C) δ: AX spin syst, δ_A 89.73, δ_X 5.99, J_{AX}= 38.90. Anal. Calcd. for $C_{56}H_{54}BN_3O_3OsP_2$ (1080.03): C, 62.28; H, 5.04; N, 3.89; Found: C, 62.08; H, 5.13; N, 3.98%; Λ_M = 51.9 $\Omega^{-1}mol^{-1}cm^2$.

$[Os(\eta^5\text{-}C_5H_5)(\kappa^1\text{-}^{15}N_3CH_2C_6H_4\text{-}4\text{-}CH_3)(PPh_3)\{P(OR)_3\}]BPh_4$ **(53b$_1$,54b$_1$)**
$[Os(\eta^5\text{-}C_5H_5)\{\kappa^1\text{-}^{15}N_3C(H)(CH_3)C_6H_5\}(PPh_3)\{P(OMe)_3\}]BPh_4$ **(53c$_1$)**

These complexes were prepared exactly like the related unlabelled derivatives **53b**, **54b** and **53c**, using labelled azides 4-$CH_3C_6H_4CH_2{}^{15}N_3$ and $C_6H_5C(H)(CH_3)^{15}N_3$ as reagents.

53b$_1$: IR (KBr, cm^{-1}) ν_{15NNN} 2114 (m); $^{31}P\{^1H\}$ NMR (CD_2Cl_2,20 °C) δ: AXN spin syst, δ_A 88.20, δ_X 5.10, J_{AX}= 37.7, J_{AN}= 3.5, J_{XN} = 2.0; 15N NMR (CD_2Cl_2, 20 °C) δ: 213.6 (s, Nα), 139.4(m, Nγ).

53c$_1$: IR (KBr, cm^{-1}) ν_{15NNN} 2105 (m); $^{31}P\{^1H\}$ NMR (CD_2Cl_2,20 °C) δ: AXN spin syst, δ_A 88.21, δ_X 5.01, J_{AX}= 38.8, J_{AN}= 4.0, J_{XN} = 1.5; 15N NMR (CD_2Cl_2, 20 °C) δ: 213.4 (s, Nα), 117.9(m, Nγ).

54b$_1$: IR (KBr, cm^{-1}) ν_{15NNN} 2117 (m); $^{31}P\{^1H\}$ NMR (CD_2Cl_2,20 °C) δ: AXN spin syst, δ_A 82.16, δ_X 5.72, J_{AX}= 38.0, J_{AN}= 4.0, J_{XN} = 1.5.

$[Os(\eta^5\text{-}C_5H_5)\{\kappa^1\text{-}NH{=}C(H)R1\}(PPh_3)\{P(OR)_3\}]BPh_4$ **(55, 56)**
[R = Me (55), Et (56); R1 = C_6H_5 (a), 4-$CH_3C_6H_4$ (b)]
$[Os(\eta^5\text{-}C_5H_5)\{\kappa^1\text{-}NH{=}C(CH_3)C_6H_5\}(PPh_3)\{P(OR)_3\}]BPh_4$ **(55c,56c)**

Method A: A solution of the appropriate azide complex $[Os(\eta^5\text{-}C_5H_5)(\kappa^1\text{-}N_3R1)(PPh_3)\{P(OR)_3\}]BPh_4$ (**53, 54**) (0.1 mmol) in CH_2Cl_2 (5 mL) was stirred at room temperature for 2 h. The solvent was removed under reduced pressure to give an oil, which was triturated with ethanol (1 mL). A

yellow-green solid slowly separated out, which was filtered and crystallised from CH_2Cl_2 and ethanol. Yield ≥85%.

Method B: In a 25 mL three-necked round-bottomed flask covered with an aluminium foil were placed 0.14 mmol of the appropriate complex [OsBr(η^5-C_5H_5)(PPh_3){$P(OR)_3$}], a slight excess of AgOTf (0.15 mmol, 39 mg) and 5 mL of toluene. The reaction mixture was stirred for 75 min and then filtered on paper to remove the AgBr formed. An excess of the appropriate azide (0.18 mmol) in 5 mL of CH_2Cl_2 was added to the resulting solution, which was stirred at room temperature for 4 h. The solvent was removed under reduced pressure to give an oil, which was triturated with ethanol (1 mL) containing an excess of $NaBPh_4$ (0.28 mmol, 96 mg). A yellow-green solid slowly separated out, which was filtered and crystallised from CH_2Cl_2 and ethanol. Yield: 75%.

55a: IR (KBr, cm^{-1}) ν_{NH} 3266 (m); ^1H NMR (CD_2Cl_2, 20 °C) δ: 10.16 (d br, 1H, NH), 8.49 (d, 1H, =CH), 7.75–6.87 (m, 40H, Ph), 4.99 (s, 5H, Cp), 3.46 (d, 9H, CH3); $^{31}P\{^1H\}$ NMR (CD_2Cl_2, 20 °C) δ: AX spin syst, δ_A 94.90, δ_X 13.69, J_{AX}= 38.2. Anal. Calcd. for $C_{57}H_{56}BNO_3OsP_2$ (1066.05): C, 64.22; H, 5.29; N, 1.31; Found: C, 64.03; H, 5.19; N, 1.37%; Λ_M = 52.6 $\Omega^{-1}mol^{-1}cm^2$.

55b: IR (KBr, cm^{-1}) ν_{NH} 3271 (m); ^1H NMR (CD_2Cl_2, 20 °C) δ: 10.30 (d br, 1H, NH), 8.41 (d, 1H, =CH), 7.75–6.87 (m, 39H, Ph), 5.08 (s, 5H, Cp), 3.46 (q, 9H, CH_3 phos), 2.36 (s, 3H, CH_3 *p*-tolyl); $^{31}P\{^1H\}$ NMR (CD_2Cl_2, 20 °C) δ: AX spin syst, δ_A 95.36,δ_X 13.87, J_{AX}= 38.15. Anal. Calcd. for $C_{58}H_{58}BNO_3OsP_2$ (1080.07): C, 64.50; H, 5.41; N, 1.30; Found: C, 64.34; H, 5.30; N, 1.38%; Λ_M = 51.4 Ω^{-1} mol^{-1} cm^2.

55c: IR (KBr, cm^{-1}) ν_{NH} 3275 (m); ^1H NMR [$(CD_3)_2CO$, 20 °C] δ: 10.33, 9.98 (s br, 1H, NH), 7.61–6.87 (m, 40H, Ph), 5.22 (s, 5H, Cp), 3.58 (d, 9H, CH_3 phos), 2.37 (br, 3H, CH_3C=); $^{31}P\{^1H\}$NMR [$(CD_3)_2CO$, 20 °C] δ: AX spin syst, δ_A 93.45, δ_X 14.97, J_{AX}= 38.40. Anal. Calcd. for $C_{58}H_{58}BNO_3OsP_2$ (1080.07): C, 64.50; H, 5.41; N, 1.30; Found: C, 64.28; H, 5.46; N, 1.41%; Λ_M = 53.3Ω^{-1} mol^{-1} cm^2.

56a: IR (KBr, cm^{-1}) ν_{NH} 3260 (m); ^1H NMR [$(CD_3)_2CO$, 20 °C] δ: 10.79 (d br, 1H, NH), 8.88 (d, 1H, =CH), 7.60–6.78 (m, 40H, Ph), 5.20 (s, 5H, Cp), 3.98 (m, 6H, CH_2), 1.14 (t, 9H, CH_3); $^{31}P\{^1H\}$ NMR [$(CD_3)_2CO$, 20 °C] δ: AX spin syst, δ_A 90.46, δ_X 14.26, J_{AX}= 37.41. Anal. Calcd. for $C_{60}H_{62}BNO_3OsP_2$ (1108.13): C, 65.03; H, 5.64; N, 1.26; Found: C, 64.86; H, 5.71; N, 1.19%; Λ_M = 52.8 $\Omega^{-1}mol^{-1}cm^2$.

56b: IR (KBr, cm^{-1}) ν_{NH} 3265 (m); ^1H NMR (CD_2Cl_2, 20 °C) δ: 10.39 (d br, 1H, NH), 8.44 (d, 1H, =CH), 7.65–6.88 (m, 39H, Ph), 4.90 (s, 5H, Cp), 3.84 (m, 6H, CH_2), 2.36 (s, 3H, CH_3 *p*-tolyl), 1.14 (t,

9H, CH_3); $^{31}P\{^1H\}$ NMR (CD_2Cl_2, 20 °C) δ: AX spin syst, δ_A 88.46, δ_X 13.72, J_{AX}= 37.91. Anal. Calcd. for $C_{61}H_{64}BNO_3OsP_2$ (1122.15): C, 65.29; H, 5.75; N, 1.25; Found: C, 65.12; H, 5.84; N, 1.17%; Λ_M = 53.5 Ω^{-1} mol^{-1} cm^2.

56c: IR (KBr, cm^{-1}) ν_{NH} 3282 (m); ^1H NMR [$(CD_3)_2CO$, 20 °C] δ: 10.46, 10.15 (s br, 1H, NH), 7.56–6.78 (m, 40H, Ph), 5.16 (s, 5H, Cp), 3.98 (m, 6H, CH_2), 1.10 (t, 9H, CH_3 phos), 2.43 (br, 3H, CH_3C=); $^{31}P\{^1H\}$ NMR [$(CD_3)_2CO$, 20 °C] δ: AX spin syst, δ_A 87.47, δ_X 14.45, J_{AX}= 38.64. Anal. Calcd. for $C_{61}H_{64}BNO_3OsP_2$ (1122.15): C, 65.29; H, 5.75; N, 1.25; Found: C, 65.13; H, 5.80; N, 1.18%; Λ_M = 52.0 $\Omega^{-1}mol^{-1}cm^2$.

$[Os(\eta^5\text{-}C_5H_5)\{\kappa^1\text{-}^{15}NH{=}C(H)C_6H_4\text{-}4\text{-}CH_3\}(PPh_3)\{P(OR)_3\}]BPh_4$ ($\mathbf{55b_1}$, $\mathbf{56b_1}$)
$[Os(\eta^5\text{-}C_5H_5)\{\kappa^1\text{-}^{15}NH{=}C(CH_3)C_6H_5\}(PPh_3)\ \{P(OR)_3\}]BPh_4$ ($\mathbf{55c_1}$, $\mathbf{56c_1}$)
[R = Me (55), Et (56)].

These complexes were prepared exactly like the related unlabelled derivatives **55b**, **56b**, **55c** and **56c**, using the labelled azides 4-$CH_3C_6H_4CH_2{}^{15}N_3$ and $C_6H_5C(H)(CH_3){}^{15}N_3$ as reagents. Yield ≥65%.

$\mathbf{55b_1}$: IR (KBr, cm^{-1}) ν_{15NH} 3272 (m); ^1H NMR (CD_2Cl_2, 20 °C) δ: AXNYZ spin syst (Y, Z = ^1H; N = ^{15}N), δ_Y 10.40, δ_Z 8.38, J_{AN} = 3.5, J_{AY} = 3.8, J_{AZ} = 0.1, J_{XN} = 2.6, J_{XY} = 1.8, J_{XZ} = 0.1, J_{NY} = 72.8, J_{NZ} = 3.0, J_{YZ} = 21.3; $^{31}P\{^1H\}$ NMR (CD_2Cl_2, 20 °C) δ: AXN spin syst, δ_A 97.02, δ_X 14.54, J_{AX} = 38.0, J_{AN} = 4.0, J_{XN} = 2.6; ^{15}N NMR(CD_2Cl_2, 20 °C) δ: AXNYZ spin syst, δ_N 161.7, J_{AX} = 38.0, J_{AN} = 4.0, J_{AY} = 4.3, J_{AZ} = 0.1, J_{XN} = 2.6, J_{XY} = 1.8, J_{XZ} = 0.1, J_{NY} = 72.6, J_{NZ} = 3.0, J_{YZ} = 21.3.

$\mathbf{55c_1}$: ^1H NMR (CD_2Cl_2, 20 °C) δ: $AXNYZ_3$ spin syst (Y, Z = ^1H; N = ^{15}N), δ_Y 10.24, δ_Z 2.36, J_{AN} = 4.0, J_{AY} = 4.55, J_{AZ} = 0.05, J_{XN} = 2.0, J_{XY} = 0.9, J_{XZ} = 1.0, J_{NY} = 71.6, J_{NZ} = 1.65, J_{YZ} = 2.00; $AXNYZ_3$ spin syst, δ_Y 9.59, δ_Z 2.16, J_{AX} = 4.65, J_{AY} = 4.15, J_{AZ} = 0.05, J_{XN} =1.9, J_{XY} = 1.65, J_{XZ} = 1.0, J_{NY} = 70.95, J_{NZ} = 1.5, J_{YZ} = 2.00; $^{31}P\ \{^1H\}$ NMR (CD_2Cl_2, 20 °C) δ: AXN spin syst, δ_A 92.56, δ_X 14.80, J_{AX} = 38.0, J_{AN} = 4.0, J_{XN} = 2.0; AXN spin syst, δ_A 93.01, δ_X 15.05, J_{AX} = 38.5, J_{AN} = 4.0, J_{XN} = 2.0; ^{15}N NMR (CD_2Cl_2, 20 °C) δ: $AXNYZ_3$ spin syst, δ_N 173.46, J_{AN} = 4.4, J_{XN} = 2.0; $AXNYZ_3$ spin syst, δ_N 182.27, J_{AN} = 4.0, J_{XN} = 2.0.

$\mathbf{56b_1}$: IR (KBr, cm^{-1}) ν_{15NH} 3266 (m); ^1H NMR (CD_2Cl_2, 20 °C) δ: AXNYZ spin syst (Y, Z = ^1H; N = ^{15}N), δ_Y 10.52, δ_Z 8.51, J_{AN} = 4.2, J_{AY} = 3.8, J_{AZ} = 0.1, J_{XN} = 2.6, J_{XY} = 1.8, J_{XZ} = 0.1, J_{NY} = 72.4, J_{NZ} = 3.0, J_{YZ} = 21.2; $^{31}P\{^1H\}$ NMR (CD_2Cl_2, 20 °C) δ: AXN spin syst, δ_A 90.35, δ_X 14.47, J_{AX} = 38.0, J_{AN} = 4.2, J_{XN} = 2.6; ^{15}N NMR (CD_2Cl_2, 20 °C) δ: AXNYZ spin syst, δ_N 163.7, J_{AN} = 4.2, J_{XN} = 2.6.

56c$_1$: IR (KBr, cm^{-1}) ν_{15NH} 3275 (m); ^{1}H NMR (CD_2Cl_2, 20 °C) δ: AXNYZ$_3$ spin syst (Y, Z = ^{1}H; N = ^{15}N), δ_Y 10.38, δ_Z 2.33, J_{AN} = 4.4, J_{AY} = 4.65, J_{AZ} = 0.05, JXN = 2.0, J_{XY} = 0.90, J_{XZ} = 1.00, J_{NY} = 71.65, J_{NZ} = 1.65, J_{YZ} = 2.00; AXNYZ$_3$ spin syst, δ_Y 10.07, δ_Z 2.22, J_{AN} = 4.0, J_{AY} = 4.15, J_{AZ} = 0.05, J_{XN} = 2.0, J_{XY} = 1.65, J_{XZ} = 1.00, J_{NY} = 70.96, J_{NZ} = 1.65, J_{YZ} = 2.00; ^{31}P{^{1}H} NMR (CD_2Cl_2, 20 °C) δ: AXN spin syst, δ_A 86.90, δ_X 14.15, J_{AX} = 38.4, J_{AN} = 4.4, J_{XN} = 2.0; AXN spin syst, δ_A 88.02, δ_X 14.75, J_{AX} = 39.2, J_{AN} = 4.0, J_{XN} = 2.0; ^{15}N NMR (CD_2Cl_2, 20 °C) δ: AXNYZ$_3$ spin syst, δ_N 174.64, J_{AN} = 4.4, J_{XN} = 2.0; AXNYZ$_3$ spin syst, δ_N 182.99, J_{AN} = 4.0, J_{XN} = 2.0.

[{Os(η^5-C$_5$H$_5$)(PPh$_3$)[P(OMe)$_3$]}$_2$(μ-N$_2$)](BPh$_4$)$_2$ (57)

Method A: A solution of the phenylazide complex [Os(η^5-C$_5$H$_5$)(κ^1-N$_3$Ph)(PPh$_3$){P(OMe)$_3$}]BPh$_4$ (**53d**) (100 mg, 0.09 mmol) in CH_2Cl_2 (5 mL) was stirred at room temperature for 1 h. The solvent was removed under reduced pressure to give an oil, which was triturated with ethanol (1 mL). A blue solid slowly separated out, which was filtered and twice crystallised from CH_2Cl_2 and ethanol. Yield ≥55%.

Method B: In a 25 mL three-necked round-bottomed flask covered with an aluminium foil were placed 0.14 mmol (100 mg) of the complex [OsBr(η^5-C$_5$H$_5$)(PPh$_3$){P(OMe)$_3$}], a slight excess of AgOTf (0.15 mmol, 39 mg) and 5 mL of toluene. The reaction mixture was stirred for 75 min and then filtered on paper to remove the AgBr formed. An excess of phenylazide (0.18 mmol, 21.5 μL) in 5 mL of dichloromethane was added to the resulting solution, and cooled to −196 °C. The reaction mixture was left to reach room temperature and then stirred for 1 h. The solvent was removed under reduced pressure to give an oil, which was triturated with ethanol (1 mL) containing an excess of $NaBPh_4$ (0.28 mmol, 96 mg). A blue solid slowly separated out, which was filtered and twice crystallised from CH_2Cl_2 and ethanol. Yield ≥45%.

^{1}H NMR [$(CD_3)_2CO$, 20 °C] δ: 7.61–6.77 (m, 70H, Ph), 5.03 (s, 10H, Cp), 3.61 (d, 18H, CH); ^{31}P{^{1}H} NMR [$(CD_3)_2CO$, 20 °C] δ: AX spin syst, δ_A 90.21, δ_X 6.24, J_{AX} = 38.5. Anal. Calcd. for $C_{100}H_{98}B_2N_2O_6Os_2P_4$ (1949.83): C, 61.60; H, 5.07; N, 1.44; Found: C, 61.41; H, 5.16; N, 1.33%; Λ_M= 58.8 $\Omega^{-1}mol^{-1}cm^2$.

[OsCl(η^6-*p*-cymene){κ^1-NH=C(H)C$_6$H$_4$-4-CH$_3$}{P(OEt)$_3$}]BPh$_4$ (58)

Method A In a 25 mL three-necked round-bottomed flask covered with an aluminium foil were placed 80 mg (0.14 mmol) of [OsCl$_2$(η^6-*p*-cymene){P(OEt)$_3$}], a slight excess of AgOTf (0.15 mmol,

39 mg) and 5 mL of dichloromethane. The reaction mixture was stirred for 24 h, filtered on paper to remove the AgCl formed, and then an excess of 4-$CH_3C_6H_4CH_2N_3$ (0.42 mmol, 62 µL) was added. The reaction mixture was stirred for 6 h and then the solvent was removed under reduced pressure. The oil obtained was triturated with ethanol (1 mL) containing an excess of NaBPh4 (0.28 mmol, 96 mg). A yellow solid slowly separated out from the resulting solution, which was filtered and crystallised from CH_2Cl_2 and ethanol. Yield ≥75%.

Method B: In a 25 mL three-necked round-bottomed flask were placed 80 mg (0.14 mmol) of [$OsCl_2(\eta^6$-*p*-cymene){$P(OEt)_3$}], an excess of $NaBPh_4$ (0.28 mmol, 96 mg), 5 mL of dichloromethane, and 5 mL of ethanol and an excess of 4-$CH_3C_6H_4CH_2N_3$ (0.42 mmol, 62 µL). The reaction mixture was stirred for 24 h and then the solvent was removed under reduced pressure. The oil obtained was triturated with ethanol (1 mL) until a yellow solid separated out from the resulting solution, which was filtered and crystallised from CH_2Cl_2 and ethanol. Yield ≥70%.

IR (KBr, cm^{-1}) ν_{NH} 3257 (m); ^{1}H NMR (CD_2Cl_2, 20 °C) δ: 10.99 (d br, 1H, NH), 8.68 (d, 1H, =CH), 7.31–6.86 (m, 24H, Ph), 5.81, 5.72, 5.60, 5.46 (d, 4H, Ph *p*-cym), 4.11 (qnt, 6H,CH_2), 2.65 (m, 1H, CH *p*-cym), 2.38 (s, 3H, CH_3 *p*-tolyl), 2.12 (s, 3H, CH_3 *p*-cym), 1.30 (t, 9H, CH_3 phos), 1.27 (m, 6H, CH3 ^{i}Pr); $^{31}P\{^1H\}$ NMR (CD_2Cl_2, 20 °C) δ: A spin syst, 67.51 (s). Anal. Calcd. for $C_{48}H_{58}BClNO_3OsP$ (964.45): C, 59.78; H, 6.06; Cl, 3.68; N, 1.45; Found: C, 59.60; H, 5.97; Cl, 3.82; N, 1.36%; Λ_M= 53.0 $\Omega^{-1}mol^{-1}cm^2$.

[$OsCl(\eta^6$-*p*-cymene)(κ^1-$NH_2C_6H_5$){$P(OEt)_3$}]BPh_4 (59)

This complex was prepared exactly like compound **58**, using both Method A and Method B, with $C_6H_5N_3$ as a reagent. Yield ≥55%.

IR (KBr, cm^{-1}) ν_{NH} 3286, 3226 (m); ^{1}H NMR (CD_2Cl_2, 20 °C) δ: 7.47–6.88 (m, 25H, Ph), 5.81, 5.52 (br, 2H, NH_2), 5.38, 5.25, 5.11, 5.00 (d, 4H, Ph *p*-cym), 4.23 (m, 6H, CH_2), 2.62 (m, 1H, CH *p*-cym), 2.10 (s, 3H, CH_3 *p*-cym), 1.39 (t, 9H, CH_3 phos), 1.18, 1.16 (d, 6H, CH_3 ^{i}Pr); $^{31}P\{^1H\}$ NMR (CD_2Cl_2, 20 °C) δ: A spin syst, 68.29 (s). Anal. Calcd. for $C_{46}H_{56}BClNO_3OsP$ (938.41): C, 58.88; H, 6.01; Cl, 3.78; N, 1.49; Found: C, 58.65; H, 5.91; Cl, 3.87; N, 1.39%; Λ_M = 51.8 Ω^{-1} mol^{-1} cm^2.

6.14 Preparation of Imine and Amine Complexes of Iridium.

$[IrCl(\eta^5\text{-}C_5Me_5)(\kappa^1\text{-}NH{=}C(H)R1)P(OR)_3]BPh_4$ **(60, 61)**
[R = Me (60), Et (61); R1 = C_6H_5 (a), 4-$CH_3C_6H_4$ (b)].

Method A: In a 25 mL three-necked round-bottomed flask were placed 80 mg (0.15 mmol) of $[IrCl_2(\eta^5\text{-}C_5Me_5)P(OR)_3]$, an excess of $NaBPh_4$ (0.30 mmol, 105 mg), 5 mL of dichloromethane, and 5 mL of ethanol and an excess of appropriate azide (0.60 mmol). The reaction mixture was stirred for 24 h and then the solvent was removed under reduced pressure. The oil obtained was triturated with ethanol (1 mL) until a yellow solid separated out from the resulting solution, which was filtered and crystallised from CH_2Cl_2 and ethanol. Yield ≥50%.

Method B: In a 25 mL three-necked round-bottomed flask covered with an aluminium foil were placed 80 mg (0.15 mmol) of $[IrCl_2(\eta^5\text{-}C_5Me_5)P(OR)_3]$, a small excess of AgOTf (0.16 mmol, 41 mg) and 5 mL of dichloromethane. The reaction mixture was stirred for 24 h, filtered on paper to remove the AgCl formed, and then an excess of 4-$CH_3C_6H_4CH_2N_3$ (0.35 mmol, 52 µL) was added. The reaction mixture was stirred for 4 h and then the solvent was removed under reduced pressure. The oil obtained was triturated with ethanol (1 mL) containing an excess of $NaBPh_4$ (0.45 mmol, 154 mg). A yellow solid slowly separated out from the resulting solution, which was filtered and crystallised from CH_2Cl_2 and ethanol. Yield ≥60%.

60b: IR (KBr, cm^{-1}) ν_{NH} 3143 (m); ^1H NMR (CD_2Cl_2, 20 °C) δ: 9.63 (d br, 1H, NH), 8.36 (d, 1H, =CH), 7.45–6.87 (m, 24H, Ph), 3.74 (d, 9H, CH_3 phos), 2.46 (s, 3H, CH_3 *p*-tolyl), 1.70 (d, 15H, CH_3 Cp*); $^{31}P\{^1H\}$ NMR (CD_2Cl_2, 20 °C) δ: 79.79 (s). Anal. Calcd. for $C_{45}H_{53}BClIrNO_3P$ (925.37): C, 58.41; H, 5.77; Cl, 3.83; N, 1.51; Found: C, 58.38; H, 5.85; Cl, 3.90; N, 1.41%; Λ_M = 51.8 $\Omega^{-1}mol^{-1}cm^2$.

61a: IR (KBr, cm^{-1}) ν_{NH} 3264 (m), $\nu_{C=N}$ 1626 (s); ^1H NMR (CD_2Cl_2, 20 °C) δ: 9.89 (d br, 1H, NH), 8.44 (d, 1H, =CH J_{HH} 21.3), 7.71–6.86 (m, 24H, Ph), 4.09 (qnt, 6H, CH_2 phos), 1.70 (d, 15H, CH_3 Cp*), 1.28 (t, 9H, CH_3 phos); $^{31}P\{^1H\}$ NMR (CD_2Cl_2, 20 °C) δ: 75.33 (s). Anal. Calcd. for $C_{47}H_{57}BClIrNO_3P$ (953.43): C, 59.21; H, 6.03; Cl, 3.72; N, 1.47; Found: C, 59.17; H, 5.96; Cl, 3.64; N, 1.52%; Λ_M = 52.0 $\Omega^{-1}mol^{-1}cm^2$.

61b: IR (KBr, cm^{-1}) ν_{NH} 3186 (m), $\nu_{C=N}$ 1625 (s); ^1H NMR (CD_2Cl_2, 20 °C) δ: 9.68 (d br, 1H, NH), 8.35 (d, 1H, =CH J_{HH} 21.3), 7.49–6.87 (m, 24H, Ph), 4.08 (qnt, 6H, CH_2 phos), 2.47 (s, 3H, CH_3 *p*-tolyl), 1.69 (d, 15H, CH_3 Cp*), 1.28 (t, 9H, CH_3 phos); $^{31}P\{^1H\}$ NMR (CD_2Cl_2, 20 °C) δ: 75.58 (s). Anal.

Calcd. for $C_{48}H_{59}BClIrNO_3P$ (967.45): C, 59.59; H, 6.15; Cl, 3.66; N, 1.45; Found: C, 59.38; H, 6.45; Cl, 3,70; N, 1.43%; Λ_M = 52.1 $\Omega^{-1}mol^{-1}cm^2$.

[IrCl(η^5-C$_5$Me$_5$)(κ^1-^{15}NH=C(H)*p*-tolyl)P(OMe)$_3$]BPh$_4$ (60b$_1$)

This complex was prepared exactly like the related unlabelled derivatives **60** and **61** using the labelled azides 4-$CH_3C_6H_4CH_2{}^{15}N_3$ and as reagents. Yield ≥47%.

IR (KBr, cm^{-1}) ν_{15NH} 3120 (m); ^{1}H NMR (CD_2Cl_2, 20 °C) δ: ANXY spin syst (A= ^{31}P; N= ^{15}N; X, Y= ^{1}H) δ_X 9.67, δ_Y 8.39, J_{NX}=75.00, J_{XY}=21.3, J_{AN}=6.8, J_{AX}=2.2, J_{NY}=1.0, J_{AY}=0.1, (2H, ^{15}NH=CH), 7.41–6.88 (m, 24H, Ph), 3.76 (d, 9H, CH_3 phos), 2.46 (s, 3H, CH_3 *p*-tolyl), 1.70 (d, 15H, CH_3 Cp*); ^{31}P{^{1}H} NMR (CD_2Cl_2, 20 °C) AN spin syst. δ_A 79.79 J_{AN} = 6.8; ^{15}N{^{1}H} NMR (CD_2Cl_2, 20 °C) AN spin syst. δ_N 174.88 J_{AN} = 6.8 (s) Anal. Calcd. for $C_{48}H_{59}BClIr^{15}NO_3P$ (968.45): C, 59.53; H, 6.14; Cl, 3.66; N, 1.55; Found: C, 59.47; H, 6.28; Cl, 3.53; N, 1.65%; Λ_M = 52.2 $\Omega^{-1}mol^{-1}cm^2$.

[IrCl(η^5-C$_5$Me$_5$)(κ^1-NH$_2$Ph)P(OR)$_3$]BPh$_4$ (62,63)
[R = Me (62), Et (63)].

In a 25 mL three-necked round-bottomed flask were placed 80 mg (0.15 mmol) of [$IrCl_2$(η^5-C_5Me_5)P(OR)$_3$], an excess of $NaBPh_4$ (0.39 mmol, 105 mg), 5 mL of dichloromethane, and 5 mL of ethanol and an excess of $C_6H_5N_3$ (0.60 mmol, 73 μL). The reaction mixture was stirred for 4 h and then the solvent was removed under reduced pressure. The oil obtained was triturated with ethanol (1 mL) until a brown solid separated out from the resulting solution, which was filtered and crystallised from CH_2Cl_2 and ethanol. Yield ≥35%.

62: IR (KBr, cm^{-1}) ν_{NH} 3277, 3220 (m); ^{1}H NMR (CD_2Cl_2, 20 °C) δ: 7.74–6.87 (m, 25H, Ph), 5.81 (br, 2H, NH_2), 3.76 (d, 9H, CH_2 phos), 1.67(d, 15H, CH_3 Cp*). ^{31}P{^{1}H} NMR (CD_2Cl_2, 20 °C) δ: 76.48 (s). Anal. Calcd. for $C_{43}H_{51}BClIrNO_3P$ (899.34): C, 57.43; H, 5.72; Cl, 3.94; N, 1.56; Found: C, 57.33; H, 5.78; Cl, 3.89; N, 1.63%; Λ_M = 51.7 $\Omega^{-1}mol^{-1}cm^2$.

63: IR (KBr, cm^{-1}) ν_{NH} 3275 (m); ^{1}H NMR (CD_2Cl_2, 20 °C) δ: 7.31–6.87 (m, 25H, Ph), 5.91 (br, 2H, NH_2), 4.28 (qnt, 6H, CH_2 phos), 1.64 (d, 15H, CH_3 Cp*), 1.39 (t, 9H, CH_3 phos). ^{31}P{^{1}H} NMR (CD_2Cl_2, 20 °C) δ: 72.77 (s). Anal. Calcd. for $C_{46}H_{57}BClIrNO_3P$ (941.42): C, 58.69; H, 6.10; Cl, 3.77; N, 1.49; Found: C, 58.58; H, 6.15; Cl, 3.70; N, 1.41%; Λ_M = 52.1 $\Omega^{-1}mol^{-1}cm^2$.

[$IrCl_2(\eta^5\text{-}C_5Me_5)(\kappa^1\text{-}NH{=}C(H)R1)$] (64)
[R1 = C_6H_5 (a), 4-$CH_3C_6H_4$ (b)].

In a 50 mL three-necked round-bottomed flask were placed 100 mg (0.13 mmol) of $[IrCl_2(\eta^5\text{-}C_5Me_5)]_2$, 15 mL of tetrahydrofuran and an excess of 4-$CH_3C_6H_4CH_2N_3$ (0.63 mmol, 93 μL). The reaction mixture was stirred at reflux temperature for 2h during which time a yellow solid precipitate. The precipitate was filtered and dried under vacuum. Yield ≥60%.

64a: IR (KBr, cm^{-1}) ν_{NH} 3176 (m), $\nu_{C=N}$ 1625 (s); ^1H NMR (CD_2Cl_2, 20 °C) δ: 10.41 (d br, 1H NH), 8.54 (d, 1H, =CH J_{HH} 21.0), 7.99, 7.66, 7.51 (d, 4H, Ph), 1.66 (s, 15H, CH_3 Cp*). Anal. Calcd. for $C_{17}H_{22}Cl_2IrN$ (503.49): C, 40.55; H, 4.40; Cl, 14.08; N, 2.78; Found: C, 40.59; H, 4.47; Cl, 13.98; N, 2.80%; Λ_M = 51.7 $\Omega^{-1}mol^{-1}cm^2$.

64b: IR (KBr, cm^{-1}) ν_{NH} 3169 (m), $\nu_{C=N}$ 1627 (s); ^1H NMR (CD_2Cl_2, 20 °C) δ: 10.22 (d br, 1H NH), 8.46 (d, 1H, =CH J_{HH} 20.8), 7.99, 7.52, 7.31 (d, 4H, Ph), 2.41 (s, 3H, CH_3 *p*-tolyl), 1.69 (s, 15H, CH_3 Cp*). Anal. Calcd. for $C_{18}H_{24}Cl_2IrN$ (517.51): C, 41.78; H, 4.67; Cl, 13.70; N, 2.71; Found: C, 41.57; H, 4.47; Cl, 13.68; N, 2.81%; Λ_M = 51.7 $\Omega^{-1}mol^{-1}cm^2$.

[$IrCl(\eta^5\text{-}C_5Me_5)(\kappa^1\text{-}NH{=}C(H)$*p-tolyl*$)_2$]$BPh_4$ (65)

In a 50 mL three-necked round-bottomed flask were placed 100 mg (0.13 mmol) of $[IrCl_2(\eta^5\text{-}C_5Me_5)]_2$, 15 mL of tetrahydrofuran and an excess of 4-$CH_3C_6H_4CH_2N_3$ (0.63 mmol, 93 μL). The reaction mixture was stirred at reflux temperature for 5h. The solvent was removed under reduced pressure to give an oil, which was triturated at 0 °C with ethanol (1 mL) containing an excess of $NaBPh_4$ (0.25 mmol, 86 mg). A yellow solid slowly separated out, which was filtered and crystallised at 0 °C from CH_2Cl_2 and ethanol. Yield ≥55%.

65: IR (KBr, cm^{-1}) ν_{NH} 3122 (m), ν_{CN} 1629 (s); ^1H NMR (CD_2Cl_2, 20 °C) δ: 11.82 (d br, 1H NH), 8.44 (d, 1H, =CH J_{HH} 20.7), 7.58-6.86 (m, 28H, Ph), 2.32 (s, 6H, CH_3 *p*-tolyl), 1.71 (s, 15H, CH_3 Cp*). Anal. Calcd. for $C_{50}H_{53}BClIrN_2$ (920.47): C, 65.24; H, 5.80; Cl, 3.85; N, 3.04; Found: C, 65.24; H, 5.80; Cl, 3.85; N, 3.04%; Λ_M = 51.8 $\Omega^{-1}mol^{-1}cm^2$.

[$Ir(\eta^5\text{-}C_5Me_5)(\kappa^1\text{-}NH{=}C(H)$*p*-tolyl$)_2${$P(OR)_3$}]$(BPh_4)_2$ (66, 67)
[R = Me (66), Et (67)].

In a 25 mL three-necked round-bottomed flask covered with an aluminium foil were placed 80 mg (0.15 mmol) of $[IrCl_2(\eta^5\text{-}C_5Me_5)P(OR)_3]$, a slight excess of AgOTf (0.32 mmol, 83 mg) and 5 mL of

dichloromethane. The reaction mixture was stirred for 24 h, filtered on paper to remove the AgCl formed, and then an excess of 4-$CH_3C_6H_4CH_2N_3$ (0.35 mmol, 52 µL) was added. The reaction mixture was stirred for 4 h and then the solvent was removed under reduced pressure. The oil obtained was triturated with ethanol (1 mL) containing an excess of NaBPh4 (0.45 mmol, 154 mg). A yellow solid slowly separated out from the resulting solution, which was filtered and crystallised from CH_2Cl_2 and ethanol. Yield ≥75%.

66: IR (KBr, cm^{-1}) ν_{NH} 3215 (m); ^1H NMR (CD_2Cl_2, 20 °C) δ: 9.15, 8.43 (d br, 1H, NH), 8.14, 8.00 (d, 1H, =CH), 7.64-6.81 (m, 28H, Ph), 3.31 (d, 9H, CH_3 phos), 2.48 (s, 6H, CH_3 *p*-tolyl), 1.77 (s, 15H, CH_3 Cp*). $^{31}P\{^1H\}$ NMR (CD_2Cl_2, 20 °C) δ: 72.70 (s). Anal. Calcd. for $C_{77}H_{82}B_2IrN_2O_3P$ (1328.32): C, 69.63; H, 6.22; N, 2.11; Found: C, 69.47; H, 6.35; N, 2.01%; Λ_M = 100.6 $\Omega^{-1}mol^{-1}cm^2$.

67: IR (KBr, cm^{-1}) ν_{NH} 3215 (m); ^1H NMR (CD_2Cl_2, 20 °C) δ: 10.74, 8.42 (d br, 1H, NH), 8.14, 7.88 (d, 1H, =CH), 7.90-6.87 (m, 28H, Ph), 3.93 (qnt, 6H, CH_2 phos), 2.48 (s, 6H, CH_3 *p*-tolyl), 1.59 (d, 15H, CH_3 Cp*), 1.20 (t, 9H, CH_3 phos). $^{31}P\{^1H\}$ NMR (CD_2Cl_2, 20 °C) δ: 72.70 (s). Anal. Calcd. for $C_{80}H_{88}B_2IrN_2O_3P$ (1370.41): C, 70.12; H, 6.47; N, 2.04; Found: C, 70.04; H, 6.58; N, 1.96%; Λ_M = 101.4 $\Omega^{-1}mol^{-1}cm^2$.

7.1 Reaction of Azines with Half-Sandwich Complexes of Ruthenium

Aldazine R(H)C=N–N=C(H)R reacts with *p*-cymene complexes of ruthenium $RuCl_2(\eta^6$-*p*-cymene)L to give κ^1-azine derivatives $[RuCl(\eta^6$-*p*-cymene$)\{\kappa^1$-$[N=C(H)R]$–$N=C(H)R\}L]BPh_4$ (**1**-**4**) (Scheme 7.1), which were isolated in good yield and characterised.

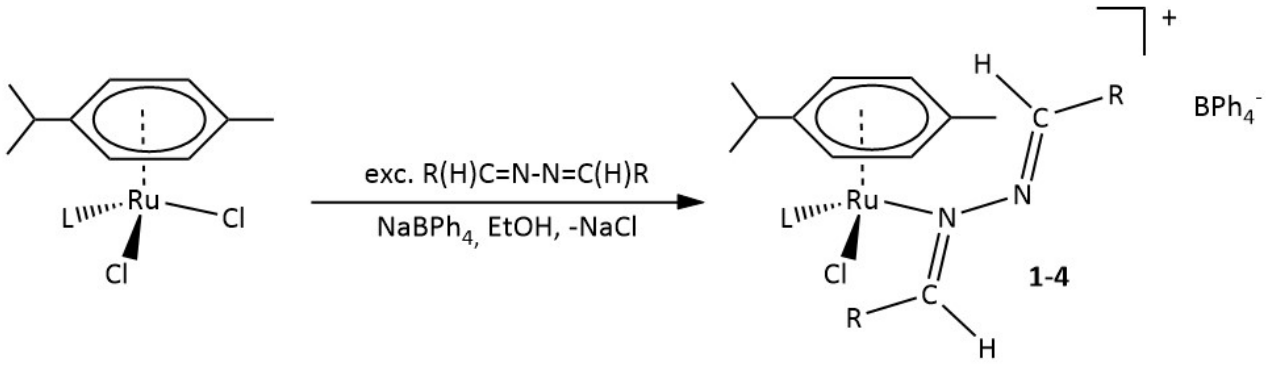

Scheme 7.1 L = $P(OMe)_3$ (1), $P(OEt)_3$ (2), $PPh(OEt)_2$ (3), P^iPr_3 (4); R = Ph (a), 4-$CH_3C_6H_4$ (b), 4-$CH_3OC_6H_4$ (c), C_2H_5 (d).

The reaction proceeds with the substitution of one chloro ligand and the formation of azine complexes **1**–**4** κ^1-coordinated through one of the nitrogen atoms. The presence of the $NaBPh_4$ salt is quite important for the labilization of the Cl^- ligand, easing the formation of final complexes **1**–**4**.

A similar behaviour was observed with both phosphite $P(OR)_3$ and triisopropylphosphine complexes $RuCl_2(\eta^6$-*p*-cymene)L [L=$P(OR)_3$ and P^iPr_3), which react with benzaldehydeazine to give κ^1-azine derivatives $[RuCl(\eta^6$-*p*-cymene$)\{\kappa^1$-$[N=C(H)Ph]$–$N=C(H)Ph\}L]BPh_4$ (**1**–**4**).

Surprisingly, the reaction of *p*-cymene complexes containing phosphite ligands $RuCl_2(\eta^6$-*p*-cymene)$[P(OR)_3]$ with acetone azine $(CH_3)_2C=N-N=C(CH_3)_2$ does not proceed with the formation of the κ^1-azine derivatives as those with the aldazine ligand, but the final products were the hydrazone complexes $[RuCl(\eta^6$-*p*-cymene$)\{NH_2N=C(CH_3)_2\}\{P(OR)_3\}]BPh_4$ (**5** and **6**), which were isolated and characterised (Scheme 7.2).

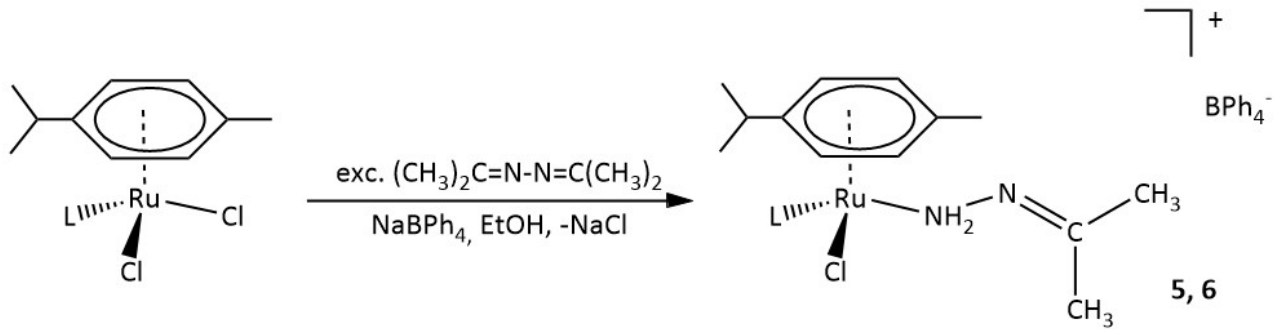

Scheme 7.2 L = $P(OMe)_3$ (5), $P(OEt)_3$ (6).

Instead, the use of the isopropylphosphine complex $RuCl_2(\eta^6\text{-}p\text{-cymene})(P^iPr_3)$ in the reaction with ketazine afford the κ^1-azine derivative $[RuCl(\eta^6\text{-}p\text{-cymene})\{\kappa^1\text{-}[N=C(CH_3)_2]\text{-}N=C(CH_3)_2\}(P^iPr_3)]BPh_4$ (**7**), which was stable and isolable (Scheme 7.3).

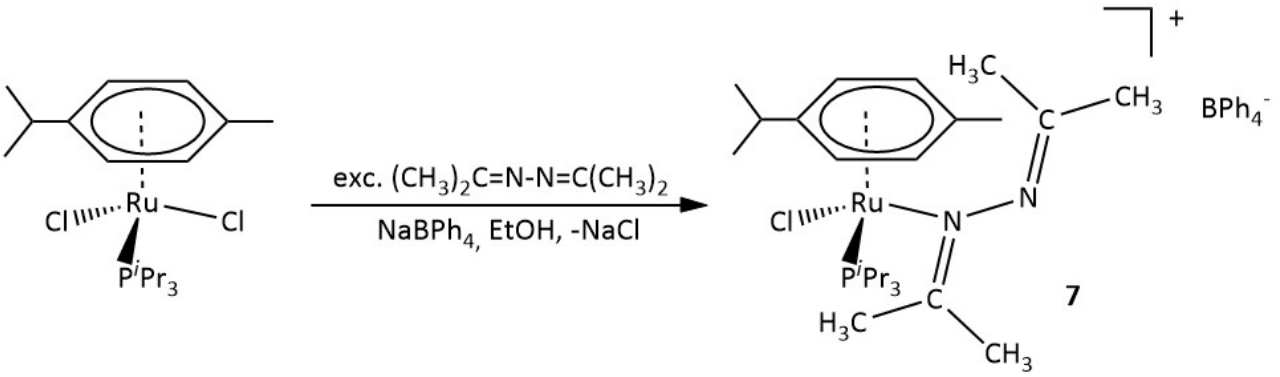

Scheme 7.3 Reaction with acetone azine

In the case of phosphite ligands, the formation of hydrazone complexes **5** and **6** was unexpected but may be explained by κ^1-coordination of the azine, followed by its fast hydrolysis by the traces of water always present in ethanol (Scheme 7.4).

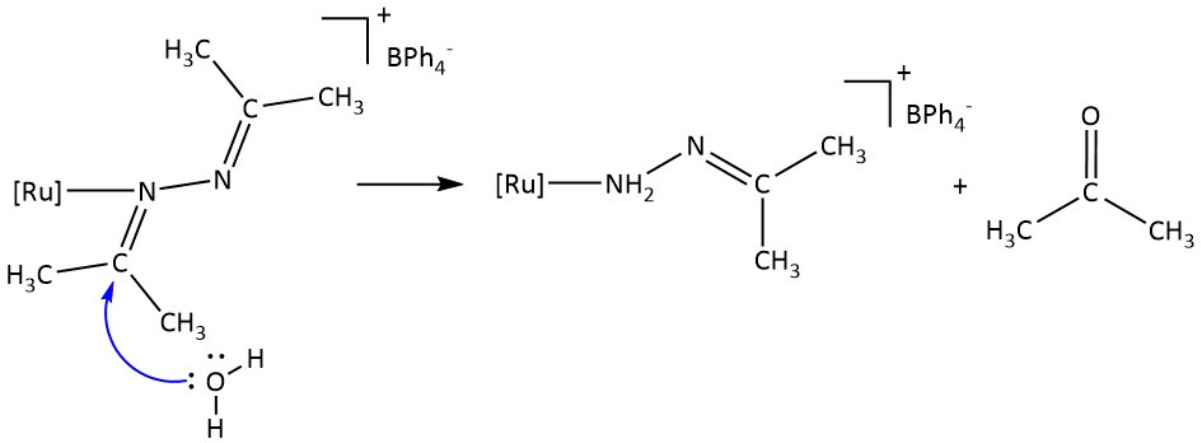

Scheme 7.4 [Ru] = $RuCl(\eta^6\text{-}p\text{-cymene})L$.

Coordination of the azine to the metal fragment [RuCl(η^6-*p*-cymene){P(OR)$_3$}]$^+$ probably activates this species towards hydrolysis, affording hydrazone derivatives **5**, **6** and acetone. Accordingly, the addition of H_2O to the reaction mixture increases the formation rate of the hydrazone, which was isolated in good yield as a yellow solid. Acetone was detected in the reaction mixture too, thus confirming the proposed reaction path for the formation of the hydrazone derivatives. It is worth noting that, in the free state, ketazine is a rather stable molecule[156], which does not undergo hydrolysis, but its κ^1-coordination to the half-sandwich fragment [RuCl(η^6-*p*-cymene){P(OR)$_3$}]$^+$ activates this species towards hydrolysis, yielding the final hydrazone derivatives under mild conditions. However, only the *p*-cymene fragment with good π-acceptor ligands such as phosphites P(OR)$_3$ activates the N-coordinated acetone azine towards hydrolysis, whereas the related P^{i}Pr$_3$ fragment instead gives stable ketazine derivative **7**.

The results obtained with aldazine and ketazine prompted us to test the behaviour of an asymmetric azine such as Ph(H)C=N–N=C(CH$_3$)Ph. The ruthenium compound RuCl$_2$(η^6-*p*-cymene)[P(OR)$_3$] turned out to react with the mixed species to give the related azine derivatives [RuCl(η^6-*p*-cymene){κ^1-[N=C(CH$_3$)Ph]–N=C(H)Ph}{P(OR)$_3$}]BPh$_4$ (**8**, **9**), which were isolated and characterised (Scheme 7.5).

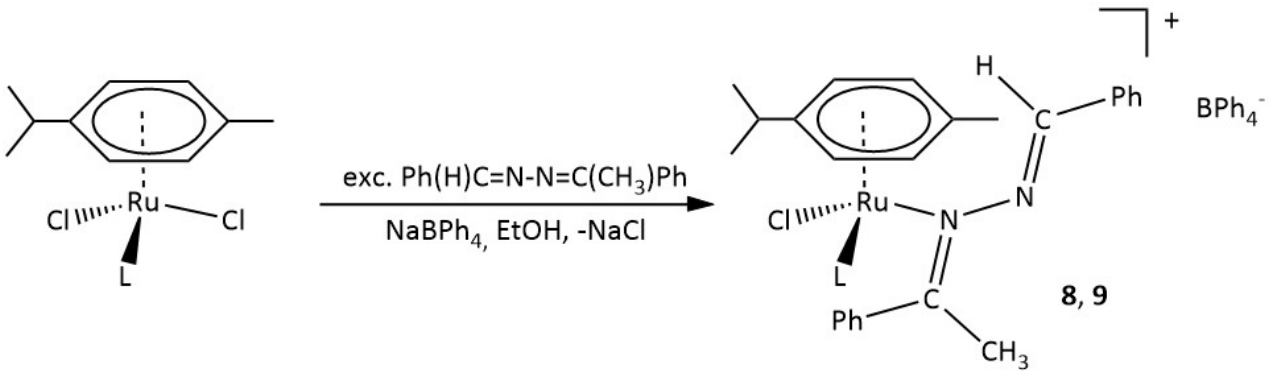

Scheme 7.5 L = P(OMe)$_3$ (8), P(OEt)$_3$ (9)

The reaction proceeds with substitution of one chloride and coordination of the azine through the "ketonic" N=C(CH$_3$)Ph group.

The coordination of the asymmetric azine through the "ketonic" nitrogen atom was not unexpected, as this atom is the more electron-rich of the two. However, in contrast with ketazine, the ketonic group of the asymmetric azine Ph(CH$_3$)C=N–N=C(H)Ph is not activated by the fragment [RuCl(η^6-*p*-cymene){P(OR)$_3$}]$^+$ towards hydrolysis under mild conditions, so complexes **8** and **9** are very stable and can be isolated in pure form.

The results obtained with the *p*-cymene complexes prompted us to extend our study to other half-sandwich fragments such as the cyclopentadienyl $RuCl(\eta^5\text{-}C_5H_5)(PPh_3)\{P(OMe)_3\}$. Unfortunately, these species do not react with azine, either at room temperature or at reflux. We therefore devised a different strategy, in an attempt to prepare azine complexes, involving treatment of the chloro complex with AgOTf followed by reaction with the appropriate azine. The results of this approach are resumed in Schemes 7.6 and 7.7.

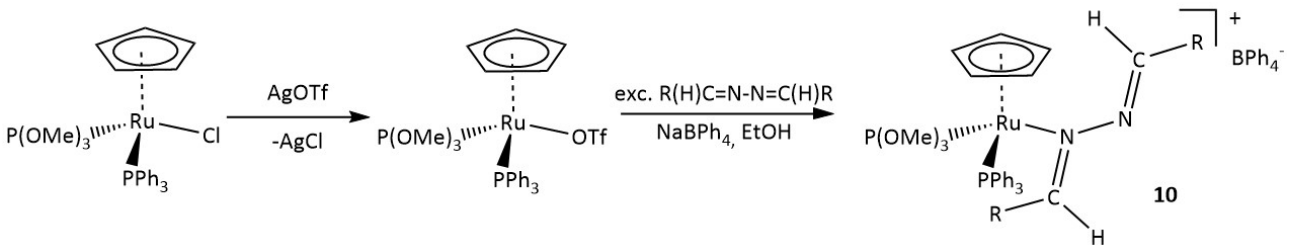

Scheme 7.6 R = Ph (a), 4-$CH_3C_6H_4$ (b), C_2H_5 (d)

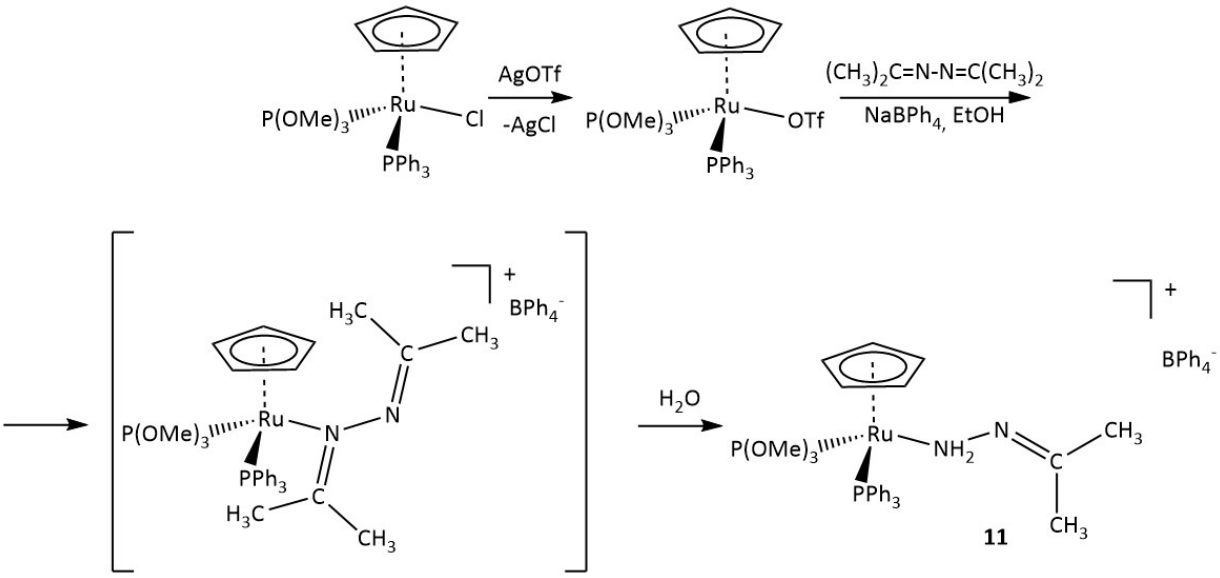

Scheme 7.7 Reaction path.

The mixed-ligand chloro complexes $RuCl(\eta^5\text{-}C_5H_5)(PPh_3)\{P(OMe)_3\}$ react with AgOTf affording, beside AgCl, the triflate intermediate $Ru(\kappa^1\text{-}OTf)(\eta^5\text{-}C_5H_5)(PPh_3)\{P(OMe)_3\}$. This complex is more reactive than the chloro precursor and reacts with aldazine R(H)C=N–N=C(H)R to give the related complex $[Ru(\eta^5\text{-}C_5H_5)\{\kappa^1\text{-}[N=C(H)R]N=C(H)R\}(PPh_3)\text{-}\{P(OMe)_3\}]^+$ (**10**), which was isolated and characterised. Unfortunately, also in this case the reaction of ketazine $(CH_3)_2C=N–N=C(CH_3)_2$ with the triflate intermediate does not afford any azine complex, but again only hydrazone species $[Ru(\eta^5\text{-}C_5H_5)\{H_2NN=C(CH_3)_2\}(PPh_3)\{P(OMe)_3\}]BPh_4$ (**11**). As previously observed with *p*-cymene

complexes, the probable initial coordination of ketazine to the ruthenium fragment is followed by hydrolysis, affording final hydrazone derivatives **11**. This hypothesis is again confirmed by the addition of H_2O to the reaction mixture, which increases the formation of hydrazone complex **11**, allowing the separation of pure samples in good yield. Those results indicated that both half-sandwich fragments $[RuCl(\eta^6\text{-}p\text{-cymene})\{P(OR)_3\}]^+$ and $[Ru(\eta^5\text{-}C_5H_5)(PPh_3)\{P(OMe)_3\}]^+$ containing phosphite ligands can activate the coordinated ketazine $(CH_3)_2C{=}N{-}N{=}C(CH_3)_2$ towards hydrolysis, even when only traces of H_2O are present in the "anhydrous" ethanol, affording the hydrazone derivatives.

It is worth mentioning that reactions with azines were also tested with bis(phosphine) $[Ru(\eta^5\text{-}C_5H_5)(PPh_3)_2]^+$ and bis(phosphite) $[Ru(\eta^5\text{-}C_5H_5)\{P(OMe)_3\}_2]^+$ derivatives, but neither azine nor hydrazone complexes were observed in either case. It therefore seems that only mixed-ligand half-sandwich fragments with both phosphine and phosphite present in the coordination sphere of the ruthenium complex $[Ru(\eta^5\text{-}C_5H_5)(PPh_3)\{P(OR)_3\}]^+$ can coordinate an azine which, in the case of acetone azine, is activated towards hydrolysis, giving the hydrazone as final derivatives.

Azine complexes of ruthenium are very rare and, before this study[157], only complexes involving a chelate pyridylazine ligand $[Ru(\eta^5\text{-}C_5H_5)(PPh_3)L]BF_4$ (L=pyridine-2-car-baldehydeazine) have been reported[158–162]. The use of half-sandwich fragments with *p*-cymene or cyclopentadienyl ligands allows the preparation of a series of stable κ^1-azine derivatives for this metal.

7.1.1 Characterisation of Complexes

Azine complexes $[RuCl(\eta^6\text{-}p\text{-cymene})\{\kappa^1\text{-}[N{=}C(H)R1]{-}N{=}C(H)R1\}(PR_3)]^+$ (**1-4**) were separated as yellow-orange solids, stable in air and in solution of polar organic solvents, where they behave as 1:1 electrolytes[163]. Their characterisation was supported by analytical and spectroscopic data (IR and ^1H, ^{13}C, ^{31}P NMR) and by X-ray crystal structure determination of $[RuCl(\eta^6\text{-}p\text{-cymene})\{\kappa^1\text{-}[N{=}C(H)Ph]\text{-}N{=}C(H)Ph\}\{P(OMe)_3\}]BPh_4$ (**1a**) and $[RuCl(\eta^6\text{-}p\text{-cymene})\{\kappa^1\text{-}[N{=}C(H)Ph]\text{-}N{=}C(H)Ph\}\text{-}\{P(OEt)_3\}]BPh_4$ (**2a**). Both **1a** and **2a** consist of tetraphenylborate salts of ruthenium complexes, however, only the corresponding cations of **1a** and **2a** are shown in Figure 7.1.

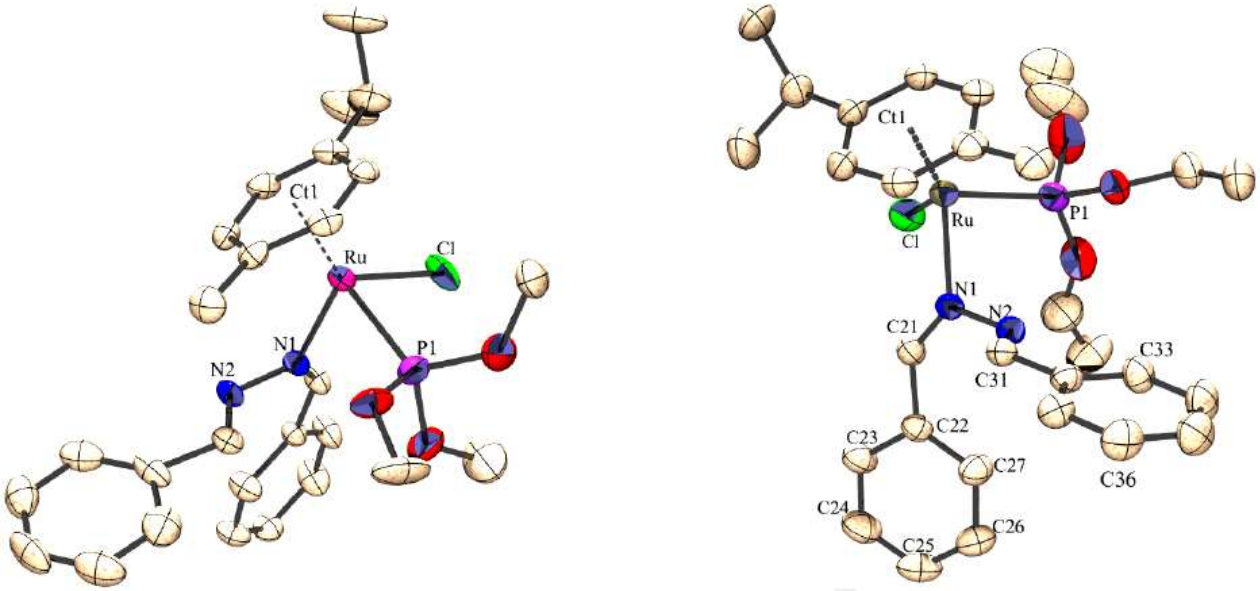

Figure 7.1 ORTEP[164] view of the cation of 1a (left) and 2a (right), drawn at 20% probability level.

The cationic complexes contain a ruthenium atom in a half-sandwich piano-stool structure, coordinated by a *p*-cymene group, one chloride ligand, the above-mentioned phosphite ligand [$P(OMe)_3$ for **1a**, $P(OEt)_3$ for **2a**], and one benzaldehydeazine ligand bound to the Ru centre via one of the nitrogen atoms. Selected bond lengths and angles are shown in Table 7.1. The geometry of the complex is octahedral and is marked by near 90° values for angles Cl-Ru-N, P-Ru-N and Cl-Ru-P, between 83.26(6) and 88.85(10)°. The *p*-cymene ligands are planar for both compounds, with a root mean square (rms) deviation of 0.0158 and 0.0119 Å for the six atoms in the benzene ring, and they are coordinated with a ring-slippage of only 0.05 Å. The Ru-C bond lengths and distances from the ruthenium atom to the centroid fall in the usual range (see Table 7.1), although some differences are found, due to the trans influence of the ligands[165,166]. The Ru-P and Ru-Cl bond lengths fall within the usual range (see Table 7.1) so they are not commented further.

The azine derivative ligand is coordinated as a N-mono-dentated donor by one of the nitrogen atoms. Metallic complexes of several metals with the benzaldehydeazine ligand are cited in the literature, either with similar monodentated behaviour, acting in a κ^2-N,N' fashion, or in a cyclometallated manner[167–169]. However, to the best of our knowledge, no ruthenium complexes have been crystallographically described before.

Table 7.1 Bond lengths [Å] and angles [°] for 1a and 2a.

	1a	2a
Ru-Cl	2.3760(14)	2.3891(16)
Ru-P(1)	2.2759(13)	2.2895(15)
Ru-N(1)	2.143(3)	2.115(4)
Ru-CT1	1.7389(4)	1.7266(4)
Ru-C(1)	2.290(5)	2.276(5)
Ru-C(2)	2.201(4)	2.202(5)
Ru-C(3)	2.194(4)	2.175(5)
Ru-C(4)	2.264(5)	2.251(5)
Ru-C(5)	2.228(5)	2.211(6)
Ru-C(6)	2.267(5)	2.260(6)
Ru-C_{av}	2.241	2.229
N(1)-N(2)	1.384(14)	1.395(5)
N(1)-N(2A)	1.42(3)	
N(1)-C(21)	1.285(6)	1.274(6)
N(2)-C(31)	1.24(3)	1.257(6)
N(2A)-C(31A)	1.24(5)	
C(21)-C(22)	1.465(6)	1.460(7)
C(31)-C(32)	1.511(16)	1.459(7)
C(31A)-C(32)	1.63(3)	
CT1-Ru-N(1)	126.96(10)	127.77(11)
CT1-Ru-P(1)	129.35(4)	127.30(4)
CT1-Ru-Cl	127.05(4)	127.85(5)
N(1)-Ru-P(1)	86.93(10)	88.74(11)
N(1)-Ru-Cl	88.85(10)	87.62(12)
P(1)-Ru-Cl	83.33(7)	83.26(6)
C(21)-N(1)-N(2)	114.7(5)	119.8(4)
C(21)-N(1)-N(2A)	120.4(7)	
C(21)-N(1)-Ru	127.1(3)	126.1(3)
N(2)-N(1)-Ru	117.2(4)	113.2(3)
N(2A)-N(1)-Ru	109.2(6)	
C(31)-N(2)-N(1)	118.9(13)	117.5(4)
C(31A)-N(2A)-N(1)	113.0(18)	
N(1)-C(21)-C(22)	132.5(4)	131.7(5)
N(2)-C(31)-C(32)	117.2(11)	121.0(5)
N(2A)-C(31A)-C(32)	106.5(15)	

The Ru-N bond lengths, 2.143(3) Å for **1a** and 2.115(4) Å for **2a**, fall between related [RuCl(η^6-*p*-cymene)(pyrazole){PPh(OEt)$_2$}]$^+$, 2.06 Å[165], 2.026(6) for guanidine [RuCl{N≡CN(H)–C(NH$_2$)=NH}(η^6-*p*-cymene){PPh(OEt)$_2$}]$^+$,[148] and 2.20 Å in azido phosphito η^6-*p*-cymene ruthenium(II) complexes[170]. The coordination of nitrogen atom N(1) to the metal slightly elongates the C=N bond[8b] (see Table 7.1) and slightly shortens the N-N bond length, compared with the free ligand[171]. In **1a** and **2a**, the azine ligand is coordinated in such a way that it is wrinkled, in contrast with the free ligand structure[171–173], and the dihedral angles between phenyl rings are 78.6(4) and 82.9(3)°, respectively. The torsion angle for the C=N–N=C chain gives values of 97.9(13)8 [for the C(21)-N(1)-N(2)-C(31) chain] and 113.9(8)° [for the C(21)-N(1)-N(2A)-C(31A) chain] for **1a** and 86.5(6)° for **2a**, revealing substantial screwing of the ligand.

If the nitrogen-metal bond is not considered, the ligand could be defined as the Z-E isomer, so that the coordinated imino moiety would be the Z isomer and the other imino moiety would not be coordinated and adopts the E configuration. Other, previously described benzaldehydeazine complexes show the ligand as almost planar, with a zig-zag shape in the C=N–N=C chain when the ligand shows monodentated behaviour in the compound [PdCl$_2$(PhHC=N–N=CHPh)$_2$][174]; if the ligand acts in a κ^2 fashion, in compound [V(C$_5$Me$_5$)(CO)$_2$(PhHC=N–N=CHPh)][175] the C=N–N=C chain is U-shape and shows a symmetry plane in the N-N bond: both shapes are found in the silver compound [Ag$_2$(bdb)$_3$(NO$_3$)$_2$ with bdb = bis(4-dimethylaminobenzylidenehydrazine)],[176] depending on the monodentated terminal or bidentated bridging behaviour of the ligand which is, in any case, mainly planar.

The IR spectra of aldazine complexes **1**–**4** show a medium-intensity band at 1630–1602 cm^{-1}, attributed to the $\nu_{N=C}$ of the azine ligand. The presence of this group was confirmed by the ^{1}H NMR spectra which, in the high-frequency region, show two singlets at 8.78-8.21 and 8.20-7.96 ppm, attributed respectively to the CH of the free and coordinated N=C(H)R1 group of the azine. In case of propionaldehyde azine (C$_2$H$_5$)(H)C=N–N=C(H)(C$_2$H$_5$) derivative **1d** and **2d** two triplets at 7.71-7.73 and 7.15-7.24 ppm were observed in the ^{1}H NMR spectra. The signals of the ancillary ligands *p*-cymene and P(OR)$_3$ or P^{i}Pr$_3$ and of the BPh$_4$ anion were also present, as well as those of the substituents *p*-CH$_3$C$_6$ H$_4$, *p*-CH$_3$OC$_6$H$_4$ or C$_2$H$_5$ of the azine. The ^{13}C NMR spectrum of **2a** shows two singlets at 164.49 and 160.62 ppm, attributed to the carbon atom of the free and coordinated N=C(H)R1 group of the azine, whereas ^{31}P NMR spectra are sharp singlets between 142 and 51 ppm, matching the proposed formulation for the complexes.

The ^{1}H NMR spectrum of ketazine complex [RuCl(η^{6}-*p*-cymene){κ^{1}-[N=C(CH$_3$)$_2$]N=C(CH$_3$)$_2$}-(P^{i}Pr$_3$)]BPh$_4$ (**7**), besides the signals of the *p*-cymene and P^{i}Pr$_3$ ligands and the BPh$_4$ anion, shows two singlets at 2.61 and 2.59 ppm and two at 1.70 and 1.58 ppm, attributed to the methyl protons of the coordinated and free N=C(CH$_3$)$_2$ groups of the azine. The ^{31}P spectrum is a singlet at 68.0 ppm, according to the proposed formulation.

The proton spectra of the asymmetric azine derivatives [RuCl(η^{6}-*p*-cymene){κ^{1}-[N=C(CH$_3$)Ph]–N=C(H)Ph}{P(OR)$_3$}]BPh$_4$ (**8**, **9**) show one singlet at 8.40 ppm, attributable to the CH proton of the "aldehydic" N=C(H)Ph group, and two others at 2.59 (**8**) and 2.50 (**9**) ppm, attributed to the methyl hydrogen atoms of the ketazine "ketonic" N=C(CH$_3$)Ph group. The shift of these signals with respect to those of the free azine Ph(H)N=C–N=C(CH$_3$)Ph [8.46 ppm for =C(H) and 2.55 ppm for =C(CH$_3$)] and, in comparison with the results obtained from other spectra, does not allow to unambiguously decide which of the two groups, "aldehydic" N=C(H)Ph or "ketonic" N=C(CH$_3$)Ph, is bonded to the metal. Support for this assignment comes from the ^{13}C NMR spectrum of **9** which, besides the ancillary ligands, shows one singlet at 158.06 ppm of the =C(H) carbon resonance and two singlets at 142.62 and 30.77 ppm of the ketonic and methyl carbon resonances respectively of the =C(CH$_3$) group of the azine. A comparison with the ^{13}C signals of the free azine [164.7 ppm for =C(H) and 157.7 and 14.92 ppm for =C(CH$_3$)] suggests coordination of the N=C(CH$_3$)Ph group of the azine, as shown in Scheme 7.5.

The IR spectra of cyclopentadienyl complexes [Ru(η^{5}-C$_5$H$_5$){κ^{1}-[N=C(H)R]N=C(CH$_3$)R}(PPh$_3$)-{P(OMe)$_3$}]BPh$_4$ (**10**) show one medium-intensity band at 1605–1602 cm^{-1}, attributed to the $\nu_{N=C}$ of the coordinated azine. The presence of this ligand was confirmed by ^{1}H NMR spectra, that shows two singlets between 7.45-8.66 ppm (**10a**, **10b**) attributed to the hydrogen atom of the coordinated and free N=C(H)R groups of the azine. Instead, in the ^{1}H NMR spectra of the propionaldehyde azine complex **10d** it is possible to identify two triplets for the CH protons of the arms of N=C(H)(C$_2$H$_5$). Further support for the proposed formulation comes from the ^{13}C NMR spectrum of **10a**, which shows two singlets at 162.20 and 156.03 ppm of the carbon resonance of the free and coordinated N=C(H)R units, whereas the ^{31}P NMR spectra appear as an AX quartet, fitting the proposed geometry for the complexes.

Hydrazone derivatives [RuCl(η^6-*p*-cymene){$NH_2N=C(CH_3)_2$}{$P(OR)_3$}]BPh_4 (**5**, **6**) and [Ru(η^5-C_5H_5)-{$NH_2N=C(CH_3)_2$}(PPh_3){$P(OMe)_3$}]BPh_4 (**11**) are stable yellow solids, which were characterised by analytical and spectroscopic data and by X-ray crystal structure determination of **11**.

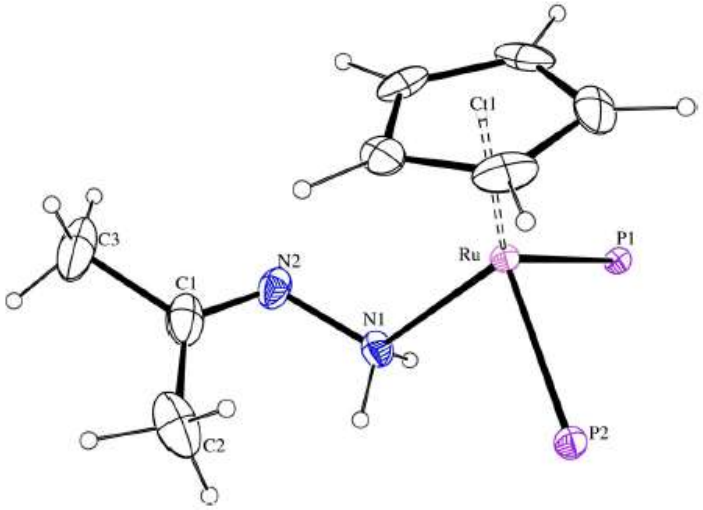

Figure 7.2 ORTEP[164] view of the cation of 11. P1 is a PPh_3 and P2 is a $P(OMe)_3$ ligand.

Compound **11** also consists of tetraphenyl borate salt of ruthenium complex, but only the cation is shown in Figure 7.2. The cationic complex contains a ruthenium atom in a half-sandwich piano-stool structure, coordinated by a cyclopentadienyl ligand (Cp), one phosphite ligand, [$P(OMe)_3$], one phosphine ligand, PPh_3, and one acetonehydrazone ligand bound to the Ru centre via the amine nitrogen atom. This coordination mode is the only one found for this ligand, and no compounds are found in the CCDC database where this hydrazone ligand is coordinated via the imino ligand as was previously suggested[177] and occurs for example with the chelating biacetyldihydrazone ligand[178].

Cp ligand (ring slippage 0.052 Å) shows Ru-C bond lengths and distance between the ruthenium atom and the centroid in the usual range (see Table 7.2) for this kind of piano-stool structures. Also the Ru-P bond lengths, either for the phosphine (P1), either for the phosphite (P2), are in the usual range (see Table 7.2)[88,90].

The acetonehydrazone ligand shows Ru-N bond lengths of 2.1806(14) Å, it is only slightly longer to those found for the three acetonehydrazone ruthenium complexes crystallographically described previously: 2.17 Å for the cation [$Ru(NH_2{=}NCMe_2)_2\{P(OMe)_3\}_4]^{2+}$,[177] 2.121(13) in the anion [(COD)$Ru(NH_2NCMe_2)(P_3O_9)$],[179] or 2.1416(13) Å in the cation [OsCl(COD)(CN^tBu)-($NH_2N=CMe_2)_2]^{2+}$.[180] Also Ru-N N and N N–C angles, 114.13(12) and 114.97(19), are similar to those found in the mentioned complex, about 115 and 116°, respectively.

Table 7.2 Selected bond lengths [Å] and angles [°] for 11.

Ru-CT1	1.87762(16)	Ru-P(1)	2.3285(5)
Ru-P(2)	2.2329(4)	Ru-N(1)	2.1806(14)
Ru-C(11)	2.2019(18)	Ru-C(12)	2.2118(18)
Ru-C(13)	2.2319(18)	Ru-C(14)	2.2536(17)
Ru-C(15)	2.2444(18)	Ru-C_{av}	2.2287
N(1)-N(2)	1.430(2)	N(1)-N(2A)	1.421(9)
N(2)-C(1)	1.289(3)	N(2A)-C(1)	1.296(9)
C(1)-C(2)	1.519(4)	C(1)-C(2A)	1.478(13)
C(1)-C(3)	1.494(3)	C(1)-C(3A)	1.463(15)
CT1-Ru-P(1)	122.996(12)	CT1-Ru-P(2)	124.576(13)
N(1)-Ru-P(1)	87.59(4)	N(1)-Ru-P(2)	88.37(4)
CT1-Ru-N(1)	127.59(4)		
Ru-N(1)-N(2)	114.13(12)	Ru-N(1)-N(2A)	111.4(4)
C(1)-N(2)-N(1)	114.97(19)	C(1)-N(2A)-N(1)	115.1(6)
N(2)-C(1)-C(3)	116.2(2)	N(2A)-C(1)-C(3A)	125.1(6)
N(2)-C(1)-C(2)	126.3(2)	N(2A)-C(1)-C(2A)	114.7(8)
C(3)-C(1)-C(2)	117.5(2)	C(3A)-C(1)-C(2A)	120.2(8)

The N-N bond distance, 1.430(2) Å is consistent with a single bond, and the N(2)-C(1), 1.289(3) Å corresponds better with a double bond, confirming the sp^2 character for C(1). Sum of angles around C(1) are in any case 360°. The whole acetonehydrazone ligand is planar (5 atoms, root-mean-square deviation of 0.0288 or 0.0094 Å) and its disposition is in such a way that is turns on the position of the Cp ligand, forming a dihedral angle between 28.87(8) and 30.75(3)°, as can be seen on the left of the schematic Figure 7.3.

Figure 7.3 Schematic figure of 11 (left) showing the spatial disposition of the hydrazone ligand, together a CpW (center) and a Ru(COD) (right) complexes.

In the lack of other Cp half-sandwich acetonehydrazone ruthenium complexes, this disposition could be compared with tungsten cation $[CpW(CO)_3(NH_2{=}NCMe_2)]^+$ (centre of Figure 7.3)[181] or with the above mentioned anion $[(COD)Ru(NH_2NCMe_2)(P_3O_9)]^-$ (right of Figure 7.3)[179].

The IR spectra of the hydrazone complexes [RuCl(η^6-pcymene){$NH_2N=C(CH_3)_2$}{$P(OR)_3$}]BPh_4 (**5,6**) and [Ru(η^5-C_5H_5){$NH_2N=C(CH_3)_2$}(PPh_3){$P(OMe)_3$}]BPh_4 (**11**) show two bands of medium intensity at 3350–3222 cm^{-1}, attributed to ν_{NH} of the hydrazone ligand. One band at 1651–1653 cm^{-1}, due to δ_{NH2}, also appears. However, the presence of the $(CH_3)_2C=NNH_2$ group is confirmed by the ^1H NMR spectra, which show two broad multiplets between 5.96 and 4.89 ppm, attributed to the NH_2 protons of the ligand. The appearance of two multiplets for the NH_2 protons can be explained owing to the presence of one stereocentre in the molecule, i. e. the Ru atom which makes the two hydrogen atoms of NH_2 diastereotopic. In the spectra, besides the resonance of the ancillary ligands such as *p*-cymene or cyclopentadienyl, PPh_3, and the BPh_4^- anion, the singlets of the methyl substituents of hydrazone $NH_2N=C(CH_3)_2$ also appear as two singlets at 1.64– 1.92 and 1.91-2.08 ppm, fitting the presence of the diazo ligand. The ^{31}P NMR spectra shows only one singlet for **5** and **6** while an AX multiplet appears for **11** in agreement with the proposed formulation for the complexes.

7.1.2 Reactivity

Some reactivity studies on azine **1**–**4** and hydrazone **5**, **6**, **11** derivatives were undertaken: unfortunately, they do not undergo ligand substitution under mild conditions, thus demonstrating that they are rather stable complexes. The azine can be substituted only at reflux condition to produce a new species (Scheme 7.8).

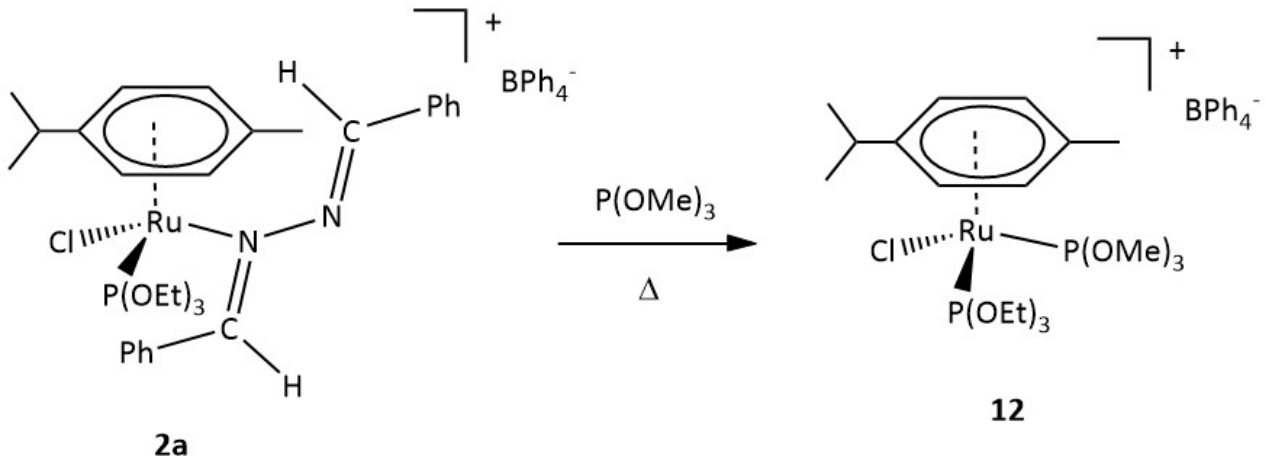

Scheme 7.8 Substitution reaction.

For example, complex **2a** reacts with $P(OMe)_3$ in refluxing 1,2-dichloroethane to give the mixed-ligand complex [RuCl(η^5-*p*-cymene){$P(OEt)_3$}{$P(OMe)_3$}]BPh_4 (**12**), whereas the reaction with CO is so slow that only traces of a carbonyl compound were observed (ν_{CO} at 1971 cm^{-1}) after 3 h at reflux in 1,2-dichloroethane.

More interesting is the reaction of hydrazone complex $[Ru(\eta^5\text{-}C_5H_5)\{NH_2N{=}C(CH_3)_2\}(PPh_3)\text{-}\{P(OMe)_3\}]BPh_4$ (**11**) with HgO in diethylether, which proceeds with oxidation of the coordinated hydrazone to provide the diazoalkane complex $[Ru(\eta^5\text{-}C_5H_5)\{N_2{=}C(CH_3)_2\}(PPh_3)\{P(OMe)_3\}]BPh_4$ (**13**), which was isolated as a solid and characterised (Scheme 7.9).

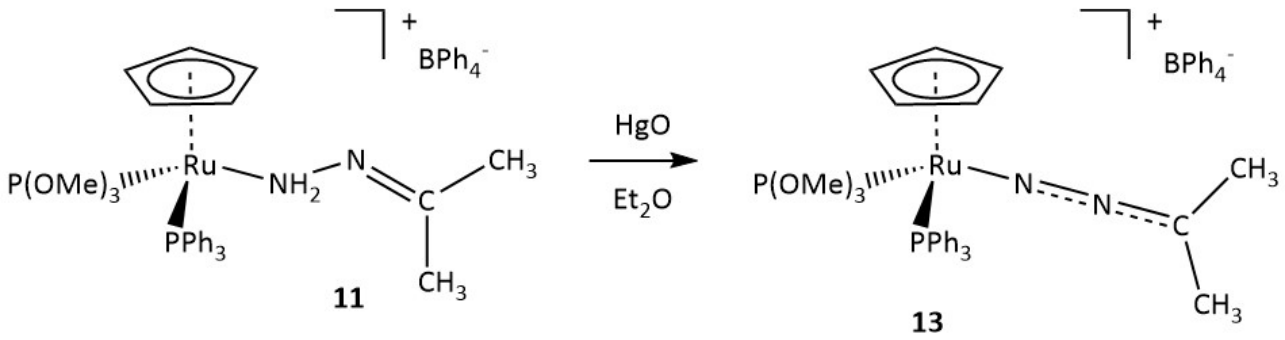

Scheme 7.9 Oxidation reaction.

The reaction of free hydrazone $NH_2N{=}CAr1Ar2$ with HgO is well-known and it is used to prepare free diazoalkane $N_2CAr1Ar2$[138,139,182]. We found that also a coordinated hydrazone can be oxidised to diazoalkane, allowing the preparation of dimethyldiazoalkane complex **13**. It is noteworthy that these types of complexes cannot be prepared by the usual method involving a substitution reaction, owing to the risk of explosive decomposition of the free dimethyldiazoalkane. The reaction with HgO on the coordinated $H_2N{-}N{=}C(CH_3)_2$ therefore appears to be an interesting new method to prepare diazoalkane complexes with alkyl substituents. We also tried this reaction with *p*-cymene derivatives $[RuCl(\eta^6\text{-}p\text{-cymene})\{NH_2N{=}C(CH_3)_2\}(PR_3)]BPh_4$ (**5**, **6**) and observed that the reaction proceeds with change of colour in the solution and the formation of metallic Hg. However, no stable complexes were isolated, probably because the metal fragment cannot stabilise dimethyldiazoalkane derivatives. Therefore, it seems that only the cyclopentadienyl fragment can stabilise alkyldiazoalkane, allowing the formation of the stable complex **13**.

The new compounds **12** and **13** were isolated as yellow and orange solids, respectively, and characterised by conductivity, IR and NMR spectra. In particular, the ^1H NMR spectrum of the mixed-ligand complex $[RuCl(\eta^5\text{-}p\text{-cymene})\{P(OEt)_3\}\{P(OMe)_3\}]BPh_4$ (**12**) shows the characteristic signals of *p*-cymene and the two phosphites $P(OEt)_3$ and $P(OMe)_3$, whereas the ^{31}P NMR spectrum is an AX quartet, fitting the proposed formulation for the complex.

The IR spectrum of diazoalkane complex $[Ru(\eta^5\text{-}C_5H_5)\{N_2{=}C(CH_3)_2\}(PPh_3)\{P(OMe)_3\}]BPh_4$ (**13**) shows a medium-intensity band at 1958 cm^{-1}, attributed to the $\nu_{N=N}$ of the diazoalkane ligand. Besides the signals of ancillary ligands C_5H_5, PPh_3 and $P(OMe)_3$ and the BPh_4 anion, the ^1H NMR spectrum

shows two singlets at 1.80 and 1.57 ppm of the methyl substituents of the diazoalkane, whereas the ^{31}P spectrum shows an AX quartet, matching the proposed formulation for the complexes.

7.2 Reaction of Azines with Half-Sandwich Complexes of Osmium

The results obtained from the study of half-sandwich azine complexes of ruthenium prompted us to extend this research to the third metals of the iron triad: osmium. However, because the direct reaction of dichloro compounds $[OsCl_2(\eta^6\text{-}p\text{-cymene})\{P(OR)_3\}]$ with $(R1C_6H_4)C(H)=N–N=C(H)R1C_6H_4$ giving only a mixture of uncharacterizable products, a different synthetic strategy was used.

Half-sandwich azine complexes of osmium of the type $[OsCl(\eta^6\text{-}p\text{-cymene})\{\kappa^1\text{-}[N=C(H)C_6H_4R1]–N=C(H)C_6H_4R1\}\{P(OR)_3\}]BPh_4$ (**14, 15**) were prepared by reacting the chloro compounds $[OsCl_2(\eta^6\text{-}p\text{-cymene})\{P(OR)_3\}]$ first with one equivalent of AgOTf and then with the appropriate azine, as shown in Scheme 7.10.

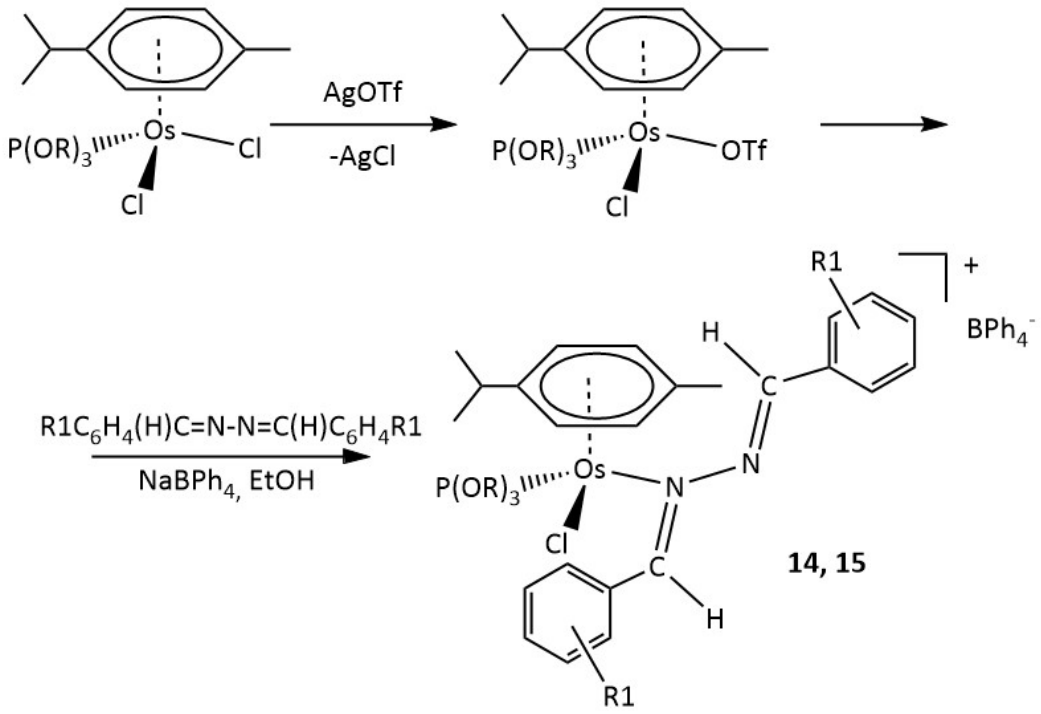

Scheme 7.10 R = Me (14), Et (15); R1 = H (a), 4-CH_3 (b), 2,6-$(CH_3)_2$ (f)

Silver triflate removes one chloride ligand from $[OsCl_2(\eta^6\text{-}p\text{-cymene})\{P(OR)_3\}]$, giving the triflate intermediate $[OsCl(\kappa^1\text{-OTf})(\eta^6\text{-pcymene})\{P(OR)_3\}]$, which reacts with azine producing κ^1-complexes **14, 15**, which were isolated as BPh_4 salts and characterised. The presence of a more labile ligand such as triflate instead of the chloro ligand is crucial for this synthesis.

Also ketazine $(CH_3)_2C{=}N{-}N{=}C(CH_3)_2$ reacts with the triflate complex $[OsCl(\kappa^1\text{-}OTf)(\eta^6\text{-}p\text{-cymene})\{P(OR)_3\}]$, producing κ^1-coordinated derivatives $[OsCl(\eta^6\text{-}p\text{-cymene})\{\kappa^1\text{-}[N{=}C(CH_3)_2]{-}N{=}C(CH_3)_2\}\{P(OR)_3\}]BPh_4$ (**16, 17**) in good yield. Instead, direct treatment of dichloro compounds $[OsCl_2(\eta^6\text{-}p\text{-cymene})\{P(OR)_3\}]$ with an excess of ketazine in ethanol gave yellow solids characterised as hydrazone derivatives $[OsCl(\eta^6\text{-}p\text{-cymene})\{NH_2N{=}C(CH_3)_2\}\{P(OR)_3\}]BPh_4$ (**18, 19**) (Scheme 7.11).

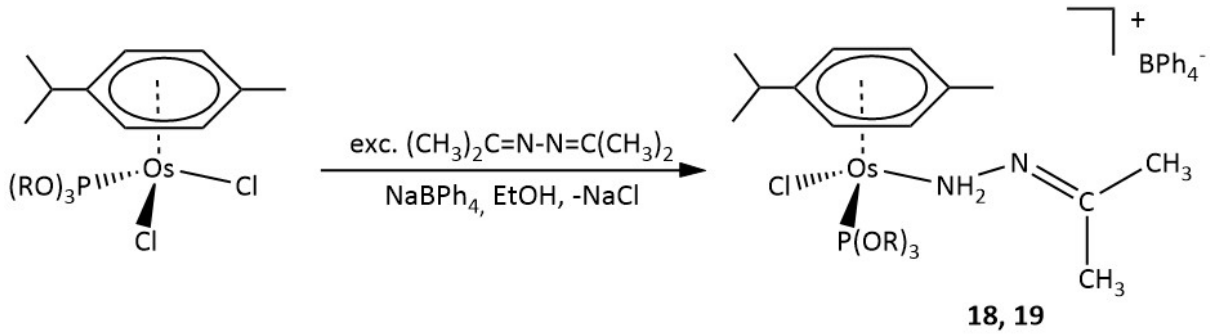

Scheme 7.11 R = Me (18), Et (19)

The formation of hydrazone complexes **18, 19** in the reaction is not unexpected, because already observed in the related azine complexes of ruthenium. The reaction may be explained by κ^1-coordination of the azine to give κ^1-complexes **16, 17** as intermediates, which subsequently undergo fast hydrolysis reacting with the traces of H_2O always present in ethanol (Scheme 7.12).

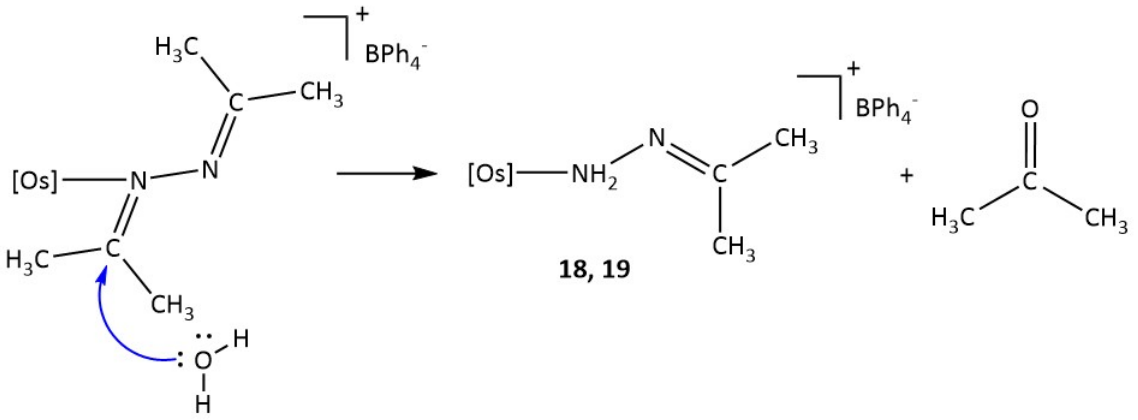

Scheme 7.12 $OsCl(\eta^6\text{-}p\text{-cymene})R$

The coordination of the azine to the metal fragment $[OsCl(\eta^6\text{-}p\text{-cymene})\{P(OR)_3\}]^+$ activates this species towards hydrolysis, producing hydrazone derivatives and acetone. Accordingly, the treatment with H_2O in the reaction mixture of $[OsCl_2(\eta^6\text{-}p\text{-cymene})\{P(OR)_3\}]$ and $(CH_3)_2C{=}N{-}N{=}C(CH_3)_2$ increases the formation rate of hydrazone, which was isolated in high yield as a yellow solid.

To confirm the proposed reaction path, we carried out the reaction of $[OsCl_2(\eta^6\text{-}p\text{-cymene})\{P(OR)_3\}]$ with ketazine in toluene, a solvent from which it is possible to eliminate almost completely the dissolved water, and, in this case, we observed that there was no the formation of any hydrazone derivatives.

We studied an interesting intramolecular reaction of κ^1-aldazine complexes $[OsCl(\eta^6\text{-}p\text{-cymene})\{\kappa^1\text{-}[N{=}C(H)C_6H_4R1]{-}N{=}C(H)C_6H_4R1\}\{P(OR)_3\}]BPh_4$, which in solution slowly give the metalated derivatives $[Os\{\kappa^2\text{-}R1C_6H_3C(H){=}N\text{-}N{=}NC(H)C_6H_4R1\}(\eta^6\text{-}p\text{-cymene})\{P(OR)_3\}]BPh_4$ (**20, 21**), as shown in Scheme 7.13.

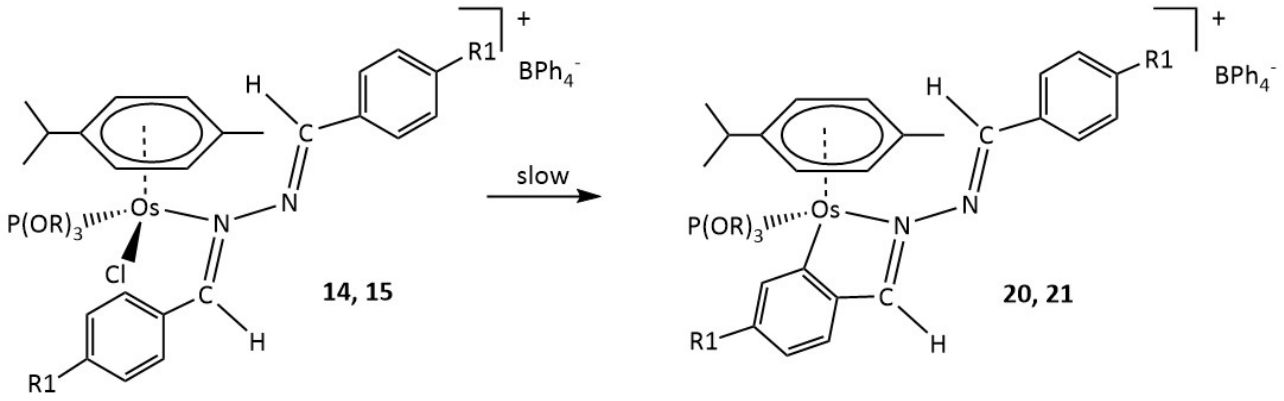

Scheme 7.13 R = Me (14, 20), Et (15, 21); R1 = H (a), 4-CH_3 (b)

The reaction proceeds through sp^2-CH activation, producing the metalated derivatives **20** and **21**, containing the κ^2-chelate aldazine. However, the metalation reaction is very slow, probably due to the need of a double cleavage, of both the C–H and Os–Cl bonds in forming the metalated complexes. To ease the formation of the metalated species, we treated the chloro compound $[OsCl_2(\eta^6\text{-}p\text{-cymene})\{P(OR)_3\}]$ with two equivalents of AgOTf, followed, after filtration of AgCl, by the addition of an excess of aldazine. The reaction quickly proceeded to give the complexes $[Os\{\kappa^2\text{-}R1C_6H_3C(H){=}N\text{-}N{=}NC(H)C_6H_4R1\}(\eta^6\text{-}p\text{-cymene})\{P(OR)_3\}]BPh_4$ (**20, 21**), which were isolated as BPh_4 salts and characterised (Scheme 7.14).

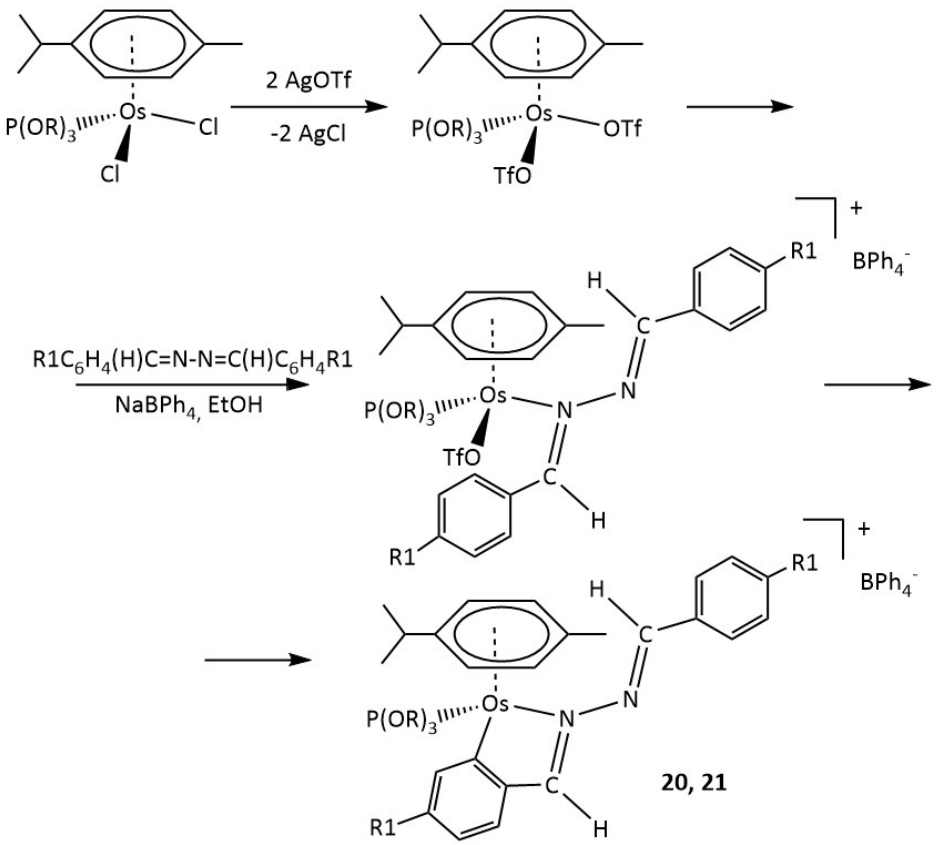

Scheme 7.14 R = Me (20), Et (21); R1 = H (a), 4-CH_3 (b)

The presence of a second labile OTf ligand, on one hand, and the excess of azine which can behave as a Brønsted base, on the other, allow the quick formation of metalated complexes **20, 21**.

This property shown by aldazine species prompted us to study the behaviour of related ketazine complexes [OsCl(η^6-*p*-cymene){κ^1-[N=C(CH_3)$_2$]–N=C(CH_3)$_2$}{P(OR)$_3$}]BPh_4 (**16, 17**). Unexpectedly, no reaction in solution was observed by these complexes and no metalation reaction occurred by treating the bis(triflate) complex [Os(κ^1-OTf)$_2$(η^6-*p*-cymene){P(OR)$_3$}] with an excess of acetone azine. In contrast with aldazine ones, κ^1-ketazine species **16, 17** are stable towards metalation and the starting complexes can be recovered unchanged after 48 h of reaction in CH_2Cl_2. Therefore, the osmium fragment [OsCl(η^6-*p*-cymene){P(OR)$_3$}]$^+$ is able to activate the C(sp^2)–H of the aldazine to give the metalated species, but not the C(sp^3)–H of the ketazine. This behaviour shown by osmium complexes towards azine also allows a comparison with the related ruthenium species [RuCl(η^6-*p*-cymene){P(OR)$_3$}]$^+$. Both fragments can coordinate the azine molecule to allow obtaining κ^1-complexes stable and isolable and, in the case of acetone azine, coordination also activates the azine towards hydrolysis, producing hydrazone derivatives. However, only osmium can promote the aldazine towards CH activation, affording a rare example of metalated complexes of the group 8.

7.2.1 Characterisation of the Complexes

Azine complexes [OsCl(η^6-*p*-cymene){k^1-[N=C(H)C_6H_4R1]–N=C(H)C_6H_4R1}{P(OR)$_3$}]BPh_4 (**14, 15**) and [OsCl(η^6-*p*-cymene){k^1-[N=C(CH_3)$_2$]–N=C(CH_3)$_2$}{P(OR)$_3$}]BPh_4 (**16, 17**) were separated as yellow-orange solids stable in air and in solution of polar organic solvents, where they behave as 1:1 electrolytes. Analytical and spectroscopic data support the proposed formulation, which is further confirmed by an X-ray crystal structure determination of [OsCl(η^6-*p*-cymene){κ^1-[N=C(H)Ph]–N=C(H)Ph}{P(OEt)$_3$}]BPh_4 (**15a**), whose ORTEP[183] is shown in Figure 7.4. The cationic complex contains an osmium atom in a half-sandwich piano-stool structure, coordinated by a *p*-cymene group, one chloride ligand, one triethoxyphosphite ligand and one dibenzylidenehydrazine ligand bound to the Os centre via one of the nitrogen atoms in similar way that was found also for the corresponding ruthenium compound.

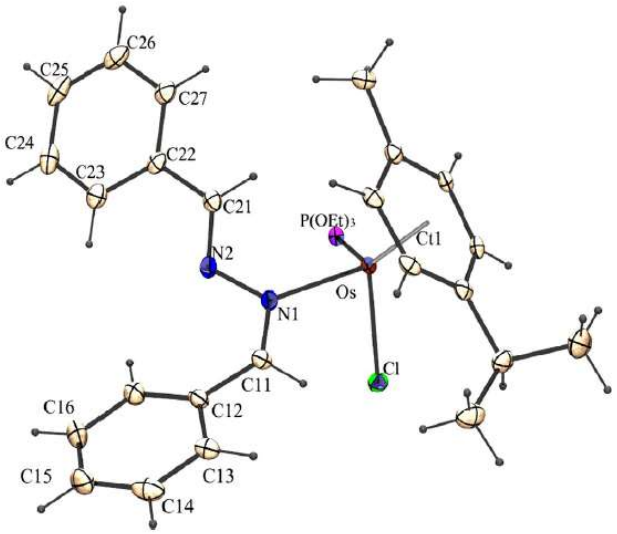

Figure 7.4 The cation [OsCl(η^6-*p*-cymene){κ^1-[N=C(H)Ph]–N=C(H)Ph}{P(OEt)$_3$}]$^+$ (15a).

Selected bond lengths and angles are shown in Table 7.3. The geometry of the complex is octahedral and is marked by near 90° values for angles Cl-Os-N, P-Os-N and Cl-Os-P, between 83.47(4) and 92.51(4)°. The *p*-cymene ligand is planar, with a RMS deviation of 0.0319 Å for the six atoms in the benzene ring, and it is coordinated with a ring-slippage of only 0.066 Å. Distances Os–C range from 2.1953(19) to 2.3123(19) Å. Osmium atom is at 1.7335(3) Å from the best calculated plane for the benzene ring and at 1.73449(12) from the centroid of the benzene ring. Os–Cl and Os–P bond distances (see Table 7.3) are expected values for this kind of compounds[184]. The azine derivative ligand is coordinated as N-monodentated donor by using one of the nitrogen atoms. The Os–N bond distance, 2.1439(16) Å, as expected due the sp2 character of the nitrogen atom and the different ancillary phosphine ligand, is shorter than that found in [OsCl(η^6-*p*-

cymene)(PhNHNH$_2$){PPh(OEt)$_2$}]$^+$ cation, 2.154(4) Å, and in the wide range found for chelating osmium half-sandwich chloro compounds, between 2.015(3) and 2.225(3) Å[185,186].

Table 7.3 Selected bond lengths [Å] and angles [°] for 15a.

Os-CT1	1.73449(12)	Os–Cl	2.3999(5)
Os-N(1)	2.1439(16)	Os–P(1)	2.2851(5)
Os-C(1)	2.3123(19)	Os–C(2)	2.2853(19)
Os-C(3)	2.2000(19)	Os–C(4)	2.2591(19)
Os-C(5)	2.1989(19)	Os–C(6)	2.1953(19)
N(1)-C(11)	1.296(2)	N(1)–N(2)	1.421(2)
N(2)-C(22)	1.276(3)	C(11)–C(12)	1.470(3)
C(21)-C(22)	1.462(3)		
N(1)–Os–P(1)	92.51(4)	CT1–Os–P(1)	129.074(13)
N(1)–Os–Cl	83.47(4)	CT1–Os–Cl	126.023(12)
P(1)–Os–Cl	85.317(17)	CT1–Os–N(1)	126.20(4)
C(11)–N(1)–N(2)	113.95(16)	C(11)–N(1)–Os	118.93(13)
N(2)–N(1)–Os	127.10(12)	C(21)–N(2)–N(1)	115.53(16)
N(1)–C(11)–C(12)	131.78(19)	N(2)–C(21)–C(22)	121.82(18)

Metallic complexes of several metals with the (1,2-dibenzylidene) hydrazine ligand are cited in the literature either with a similar monodentated behaviour, or acting in a η^2-N,N fashion or in a cyclometallated manner. However, to the best of our knowledge, this is the first osmium complex crystallographically described with this type of ligand, although some osmium *p*-cymene chloro complexes of several hydrazine derivatives can be found in the literature[162,187,188]. The Os–N distances for those complexes are shorter than in **15a**, probably due the chelating fashion of those ligands. The coordination of the nitrogen atom N(1) to the metal slightly stretches the C=N bond of 0.02 Å (see Table 7.3) and slightly shortens the N–N bond length when compared with free ligand[171,172]. Also the hydrazine ligand is coordinated in such a way that the ligand resulted wrinkled, in contrast with the free ligand structure[187] or when compared with substituted ones[173,189–192], and the dihedral angle between phenyl rings is 38.51(9)°. However, the torsion angle for the C–N–N–C chain shows a value of 157.05 (19)° [for the C(11)–N(1)–N(2)–C(21) chain], much more linear than in the related ruthenium complexes [97.9(13)° and 113.9(8)°]. Such differences are evident in Figure 7.5, where both complexes were drawn in a superimposed manner.

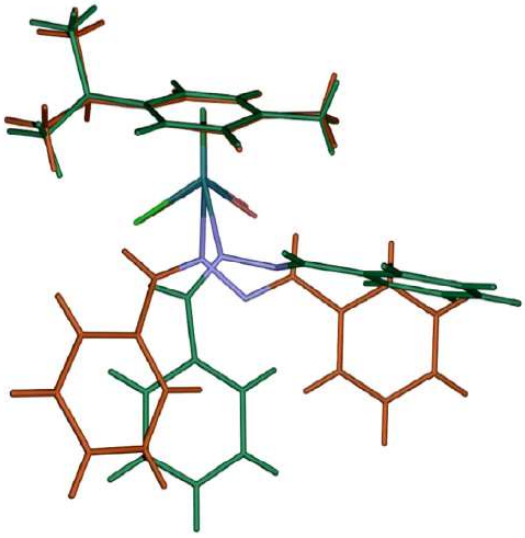

Figure 7.5 Comparison between Ru and Os complexes. Carbon atoms drawn in green for the ruthenium complex [9], in brown for the osmium complex [15a].

The IR spectra of aldazine complexes [OsCl(η^6-*p*-cymene){κ^1-[N=C(H)C$_6$H$_4$R1]–N=C(H)C$_6$H$_4$R1}{P(OR)$_3$}]BPh$_4$ (**14, 15**) show a medium-intensity band at 1619–1603 cm^{-1}, attributed to the $\nu_{C=N}$ of the azine ligand. Its presence is confirmed by the ^{1}H NMR spectra, which show two singlets at 8.96–8.58 and 7.88–7.83 ppm respectively attributed to the CH of the free and coordinated end of the azine. In the spectra also appear the signals of the ancillary ligands *p*-cymene, P(OR)$_3$ and the anion BPh$_4$ as well as those of the substituents R1 of the azine. The ^{13}C NMR spectra show two characteristic singlets at 166.90–164.21 and 158.41–161.22 ppm, attributed to the =C(H) carbon resonances of the free and coordinated end of the aldazine, whereas the ^{31}P NMR spectra show one singlet at 71.53–65.20 ppm, fitting the proposed formulation for the complexes. The proton NMR spectra of ketazine complexes [OsCl(η^6-*p*-cymene){κ^1-[N=C(CH$_3$)$_2$]–N=C(CH$_3$)$_2$}{P(OR)$_3$}]BPh$_4$ (**16, 17**) also support the proposed formulation showing, beside the signals of the ancillary ligands, two singlets at 2.37–2.30 and 2.23–2.30 ppm of the methyl groups of the κ^1-N=C(CH$_3$)$_2$ end and a singlet at 2.07–2.06 ppm of the free end of the ketazine.

The IR spectra of metalated complexes [Os{κ^2-R1C$_6$H$_3$C(H)=N-N=NC(H)C$_6$H$_4$R1}(η^6-*p*-cymene){P(OR)$_3$}]BPh$_4$ (**20, 21**) show a medium-intensity band at 1621–1614 cm^{-1}, attributed to the $\nu_{C=N}$ of the azine. However, the presence of this ligand is confirmed by the ^{1}H NMR spectra, which show one doublet at 8.88–8.76 ppm (J_{PH} = 2.65 and 2.62 Hz) and one singlet at 8.60-8.53 ppm, attributed to the =C(H) proton resonances of the chelate and free –N=C(H) end of the azine. The presence of a doublet is due to the small coupling (ca. 2.6 Hz) with the phosphorus of the phosphine. The ^{13}C spectra support the proposed formulation showing, beside the resonances of

the ancillary ligands, two singlets at 174.70–174.89 and 162.07–162.00 ppm, attributed to the (H)C=N- carbon resonances of the chelate and free –N=C(H) end respectively, of the azine. The resonance of the metalated carbon Os–C falls near 140 ppm, whereas ^{31}P spectra are singlets at 76.70–72.47 ppm, fitting the proposed formulation for the complexes.

The IR spectra of hydrazone complexes [OsCl(η^6-*p*-cymene){$NH_2N=C(CH_3)_2$}{$P(OR)_3$}]BPh_4 (**18, 19**) show two bands of medium intensity at 3263–3201 cm^{-1}, due to the ν_{NH} of the $NH_2N=C(CH_3)_2$ ligand, while the $\nu_{C=N}$ appears at 1647–1643 cm^{-1}. The ^1H NMR spectra show two broad signals at 6.69–6.66 and 6.37–6.23 ppm, due to the prochiral protons of NH_2. Two singlets also appear at 2.23–2.10 and 1.98–1.92 ppm, which were attributed to the methyl substituents of the hydrazone. The ^{13}C NMR spectra support the proposed formulation showing, beside the resonances of the ancillary ligands, a singlet at 166.93 ppm (**18**) of the quaternary carbon $N=C(CH_3)_2$ and two singlets at 25.33 and 18.58 ppm of the methyl groups, confirming the presence of the hydrazone.

The reactivity of these complexes was also tested, unfortunately with poor results. Whereas the homologous ruthenium compounds, under certain conditions, were able to give substitution reactions, the osmium derivatives **14-21** are so stable that every reaction gave as results either the formation of decomposition products or the isolation of the unchanged reagent.

7.3 Reaction of Azines with Half-Sandwich Complexes of Rhodium

The interesting results obtained of the synthetic studies of azine with ruthenium and osmium complexes suggested to extend this line of research to the transition metals of the cobalt triad too. In particular, the reactivity of different kind of azines, in rhodium and iridium complexes stabilized by pentamethylcyclopentadiene, was tested.

Only a few preliminary tests were made with the rhodium complexes because we observed that half-sandwich rhodium compounds have the same behaviour as the osmium ones. Indeed, chloro complex $RhCl_2(\eta^5\text{-}C_5Me_5)[P(OEt)_3]$, like osmium compounds $OsCl_2$(*p*-cymene)$P(OR)_3$, reacts first with one equivalent of AgOTf and then with both aldazines R1(H)C=N–N=C(H)R1 and the ketazine $(CH_3)_2C=N–N=C(CH_3)_2$ to give respectively κ^1-azine complexes [RhCl(η^5-C_5Me_5){κ^1-[N=C(H)R1]–N=C(H)R1}{$P(OEt)_3$}]BPh_4 (**22**) and [RhCl(η^5-C_5Me_5){κ^1-[$N=C(CH_3)_2$]–$N=C(CH_3)_2$}{$P(OEt)_3$}]BPh_4 (**23**), which were isolated as BPh_4^- salts and characterised (Schemes 7.15 and 7.16).

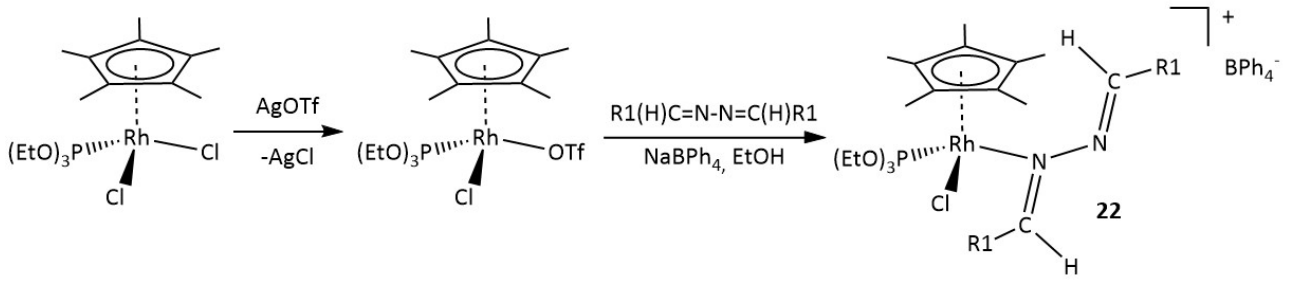

Scheme 7.15 R1 = Ph, *p*-tolyl.

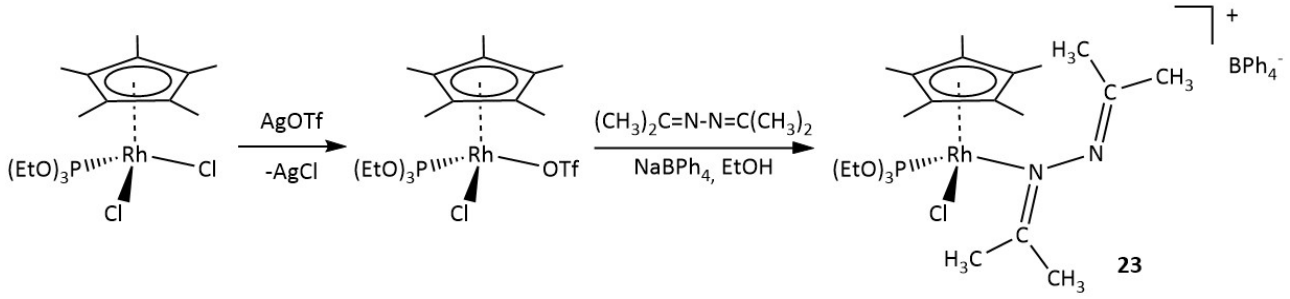

Scheme 7.16 Synthesis of ketazine complex of rhodium.

The reaction proceeds with substitution of one chloride ligand by AgOTf and formation of the triflate intermediate RhCl(κ^1-OTf)(η^5-C_5Me_5)[P(OEt)$_3$], which was not isolated. The replacement of the labile κ^1-OTf group produced κ^1-azine derivatives **22, 23**. It is worth noting that the formation of the triflate complex RhCl(κ^1-OTf)(η^5-C_5Me_5)[P(OEt)$_3$] is crucial for the preparation of κ^1-azine derivatives **22** and **23**, because dichloro species $RhCl_2$(η^5-C_5Me_5)[P(OEt)$_3$] do not react directly with azine.

More studies on κ^1-azine derivative **22a** have shown that this complex is unstable in solution, and slowly undergo metalation reaction, generating the chelate complex [Rh{κ^2-C_6H_4(H)C=N–N=C(H)(C_6H_5)}(η^5-C_5Me_5){P(OEt)$_3$}]BPh_4 (**24**).

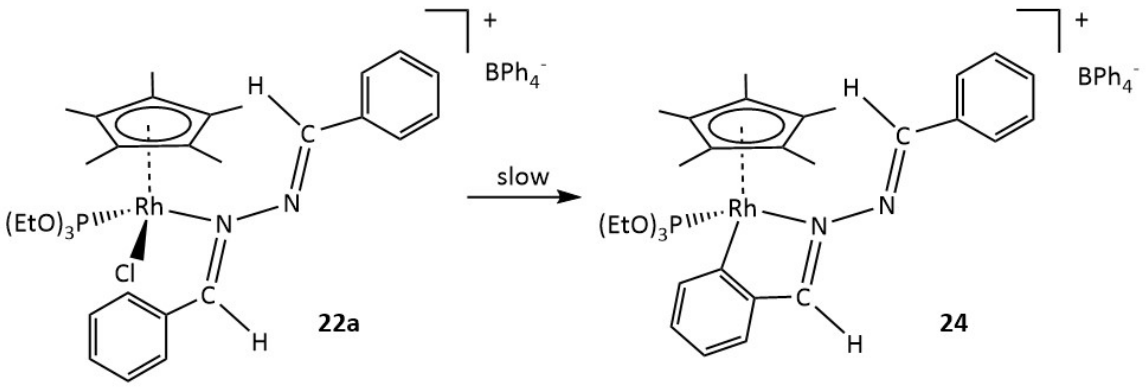

Scheme 7.17 Metalation reaction

The reaction proceeds with sp^2 CH activation and, after the formal loss of HCl, we obtained chelate κ^2 derivative **24**, which was isolated and characterized: the metalation reaction is rather slow and

at room temperature requires more than one day. However, complex **24** can also be quickly prepared in a one-pot synthesis, by reacting chloro complex $RhCl_2(\eta^5\text{-}C_5Me_5)[P(OEt)_3]$ first with two equivalents of AgOTf and, after removing AgCl (filtration), with an excess of benzaldehydeazine, as shown in Scheme 7.18.

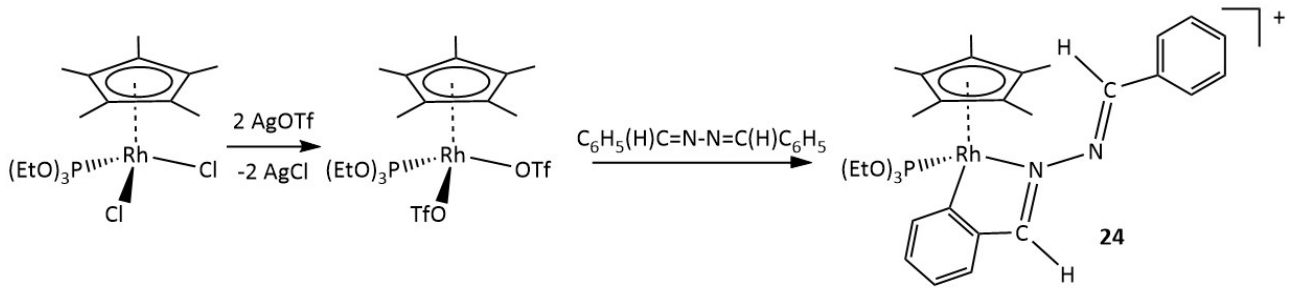

Scheme 7.18 One-pot synthesis.

The presence of two labile ligands such as OTf in the precursor favours not only κ^1-coordination of the azine but the subsequent metalation too, rapidly affording the final chelate species **24**. Moreover, the excess of azine is essential because its Brønsted basicity favours the formal removal of HOTf.

Unfortunately, the low yield, the difficulty in having non-oil products and the impossibility to obtain crystals suitable for X-ray structure determination of complexes **22-24** have discouraged us from extending our research in this direction.

7.4 Reaction of Azines with Half-Sandwich Complexes of Iridium

Parallel to the studies of azine complexes of rhodium, the reactivity of iridium half-sandwich complexes $IrCl_2(\eta^5\text{-}C_5Me_5)[P(OR)_3]$ with azines has been investigated. The first reaction tested, a direct reaction between the chloro complex precursor and azine in the presence of $NaBPh_4$, led to the formation of a mixture of unidentifiable products. Thus, we decided to apply the same synthetic route used with the osmium and rhodium compounds.

Half-sandwich complexes $IrCl_2(\eta^5\text{-}C_5Me_5)[P(OR)_3]$ react first with one equivalent of AgOTf and then with both aldazines R1(H)C=N–N=C(H)R1 and the ketazine $(CH_3)_2\text{-}C=N–N=C(CH_3)_2$ to give κ^1-azine complexes $[IrCl(\eta^5\text{-}C_5Me_5)\{\kappa^1\text{-}[N=C(H)R1]–N=C(H)R1\}\{P(OR)_3\}]BPh_4$ (**25, 26**) and $[IrCl(\eta^5\text{-}C_5Me_5)\{\kappa^1\text{-}[N=C(CH_3)_2]N=C(CH_3)_2\}\{P(OR)_3\}]BPh_4$ (**27, 28**), which were isolated as BPh_4^- salts and characterised (Schemes 7.19 and 7.20).

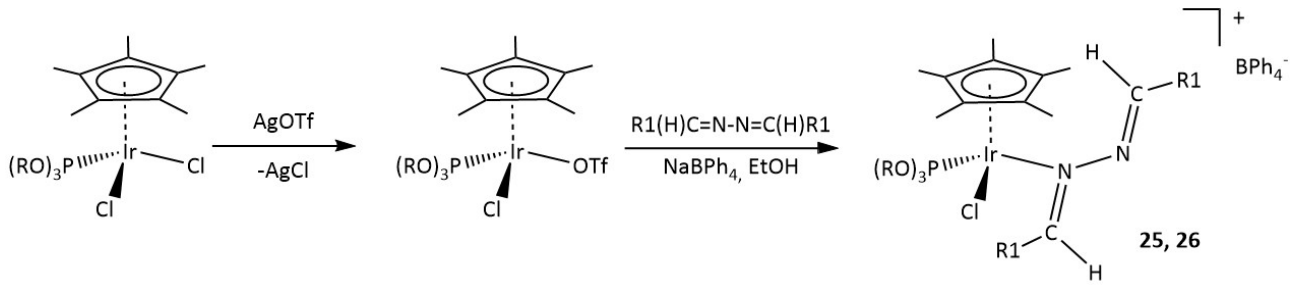

Scheme 7.19 R = Me (25), Et (26); R1 = Ph (a), 4-$CH_3C_6H_4$ (b), 2,6-$(CH_3)_2C_6H_3$ (f).

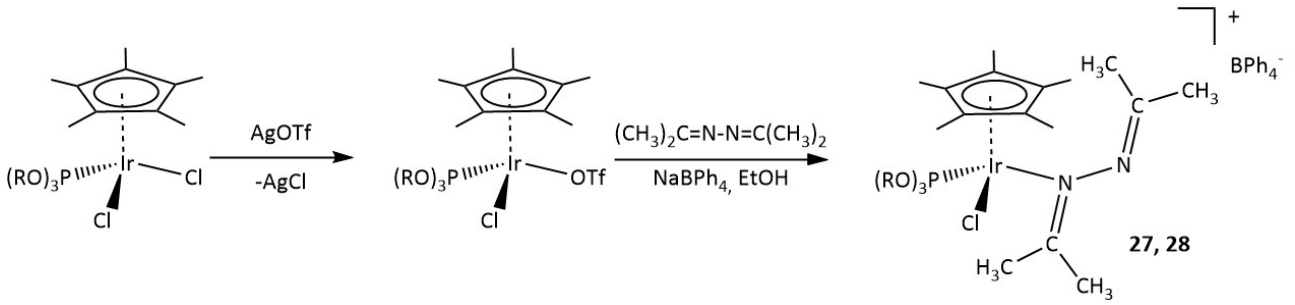

Scheme 7.20 R1 = Me (27), Et (28).

The reaction proceeds with abstraction of the Cl^- by Ag^+ and formation of the triflate intermediates $IrCl(\kappa^1\text{-}OTf)(\eta^5\text{-}C_5Me_5)[P(OR)_3]$. Because the κ^1-OTf group is more labile than the chloride ligand this can be easily replaced by azine to produce the κ^1-azine derivatives **25–28**, isolable as solids in good yield. κ^1-Azine derivatives **25–28** were found to be unstable in solution, in which they undergo a intramolecular reaction, giving the chelate complexes $[Ir\{\kappa^2\text{-}R1C_6H_3(H)C{=}N{-}N{=}C(H)(R1C_6H_4)\}(\eta^5\text{-}C_5Me_5)\{P(OR)_3\}]BPh_4$ (**29, 30**) and $[Ir\{\kappa^2\text{-}CH_2(CH_3)C{=}N{-}N{=}C(CH_3)_2\}(\eta^5\text{-}C_5Me_5)\text{-}\{P(OR)_3\}]BPh_4$ (**31, 32**) in good yields (Scheme 7.21).

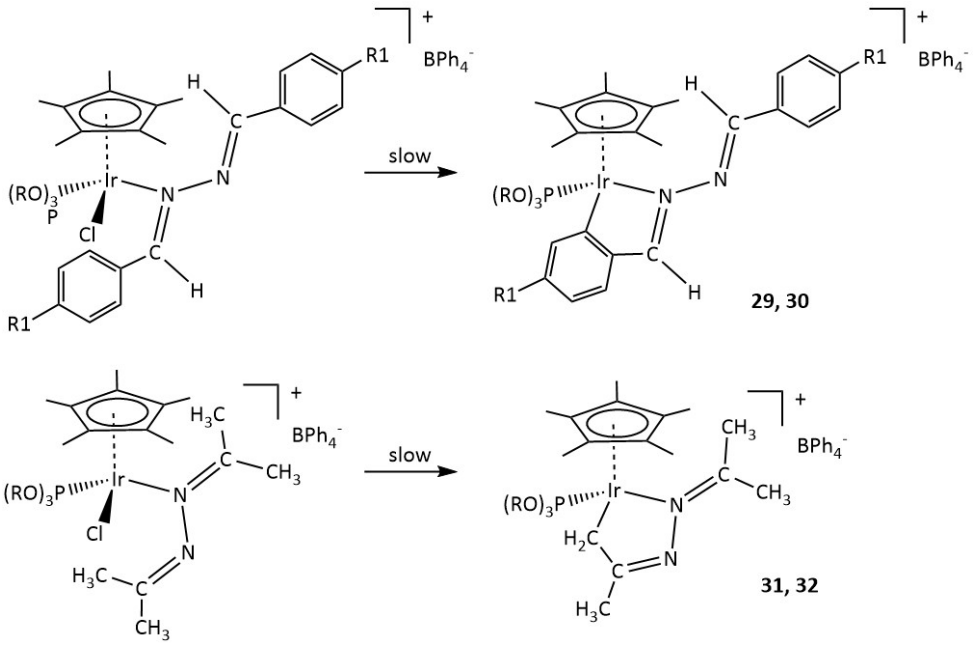

Scheme 7.21 R = Me (5, 7), Et (6, 8); R1 = H (a), 4-CH_3 (b), 4-CH_3O (c), 4-F (d), 4-NO_2 (e).

The reaction proceeds through sp^2-CH activation to produce, after loss of the HCl, chelate κ^2 derivatives **29–32**, which were isolated and characterised. The metalation reaction is quite slow at room temperature and, in some cases, the complete formation of the chelate species requires more than one day. However, the complexes **29–32** can also be effortlessly prepared by one-pot synthesis, by reacting chloro complexes $IrCl_2(\eta^5\text{-}C_5Me_5)[P(OR)_3]$ first with two equivalents of AgOTf and, after removing AgCl, with an excess of the appropriate azine, as shown in Scheme 7.22.

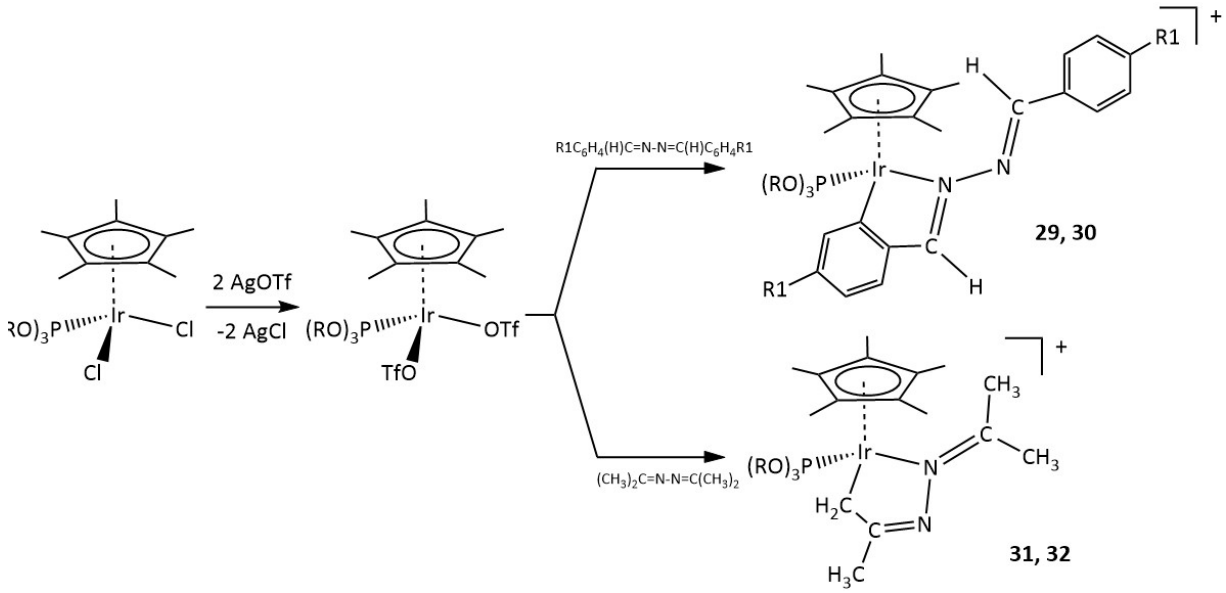

Scheme 7.22 R = Me (29, 31), Et (30, 32); R1 = H (a), 4-CH_3 (b), 4-CH_3O (c), 4-F (d), 4-NO_2 (e).

The presence of two labile ligands such as OTf in the precursor favours not only the κ^1-coordination of the azine but also the subsequent metalation, rapidly giving the final chelate species **29–32** in good yield. The tendency towards metalation of the κ^1-azine ligands in the presence of a free coordination site on the iridium(III) centre is highlighted by the DFT-optimised structure of the cation $[Ir\{\kappa^1\text{-}C_6H_5(H)C{=}N{-}N{=}C(H)(C_6H_5)\}(\eta^5\text{-}C_5Me_5)\{P(OMe)_3\}]^{2+}$ (Fig. 7.6), which shows the deviation of the *ortho*-hydrogen atom of the aromatic substituent close to the metal centre by about 0.32 Å with respect to the ring plane.

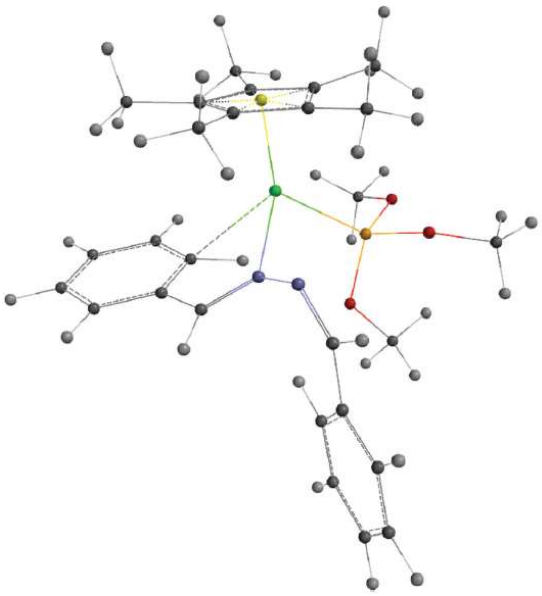

Figure 7.6 DFT-optimised structure of the cation $[Ir\{\kappa^1\text{-}C_6H_5(H)C{=}N{-}N{=}C(H)(C_6H_5)\}(\eta^5\text{-}C_5Me_5)\{P(OMe)_3\}]^{2+}$. Color map: dark gray, C; light gray, H; blue, N; red, O; orange, P; green, Ir; yellow, centroid.

It should be noted that metalation occurs with all the $R1C_6H_4$ aryl substituents of the involved aldazines, except for the complex $[IrCl(\eta^5\text{-}C_5Me_5)\{\kappa^1\text{-}[N{=}C(H)\{2,6\text{-}(CH_3)_2C_6H_3\}]{-}N{=}C(H)[2,6\text{-}(CH_3)_2\text{-}C_6H_3]\}\{P(OEt)_3\}]BPh_4$ (**25f**). In this case, the formation of the chelate ring is probably hampered by a too wide bite angle.

Oddly, the rate of metalation reaction in complexes of the type $[IrCl(\eta^5\text{-}C_5Me_5)\{\kappa^1\text{-}[N{=}C(H)(R1C_6H_4)]{-}N{=}C(H)(R1C_6H_4)\}\{P(OR)_3\}]BPh_4$ (**25, 26**) is comparable with those of the formation of the κ^1-species. As a result, κ^1-azine complexes cannot be separated in pure form, owing to the presence of large amounts of the chelate species **29** and **30** in the reaction products. The formation of these κ^2-species also entails a CH activation step (either sp^2 CH activation, in the case of the aldazine species **25** and **26**, or sp^3 CH activation, in the ketazines **27** and **28**) promoted by the iridium fragment and, in the case of ketazine, is a rare example involving an aliphatic group.

Good analytical data were obtained for all κ^1- and κ^2-azine complexes, which were obtained as yellow or orange solids stable in air and in solution of polar organic solvents, where they behave as 1 : 1 electrolytes[163]. Infrared and NMR data support the proposed formulation, which was further confirmed by X-ray crystal structure determination of $[Ir\{\kappa^2\text{-}C_6H_4(H)C{=}N{-}N{=}C(H)(C_6H_5)\}(\eta^5\text{-}C_5Me_5)\{P(OEt)_3\}]BPh_4$ (**30a**), whose ORTEP[164] is shown in Fig. 7.7.

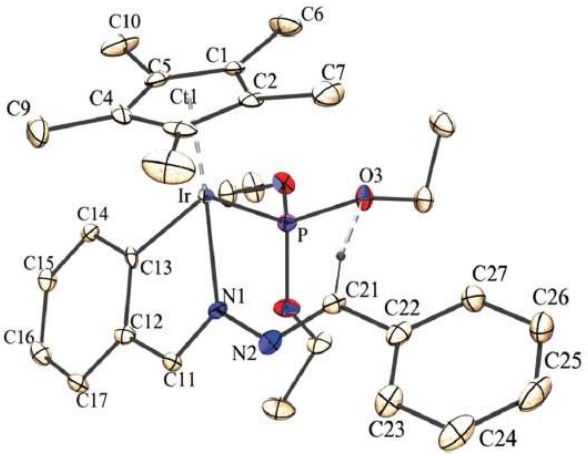

Figure 7.7 ORTEP view of the cation of 30a drawn at the 50% probability level. The tetraphenylborate anion is not shown and hydrogen atoms are not represented, except that forming the intramolecular H-bond.

The structure of the compound **30a** consists of a tetraphenylborate anion and a cation formed of an iridium atom η^5-coordinated (ring-slippage of 0.082 Å) to a pentamethylcyclopentadienyl ligand (Cp*) and three donor atoms, leading to the formation of a "three-legged piano stool" structure. These donor atoms are one phosphorus atom from a $P(OEt)_3$ phosphite ligand and a bidentate κ^2-C,N-benzaldehydeazine ligand. The overall geometry of the complex is pseudo octahedral, in which three of the positions are occupied by the Cp* ligand. The angles between legs (see Table 7.4) should be near 90°, but it is worth noting that one of these, the N–Ir–C angle, is 77.35(12)° and is constrained by the nature of the bidentate ligand, whereas the other two have almost the same value, 89.43(9) versus 89.52(8)°.

Table 7.4 Selected bond lengths [Å] and angles [°] for 30a

Ir–CT1	1.87764(13)	Ir–C(13)	2.076(3)
Ir–N(1)	2.096(3)	Ir–P	2.2295(9)
Ir–C(1)	2.229(3)	Ir–C(2)	2.276(3)
Ir–C(3)	2.264(3)	Ir–C(4)	2.238(3)
Ir–C(5)	2.184(3)	Ir–Cav	2.238
N(1)–N(2)	1.403(4)	N(1)–C(11)	1.297(4)
N(2)–C(21)	1.277(5)	C(11)–C(12)	1.427(4)
C(21)–C(22)	1.466(4)		
CT1–Ir–C(13)	126.63(9)	CT1–Ir–N(1)	129.14(7)
CT1–Ir–P	128.77(2)	N(1)–Ir–P	89.52(8)
C(13)–Ir–P	89.43(9)	C(13)–Ir–N(1)	77.35(12)
C(11)–N(1)–N(2)	113.6(3)	C(11)–N(1)–Ir	116.8(2)
N(2)–N(1)–Ir	129.7(2)	C(21)–N(2)–N(1)	115.6(3)
N(2)–C(21)–C(22)	120.2(3)	N(1)–C(11)–C(12)	116.6(3)

The sum of these three values, 270°, is lower than expected: that is, the angles between the Cp* centroid and the donor atoms (expected 125.3°) are all larger than usual [between 126.63(9) and 129.14(7)°], probably due to the steric requirement of the Cp* ligand and the formation of a C–H···O bond interaction between the C(21) imine carbon and one oxygen atom of one of ethoxy groups (Table 7.5).

Table 7.5 Parameters of the hydrogen bond interaction [Å and °]

D-H···A	*d*(D-H)	*d*(H···A)	*d*(D···A)	<(DHA)
C(21)–H(21)···O3	0.95	2.58	3.431(4)	149.4

The centroid of the Cp* ligand is located at 1.87764(13) Å from the iridium atom, and the average Ir–C bond distance for the Cp* ligand is 2.238 Å (Table 7.4), both values being similar to those found in the literature[193–195]. The bond length of Ir–P [2.2295(9) Å] is only slightly shorter, for example, than the cations $[IrCp^*Cl[H_2N\text{-}NHR]\{P(OEt)_3\}]^+$ R = H, 2.2362(6) Å and R = Me, 2.2500(5) Å[150]. To the best of our knowledge, the literature does not contain any crystallographically described benzaldehydeazine iridium complex, so we should compare ours with other metal compounds. In the literature, this ligand is reported to show a different coordinative behaviour, but it can be found coordinated to the metal through one of the imine nitrogen atoms and by one of the ortho carbon atoms in the benzyl rings with several metals such as Co, Ni, and Mn. This coordinative fashion allows the formation of a planar [root mean square deviation of 0.022 Å] five-membered metallacycle $IrNC_3$. Two of these carbon atoms in the cycle also belong to the benzene ring, and both fused rings form a dihedral angle between planes of only 1.99(16)°. The other iminobenzyl moiety remains uncoordinated and is twisted, forming a dihedral angle between both benzenes in the ligand of 36.93(13)°. This value is similar to that found in the *o*-difluorinated benzaldehydeazine ligand (L) in $[CoMeCl(PMe_3)L]$,[196] 43.6(1)°, but it is in contrast with the values of 78.6(4) and 82.9(3)° found in N-monodentated Ru complexes, and also with the plane conformation found both in the free ligand[171–173] and in the cyclometallated $MnL(CO)_4$ compound[167] or $NiLCl(PMe_3)$ compounds,[169] which are almost planar. The torsion angle for the C–N–N–C chain has a value of 154.1(3)° and also differs from the values found in the above-mentioned N-monodentated Ru complexes, between 86.5(6)° and 113.9(8)°. The N(1)–N(2) bond length, 1.403(4) Å is similar to that found in most of the above-mentioned complexes and reveals a certain amount of delocalisation, since it is slightly shorter than the value of 1.45 Å expected for a single bond. The C=N bond length of the coordinated nitrogen, [N(1)–C(11), 1.297(4) Å], is longer

than that of the free C=N, [N(2)–C(21), 1.277(5) Å], whereas C(11)–C(12) [1.427(4) Å] is shorter than that of the free imino moiety C(21)–C(22) [1.466(3) Å]. The Ir–C(13) bond length (into the metallacycle), 2.076(3) Å, is similar to that found in the cation $[IrCp^*(oxazoline)(ppy)]^+$, 2.080(5) Å, although longer than that found in $[IrCl_2(ppy)(Hppy)]$,[197] 2.021(4) Å, and also in the plethora of cyclometallated 2-phenylpyridine (ppy) iridium(III) complexes found in the literature, with Ir–C bond lengths which are also in the range of 1.99 to 2.01 Å, although this distance may increase to 2.04 Å if the compound contains the Cp* ligand[198,199], e.g., 2.0482(18) and 2.0346(19) Å in $IrClCp^*(F\text{-}ppy)$[200] or 2.038(2) Å in $IrClCp^*(PhCHNPr)$.[201]

The IR spectra of κ^1-azine complexes $[IrCl(\eta^5\text{-}C_5Me_5)\{\kappa^1\text{-}[N=C(H)R1]\text{–}N=C(H)R1\}\{P(OR)_3\}]BPh_4$ (**25, 26**) show a medium-intensity band at 1619–1615 cm^{-1}, attributed to the $\nu_{N=C}$ of the azine ligand. However, the presence of this group is confirmed by the ^1H NMR spectra, which show two singlets at 8.96–8.64 and 8.62–8.02 ppm, attributed to the CH protons of the free and coordinated N=C(H) groups, respectively. Besides the signals of the ancillary ligands C_5Me_5, $P(OR)_3$ and the anion BPh_4^-, the spectra show two singlets of the methyl substituents of the 4-$CH_3C_6H_4$ group (**26b**) and three for the 2,6-$(CH_3)_2C_6H_3$ one (**26f**), whereas the ^{31}P NMR spectra are sharp singlets, fitting the proposed formulation for the complexes. In addition, the ^{13}C NMR spectrum of **26a** supports the presence of the κ^1-azine, showing two singlets at 165.80 and 162.84 ppm, attributed to the coordinated and free N=C(H) carbon resonances of the aldazine. The proton spectra of the ketazine complexes $[IrCl(\eta^5\text{-}C_5Me_5)\{\kappa^1\text{-}[N=C(CH_3)_2]\text{–}N=C(CH_3)_2\}\{P(OR)_3\}]BPh_4$ (**27, 28**), besides the resonances of the ancillary ligands, show two singlets at 2.19 and 2.14 (**27**) and at 2.35 and 2.22 ppm (**28**) of the methyl groups of the coordinated and free ends of the azine. Instead, the ^{31}P NMR spectrum is a singlet, matching the proposed formulation.

The ^1H NMR spectra of the metalated complexes $[Ir\{\kappa^2\text{-}R1C_6H_3(H)C=N\text{–}N=C(H)(R1C_6H_4)\}(\eta^5\text{-}C_5Me_5)\{P(OR1)_3\}]BPh_4$ (**29, 30**) show one doublet at 8.84–8.45 ppm, attributed to the N=C(H) resonances of the cyclometallated group, and one singlet at 8.60–8.03 ppm of the other, free N=C(H) group of the κ^2-azine; the doublet is due to a light coupling with the ^{31}P of the phosphine. The spectra also show the signals of ancillary ligands and the singlets of the methyl or methoxy substituents of the $R1C_6H_3$ and $R1C_6H_4$ moieties of the azine, whereas the ^{31}P spectra are sharp singlets. The ^{13}C NMR spectra also support the presence of the metalated ligand, showing two singlets at 175.76 and 163.19 ppm (**30a**) of the two N=C(H) carbon resonances of the κ^2-azine, and

one singlet at 156.76 ppm of the metalated carbon resonance, matching the proposed formulation for the complexes.

^{1}H NMR spectra of κ^{2}-ketazine derivatives [Ir{κ^{2}-$CH_2C(CH_3)$=N–N=$C(CH_3)_2$}(η^{5}-C_5Me_5){P(OR1)$_3$}]BPh_4 (**31, 32**) show a multiplet between 2.93–2.07 ppm, which may be simulated with an ABC_3X model (X = ^{31}P) with the parameters reported in the Experimental section and attributed to the metal-bonded methylene protons κ^{2}-$CH_2C(CH_3)$=N of the metalated azine. The presence of a stereocentre in the molecule, i.e., the iridium atom, makes the two κ^{2}-CH_2 protons diastereotopic and their coupling with both the ^{31}P of the phosphine and the methyl protons give an ABC_3X multiplet. In the spectra, the signals of the methyl protons =N(CH_3) appear as a multiplet at 2.09–2.07 ppm, whereas the other two methyl substituents of the free end of ketazine N–N=$C(CH_3)_2$ appear as two singlets at 1.34–1.32 and 1.12–1.11 ppm, matching the proposed formulation. Besides the signals of the ancillary ligands, the ^{13}C NMR spectra of the complexes **31** and **32** show the characteristic signals of the chelate ketazine group. Broad singlets appear at 52.81 (**31**) and 52.70 (**32**) ppm which, in a HMQC experiment, were correlated with the multiplet near 2.92 ppm observed in the proton spectra and attributed to the Ir–CH_2 carbon resonance of the chelate azine. The singlet appearing at 18.93–18.89 ppm, correlated with the proton singlets at 2.09–2.07 ppm in an HMQC experiment, was assigned to the methyl carbon resonance of the Ir–$CH_2C(CH_3)$=N group, and the signals of the quaternary carbon appear at 164.61–163.50 ppm. Instead, the methyl signals of the free end of the ketazine N=$C(CH_3)_2$ appear as two singlets at 27.26–27.17 and 26.92–26.91 ppm, and the quaternary carbon as a singlet at 61.54–61.31 ppm, fitting the proposed formulation.

7.4.1 Photophysical Properties

Upon excitation with light in the near UV–violet range, solid samples of the metalated aromatic κ^{2}-azine complexes [Ir{κ^{2}-$C_6H_4(H)C$=N–N=$C(H)(C_6H_5)$}(η^{5}-C_5Me_5){P(OR)$_3$}]BPh_4 (R = Me, **29a**; Et, **30a**) showed emission in the red region centred at about 650 nm, with FWHM between 3100 and 3400 cm^{-1} (Graphic 7.1). The change of the phosphite ligand does not greatly affect the emission band. Several red-emitting Ir(III) complexes with metalated ligands are known[202].

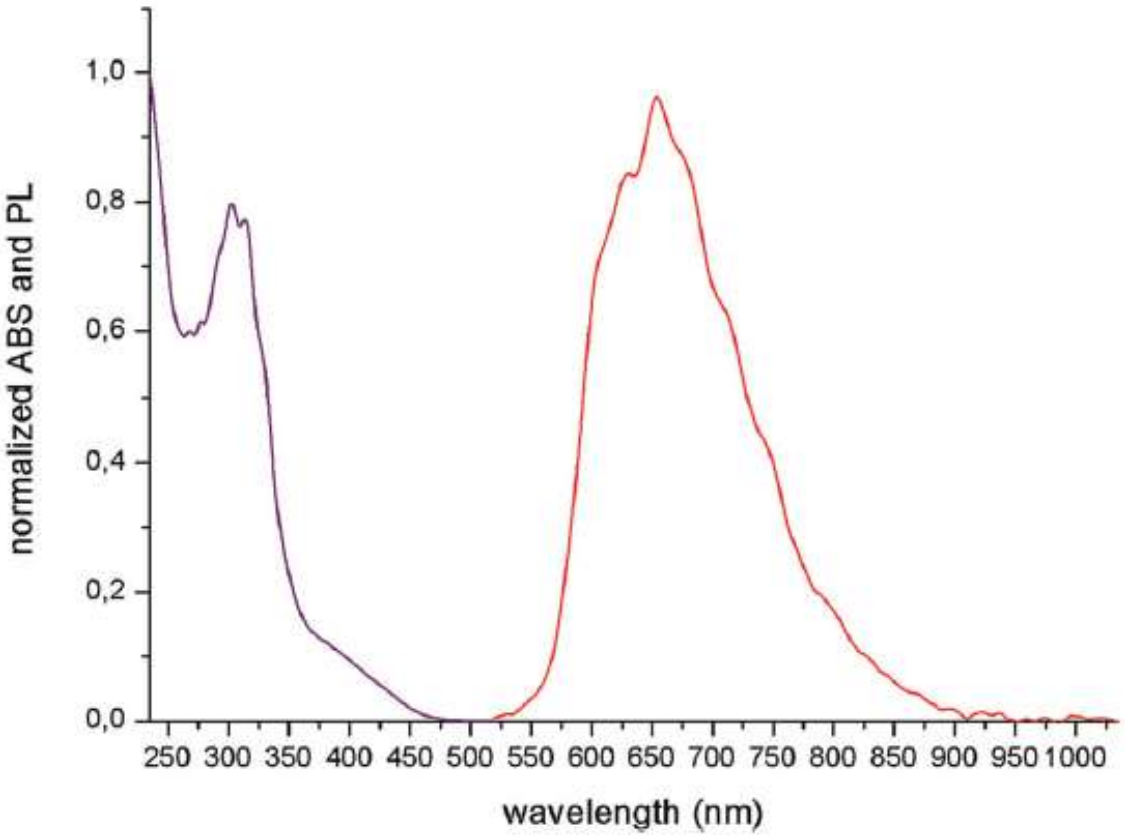

Graphic 7.1 Normalised absorption (CH_2Cl_2 solution, room temperature, violet line) and emission (solid sample, room temperature, $l_{excitation}$ = 405 nm, red line) spectra of [Ir{κ²-C_6H_4(H)C=N–N=C(H)(C_6H_5)}(η⁵-C_5Me_5){P(OEt)₃}]BPh_4 (30a).

Selected current examples of luminescent Ir(III) derivatives with emission centred at wavelengths higher than 600 nm are cationic complexes based on the $[Ir(ppy)_2(bpy)]^+$ skeleton (bpy = 2,2'-bipyridine), but bearing methoxy groups on the cyclometallating ligands,[203] or with 1,10-phenanthroline ligands featuring aryl acetylene chromophores instead of bpy.[204] Other recent representative red-emitting Ir(III) species are organometallic compounds having a metalated naphthalimide N-heterocyclic carbene in the coordination sphere,[205] and the compounds $Ir(th\text{-}pq)_3$ (th-pq = metalated 4-phenyl-2-(thiophen-2-yl)quinoline),[206] $[Ir(ppy)_2(pytpy)](PF_6)$ (pytpy = 4'-pyridyl-2,2':6',2''-terpyridine),[207] $Ir(nbt)_2$(cz-acac-allyl) (nbt = metalated 2-(1-naphthyl)benzothiazole; cz-acac-allyl = 1-(9-butyl-9H-carbazol-3-yl)hept-6-ene-1,3-dionate),[208] $[Ir(thpy)_2(bpySMe_2)][PF_6]$ (thpy = metalated 2-thienylpyridine; $bpySMe_2$ = 4,4'-dimethylthio-2,2'-bipyridine),[209] and $(Ir(mpiq)_3)$ (mpiq = metalated (4'-methylphenyl)isoquinoline).[210] The [Ir{κ²-C_6H_4(H)C=N–N=C(H)(C_6H_5)}(η⁵-C_5Me_5){P(OR)₃}]BPh_4 complexes **29a** and **30a** absorb radiation throughout the UV range and the violet region (Graphic 7.1). The lowest energy band, the selective excitation of which causes the red emission, is absent in the absorption spectra of both the free aldazine and the iridium precursor. TD-DFT calculations on the cation [Ir{κ²-C_6H_4(H)C=N–N=C(H)(C_6H_5)}(η⁵-C_5Me_5){P(OMe)₃}]⁺ allowed us to attribute this transition (computed value for

the absorption wavelength = 412 nm) to the population of the singlet excited state derived from the transfer of one electron from the HOMO of the complex ($\varepsilon_{\mathrm{HOMO}}^{\mathrm{DFT}}$ = -8.31 eV) to the LUMO ($\varepsilon_{\mathrm{LUMO}}^{\mathrm{DFT}}$ = -4.69 eV). The HOMO is centred on iridium, the metalated aromatic ring, the [N=C] donor moiety and, to a lesser extent, the pentamethylcyclopentadienyl ligand. Instead, the LUMO is located on both the coordinated and non-coordinated aromatic rings of aldazine and the N-donor fragment; the participation of the Ir centre is less important (Fig. 7.8).

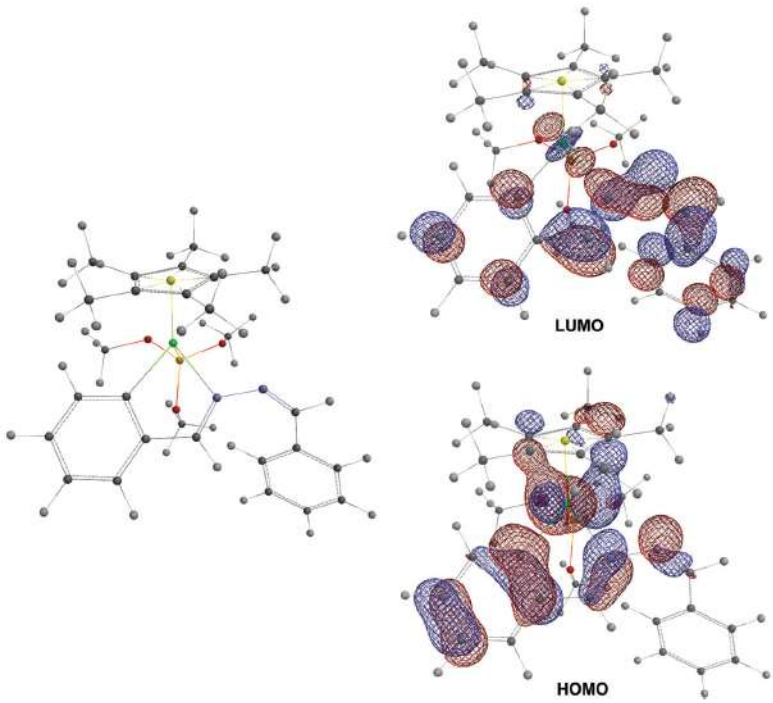

Figure 7.8 DFT-optimised singlet ground-state geometry of [Ir{κ²-C₆H₄(H)C=N–N=C(H)(C₆H₅)}(η⁵-C₅Me₅){P(OMe)₃}]⁺ and HOMO and LUMO molecular orbitals (surface isovalue = 0.04 a.u.). Colour map: dark grey, C; light grey, H; blue, N; red, O; orange, P; green, Ir; yellow, centroid

In view of the DFT outcomes, the lowest energy absorption therefore has a mixed ^{1}MLCT/^{1}LC character. Computational optimisation of the first excited triplet state geometry of [Ir{κ²-C₆H₄(H)C=N–N=C(H)(C₆H₅)}(η⁵-C₅Me₅){P(OMe)₃}]⁺ afforded a stationary point having a similar coordination sphere with respect to the singlet ground state (RMSD = 0.439 Å). The most striking differences involve the C–N–N–C dihedral angle of the azine ligand, from the 66.5° of the singlet geometry to 2.0°, that of the triplet. In addition, the triplet geometry has shorter N–N distances and longer C=N bonds (Table 7.6), as a consequence of the radical character of the azine ligand in this configuration.

Table 7.6 Selected computed distances (Å) for the ground state singlet and first excited state triplet geometries of [Ir{κ²-$C_6H_4(H)C=N–N=C(H)(C_6H_5)$}(η⁵-$C_5Me_5$){$P(OMe)_3$}]⁺.

	Singlet	Triplet
Ir–C(azine)	2.056	2.049
Ir–N	2.107	2.090
N–N	1.377	1.291
C–N	1.299	1.361
	1.286	1.386

Lastly, in the triplet excited state, the donor atoms of the azine ligand are slightly closer to the metal centre, whereas the other metal–ligand distances are almost unchanged. Triplet-configuration α-HOMO and α-HOMO-1 (Fig. 7.9) are, respectively, comparable with the LUMO and HOMO of the singlet ground structure. The most noticeable difference concerns the negligible participation of iridium orbitals to the triplet α-HOMO with respect to the singlet-LUMO; the non-coordinated aromatic ring is involved to a greater extent.

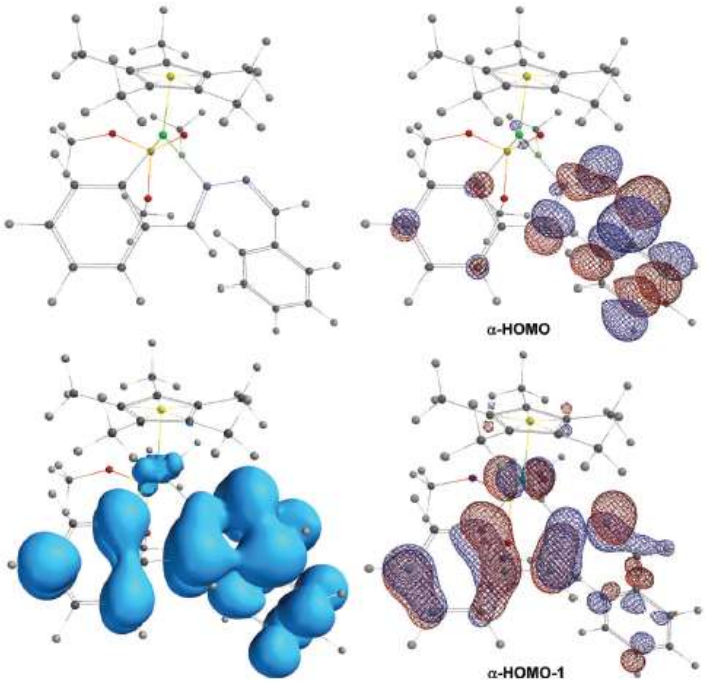

Figure 7.9 DFT-optimised first excited triplet-state geometry of [Ir{κ²-$C_6H_4(H)C=N–N=C(H)(C_6H_5)$}(η⁵-$C_5Me_5$){$P(OMe)_3$}]⁺, spin density surface (blue, isovalue = 0.001 a.u.), and a-HOMO and a-HOMO_1 molecular orbitals (surface isovalue = 0.04 a.u.). Color map: dark gray, C; light gray, H; blue, N; red, O; orange, P; green, Ir; yellow, centroid.

As shown also by the spin density surface (Fig. 7.9), the first triplet state is mainly located on the metalated azine ligand. The computed emission wavelength from the triplet state is at around 700 nm, matching the experimental value to an acceptable extent. According to DFT calculations, the

emission band was attributed to the ^{3}MLCT/^{3}LC transition. From the above-described molecular orbitals, the widths of the emission bands are primarily associated with the coordinated aldazine vibrational structure.

Emission lifetime measurements on solid samples of [Ir{κ^2-C$_6$H$_4$(H)C=N–N=C(H)(C$_6$H$_5$)}(η^5-C$_5$Me$_5$){P(OR)$_3$}]BPh$_4$ (**29a, 30a**) confirm the phosphorescent nature of the transition, ranging between 0.36 and 0.41 μs, and, respectively, corresponding to R = Et and Me (Graphic 7.2). These values are in line with the data reported for other Ir(III) complexes emitting in the same range[211].

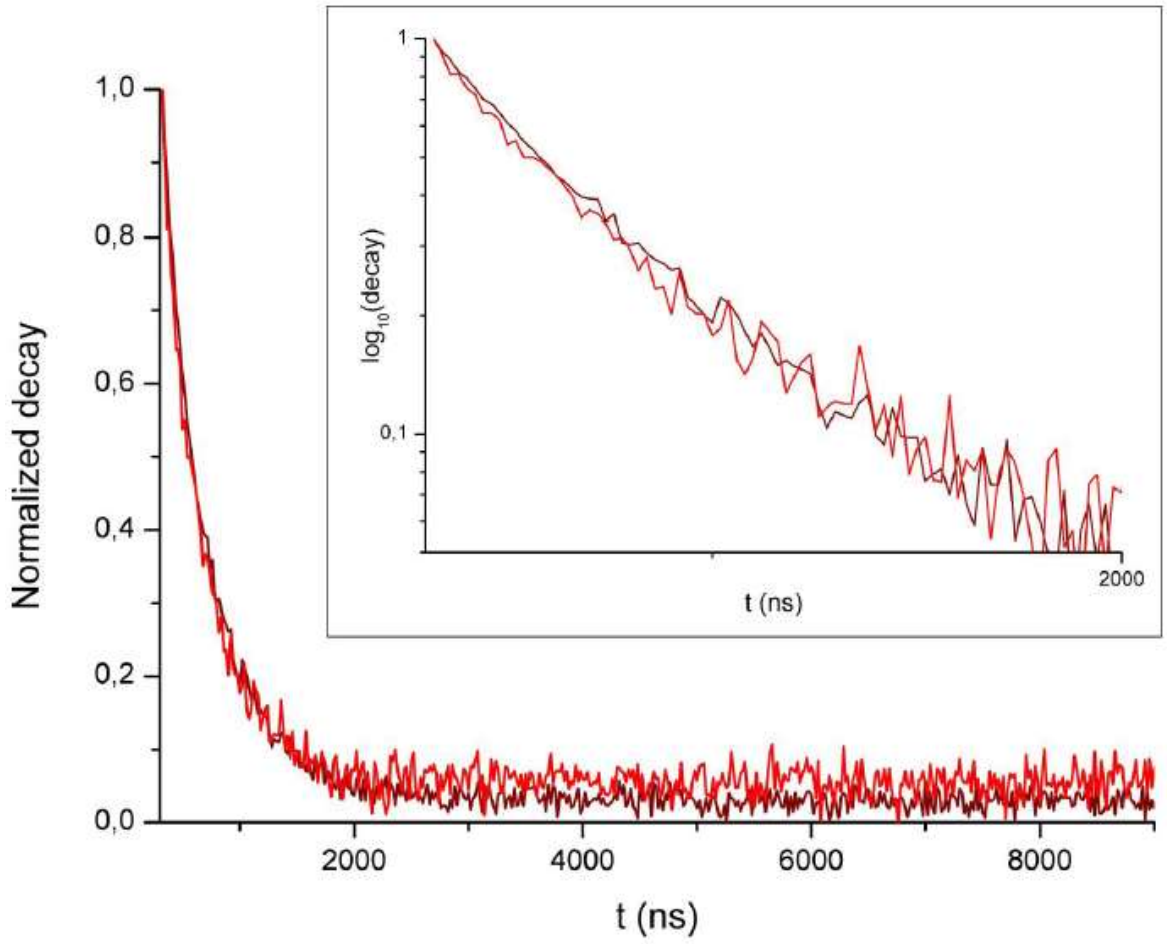

Graphic 7.2 Luminescence decay curves of [Ir{κ^2-C$_6$H$_4$(H)C=N-N=C(H)(C$_6$H$_5$)}(η^5-C$_5$Me$_5$){P(OR)$_3$}]BPh$_4$ complexes (R = Me, wine line; R = Et, red line). Inset: semi-log plot

As an example, 0.42 μs were measured at 298 K for [Ir(μ-Cl)(ppy-NO$_2$)$_2$]$_2$ (ppy-NO$_2$ = metalated 5-nitro-2-phenylpyridine),[212] the emission maximum of which peaks at 651 nm. These quite short lifetimes indicate the strong influence of non-radiative decay processes. The vibronic coupling of the triplet state to the ground state probably explains the quite low quantum yields (ϕ_P) measured for [Ir{κ^2-C$_6$H$_4$(H)C=N–N=C(H)(C$_6$H$_5$)}(η^5-C$_5$Me$_5$){P(OR)$_3$}]BPh$_4$ (**29a, 30a**) complexes at room temperature, around 1%. However, these results were expected for emitters in the deep red region, as luminescent Ir(III) complexes are known to obey the energy gap law[213]. Despite the

relatively weak emissions exhibited by the κ^2-aldazine derivatives, it should be noted that the negligible participation of ancillary ligands to the ground-state LUMO with respect to the HOMO may facilitate changes in photophysical features as the supporting ligands vary. Instead, introduction of substituents in the aldazine moiety appears to be a less viable route. The presence of CH_3-, CH_3O- or F-substituents in the *para*-position in the aldazine aromatic rings only caused very small changes in emission maxima, bandwidths, and relative intensities, as shown in Graphic 7.3.

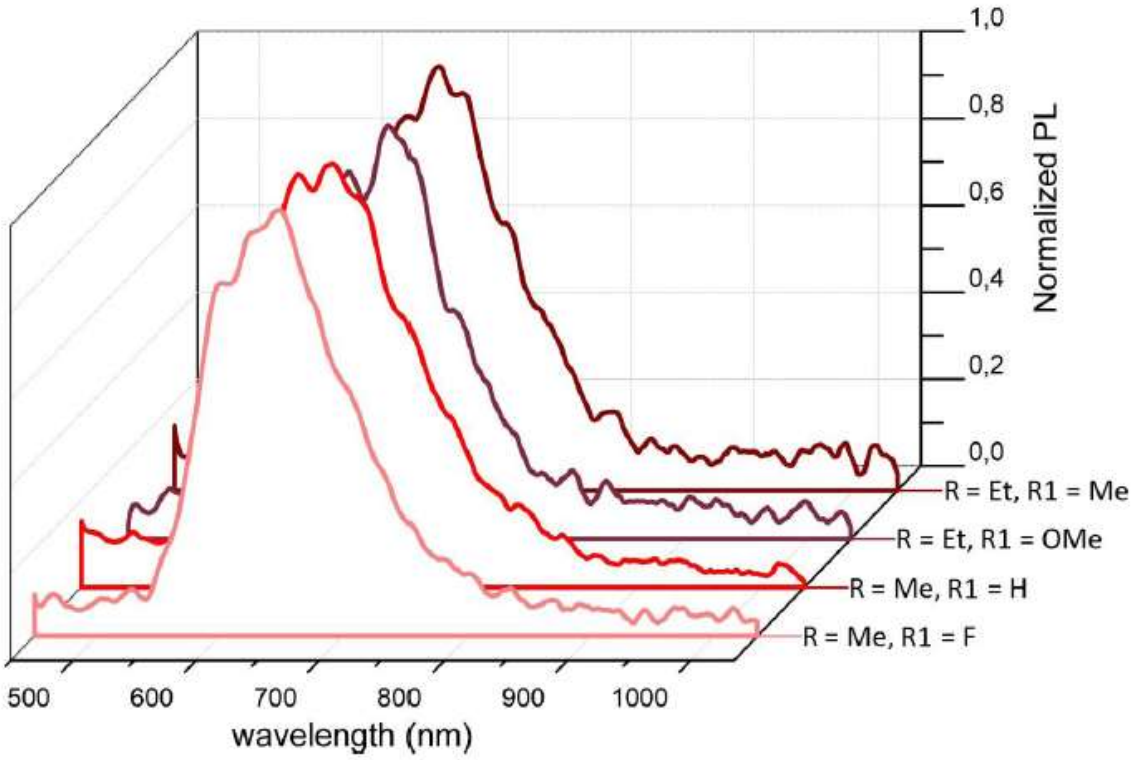

Graphic 7.3 Normalised emission spectra of $[Ir\{\kappa^2\text{-}R1C_6H_3(H)C{=}N{-}N{=}C(H)(R1C_6H_4)\}(\eta^5\text{-}C_5Me_5)\{P(OR)_3\}]BPh_4$ complexes. Solid samples, room temperature, $\lambda_{excitation}$ = 405 nm.

The emissions of complexes **29a, 29d, 30a, 30b** and **30c** are characterized by good colour purity, between 0.83 and 0.91, suggesting that the metalated κ^2-aldazine iridium complexes could be of technological interest, in particular if proper changes in the coordination sphere will increase the quantum yields. The CIE chromaticity diagram showing the emission colours of the complexes is depicted in Graphic 7.4.

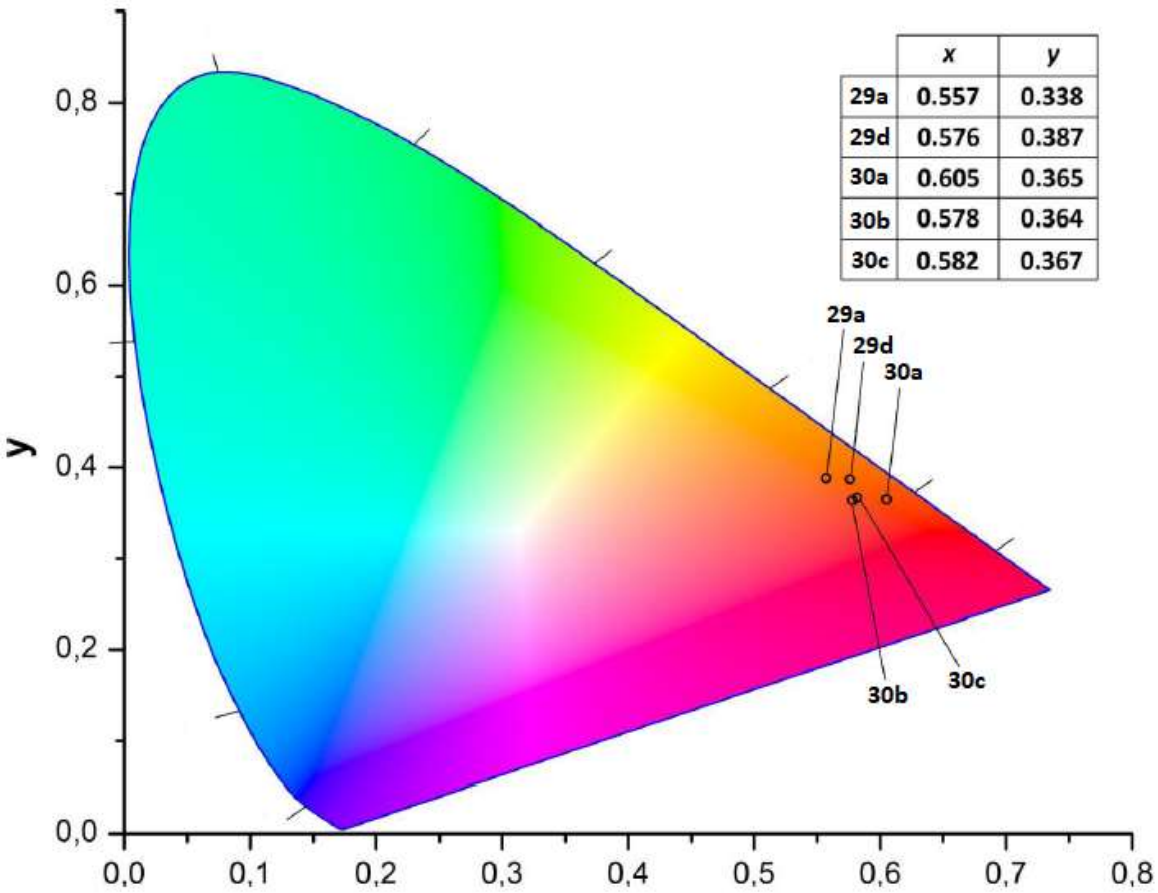

Graphic 7.4 CIE chromaticity diagram (1931 method) showing the emission colours of 29a, 29d, 30a, 30b, 30c. Inset: chromaticity coordinates.

Differently from the previously described compounds, no appreciable emission was observed for the nitro-substituted derivatives (Graphic 7.5). The π-delocalisation caused by the NO_2 groups extends the absorption of the complexes to about 700 nm. If we presume that the Stokes shift for the nitro-substituted derivative is comparable with those measured for the other κ^2-aldazine complexes, around 10 000 cm^{-1}, the corresponding emission should fall in the near-infrared region, but was not observed, probably because it had been quenched by non-radiative decay.

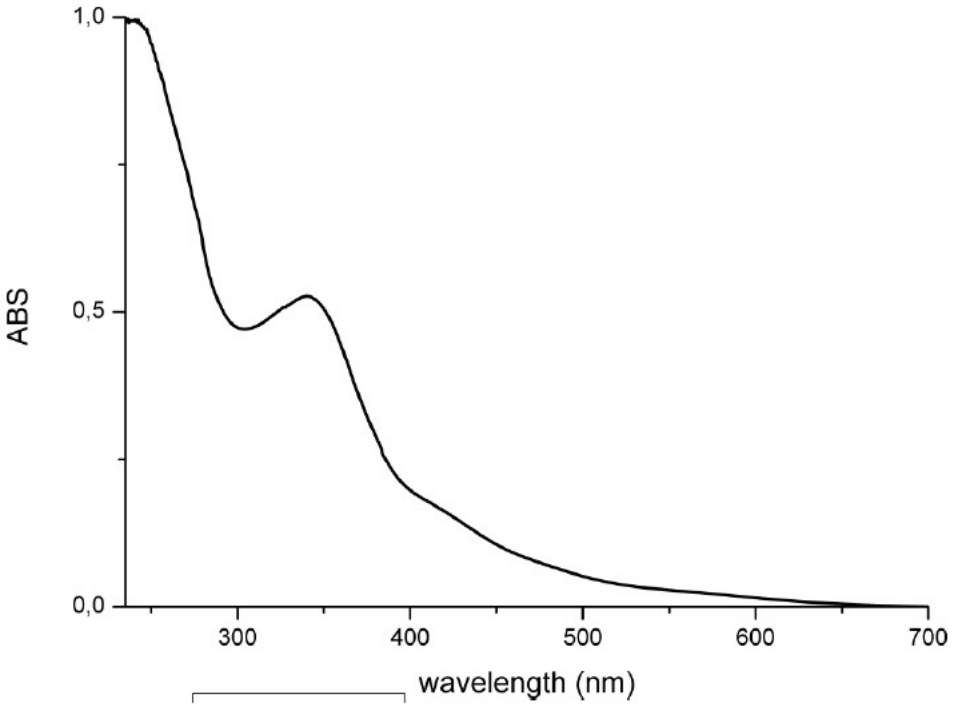

Graphic 7.5 Emission spectrum of [Ir{κ²-4-$NO_2C_6H_3$(H)C=N–N=C(H)(C_6H_4-4-NO_2)}(η⁵-C_5Me_5){$P(OMe)_3$}]BPh_4 29e (CH_2Cl_2 solution, room temperature)

Lastly, examining the previously described attribution of the emission bands of the κ²-aldazine complexes, it is not surprising that no emissions were detected for the aliphatic metalated κ²-ketazine complexes **31** and **32**.

7.5 Reaction of Diazoalkanes with Half-Sandwich Complexes of Osmium

Satisfied with the remarkable results obtained from the systematic study of the reactivity of azines with half-sandwich complexes of ruthenium, rhodium, osmium and iridium, we decided to extend the doctoral project to other diazo ligands. In particular, in literature, it is easy to find references of diazoalkane complexes with iron and ruthenium, however no osmium complex capable of stabilizing the diazotate ligand has ever been reported. We here report the results obtained by the isolation and characterization of different diazoalkane osmium complexes stabilized by pentamethylcyclopentadiene ligand.

Diazoalkane complexes of osmium [Os(η⁵-C_5Me_5)(N_2CAr1Ar2)(PPh_3){$P(OR)_3$}]BPh_4 (**33, 34**) were prepared by reacting bromo-compounds [OsBr(η⁵-C_5Me_5)(PPh_3){$P(OR)_3$}] with an excess of diazoalkane in the presence of $NaBPh_4$, as shown in Scheme 7.23.

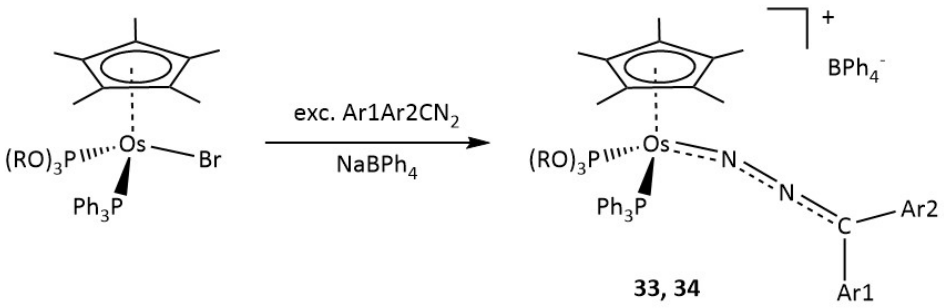

Scheme 7.23 R = Me (33), Et (34); Ar1 = Ar2 = Ph (a); Ar1 = Ph, Ar2 = *p*-tolyl (b); Ar1Ar2 = $C_{12}H_8$ (c).

The reaction proceeds with substitution of the bromide ligand and formation of diazoalkane complexes **33**, **34** which were isolated in good yields and characterized. Crucial for the success of the syntheses was the presence of the $NaBPh_4$ salt which, favouring the substitution of the Br^-, rapidly afford the final species **33, 34** in good yield. Anyway, the reaction is quite slow at room temperature and takes two days to be completed; reflux conditions can not be used leading to the formation of decomposition products.

The bis(triphenylphosphine) complex $[OsBr(\eta^5\text{-}C_5Me_5)(PPh_3)_2]$ was also reacted with diazoalkane in different conditions, but no diazoalkane complex was obtained. It turns out that only mixed-ligands pentamethylcyclopentadienyl fragments are able to stabilize diazoalkane derivatives.

The new complexes **33, 34** were isolated as yellow-orange solids stable in air and in solution of polar organic solvents, where they behave as 1:1 electrolytes. Analytical and spectroscopic (IR, NMR) data support the proposed formulation.

The IR spectra show a medium-intensity band at 1935-1946 cm^{-1}, attributed to the ν_{N_2} of the coordinate diazoalkane group. Besides the signals of the ancillary ligands C_5Me_5, PPh_3, $P(OR)_3$ and of the BPh_4^- anion, the ^1H NMR spectra show the resonances characteristic of the substituents $C_{12}H_8$ and 4-$CH_3C_6H_4$ of the diazoalkane $Ar1Ar2CN_2$. Their presence is further supported by the ^{13}C NMR spectra of **33c** and **34a**, which show a broad signal at 83.5-85.8 ppm attributed to the CN_2 carbon resonance of the diazoalkane. In the temperature range between +20 and -80 °C, the ^{31}P NMR spectra appear as an AX quartet fitting the proposed geometry for the complexes.

Reactivity studies on our diazoalkane complexes **33**, **34** with alkenes and alkynes were undertaken, with the aim of testing whether a (3+2) cycloaddition may occur. The results are summarized in Scheme 7.24.

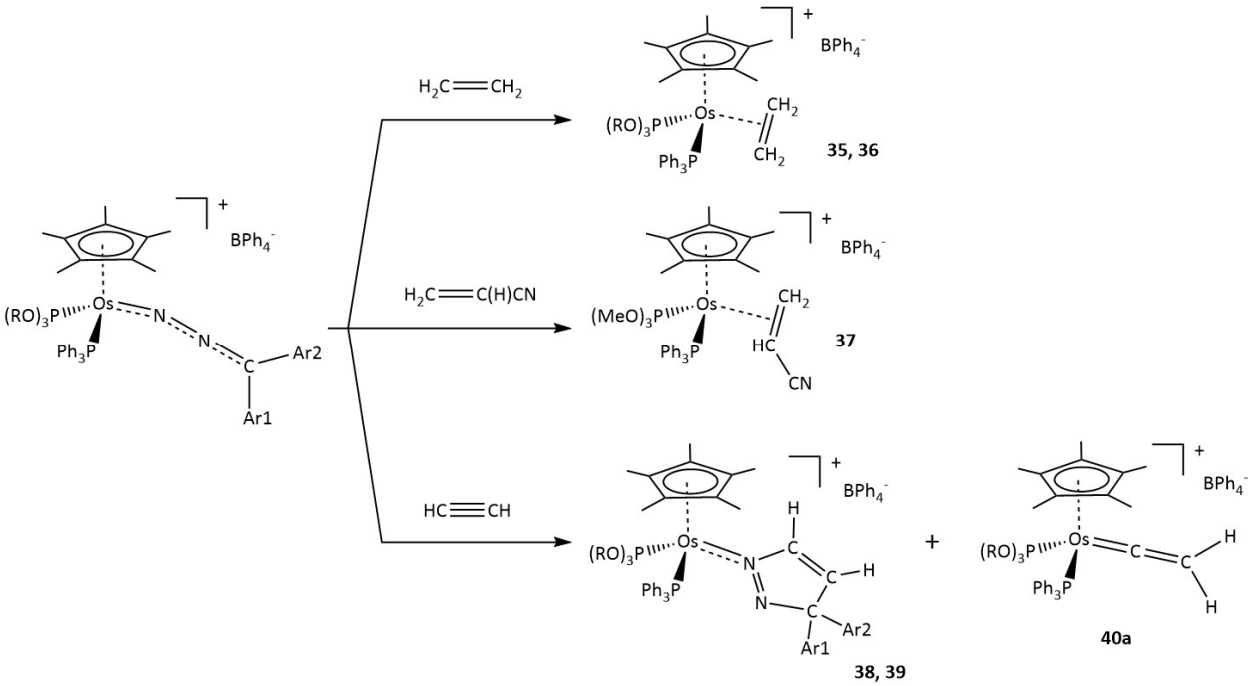

Scheme 7.24 R = Me (35, 38), Et (39); Ar1Ar2 = $C_{12}H_8$.

Under mild conditions (1 atm, room temperature) ethylene reacted with diazoalkane complexes **33** and **34** to give ethylene derivatives $[Os(\eta^5\text{-}C_5Me_5)(\eta^2\text{-}CH_2{=}CH_2)(PPh_3)\{P(OR)_3\}]BPh_4$ (**35, 36**). However, the reaction is very slow and takes several days to complete. Instead, in refluxing 1,2-dichloroethane the $\eta^2\text{-}CH_2{=}CH_2$ complexes **35** and **36** quickly form and can be isolated in good yield and characterised. The reaction proceeds with substitution of the diazoalkane ligand and no cyclisation reaction yielding 3H pyrazole derivatives was observed.

Substitution of diazoalkane also occurs with activate alkenes such as acrylonitrile, forming the complex $[Os(\eta^5\text{-}C_5Me_5)\{\kappa^2\text{-}CH_2{=}C(H)CN\}(PPh_3)\{P(OMe)_3\}]BPh_4$ (**37**) in which the acrylonitrile seems to be π-coordinated to the metal centre.

Under mild conditions, acetylene HC≡CH slowly reacted with diazoalkane complexes **33** and **34,** giving 3H pyrazole derivatives $[Os(\eta^5\text{-}C_5Me_5)(\kappa^1\text{-}N{=}NC(C_{12}H_8)CH{=}CH)(PPh_3)\{P(OR)_3\}]BPh_4$ (**38, 39**) which were isolated and characterized. The reactions proceed with dipolar (3+2) cycloaddition of acetylene to the coordinated diazoalkane giving 3-H pyrazole complexes **38** and **39**, in which the heterocycle acts as a ligand. However, in the reaction mixture is also possible to identify a small amount of a substitution product characterized as the vinylidene species **40a** which quickly decompose in solution (see below).

This last result prompted us to extend the study of the reactivity of the diazoalkanes complexes **33, 34** with terminal alkynes R1C≡CH too. The reactions led to the formation of vinylidene

complexes $[Os(\eta^5\text{-}C_5Me_5)\{=CH=C(H)R1\}(PPh_3)\{P(OR)_3\}]BPh_4$ (**40, 41**) which were isolated and characterized.

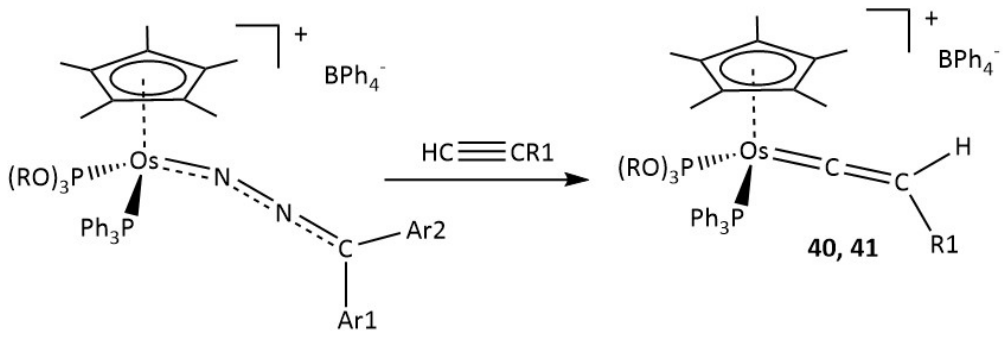

Scheme 7.25 R= Me (40), Et (41); R1 = Ph (b), *p*-tolyl (c), COOMe (d)

Substitution of diazoalkane probably gives rise to the η^2-alkyne complex which undergoes the well-known tautomerization of π-coordinated R1C≡CH, yielding vinylidene as the final derivative. These results highlight the important influence of the substituents on the alkyne in determining the cyclisation reaction, which only proceeds with acetylene HC≡CH, whereas substitution of the $Ar1Ar2CN_2$ ligand and formation of the vinylidene take place with monosubstituted alkynes R1C≡CH.

All our results on the reactivity of diazoalkane complexes **33** and **34** towards alkenes and alkynes indicate that the pentamethylcyclopentadienyl fragment $[Os(\eta^5\text{-}C_5Me_5)(PPh_3)\{P(OR)_3\}]^+$ can activate the coordinated diazoalkane towards dipolar (3+2) cycloaddition, but only with acetylene HC≡CH, giving the 3-H pyrazole complexes **38** and **39**. With alkenes and terminal alkynes only substitution occurs affording η^2-alkene or vinylidene, respectively, as the final product. In addition, comparison with previous results[90] on the pentamethylcyclopentadienyl fragment $[Ru(\eta^5\text{-}C_5Me_5)(PPh_3)\{P(OR)_3\}]^+$ points out a similar behaviour of the two metal fragments which are able to activate the coordinated $Ar1Ar2CN_2$ group towards (3+2) cycloaddition exclusively with acetylene. The substitution of the diazoalkane ligand giving the η^2-alkene or vinylidene derivatives is predominant with both metals.

The lability of the coordinated diazoalkane in **33** and **34** was also observed as an unexpected reactivity simply working up the complex in the air, and yielded the new dioxygen complexes $[Os(\eta^5\text{-}C_5Me_5)(\eta^2\text{-}O_2)(PPh_3)\{P(OR)_3\}]BPh_4$ (**42, 43**), which were isolated and characterized (Scheme 7.26).

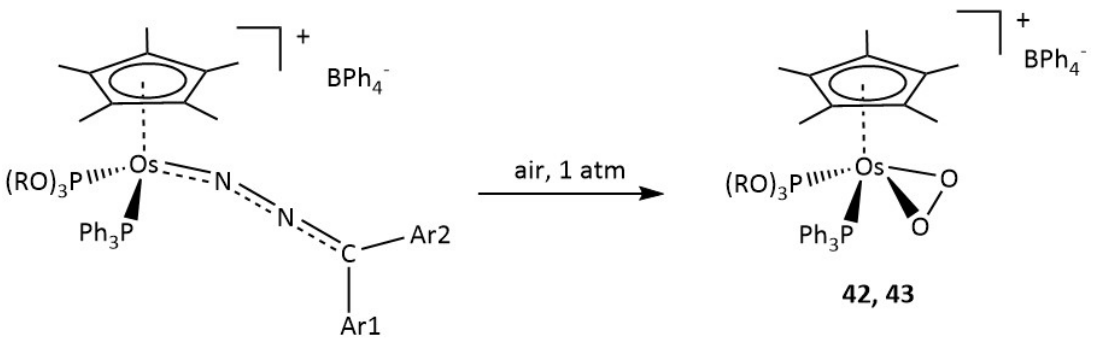

Scheme 7.26 R = Me (42), Et (43).

The reaction proceeded with substitution of the Ar1Ar2CN$_2$ group with an O_2, producing the η^2-O_2 derivatives in good yields. It is worth noting that dioxygen complexes **42** and **43** can also be prepared by substituting the Br^- ligand in [OsBr(η^5-C_5Me_5)(PPh_3){$P(OR)_3$}] using $NaBPh_4$ as a labilising agent, as shown in Scheme 7.27.

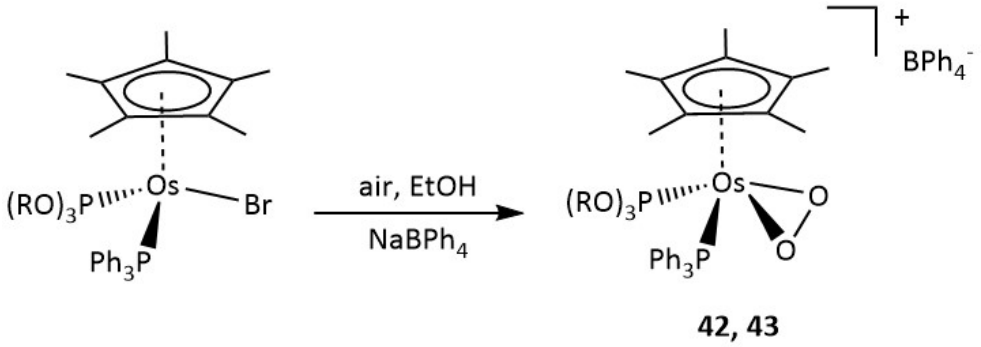

Scheme 7.27 R = Me (42), Et (43).

The coordination of the O_2 molecule to the [Os(η^5-C_5Me_5)(PPh_3){$P(OR)_3$}]$^+$ fragment is interesting as dioxygen complexes of osmium are rare and mainly contain bidentate phosphine ligands. Complexes **42** and **43** are the first members of a new family of Os(η^2-O_2) compounds with pentamethylcyclopentadienyl as a supporting ligand.

The new pentamethylcyclopentadienyl complexes of osmium **35–43** were all isolated as their BPh_4^- salts and are stable in air and in solution of polar organic solvents, where they behave as 1:1 electrolytes. Analytical and spectroscopic (IR, NMR) data support the proposed formulation, which was further confirmed by an X-ray crystal structure determination of complexes [Os(η^5-C_5Me_5){=C=C(H)Ph}(PPh_3){$P(OEt)_3$}]BPh_4 (**41b**) and [Os(η^5-C_5Me_5)(η^2-O_2)(PPh_3){$P(OMe)_3$}]BPh_4 (**42**) whose ORTEPs[164] are shown in Figures 7.10 and 7.11.

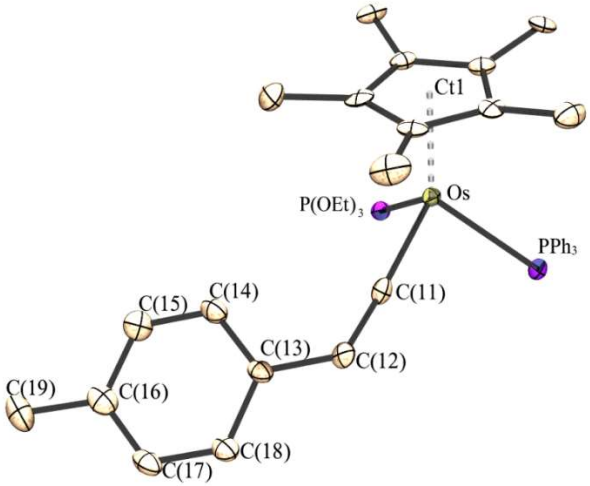

Figure 7.10 ORTEP scheme of the molecular structure of 41b cation.

The **41b** cation complex contains an osmium atom in a half-sandwich piano-stool structure, coordinated by a pentamethylcyclopentadiene group (Cp*), one $P(OEt)_3$ phosphite ligand, one PPh_3 phosphine ligand and a *p*-tolylvinylidene ligand. The overall geometry of the complex is a slightly-distorted octahedron and is marked by the angles between the centroid of the Cp* ligand (Ct1) and the legs close to the theoretical 125.3°, or by near 90° values for angles formed by the legs of the piano-stool (see Table 7.7).

7.7 Selected list of bond lengths [Å] and angles [°] for 41b

Os–C(11)	1.859(5)	Os–CG1	1.9495(2)
Os–P(1)	2.3283(11)	Os–P(2)	2.2725(11)
Os–C(1)	2.274(4)	Os–C(4)	2.338(4)
Os–C(2)	2.267(4)	Os–C(5)	2.306(4)
Os–C(3)	2.315(4)	Os–C_{av}	2.300
C(11)–C(12)	1.306(6)	C(12)–C(13)	1.476(6)
C(11)-Os-CG1	124.04(13)	C(11)-Os-P(1)	91.32(13)
CG1-Os-P(1)	126.23(3)	P(2)-Os-P(1)	93.35(4)
CG1-Os-P(2)	122.14(3)	C(11)-Os-P(2)	89.89(13)
Os-C(11)-C(12)	174.4(4)	C(11)-C(12)-C(13)	126.2(4)

Coordination of the Cp* ligand (ring slippage, 0.077 Å) shows Os–C distances between 2.267(4) and 2.338(4) Å (average, 2.300 Å), the longest Os–C bond corresponding to that *trans* to the vinylidene ligand. These values are in agreement with the Os–P bond lengths, which also depend of the nature of the ligand, 2.2725(11) Å for the phosphite and 2.3283(11) Å for the triphenylphosphine. These values are analogous to those found in the above-mentioned compounds.

The vinylidene ligand comprises a Os–C bond length of 1.859(5) Å with an angle of 174.4(4)°, close to linearity. The C(11)–C(12) bond distance of 1.306(6) Å indicates a double bond character. This fact and a C(11)-C(12)-C(13) angle of 126.2(4)° confirm the vinylidene formulation.

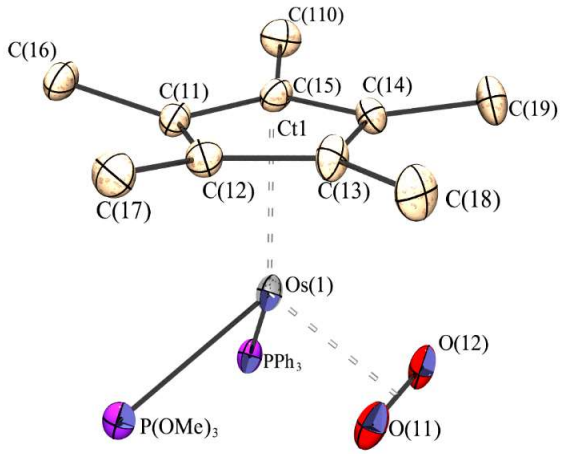

7.11 ORTEP scheme of the molecular structure of 42 cation.

The asymmetric unit of **42** contains four molecular formulae, that is, four cations and four anions and, also, any kind of unknown solvent. Reflections caused by the latter were eliminated in a usual procedure. In Figure 7.11 only one cation is sketched. A selection of bond distances and angles are set out in Table 7.8.

Table 7.8 Selected bond lengths [Å] and angles [°] for 42

Os(1)–CT1	1.91834(14)	Os(3)–CT3	1.9177(2)
Os(1)–O(12)	2.026(3)	Os(3)–O(31)	2.031(3)
Os(1)–O(11)	2.041(3)	Os(3)–O(32)	2.019(3)
Os(1)–P(11)	2.3666(10)	Os(3)–C(31)	2.255(5)
Os(1)–P(12)	2.2893(11)	Os(3)–C(32)	2.240(5)
Os(1)–C(11)	2.242(4)	Os(3)–C(33)	2.222(5)
Os(1)–C(12)	2.240(4)	Os(3)–C(34)	2.314(5)
Os(1)–C(13)	2.274(4)	Os(3)–C(35)	2.319(4)
Os(1)–C(14)	2.323(4)	Os(3)–P(31)	2.3678(11)
Os(1)–C(15)	2.297(4)	Os(3)–P(32)	2.3034(12)
Os(1)–C_{av}	2.2756	Os(3)–C_{av}	2.2702
O(11)–O(12)	1.429(4)	O(31)–O(32)	1.430(5)
Os(2)–CT2	1.9142(2)	Os(4)–CT4	1.9214(2)
Os(2)–O(21)	2.028(3)	Os(4)–O(41)	2.032(3)
Os(2)–O(22)	2.044(3)	Os(4)–O(42)	2.024(3)
Os(2)–P(21)	2.3663(11)	Os(4)–C(41)	2.235(5)
Os(2)–P(22)	2.2922(12)	Os(4)–C(42)	2.287(4)

Os(2)–C(21)	2.238(4)	Os(4)–C(43)	2.302(4)
Os(2)–C(22)	2.238(4)	Os(4)–C(44)	2.294(5)
Os(2)–C(23)	2.268(4)	Os(4)–C(45)	2.256(5)
Os(2)–C(24)	2.304(5)	Os(4)–P(41)	2.3595(11)
Os(2)–C(25)	2.280(4)	Os(4)–P(42)	2.2885(13)
Os(2)–C_{av}	2.2656	Os(4)–C_{av}	2.275
O(21)–O(22)	1.425(5)	O(41)–O(42)	1.413(5)
CT01-Os(1)-O(11)	119.27(9)	CT03-Os(3)-O(31)	120.32(10)
CT01-Os(1)-O(12)	114.60(9)	CT03-Os(3)-O(32)	113.44(9)
CT01-Os(1)-P(11)	129.96(3)	CT03-Os(3)-P(31)	130.84(3)
CT01-Os(1)-P(12)	120.04(3)	CT03-Os(3)-P(32)	120.32(3)
O(11)-Os(1)-P(11)	103.77(9)	O(31)-Os(3)-P(31)	100.69(10)
O(11)-Os(1)-P(12)	85.61(9)	O(31)-Os(3)-P(32)	86.00(10)
O(12)-Os(1)-O(11)	41.14(12)	O(32)-Os(3)-O(31)	41.35(13)
O(12)-Os(1)-P(11)	81.23(9)	O(32)-Os(3)-P(31)	79.26(9)
O(12)-Os(1)-P(12)	117.80(9)	O(32)-Os(3)-P(32)	119.20(10)
P(12)-Os(1)-P(11)	85.52(4)	P(32)-Os(3)-P(31)	86.00(4)
CT02-Os(2)-O(21)	115.27(10)	CT04-Os(4)-O(41)	120.62(10)
CT02-Os(2)-O(22)	120.43(10)	CT04-Os(4)-O(42)	116.13(10)
CT02-Os(2)-P(21)	129.87(3)	CT04-Os(4)-P(41)	129.13(3)
CT02-Os(2)-P(22)	119.24(3)	CT04-Os(4)-P(42)	118.76(3)
O(21)-Os(2)-O(22)	40.96(14)	O(41)-Os(4)-P(41)	103.58(10)
O(21)-Os(2)-P(21)	79.60(9)	O(41)-Os(4)-P(42)	85.70(10)
O(21)-Os(2)-P(22)	118.85(11)	O(42)-Os(4)-O(41)	40.78(13)
O(22)-Os(2)-P(21)	102.15(10)	O(42)-Os(4)-P(41)	80.98(10)
O(22)-Os(2)-P(22)	86.88(11)	O(42)-Os(4)-P(42)	117.75(10)
P(22)-Os(2)-P(21)	85.90(4)	P(42)-Os(4)-P(41)	86.29(4)

All cation complexes in the asymmetric unit are similar and each one contains an osmium atom in a half-sandwich structure, coordinated by a pentamethylcyclopentadienyl group (Cp*), one $P(OMe)_3$ phosphite ligand, one PPh_3 phosphine ligand and a dioxygen ligand coordinated η^2-O_2. The coordination of the Cp* (ring slippage between 0.062 to 0.088 Å) shows Os–C distances between 2.222(5) and 2.319(5) Å, with Os–C average between 2.2656 and 2.275 Å. Phosphite Os–P bond lengths, between 2.2893(11) and 2.3034(12) Å, are shorter than phosphine ones, which are between 2.3595(11) and 2.3679(11) Å. Os–O bond lengths range from 2.020(3) to 2.044(3) Å and distances are calculated between 1.412(5) and 1.430(5) Å. These last values are in the range

observed for Os(η^2-O_2) derivatives (1.31−1.49 Å), so we can propose a peroxide structure rather than a dioxygen compound[214–218].

Besides the signals of the ancillary ligands C_5Me_5, PPh_3, $P(OR)_3$ and of the BPh_4^- anion, the ^1H NMR spectra of ethylene complexes **35** and **36** show two broad signals at 2.36-2.38 and at 2.05 ppm, attributed to the protons of the ethylene ligand. Lowering the sample temperature caused some variations in the spectra but even at -90 °C the two multiplets that appeared at 2.86 and at 2.25-2.20 ppm remained broad, indicating that rotation of CH_2=CH_2 still took place at this temperature, preventing the exact determination of the NMR parameters. However, the presence of the η^2-CH_2=CH_2 ligand is confirmed by the ^{13}C spectra which show a broad singlet at 26.46-26.43 ppm correlated, in an HMQC experiment with the two multiplets at 2.36-2.38 and at 2.05 ppm that appear in the proton spectra and is attributed to the ethylene carbons resonances. In the temperature range between +20 and-80 °C, the $^{31}P\{^1H\}$ NMR spectra are AX quartets, fitting the proposed formulation for the complexes.

The IR spectrum of the acryls nitrile complex **37** shows a weak band at 2207 cm^{-1}, attributed to the ν_{CN} of the ligand. The lowering of this value in **37** compared to the free CH_2=CHCN suggests η^2-coordination of the nitrile, as a N-bond should lead to an increase of the ν_{CN}. Support for this coordination came from the ^1H NMR spectrum which, besides the signals of the ancillary ligands C_5Me_5, PPh_3 and $P(OMe)_3$, shows a multiplet between 6.92 and 5.30 ppm, attributed to the CH_2=C(H)CN protons. This multiplet comes from the ethylene protons which couple also with the ^{31}P nuclei of the P-ligands and can be simulated using an A_2BCXY model (A, B, C = ^1H; X, Y = ^{31}P) with the parameters reported in the Experimental section. The good fit between the calculated and experimental spectra strongly suggests a η^2-coordination of the acrylonitrile.

The ^1H NMR spectra of the 3H pyrazole complexes [Os(η^5-C_5Me_5)(κ^1-N=NC($C_{12}H_8$)CH=CH)-(PPh_3){$P(OR)_3$}]BPh_4 (**38, 39**) show two doublets at 7.53-7.87 and at 6.72-6.73 ppm, attributed to H5 and H4 of the heterocycle (Scheme 7.24), and the characteristic signals of the $C_{12}H_8$ substituent at C3. The ^{13}C NMR spectra confirm the presence of the 3-H pyrazole ligand showing two singlets at 158.13-157.47and at 139.39-139.50 ppm which, in a HMQC experiment, were correlated with the doublets at 7.53-7.87 and at 6.72-6.73 ppm observed in the proton spectra and consequently attributed to C5 and C4 carbon resonances of the heterocycle; a singlet at 105.38 ppm was attributed to C3. In the spectra, the signals of the ancillary ligands, BPh_4^- anion and $C_{12}H_8$

substituent appear too. The ^{31}P spectra are AX systems fitting the proposed formulation for the complexes.

The IR spectra of vinylidene complexes **40** and **41** show a medium-intensity band at 1650–1628 cm^{-1}, attributed to the $\nu_{Os=C=C}$ of the vinylidene ligand. However, its presence is confirmed by the multiplet at 2.80–4.15 ppm in the proton NMR spectra, attributed to the =C(H)R vinylidene proton. The ^{13}C NMR spectra show a doublet of doublets at 390–317 ppm of the C_α carbene carbon resonance $=C_\alpha=C_\beta(H)$ and a broad singlet near 115 ppm which, in a HMQC experiment, is correlated with the multiplet at 2.80–4.15 ppm in the ^1H NMR spectra and was attributed to the C_β carbon resonance of the =C=C(H)R1 group. The ^{31}P NMR spectra appear as AX quartets, in agreement with the proposed formulation for the complexes.

Besides the signals of the phosphines and the BPh_4^- anion, the ^1H NMR spectrum of the dioxygen complexes **42** and **43** show a singlet at 1.47–1.53 ppm of the methyl protons of the C_5Me_5, whereas the ^{31}P NMR spectra are AX quartets, suggesting that a geometry like that observed in the solid state for **42** also occurs in solution.

7.5.1 Vinylidene and Propadienylidene Derivatives.

As previously reported, substitution of diazoalkane **33, 34** with terminal alkynes R1C≡CH gives κ^2-alkyne complex which undergoes the known tautomerization of the coordinated R1C≡CH yielding the final vinylidene derivative.

However, vinylidene complexes $[Os(\eta^5\text{-}C_5Me_5)\text{-}\{=CH=C(H)R1\}(PPh_3)\{P(OR)_3\}]BPh_4$ (**40, 41**) were also directly prepared by reacting bromo-complexes $[OsBr(\eta^5\text{-}C_5Me_5)(PPh_3)\{P(OR)_3\}]$ with terminal alkynes HC≡CR1 in the presence of $NaBPh_4$, as shown in Scheme 7.28.

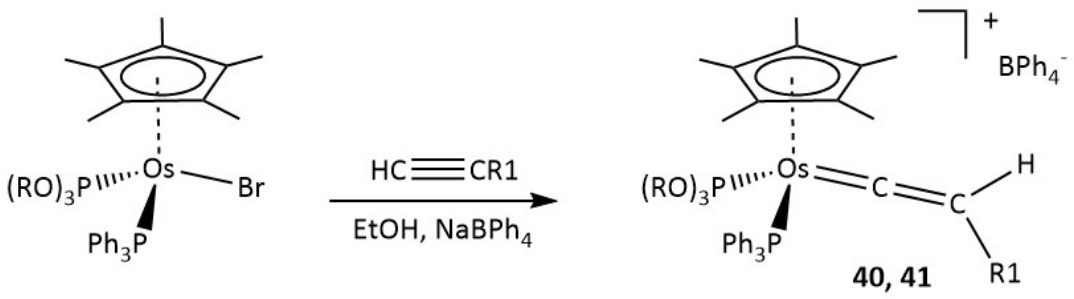

Scheme 7.28 R = Me (40), Et (41); R1 = H (a), Ph (b), *p*-tolyl (c), COOMe (d).

The $NaBPh_4$ salt favours the substitution of Br^- by alkyne, which tautomerizes on the metal centre yielding vinylidene derivatives **40** and **41**.

These results prompted us to move our study to propargylic alcohols HC≡CC(OH)R1R2, with the aim of testing whether allenylidene complexes may be prepared. The results are summarised in Scheme 7.29.

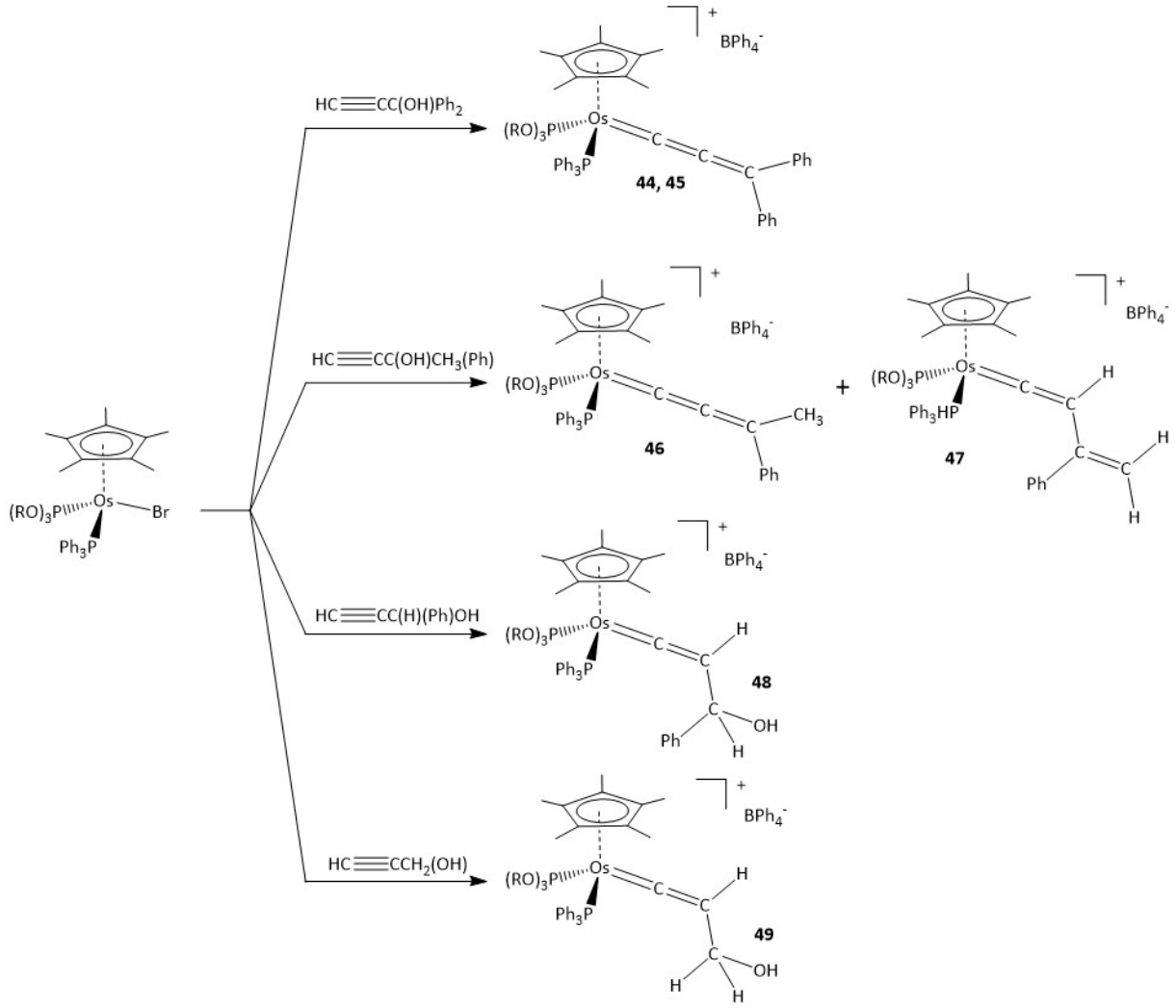

Scheme 7.29 R = Me (44, 46, 47, 48, 49), Et (45)

Depending on the nature of substituents R1 and R2, the reaction of bromo-complexes $[OsBr(\eta^5\text{-}C_5Me_5)(PPh_3)\{P(OR)_3\}]$ with propargylic alcohols HC≡CC(OH)R1R2 afforded propadienylidene [Os]=C=C=CR1R2 (**44-46**), vinylvinylidene $[Os]=C=C(H)C(Ph)=CH_2$ (**47**) or 3-hydroxyvinylidene [Os]=C=C(H)C(H)R2(OH) (**48, 49**) derivatives, which were isolated and characterised. As usual the presence of $NaBPh_4$ labilised the Br^- ligand, favouring the formation of the carbene derivatives. The reactions proceed with the substitution of the bromo ligand and the

formation, after tautomerization on the metal centre, of the hydroxyvinylidene intermediate **[A]** (Scheme 7.30).

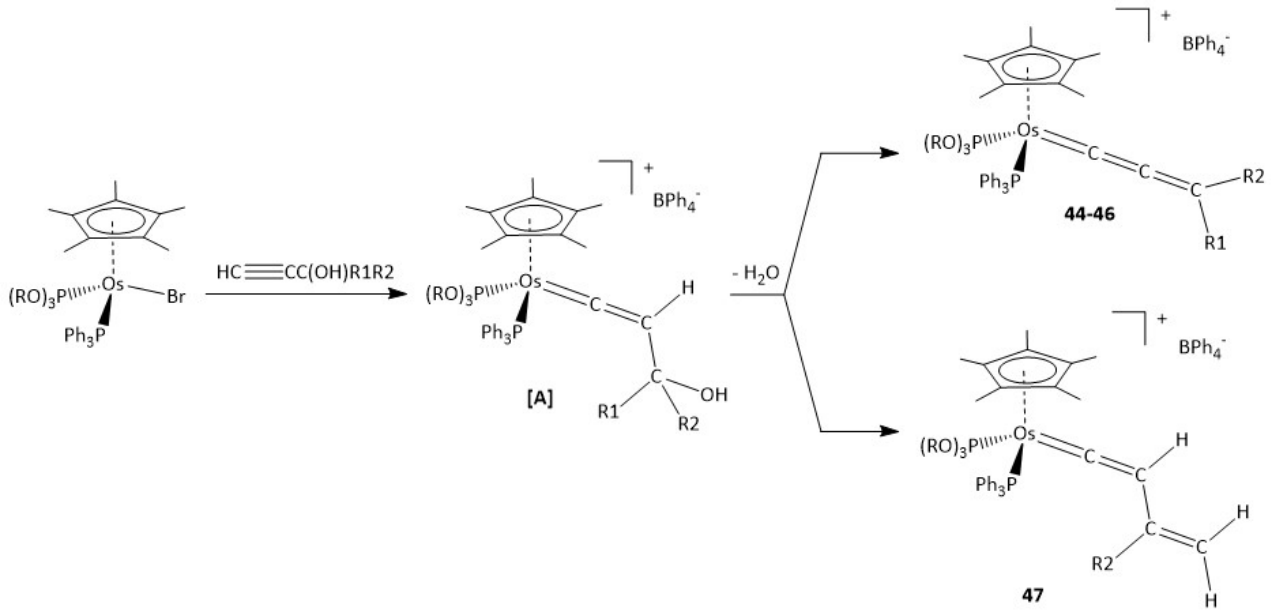

Scheme 7.30 R = Me (44, 46, 47), Et (45); R1 = R2 = Ph, (44, 45); R1 = Me, R2 = Ph, (46, 47);

The loss of one water molecule from this 3-hydroxyvinylidene can afford either allenylidene **44-46** or alkenylvinylidene **47** derivatives, depending on the presence of hydrogen atoms in β position with respect to the hydroxy group. As a matter of fact, 1,1-diphenyl-2-propyn-1-ol yielded the allenylidene complexes [Os]=C=C=C=Ph_2 (**44, 45**), whereas 2-phenyl-3-butyn-1-ol afforded a mixture of allenylidene [Os]=C=C=C=(CH_3)(Ph) (**46**) and vinylvinylidene [Os]=C=C(H)C(Ph)=CH_2 (**47**). Surprisingly, the reaction of the bromo compound [OsBr(η^5-C_5Me_5)(PPh_3){$P(OR)_3$}] with 2-propyn-1-ol and 1-phenyl-2-propyn-1-ol afforded hydroxyvinylidene derivatives [Os]=C=C(H)CH(Ph)OH (**48**) and [Os]=C=C(H)CH_2(OH) (**49**) which are very stable and do not undergo loss of water giving the corresponding allenylidene derivatives. The reluctance to dehydration of these 3-hydroxyvinylidene complexes even in protic solvents (EtOH) may be attributed both to the nature of the substituents of the vinylidene and to the properties of the pentamethylcyclopentadienyl osmium fragment, which stabilises 3-hydroxyvinylidene **48** and **49**, preventing the formation of allenylidene [Os]=C=C=C(H)R1 (R1 = H, Ph).

Despite the large number of reported analogue complexes of ruthenium, allenylidene of osmium are rather rare and involve mainly η^5-cyclopentadienyl and η^6-arene complexes. The use of the mixed-ligands fragments [Os(η^5-C_5Me_5)(PPh_3){$P(OR)_3$}]$^+$ allowed the preparation of the first

vinylidene and allenylidene complexes of Os containing the pentamethylcyclopentadienyl as a supporting ligand.

Vinylidene complexes were found to be stable with all substituents except [Os(η^5-C_5Me_5)-(=C=CH_2)(PPh_3){P($OR)_3$}]BPh_4 (**40a**, **41a**) which quickly decomposed in solution preventing its complete characterisation. However, in the presence of PPh_3, vinylidene can be "stabilised" by reaction with phosphine affording the alkenylphosphonium derivative [Os(η^5-C_5Me_5){η^1-C(H)=C(H)PPh_3}(PPh_3){P($OMe)_3$}]BPh_4 (**50**) which is stable and isolable (Scheme 7.31).

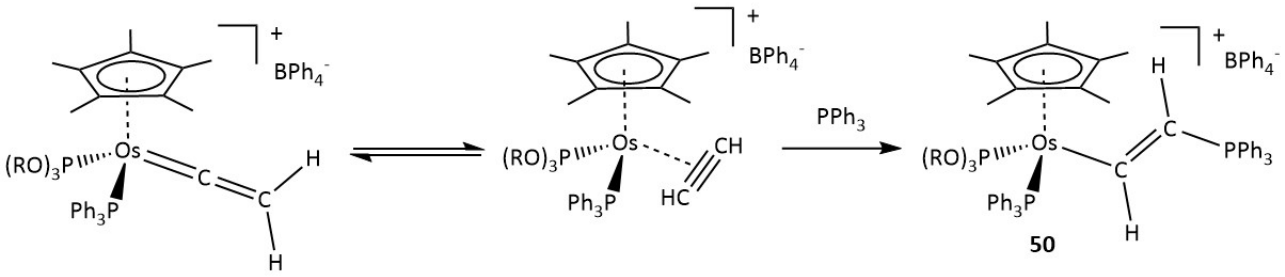

Scheme 7.31 Reaction of compound 40a with PPh_3

As proposed for the comparable [Ru(η^5-1,2,3-$R_3C_9H_4$){η^1-C(H)=C(Ph_3)Ph}(CO)(PPh_3)]BF_4, alkenylphosphonium derivatives, compounds **50**, are probably formed by a nucleophilic attack of phosphine on the carbon atom of the η^2-alkyne in equilibrium with the vinylidene species (Scheme 7.31). It is worth noting that the other vinylidene complexes with aryl or carboxyl substituents **40** and **41** do not react with phosphine in mild conditions probably owing to the absence of η^2-alkyne.

Instead, those vinylidene derivatives [Os]=C=C(H)R1 (R1 = Ph, 4-$CH_3C_6H_4$, $COOCH_3$) undergo easy hydrolysis in solution at room temperature yielding the carbonyl compounds [Os(η^5-C_5Me_5)(CO)(PPh_3){P($OR)_3$}]BPh_4 (**51, 52**), which were isolated and characterised (Scheme 7.32).

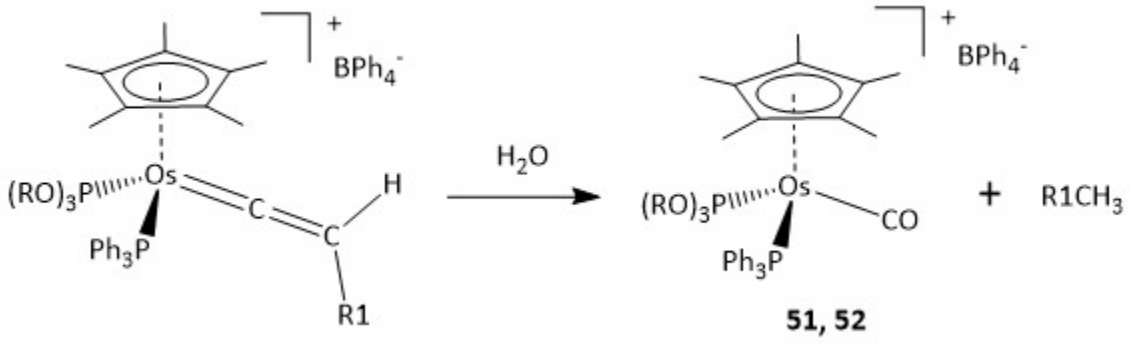

Scheme 7.32 R = Me (51), R = Et (52)

The formation of the carbonyl derivatives **51** and **52** could be the result of the nucleophilic attack of H_2O on the vinylidene C_α, giving an unstable carbene intermediate (**[B]**, Scheme 7.33).

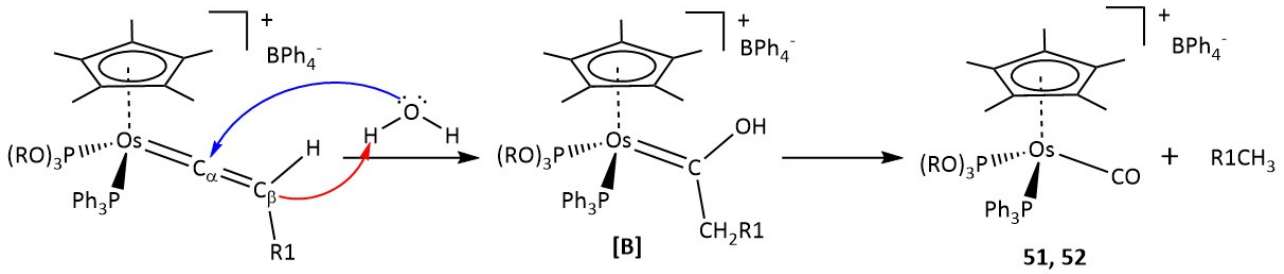

Scheme 7.33 R = Me (51), R = Et (52)

Decomposition of intermediate **[B]** may involve the H-shift from the hydroxo group to the alkyl carbon atom of the carbene yielding the carbonyls **51** and **52** and free hydrocarbon $R1CH_3$. The presence of $R1CH_3$ in the reaction mixture was confirmed by GC analysis, thus fitting the reaction path proposed in Scheme 7.33. The reaction, therefore, entails hydrolysis of the terminal alkyne with C=C bond cleavage and formation of carbonyl derivatives **51** and **52** and free hydrocarbon.

The reaction of vinylidene with H_2O suggested to study the reactivity with other nucleophiles such as alcohol and amine, in an attempt to prepare stable carbene complexes. Surprisingly, no reaction was observed with alkylamine RNH_2 in refluxing 1,2-dichloroethane as well as in refluxing EtOH or MeOH, indicating some reluctance of our vinylidenes to form carbene derivatives.

The new η^5-C_5Me_5 complexes were all isolated as solids stable in air and in solution of polar organic solvents where they behave as 1:1 electrolytes. Analytical and spectroscopic (IR, ^1H, ^{13}C, ^{31}P NMR) data support the proposed formulation which, in the case of $[Os(\eta^5\text{-}C_5Me_5)(CO)(PPh_3)\text{-}\{P(OMe)_3\}]BPh_4$ (**51**), was further confirmed by X-ray crystal structure determination, whose ORTEP[164] is shown in Figure 7.12.

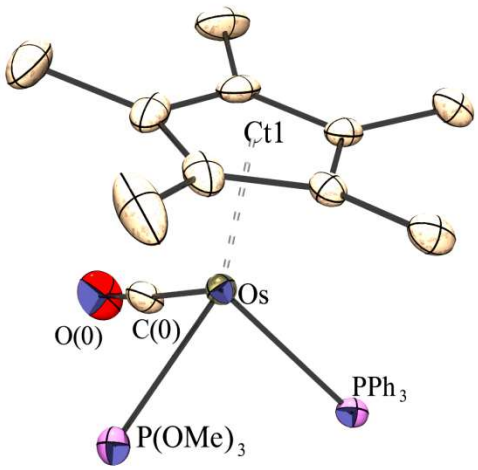

Figure 7.12 ORTEP scheme of the molecular structure of 51 cation.

The cationic complex of compound **51** contains an osmium atom in a half-sandwich piano-stool structure, coordinated by a pentamethylcyclopentadiene group (Cp*), one $P(OMe)_3$ phosphite ligand, one PPh_3 phosphine ligand and a carbonyl ligand. The overall geometry of the half-sandwich piano-stool complex is a slightly distorted octahedral and is marked by the angles between the centroid of the Cp* ligand (Ct1) and the legs close to the theoretical 125.3°, or by near 90° values for angles formed by the legs of the piano-stool (see Table 7.9).

Table 7.9 Selected bond lengths [Å] and angles [º] for 51

Os–C(0)	1.865(3)	**9**	1.92863(12)
Os–P(1)	2.3365(7)	Os–P(2)	2.2509(7)
Os–C(1)	2.258(3)	Os–C(2)	2.279(3)
Os–C(3)	2.299(3)	Os–C(4)	2.289(3)
Os–C(5)	2.281(3)	$Os–C_{av}$	2.281
C(0)–O(0)	1.153(3)	P(1)–C(11)	1.827(3)
C(0)-Os-CT1	124.64(9)	C(0)-Os-P(2)	89.10(9)
CT1-Os-P(2)	123.750(18)	P(2)-Os-P(1)	93.24(2)
C(0)-Os-P(1)	90.99(9)	CT1-Os-P(1)	124.975(17)
O(0)-C(0)-Os	175.5(3)		

Coordination of the Cp* ligand (ring slippage, 0.031 Å) shows Os–C distances between 2.258(3) and 2.299(3) Å (average, 2.281 Å). The shorter Os–C bond corresponds to that *trans* to the phosphine ligand, the longer one is *trans* (not exactly) to the phosphite ligand. These values are in agreement with the Os–P bond lengths, which also depend on the nature of the ligand,

2.2509(7) Å for the phosphite ligand and 2.3365(7) Å for the triphenylphosphine ligand respectively. Those values are analogous to those found, for example, in $Cp^*OsCl(PPh_3)_2$. Carbonyl ligand shows a C–Os bond length of 1.865(3) Å and the angle O-C-Os is 175.5(3)º. These values are close to those fond, for example, in $[Os(\eta^1\text{-}CH_2Ph)(CO)(\eta^6\text{-}p\text{-cymene})\{PPh(OEt)_2\}]BPh_4$, in $Os(\eta^4\text{-}C_4H_5Ph)(CO)\text{-}(P^iPr_3)_2$ or for the 1-(methylthio)cyclopentadienyl cationic compound $[Os(\eta^5\text{-}C_5H_4SMe)(CO)\text{-}(PPh_3)_2]^+$. Worth noting, the latter is the only half-sandwich complex $Os(CO)P_2$ compound found in the CCDC data base, either with any kind of cyclopentadienyl derivative or benzene derivatives, including *p*-cymenes.

The IR spectra of propadienylidene complexes $[Os(\eta^5\text{-}C_5Me_5)(=C=C=CPh_2)(PPh_3)\text{-}\{P(OMe)_3\}]BPh_4$ (**44, 45**) show a strong band at 1925-1930 cm^{-1} attributed to the $\nu_{=C=C=C}$ of the propadienylidene ligand. Its presence is confirmed by the ^{13}C NMR spectra, which show a doublet of doublets at 260.7 ppm attributed to the Cα resonance of the =Cα=Cβ=Cγ ligand. The resonances of the Cβ and Cγ appear at 219 and 149 ppm, respectively, and their attribution is supported by the HMQC and HMBC experiments. The ^{31}P NMR spectra appear as AX quartets fitting the proposed formulation for the complexes.

The IR spectra of the non-separable mixture containing the propadienylidene **46** and the vinylvinylidene **47** complexes show two characteristic bands, one at 1933 cm^{-1} attributed to the $\nu_{=C=C=C}$ of **46**, and the other at 1631 cm^{-1} attributed to the $\nu_{=C=C}$ of **47**. However, diagnostic for the presence of the two species are ^{13}C NMR spectra, which show two doublets of doublets at 314.65 and 260.99 ppm assigned to the carbenic Cα of the vinylidene **46** and propadienylidene **47**, respectively. These values of chemical shift are in accord with those of vinylidene complexes **40** and **41** and propadienylidene **44** and **45**, so supporting the presence of the two derivatives in the mixture. In the ^{13}C NMR spectra also appear two signals at 210 and 113 ppm attributed to Cβ and Cγ of the propadienylidene ligands, respectively, and a singlet at 114.04 ppm of Cβ of the vinylidene. In the ^{31}P NMR spectra, two AX quartets appear, in agreement with the proposed formulation for the mixture of **46** and **47**.

The presence of the 3-hydroxyvinylidene ligand in the complexes $[Os(\eta^5\text{-}C_5Me_5)\text{-}\{=C=C(H)C(H)R2(OH)\}(PPh_3)\{P(OMe)_3\}]BPh_4$ (**48, 49**) is mainly confirmed by both IR and ^{13}C NMR spectra. In particular, a medium-intensity band at 1647-1653 cm^{-1} due to the $\nu_{=C=C}$ of vinylidene appears in the IR spectra, whereas one doublet of doublets at 309.65 ppm for **49** and two at 308.24 and 308.65 ppm for **48** were observed in the ^{13}C NMR spectra of the complex and were

attributed to the carbenic Cα carbon resonance of the =C=C(H)C(H)R2(OH) moiety. The presence of two doublets of doublets in the spectra of complex $[Os(\eta^5\text{-}C_5Me_5)\{=C=C(H)C(H)Ph(OH)\}(PPh_3)\{P(OMe)_3\}]BPh_4$ (**48**) confirms that it was obtained as a mixture of two diastereoisomers, owing to the presence of two chiral centres in the molecule, *i.e.*, the osmium atom and the carbon atom bonded to the C_β of the vinylidene. In the ^{13}C NMR spectra there is a singlet at 107-115 ppm which is correlated in a HMQC experiment with the multiplet that appears in the proton spectra at 2.55-2.49 ppm and was assigned to the C_β carbon resonance of the vinylidene. In the proton spectra are present the signals of the substituents CH_2OH and CH(Ph)OH of the vinylidene, which appear as a doublet at 4.19 ppm (**49**) and a doublet of doublets at 5.10 ppm (**48**). In the temperature range between +20 and -80 °C, the ^{31}P NMR spectra are an AX quartet for **49** and two AX quartets for **48**, fitting the proposed formulation for the complexes.

The IR spectra of carbonyl complexes $[Os(\eta^5\text{-}C_5Me_5)(CO)(PPh_3)\{P(OR)_3\}]BPh_4$ (**51, 52**) show a strong band at 1944-1951 cm^{-1} attributed to the ν_{CO} of the carbonyl ligand; its presence confirmed by the ^{13}C NMR spectrum of **51** showing a doublet of doublets at 183.65 ppm for the CO carbon resonance. The proton spectra show the characteristic signals of the ancillary ligands, whereas the ^{31}P spectra are AX multiplets suggesting a geometry in solution like those found in the solid state.

7.6 Reaction of Azides with Half-Sandwich Complexes of Osmium

In the last part of this PhD project we further extended our studies on half-sandwich complexes of osmium and iridium to another type of azo ligand, the organic azides. The results show that azide complexes of the type $[Os(\eta^5\text{-}C_5H_5)(\kappa^1\text{-}N_3R1)(PPh_3)\{P(OR)_3\}]BPh_4$ (**53, 54**) can be prepared by reacting the bromo-compounds $[OsBr(\eta^5\text{-}C_5H_5)(PPh_3)\{P(OR)_3\}]$ first with AgOTf and then with an excess of the appropriate azide in toluene, as shown in Scheme 7.34.

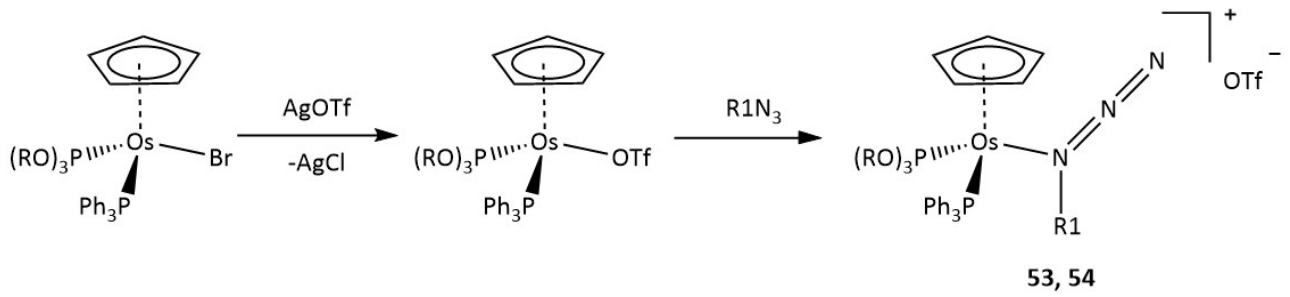

Scheme 7.34 R = Me (53), Et (54); R1 = $CH_2C_6H_5$ (a), $CH_2C_6H_4$-4-CH_3 (b), $CH(CH_3)C_6H_5$ (c), C_6H_5 (d).

The reaction of bromo-compounds [OsBr(η^5-C_5H_5)(PPh_3){$P(OR)_3$}] with AgOTf proceeds with the separation of solid AgBr, removed by filtration, and the formation of triflato complexes [Os(κ^1-OTf)(η^5-C_5H_5)(PPh_3){$P(OR)_3$}]. The treatment of this species with an excess of organic azide $R1N_3$ afforded azide derivatives [Os(η^5-C_5H_5)(κ^1-N_3R1)(PPh_3){$P(OR)_3$}]OTf, which separated out from their toluene solutions as dark-green sticky oil. The related tetraphenylborate salts [Os(η^5-C_5H_5)(κ^1-N_3R1)(PPh_3){$P(OR)_3$}]BPh_4 (**53, 54**), which are green solids stable in air but rather unstable in a solution of polar organic solvents, were obtained by treating the triflate species with an excess of $NaBPh_4$ in ethanol. Analytical and spectroscopic data (IR, ^1H, ^{15}N, ^{31}P NMR) support the proposed formulation.

It is worth noting that the related bis(triphenylphosphine) complex [OsBr(η^5-C_5H_5)$(PPh_3)_2$] does not give any azide complex following the same synthetic route of complexes **53, 54**. Therefore, it seems that only mixed-ligand fragments [Os(η^5-C_5H_5)(PPh_3){$P(OR)_3$}] can stabilize the [Os]-κ^1-N_3R1 derivatives.

The IR spectra of complexes **53** and **54** show a medium-intensity band at 2164–2145 cm^{-1}, attributed to ν_{N3} of the coordinate azide ligand. These values are higher than those of free RN_3 and are instead comparable with that of Ir, Pd, Cu, and Ag complexes, in which N_γ coordination was confirmed by X-ray crystal structure determination. Such coordination through substituted N_γ is favoured by the greater Lewis basicity[219,220] of the site and is probably the most common type of azide complex with linear NNN geometry.

Support for this attribution comes from the spectra of the labelled compounds [Os(η^5-C_5H_5)(κ^1-$^{15}N_3R1$)(PPh_3){$P(OR)_3$}]BPh_4 (**53b$_1$, 54b$_1$**, and **53c$_1$**), which show the ν_{15N3} at 2116–2105 cm^{-1} shifted to a lower wavenumber by 30–50 cm^{-1} with respect to unlabelled compounds **53b**, **54b** and **53c** (Fig. 7.13).

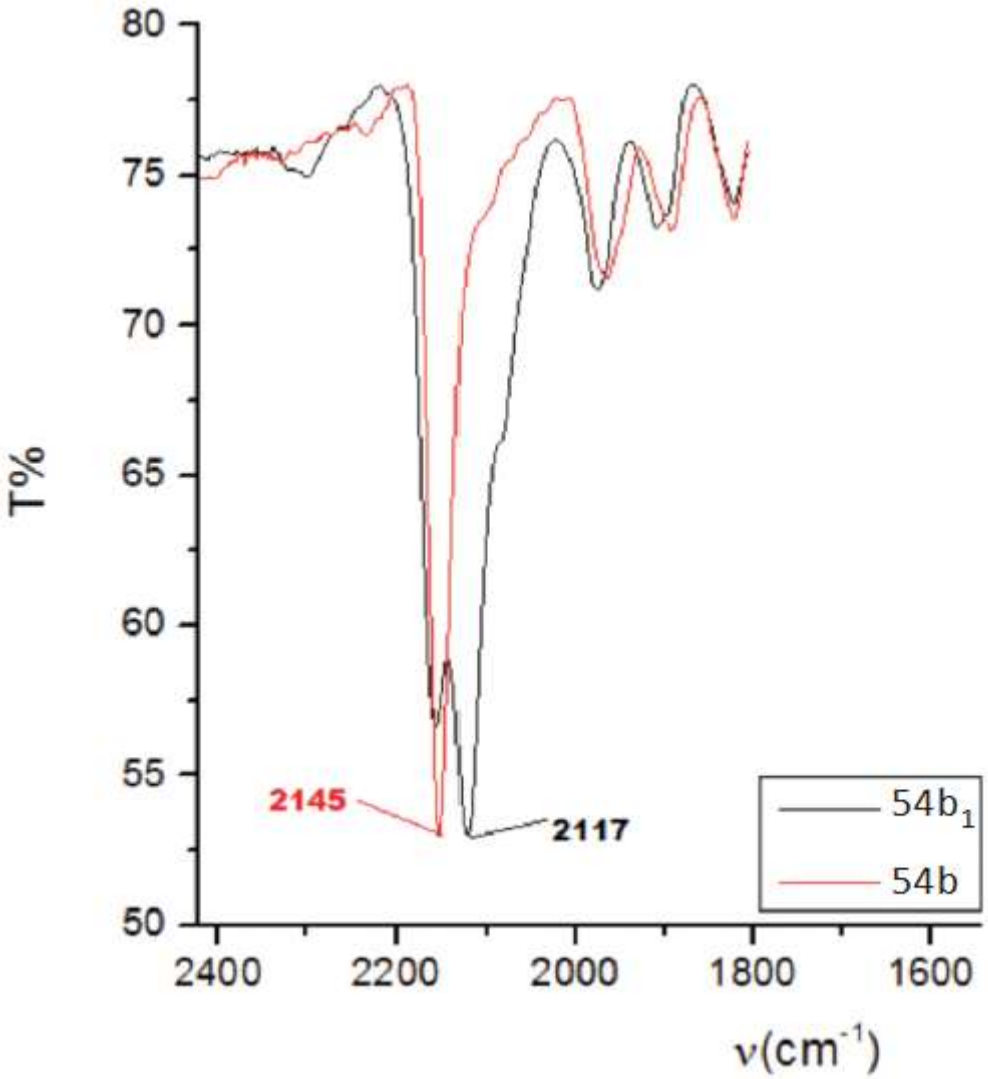

Figure 7.13 IR spectra in KBr of the labelled [Os(η^5-C_5H_5)(κ^1-$^{15}N_3CH_2C_6H_4$-4-CH_3)(PPh_3){$P(OEt)_3$}]BPh_4 (54b_1) and unlabelled compound [Os(η^5-C-H_5)(κ^1-$N_3CH_2C_6H_4$-4-CH_3)(PPh_3){$P(OEt)_3$}]BPh_4 (54b).

In addition, the higher ν_{N3} values of our complexes, compared to those of azide complexes, the X-ray structures of which are known,[122,221–223] suggest a κ^1-diazoamino coordination mode (Figure 7.14) for the azide ligand.

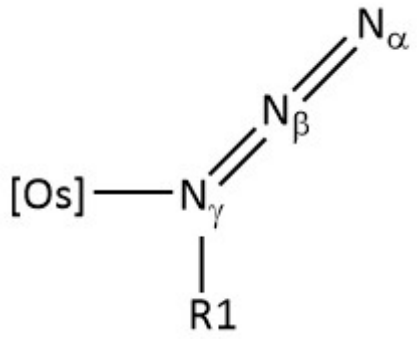

Figure 7.14 [Os] = [Os(η^5-C_5H_5)(PPh_3){$P(OR)_3$}].

Further support to the supposed coordination of the azide is given by the ^{15}N NMR and ^{31}P NMR spectra of the labelled complexes $[Os(\eta^5\text{-}C_5H_5)(\kappa^1\text{-}^{15}N_3R1)(PPh_3)\{P(OR)_3\}]BPh_4$ (**53b$_1$** and **53c$_1$**). The former shows a multiplet between 139 and 117 ppm and a singlet near 213 ppm, attributed to the N_γ and N_α nitrogen nuclei, respectively, of the coordinate $^{15}N_3R1$ group. The latter (Figure 7.15) show a multiplet due to coupling with the ^{15}N nuclei of $\kappa^1\text{-}^{15}N_3R1$, which can be simulated using an AXN model (A, X = ^{31}P; N = ^{15}N). In addition to the resonances of the substituents of the organic azides $R1N_3$, the ^1H NMR spectra of **53, 54** show the characteristic signals of the ancillary ligands $\eta^5\text{-}C_5H_5$, PPh_3, and $P(OR)_3$ and of the BPh_4^- anion, in agreement with the half-sandwich geometry shown in Scheme 7.34.

Transition metal complexes containing organic azides $R1N_3$ as ligands are rare[221,224–230] and only one example is known for osmium,[231] $[OsCl(\eta^1\text{-}N_3CH_2Ar)(CO)(PPh_3)_2\{P(OR)_3\}]BPh_4$, involving carbonyl and phosphines as supporting ligands. The use of the half-sandwich fragment $[Os(\eta^5\text{-}C_5H_5)(PPh_3)\{P(OR)_3\}]^+$ allows the synthesis of new stable organic azide complexes. Unfortunately, the bonding mode of the RN_3 in compounds **53** and **54** could not be established by X-ray determination, owing to their instability in solution, which prevented the preparation of suitable crystals.

Azide complexes $[Os(\eta^5\text{-}C_5H_5)(\kappa^1\text{-}N_3CH_2Ar)(PPh_3)\{P(OR1)_3\}]BPh_4$ and $[Os(\eta^5\text{-}C_5H_5)\{\kappa^1\text{-}N_3CH(CH_3)\text{-}C_6H_5\}(PPh_3)\{P(OR1)_3\}]BPh_4$ (**53a–c, 54a–c**) are stable as solids but in solution react to give the imine species $[Os(\eta^5\text{-}C_5H_5)\{\kappa^1\text{-}NH{=}C(H)Ar\}(PPh_3)\{P(OR)_3\}]BPh_4$ and $[Os(\eta^5\text{-}C_5H_5)\{\kappa^1\text{-}NH{=}C(CH_3)C_6H_5\}(PPh_3)\{P(OR)_3\}]BPh_4$ (**55, 56**) (Scheme 7.35).

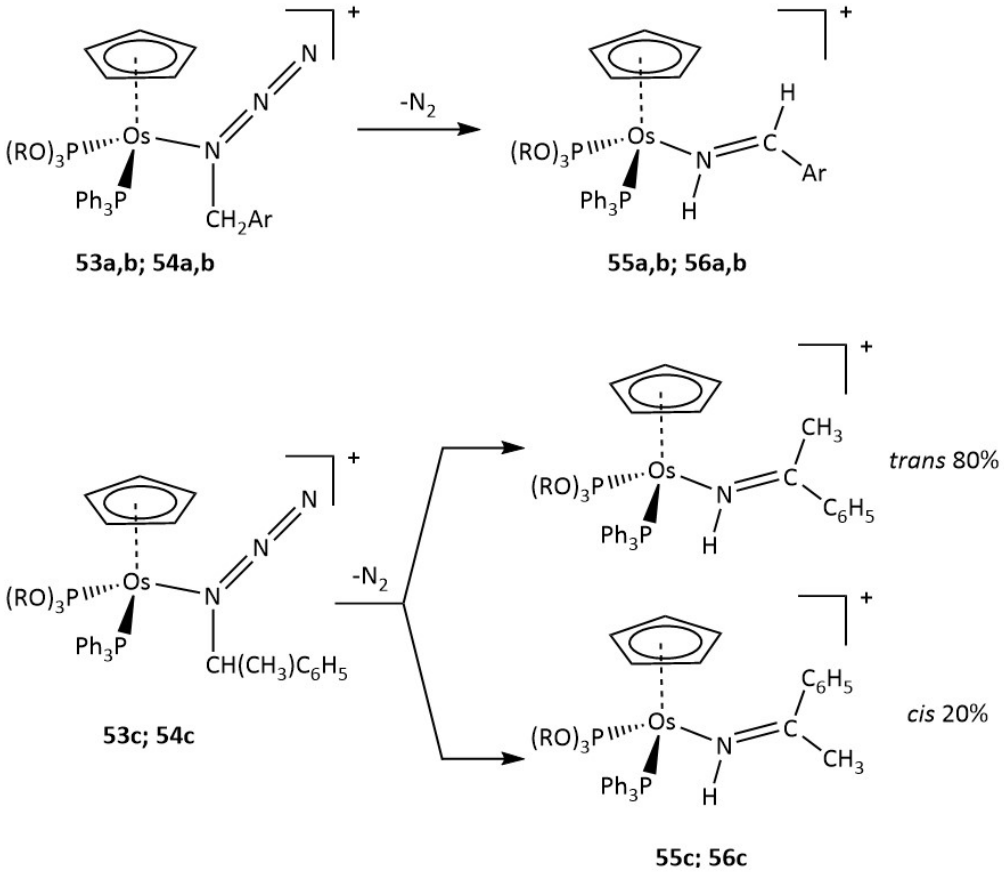

Scheme 7.35 Ar = C_6H_5 (a), 4-$CH_3C_6H_4$ (b).

The formation of the imino derivatives **55** and **56** can be easily explained with the extrusion of N_2 in the coordinated azide complexes **53** and **54** followed by the 1,2-shift of one hydrogen atom. Both the cis and trans isomers of the imine ligand are formed in the reaction of (1-azidoethyl)benzene derivatives **53c** and **54c** in approximately 1:4 ratio, whereas, with the benzylazide, only trans isomers **55a,b** and **56a,b** are observed.

Surprisingly, the phenylazide complex $[Os(\eta^5\text{-}C_5H_5)(\kappa^1\text{-}N_3Ph)(PPh_3)\{P(OMe)_3\}]BPh_4$ (**53d**) is also quite unstable in solution, but in this case a moderate yield of a blue solid can be isolated, whose structure by X-ray crystal determination revealed a binuclear μ-N_2 complex of the type $[\{Os(\eta^5\text{-}C_5H_5)(PPh_3)[P(OMe)_3]\}_2(\mu\text{-}N_2)](BPh_4)_2$ (**57**), which ORTEP[164] is shown in Figure 7.17.

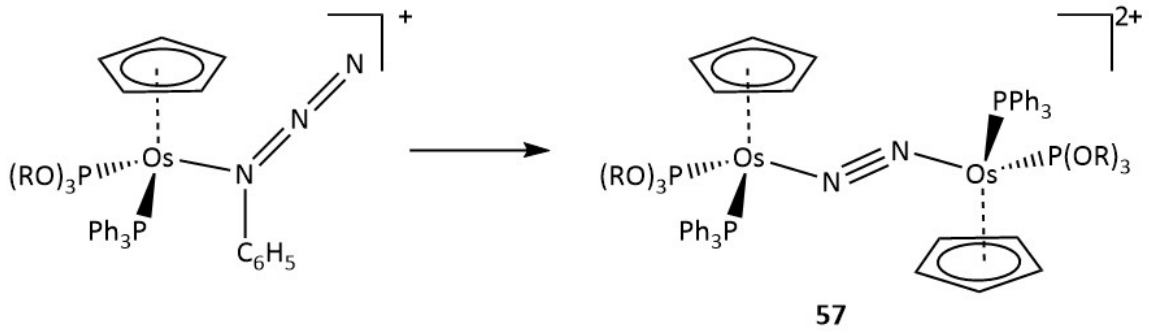

Scheme 7.36 Binuclear complex of osmium

The formation of the μ-dinitrogen complex is not totally unexpected because, unlike the other azides studied, the decomposition of the coordinated phenylazide with the extrusion of N_2 cannot give an imine owing to the absence of appropriate carbon and hydrogen atoms adjacent to the coordinate nitrogen. Therefore, the fragment $[Os(\eta^5\text{-}C_5H_5)(PPh_3)\{P(OMe)_3\}]^+$ could coordinate either the C_6H_5N fragment giving imido $[Os]{=}NC_6H_5$, or N_2 affording binuclear $\mu\text{-}N_2$ (**57**) as the final product.

Alternatively, the formation of the dinitrogen complex may be explained on the basis of a mechanism proposed for the formation of the nitrene complexes of vanadium and here described in Scheme 7.37[232].

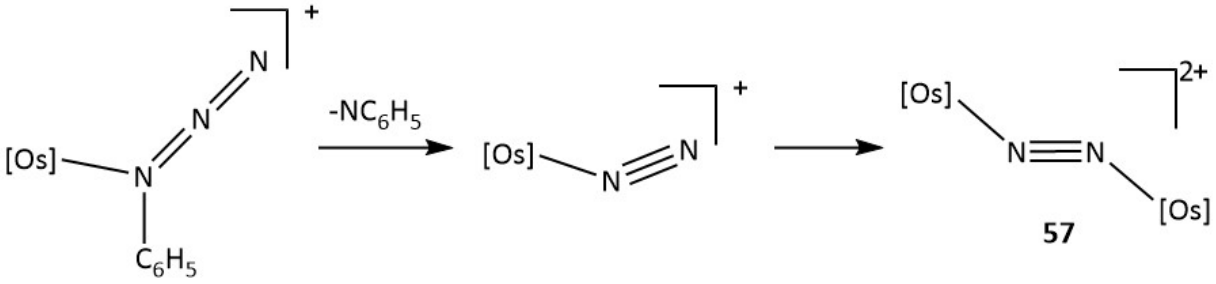

Scheme 7.37 [Os] = $Os(\eta^5\text{-}C_5H_5)\{(PPh_3)\{P(OMe)_3\}$

The loss of nitrene could occur directly from the azide complex **53d** affording a dinitrogen intermediate, which then dimerises to give the final product **57**. Also, the nitrene fragments thus generated could dimerise to give azobenzene $C_6H_5N{=}NC_6H_5$. The formation of **57** highlights the greater affinity of the fragment $[Os(\eta^5\text{-}C_5H_5)(PPh_3)\{P(OMe)_3\}]^+$ for the dinitrogen molecule allowing the formation of $\mu\text{-}N_2$ complexes. In addition, whatever the mechanism may be, the formation of **57** is interesting and has no precedent in azide derivatives reactions.

Imine complexes $[Os(\eta^5\text{-}C_5H_5)\{\kappa^1\text{-}NH{=}C(H)Ar\}(PPh_3)\{P(OR1)_3\}]BPh_4$ and $[Os(\eta^5\text{-}C_5H_5)\{\kappa^1\text{-}NHvC(CH_3)C_6H_5\}(PPh_3)\{P(OR1)_3\}]BPh_4$ (**55, 56**) and the dinitrogen derivative $[Os(\eta^5\text{-}C_5H_5)(PPh_3)\text{-}\{P(OMe)_3\}_2(\mu\text{-}N_2)](BPh_4)_2$ (**57**) were separated as green-yellow (**55, 56**) or blue (**57**) solids, stable in air and in solution of polar organic solvents, where they behave as 1:1 (**55, 56**) or 2:1 (**57**) electrolytes.[163] Analytical and spectroscopic data (IR, ^1H, ^{31}P, ^{15}N NMR) support the proposed formulation for the complexes.

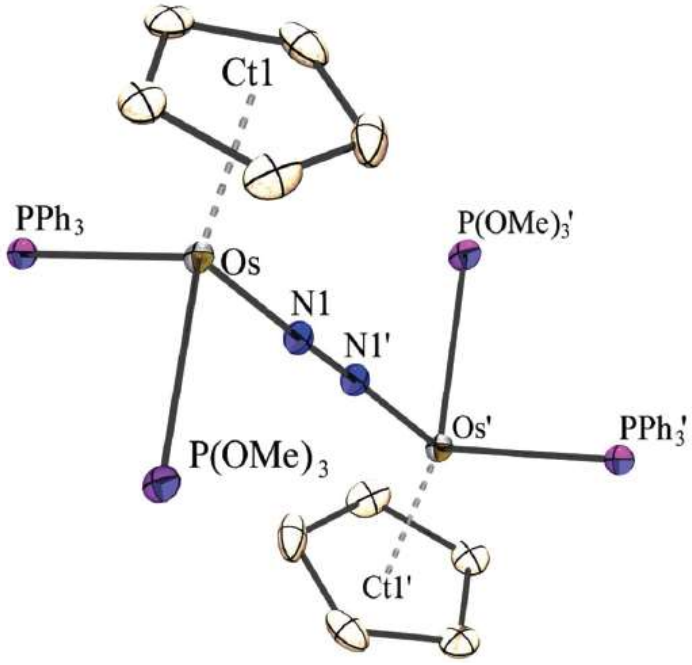

Figure 7.15 ORTEP of complex 57.

The asymmetric unit contains a tetraphenylborate anion, a dichloromethane solvent molecule and one half of the osmium cation complex so that the whole cation contains two symmetrically related osmium atoms in a half-sandwich piano-stool coordination. Each is bonded by one cyclopentadienyl (Cp), one $P(OMe)_3$ phosphite, one PPh_3 phosphine and one bridging N–N'-dinitrogen ligand, where the last ligand presents the inversion centre in the middle of the N–N bond. The overall geometry of the half-sandwich piano-stool complex is a slightly distorted octahedral and is marked by the angles between the centroid of the Cp ligand (Ct1) and the legs close to the theoretical 125.3°, or by near 90° values for angles formed by the legs of the piano-stool (Table 7.10). The two $OsCpP_2$ fragments are rotated about the Os–Os vector by 180°. Coordination of the Cp ligand (ring-slippage, 0.025 Å) with Os–C distances between 2.229(4) and 2.260(4) Å (average, 2.244 Å) do not require further comments as they are similar, for example, to those found in the cation $[CpOs(=C=CH_2)(PPh_3)_2]^+$, Os–C(Cp) 2.25–2.30(2), av. 2.27 Å.16 The Os–P distances are 2.261(1) and 2.342(1), longer than that of the phosphine ligand, but with less back-

bonding than the phosphite ligand. The bond length Os–N(1), 1.957(3) Å, is quite similar to those found for the Os(II) cation $[\{(\mu\text{-}N_2)Cp^*Os(Me_3P)_2\}_2]^{2+}$, 1.959(8) and 1.979(7) Å,17 and slightly longer than those found in mixed-valence (II + III) CpOs complexes, between 1.883(6) and 1.895(5) Å.[233–235]

Table 7.10 Selected bond lengths [Å] and angles [°] for 5

Os–CT1	1.8918(3)	Os–P(1)	2.3416(10)
Os–P(2)	2.2611(10)	Os–N(1)	1.957(3)
Os–C(1)	2.235(4)	Os–C(2)	2.236(4)
Os–C(4)	2.262(4)	Os–C(3)	2.229(4)
Os–C(5)	2.260(4)	Os–Cav	2.244(4)
N(1)–N(1^i)	1.116(6)		
CT1–Os–N(1)	126.05(9)	CT1–Os–P(2)	123.98(3)
N(1)–Os–P(2)	88.26(9)	CT1–Os–P(1)	123.31(2)
N(1)–Os–P(1)	89.76(9)	P(2)–Os–P(1)	95.43(3)
N(1^i)–N(1)–Os	177.2(4)		

Symmetry transformations used to generate equivalent atoms: i: 1 − x; 1 − y, 2 − z.

The N–N bond length, 1.116(6) Å is, however, shorter than those found in the above-mentioned compounds and, namely, between 1.135(6) and 1.165(8) Å. Conversely, the Os–N–N angle, 177.2(4)°, is more linear than the one found in the above-mentioned complexes (around 170°) or even in the ruthenium analogous complex $[\{(\mu\text{-}N_2)CpRu(PEt_3)_2\}_2]^{2+}$.[140]

The IR spectra of the imine complexes **55** and **56** show a medium-intensity band at 3260–3282 cm^{-1}, attributed to the ν_{NH} of the imine ligand. Its presence is confirmed by ^1H NMR spectra which, in monosubstituted species [Os]–NH=C(H)Ar (**55a, 55b, 56a, 56b**), show a broad doublet between 10.16 and 10.79 ppm, attributed to the NH imine resonance. This attribution is supported by the spectra of the labelled complexes [Os]–^{15}NH=C(H)Ar (**55b$_1$, 56b$_1$**), which show a doublet of multiplets due to the coupling of the imine proton NH with the =C(H) proton and the ^{31}P and the ^{15}N nuclei, Figure 7.16.

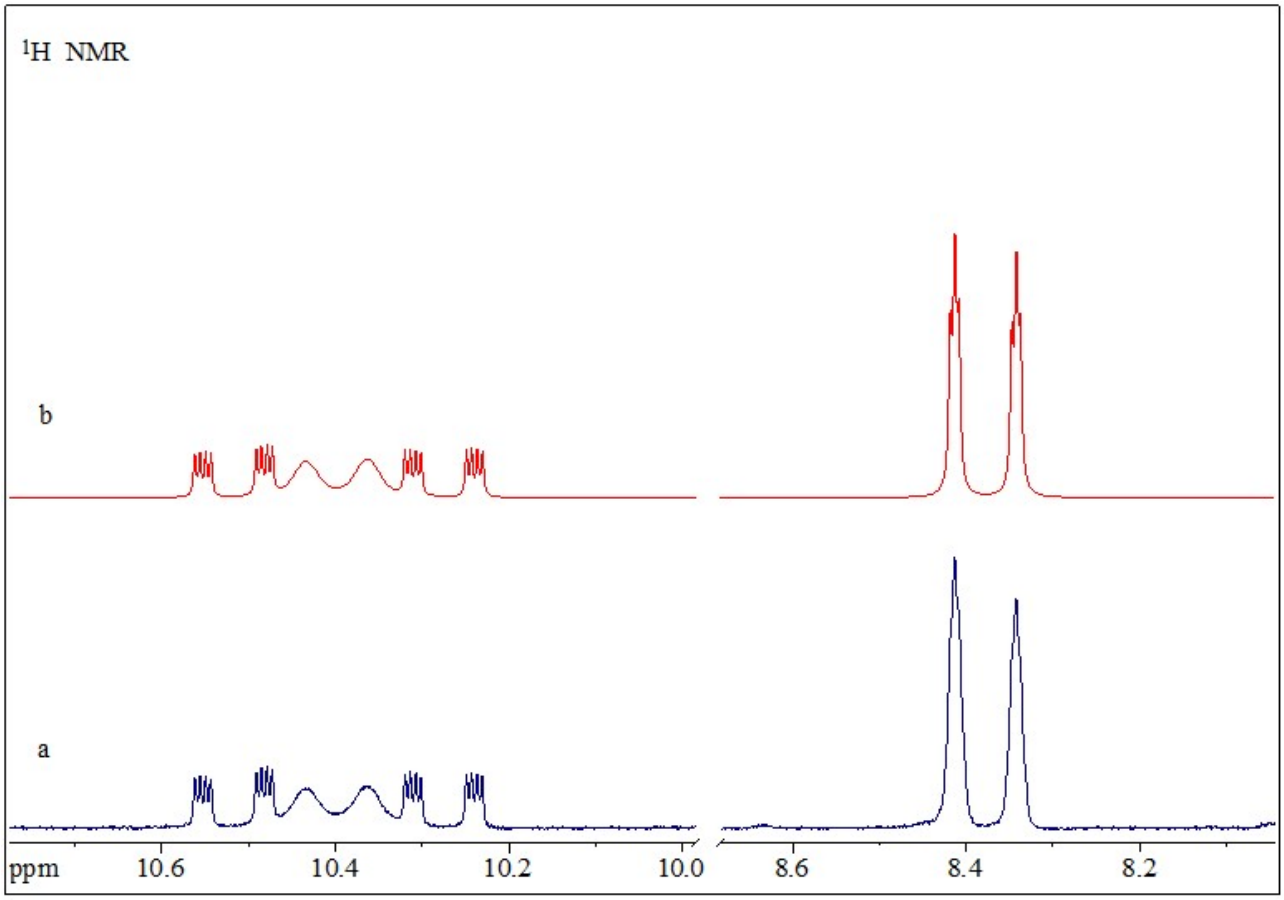

Figure 7.16 ^{1}H NMR spectra of complex $[Os(\eta^5\text{-}C_5H_5)\{\kappa^1\text{-}^{15}NH{=}C(CH_3)C_6H_4\text{-}4\text{-}CH_3\}(PPh_3)\{P(OMe)_3\}]BPh_4$ ($\mathbf{55b_1}$) in CD_2Cl_2 at 295 K. Lower, experimental; upper, simulated

These spectra may be simulated using an AXNYZ model (A, X = ^{31}P; N = ^{15}N; Y, Z = ^{1}H). Moreover, a doublet between 8.41 and 8.80 ppm also appears in the spectra, which is correlated, in a COSY experiment, with the doublet at 10.16–10.79 ppm of the NH proton. This signal was attributed to the =C(H) of the imine.

In the temperature range between +20 and −80 °C, the ^{31}P NMR spectra of the imine derivatives **55a, 55b, 56a** and **56b** are AX quartets, whereas those of the labelled compounds $\mathbf{55b_1}$ and $\mathbf{55b_1}$ appear as AXN multiplets (N = ^{15}N). In addition, the proton-coupled ^{15}N NMR spectra are doublets of multiplets that have been simulated by using of an AXNYZ model, supporting the proposed formulation.

The ^{1}H NMR spectra of the complexes $[Os(\eta^5\text{-}C_5H_5)\{\kappa^1\text{-}NH{=}C(CH_3)C_6H_5\}(PPh_3)\{P(OR1)_3\}]BPh_4$ (**55c, 56c**) show two broad signals between 10.46 and 9.98 ppm, which may be attributed to the NH imine protons of the two isomers *cis* and *trans* (Scheme 7.35) present in the sample.

This attribution is also supported by the ^{1}H NMR spectra of the labelled complexes $[Os(\eta^5\text{-}C_5H_5)\{\kappa^1\text{-}^{15}NH{=}C(CH_3)C_6H_5\}(PPh_3)\{P(OR1)_3\}]BPh_4$ (**55c$_1$, 56c$_1$**), Figure 7.17.

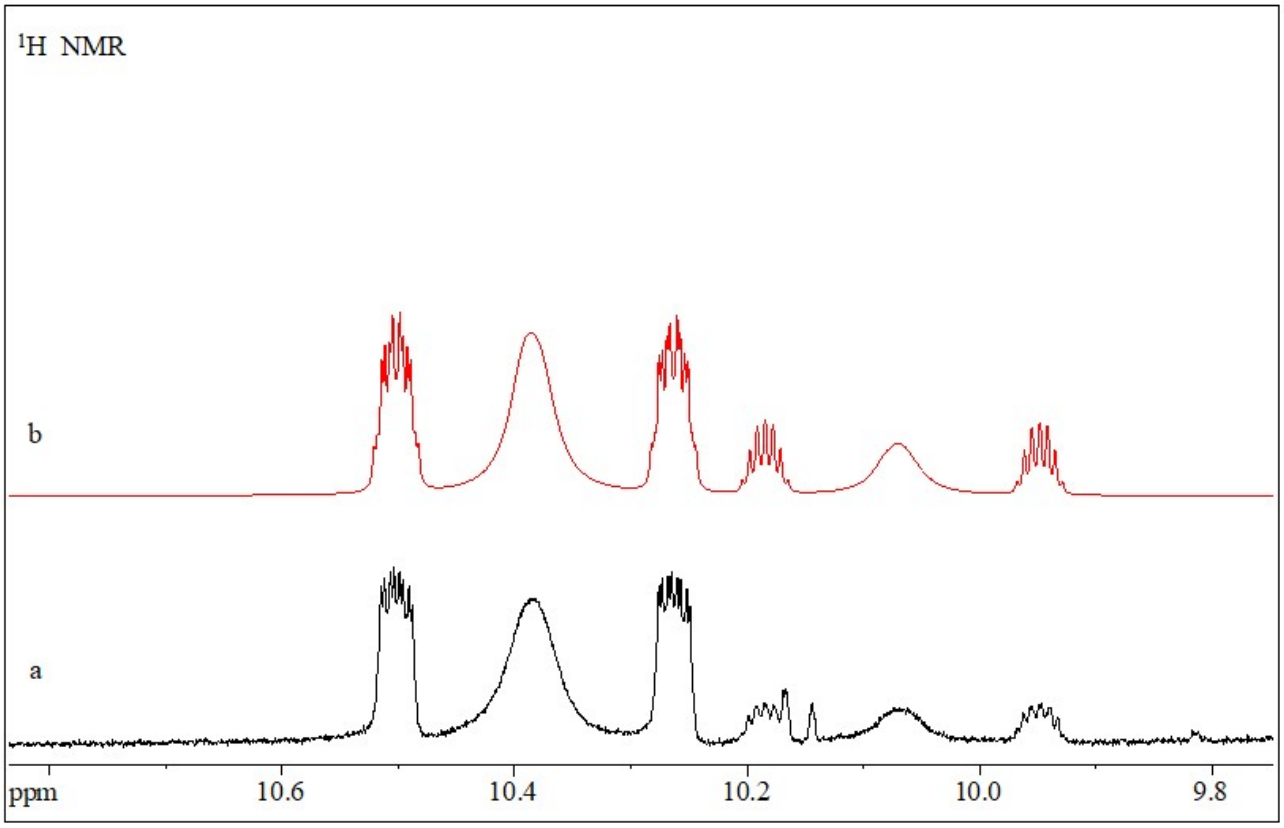

Figure 7.17 ^{1}H NMR spectra of complex $[Os(\eta^5\text{-}C_5H_5)\{\kappa^1\text{-}^{15}NH{=}C(CH_3)C_6H_5\}(PPh_3)\{P(OEt)_3\}]BPh_4$ (55c$_1$) in CD_2Cl_2 at 295 K. Lower, experimental; upper, simulated.

The Figure 7.17 shows two multiplets centred at the same chemical shift of the unlabelled species. This NMR spectra can be simulated by using two $AXNYZ_3$ models (A, X = ^{31}P; N = ^{15}N; Y, Z = ^{1}H). NOESY and COSY experiments are used to attribute the geometry of the two isomers. The proton-coupled ^{15}N NMR spectra (Figure 7.18), as well as those of $^{31}P\{^{1}H\}$, of the complexes **54c$_1$** and **55c$_1$** show two doublets of multiplets, which further support the proposed formulation.

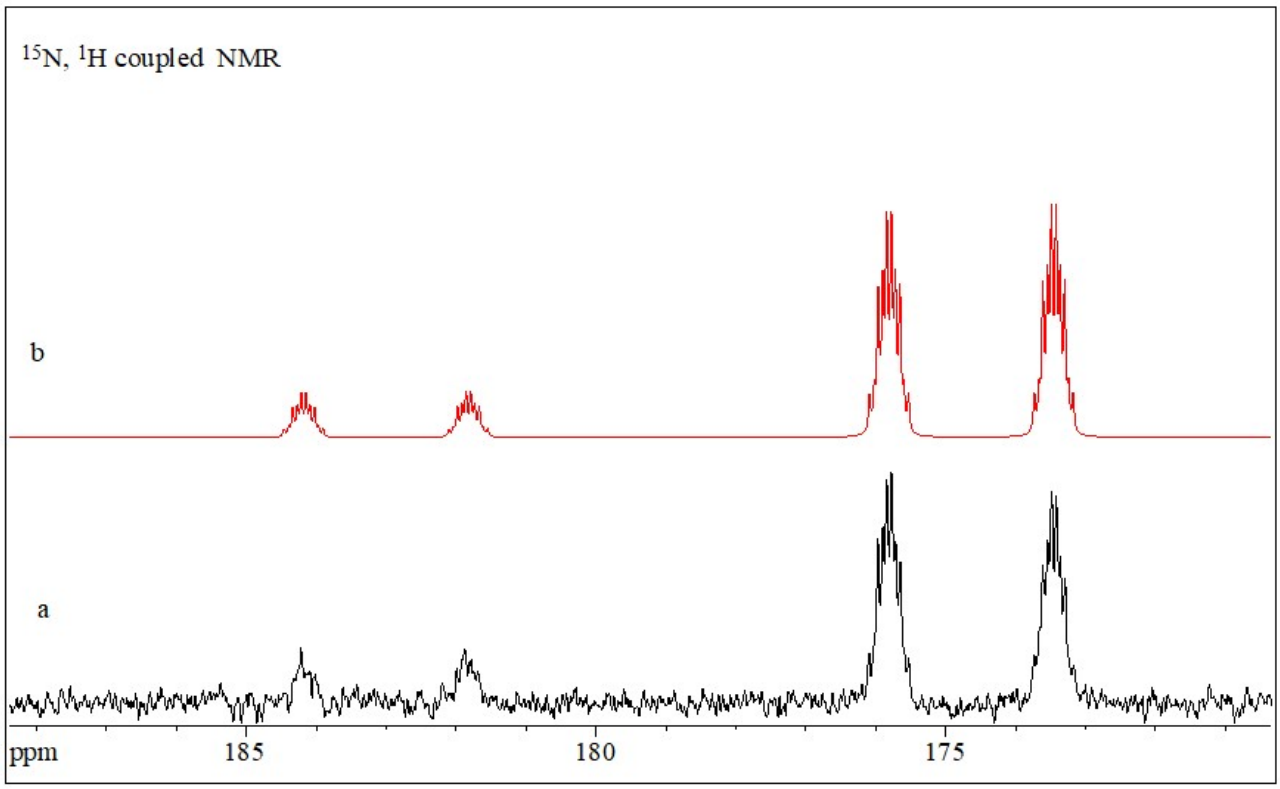

Figure 7.18 Proton-coupled ^{15}N NMR spectra of complex $[Os(\eta^5\text{-}C_5H_5)\{\kappa^1\text{-}^{15}NH{=}C(CH_3)C_6H_5\}(PPh_3)\{P(OEt)_3\}]BPh_4$ ($55c_1$) in CD_2Cl_2. Lower, experimental; upper, simulated.

The results obtained from the reaction of cyclopentadienyl complexes of the Os with organic azide prompted us to extend the studies to other half-sandwich derivatives of osmium of the type $[OsBr(\eta^5\text{-}C_5Me_5)(PPh_3)\{P(OR)_3\}]$ and $[OsCl_2(\eta^6\text{-}p\text{-cymene})(PPh_3)\{P(OEt)_3\}]$.

While the reaction of pentamethylcyclopentadienyl derivatives with the organic azide does not give any clear and reproducible results, *p*-cymene complexes quickly react with the organic azide, but do not afford κ^1-azide derivatives (Scheme 7.38).

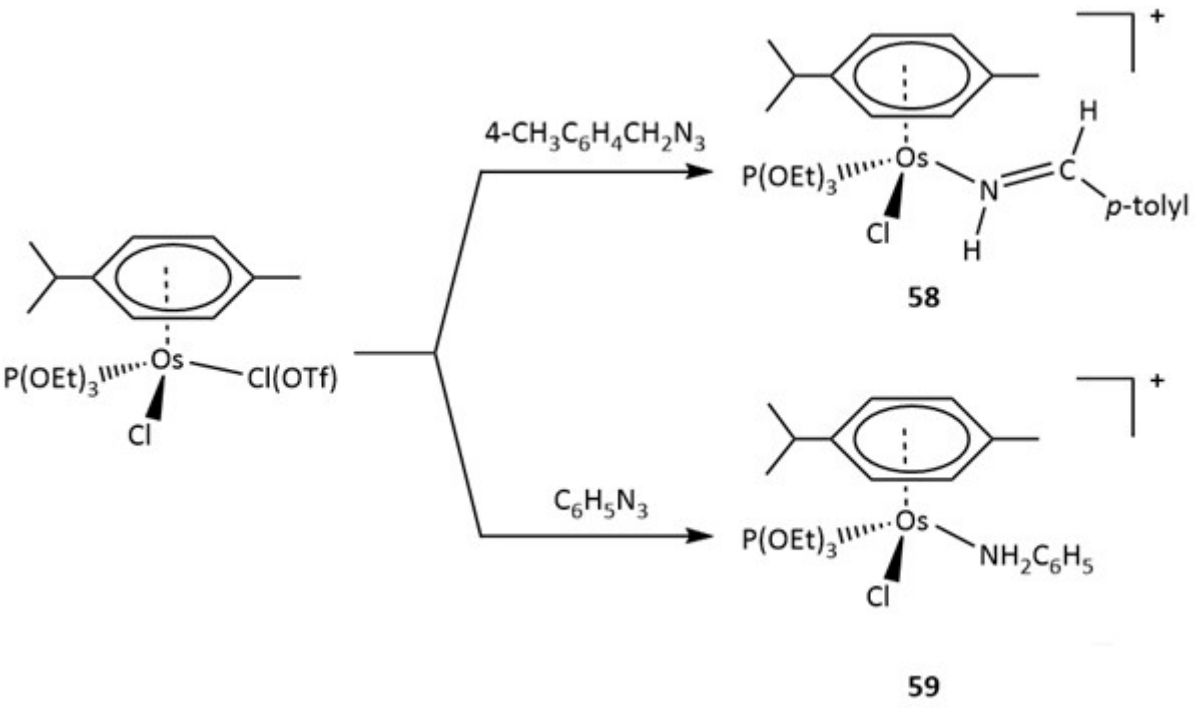

Scheme 7.38 Reaction of azides with complexes of osmium stabilized by *p*-cymene.

Depending on the nature of the substituents, the reaction of organic azides with both dichloro and chloro-triflate *p*-cymene derivatives $[OsCl_2(\eta^6\text{-}p\text{-cymene})\{P(OEt)_3\}]$ and $[OsCl(\kappa^1\text{-}OTf)(\eta^6\text{-}p\text{-cymene})\{P(OEt)_3\}]$ leads to the formation of κ^1-imine complex $[OsCl(\eta^6\text{-}p\text{-cymene})\{\kappa^1\text{-}NH{=}C(H)\text{-}C_6H_4\text{-}4\text{-}CH_3\}\{P(OEt)_3\}]BPh_4$ (**58**) and κ^1-amine derivative $[OsCl(\eta^6\text{-}p\text{-cymene})(\kappa^1\text{-}NH_2C_6H_5)\text{-}\{P(OEt)_3\}]BPh_4$ (**59**), while no evidence for the formation of κ^1-azide complexes was detected. However, based on the results obtained with half-sandwich osmium complexes stabilized by Cp*, we can hypothesize that the azide RN_3 could first substitute the Cl^- or OTf^- ligand in the *p*-cymene precursors, affording the intermediate κ^1-azide derivative $[OsCl(\eta^6\text{-}p\text{-cymene})(\kappa^1\text{-}N_3R)\{P(OEt)_3\}]BPh_4$ (Scheme 7.39).

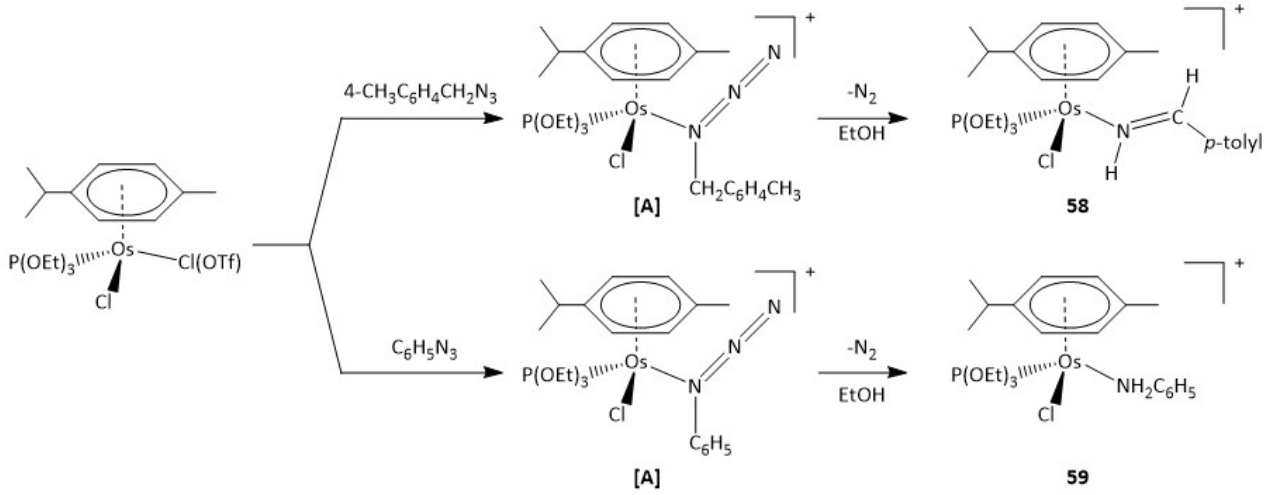

Scheme 7.39 proposed mechanism

This intermediate is unstable and decomposes, in the case of *p*-tolylbenzylazide, to form the κ^1-imine derivative **58**. Instead, in presence of ethanol, decomposition of the phenylazide intermediate affords the aniline derivative **59**. This last product is not unexpected because it is well known in literature[236] that an azide, when catalysed by transition metal complexes, can be reduced to an amine by an alcohol. As phenylazide cannot give an imine after the extrusion of N_2 and the fragment $[OsCl(\eta^6\text{-}p\text{-cymene})\{P(OEt)_3\}]^+$ does not bind N_2, reduction by alcohol of the coordinate $C_6H_5N_3$ could be the easiest reaction for the intermediate giving **59**.

Good analytical data were obtained for the *p*-cymene complexes **58** and **59**, which were separated as yellow solids stable both in air and in solution of polar organic solvents, where they behave as 1:1 electrolytes.[163] Infrared and NMR spectra support the proposed formulation. In particular, the ^1H NMR spectrum of the imine complex $[OsCl(\eta^6\text{-}p\text{-cymene})\{\kappa^1\text{-}NH{=}C(H)C_6H_4\text{-}4\text{-}CH_3\}\{P(OEt)_3\}]BPh_4$ (**58**) shows a broad doublet at 10.99 ppm, attributed to the iminic NH proton. Besides the signals of the ancillary ligands *p*-cymene and $P(OEt)_3$ and of anion BPh_4^-, the proton spectra also show a doublet at 8.68 ppm, which, in a COSY experiment, is correlated with the broad doublet at 10.99 ppm, and is attributed to the =CH proton of the imine ligand. The $^{31}P\{^1H\}$ NMR spectrum is a sharp singlet at 67.51 ppm fitting the proposed formulation for the complex. The IR spectrum of the amine complex $[OsCl(\eta^6\text{-}p\text{-cymene})(\kappa^1\text{-}NH_2Ph)\{P(OEt)_3\}]BPh_4$ (**59**) shows two medium-intensity bands at 3286 and 3226 cm^{-1}, attributed to the =NH of the aniline ligand. Its presence is confirmed using the ^1H NMR spectrum, which shows two broad signals at 5.52 and 5.81 ppm, attributed to the NH_2 protons of the coordinate aniline. The presence of the two signals is due to the chiral centre at osmium atom in the molecule. Signals of the supporting ligands are also present in the spectra, whereas the ^{31}P spectrum is a singlet at 68.29 ppm, in agreement with the proposed formulation for the complex.

7.7 Reaction of Azides with Half-Sandwich Complexes of Iridium

The reaction of half-sandwich fragments $[IrCl_2(\eta^5\text{-}C_5Me_5)P(OR)_3]$ with an excess of the appropriate aliphatic azide $R1CH_2N_3$ led to the formation of κ^1-imine complexes $[IrCl(\eta^5\text{-}C_5Me_5)(\kappa^1\text{-}NH{=}C(H)R1)P(OR)_3]BPh_4$ (**60**, **61**), while the same reaction with phenyl azide PhN_3 afforded the κ^1-aniline derivatives $[IrCl(\eta^5\text{-}C_5Me_5)(\kappa^1\text{-}NH_2Ph)P(OR)_3]BPh_4$ (**62, 63**), as shown in Scheme 7.40:

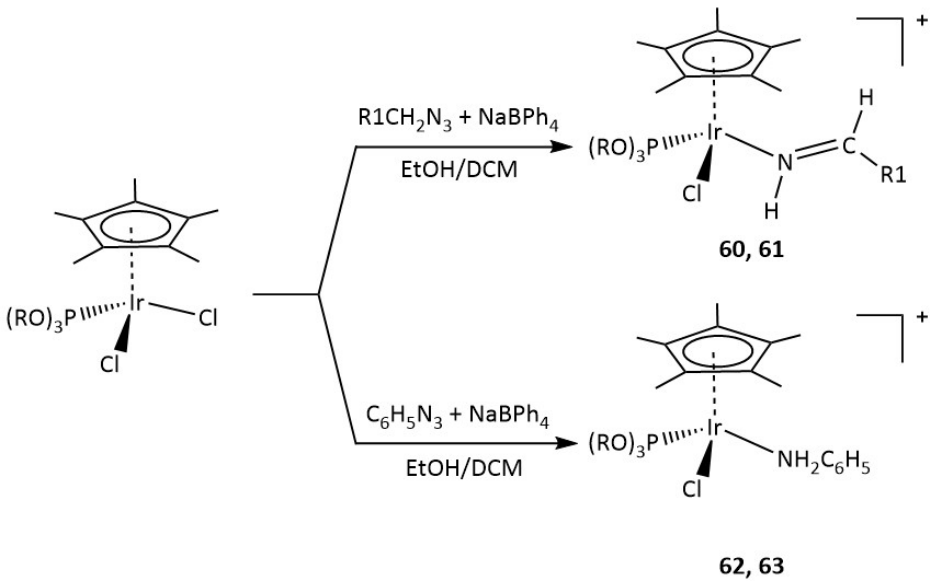

Scheme 7.40 R = Me (60, 62), Et (61, 63); R1 = C_6H_5 (a), 4-$CH_3C_6H_4$

As previously proposed for the reaction of *p*-cymene osmium complex [$OsCl_2(\eta^6$-*p*-cymene)$P(OR)_3$], the reaction probably involve a first coordination of the azide ArN_3 affording the intermediates κ^1-azide derivatives [$IrCl(\eta^5$-$C_5Me_5)(\kappa^1$-$N_3Ar)\{P(OR)_3\}]BPh_4$ **[A]** (Scheme 7.41).

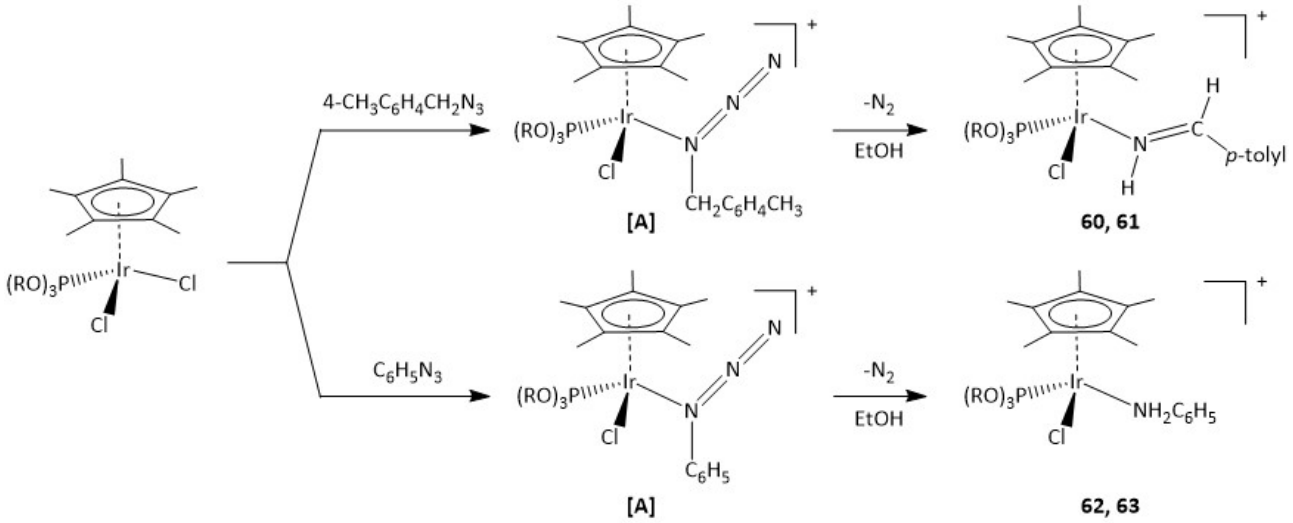

Scheme 7.41 R = Me (60, 62), Et (61, 63).

Those intermediates are unstable and decomposes producing, in the case of aliphatic azide $R1CH_2N_3$, the κ^1-imine derivative **60, 61**. Instead, in the presence of ethanol, reaction of the phenylazide intermediate **[A]** yielded the aniline derivative **62, 63**[236] which were isolated and characterized.

It is worth noting that the treatment of the chloro complexes [$IrCl_2(\eta^5$-$C_5Me_5)P(OR)_3$] first with AgOTf, and then with an excess of the appropriate azide ArN_3 also led to the formation of both κ^1-

imine complex complexes [IrCl(η^5-C$_5$Me$_5$)(κ^1-NH=C(H)R1)P(OR)$_3$]BPh$_4$ (**60**, **61**) and κ^1-amine derivatives [IrCl(η^5-C$_5$Me$_5$)(κ^1-NH$_2$Ph)P(OR)$_3$]BPh$_4$ (**62, 63**), as shown in Scheme 7.42.

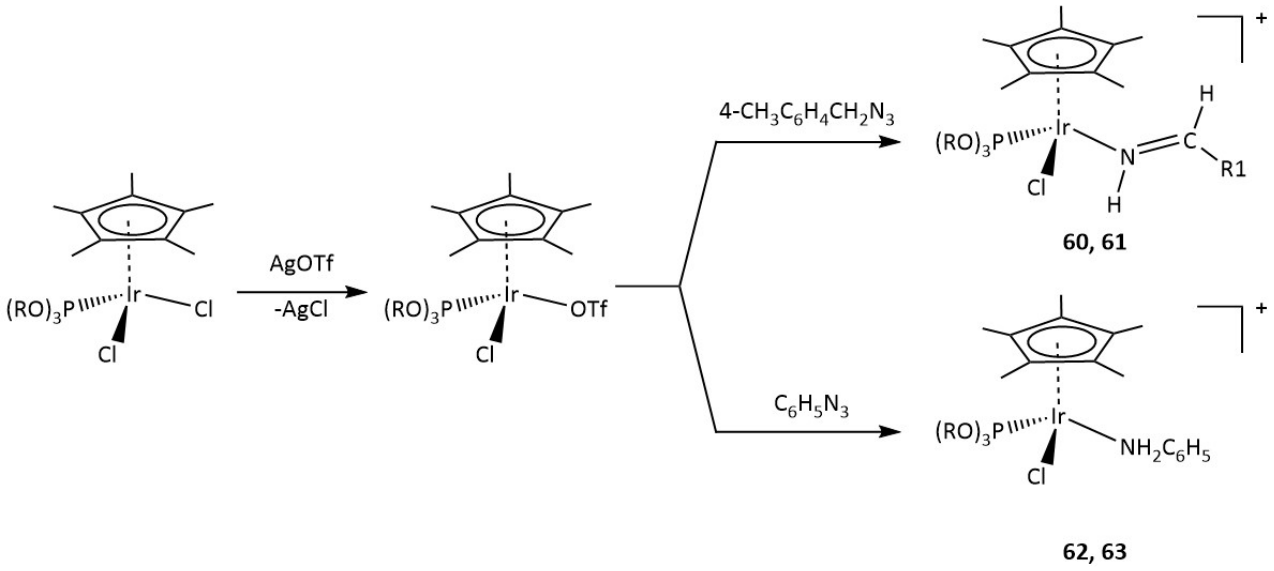

Scheme 7.42 R = Me (60, 62), Et (61, 63); R1 = C$_6$H$_5$ (a), 4-CH$_3$C$_6$H$_4$ (b).

The new iridium **60-63** complexes were isolated as solids of yellow to orange colour, stable in the air and in solution of the most common polar organic solvents, in which they behave as 1:1 electrolytes. The elemental analyses and the spectroscopic properties (IR and NMR) confirm the proposed formulation, which was further supported by the X-ray crystal structure determination of the complex **61b** [IrCl(η^5-C$_5$Me$_5$)(κ^1-NH=C(H)*p*-tolyl)P(OEt)$_3$]BPh$_4$, which ORTEP is shown in Figure 7.19.

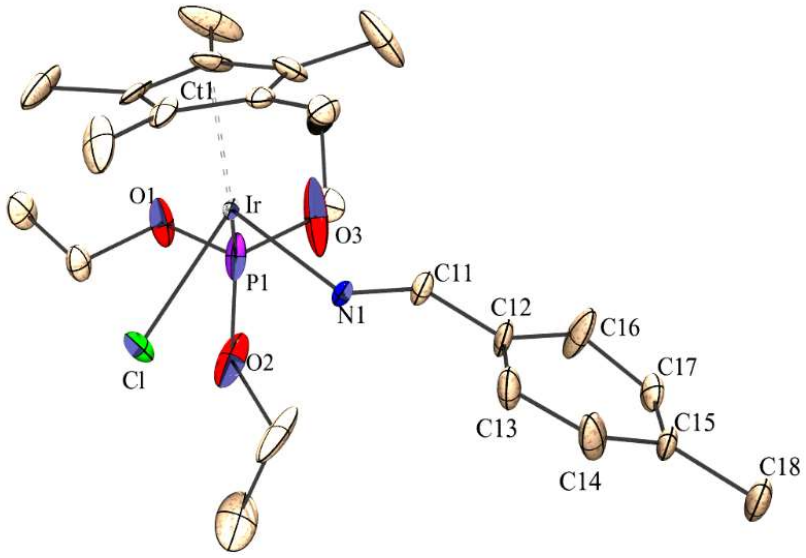

Figure 7.19 ORTEP of compound 61b

FIgure 7.19 portrays only the cation of complex **61b**, the BPh_4^- anion is not shown. And, even if there is an important disorder on the tolyl groups, only the most populated positions are drawn. The structure clearly shows an iridium atom in a half-sandwich piano-stool structure, coordinated to a pentamethylcyclopentadiene group (Cp*), one $P(OEt)_3$ phosphite ligand, a chloride ligand and a *p*-tolylmethanimine ligand. The overall geometry of the half-sandwich piano-stool complex is a slightly distorted octahedral and is marked by the angles between the centroid of the Cp* ligand (Ct1) and the legs close to the theoretical 125.3°, or by near 90° values for angles formed by the legs of the piano-stool (see Table 7.11).

Table 7.11 Selected bond lengths [Å] and angles [°] for 61b.

Ir-CT1	1.83131(16)	Ir-Cl	2.4103(5)
Ir-P(1)	2.2423(6)	Ir-N(1)	2.0933(16)
Ir-C(1)	2.246(2)	Ir-C(2)	2.171(2)
Ir-C(3)	2.181(2)	Ir-C(4)	2.160(2)
Ir-C(5)	2.245(2)	Ir-C_{av}	2.201
N(1)-C(11)	1.276(3)		
CT1-Ir-Cl	124.947(15)	N(1)-Ir-Cl	86.25(5)
P(1)-Ir-Cl	89.28(2)	CT1-Ir-N(1)	123.01(5)
CT1-Ir-P(1)	128.130(19)	N(1)-Ir-P(1)	93.48(5)
Ir-N(1)-C(11)	128.70(15)	N(1)-C(11)-C(12)	126.9(2)

Coordination of the Cp* ligand (ring slippage of 0.086 Å) leaves its centroid at a distance of 1.8313(2) Å from the iridium atom, and the average Ir–C bond distances for the Cp* ligand is 2.201 Å, values very similar to those found in the literature. While the Ir-P [2.2423(6) Å] and the Ir-Cl [2.4103(5) Å] bond lengths are similar to those found in the cations $[Cp^*IrCl(NH_2NH_2)\{P(OEt)_3\}]^+$ and $[Cp^*IrCl(CH_3NHNH_2)\{P(OEt)_3\}]^+$.[237]

The *p*-tolylmethanimine ligand is bonded to the iridium through the nitrogen atom, coordination mode κ^1-N. The Ir-N bond distance, 2.0933(16) Å, is a bit shorter than that found in the literature for the similar iridium complex, the cation $[IrCl_2\{\kappa^1\text{-}NH{=}C(H)C_6H_5\}\{P(OEt)_3\}_3]^+$, 2.130(4) Å. The shorter Ir-N bond length in **61b** with respect to the octahedral complex $[IrCl_2\{\kappa^1\text{-}NH{=}C(H)C_6H_5\}\{P(OEt)_3\}_3]^+$ can be explained on considering that the pentamethylcyclopentadiene ligand is only formally a 6-electron donor, therefore the metal centre can be less electronically saturated than in true octahedral compounds. Moreover, the Ir-N(1)-C(11) angle, 128.70(15)° as also the N(1)-C(11)-C(12) one, 126.9(2)° are surprisingly large for an sp^2-hybridized nitrogen and

carbon atoms, but similar values are found for all the *p*-tolylmethanimine complexes described in the literature[166,223,231,238–240].

The IR spectrum of the imine complex $[IrCl(\eta^6\text{-}C_5Me_5)(\kappa^1\text{-}NHC(H)R1)\{P(OR)_3\}]BPh_4$ (**60, 61**) shows a medium-intensity bands at 3143 cm^{-1}, attributed to $\nu_{=NH}$ of the imine ligand. The precence of the ligand is also confirmed by the proton NMR spectrum, showing a broad doublet at 9.6 ppm (**60**) and at 6.9 (**61**), attributed to the iminic NH proton. Besides the signals of the ancillary ligands Cp* and $P(Or)_3$ and of anion BPh_4^-, the proton spectra also show a doublet at 8.3 ppm (**60**) and at 8.4 (**61**), which, in a COSY experiment, is correlated with the broad doublet 9.6 ppm (**60**) and at 9.9 (**61**) and is attributed to the =CH proton of the imine ligand. The $^{31}P\{^1H\}$ NMR spectrum is a sharp singlet at 78 ppm for $P(OMe)_3$ or 75 ppm for $P(OEt)_3$, fitting the proposed formulation for the complex and suggesting a geometry like those found in the solid state.

The IR spectrum of the amine complex $[IrCl(\eta^6\text{-}C_5Me_5)(\kappa^1\text{-}NH_2Ph)\{P(OR)_3\}]BPh_4$ (**62, 63**) shows two medium-intensity bands at 3275 and 3126 cm^{-1}, attributed to $\nu_{=NH}$ of the aniline ligand. Its presence is confirmed by the ^1H NMR spectra, which shows a broad doublet at 5.8 (**62**) and at 5.9 (**63**) attributed to the NH_2 protons of the coordinate aniline. The presence of the two signals is due to the chiral centre at osmium atom in the molecule. Signals of the supporting ligands are also present in the spectra, whereas the ^{31}P spectrum is a singlet at 76.5 ppm (**62**) or 72.8 (**63**), in agreement with the proposed formulation for the complex.

Interestingly, the reaction between the dimer complexes $[IrCl_2(\eta^5\text{-}C_5Me_5)]_2$ and aliphatic azines $R1CH_2N_3$ in tetrahydrofuran under reflux condition, led to the fragmentation of the dimer and, depending on the reaction time, to the formation of both mono (**64**) and bis-imino (**65**) complexes as shown in Scheme 7.43:

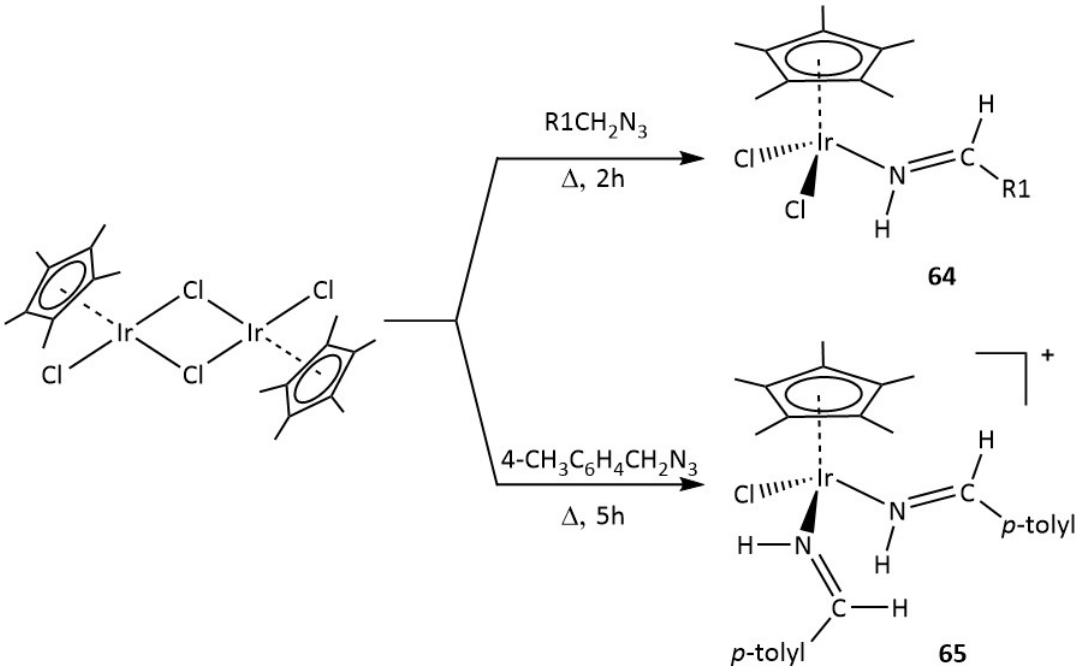

Scheme 7.43 R1 = C_6H_5 (a), 4-$CH_3C_6H_4$ (b)

The mono-imino complex [$IrCl_2(\eta^5\text{-}C_5Me_5)(\kappa^1\text{-}NH{=}C(H)p\text{-tolyl})$] (**64**) is neutral and could be separated from the reaction mixture as a yellow solid, whereas the bis imino derivative [$IrCl(\eta^5\text{-}C_5Me_5)(\kappa^1\text{-}NH{=}C(H)p\text{-tolyl})_2]BPh_4$ (**65**) was precipitated from ethanol, as tetraphenylborate salt. Both mono e bis imino compounds (**64, 65**) were isolated as solids in good yield and characterized by the standard methods. In particular, the IR spectrum of the mono-imino complex **64** shows a medium intensity band at 3169 cm^{-1}, attributable to $\nu_{N\text{-}H}$ of the imine and one to 1627 cm^{-1} due to $\nu_{C=N}$. The presence of the ligand in the coordination sphere is also confirmed by the ^1H NMR spectrum, which shows two doublets, one broad at 10.22 ppm and one sharp at 8.46 ppm, of the two iminic hydrogen atom =NH and =CH respectively. Signals of the *p*-tolyl substituent and of the C_5Me_5 are also present in the spectra.

Like the mono imino complex, also the proton spectra of the bis-imino derivative [$IrCl(\eta^5\text{-}C_5Me_5)(\kappa^1\text{-}NH{=}C(H)p\text{-tolyl})_2]BPh_4$ (**65**) shows, beside the signals of the *p*-tolyl substituent, of the C_5Me_5 and of the BPh_4^- anion, two doublets: one broad at 11.82 ppm and one sharp at 8.44 ppm attributed to the two =NH and =CH protons, according to the proposed formulation.

To verify whether also the fragment $[Ir(\eta^5\text{-}C_5Me_5)\{P(OR)_3\}]^{2+}$ could stabilize the relative bis imino derivatives, the chloro complexes $[IrCl_2(\eta^5\text{-}C_5Me_5)P(OR)_3]$ were first reacted with two equivalents of AgOTf. The reaction proceeds with the separation of solid AgCl, removed by filtration, and the probable formation of the bis-triflato complexes $[Ir(\kappa^1\text{-}OTf)_2(\eta^5\text{-}C_5Me_5)\{P(OR)_3\}]$.

The treatment of this species with an excess of organic azide 4-$CH_3C_6H_4CH_2N_3$ afforded the bis imino derivatives $[Ir(\eta^5\text{-}C_5Me_5)(\kappa^1\text{-}NH{=}C(H)p\text{-tolyl})_2\{P(OR)_3\}](OTf)_2$, as shown in Scheme 7.44.

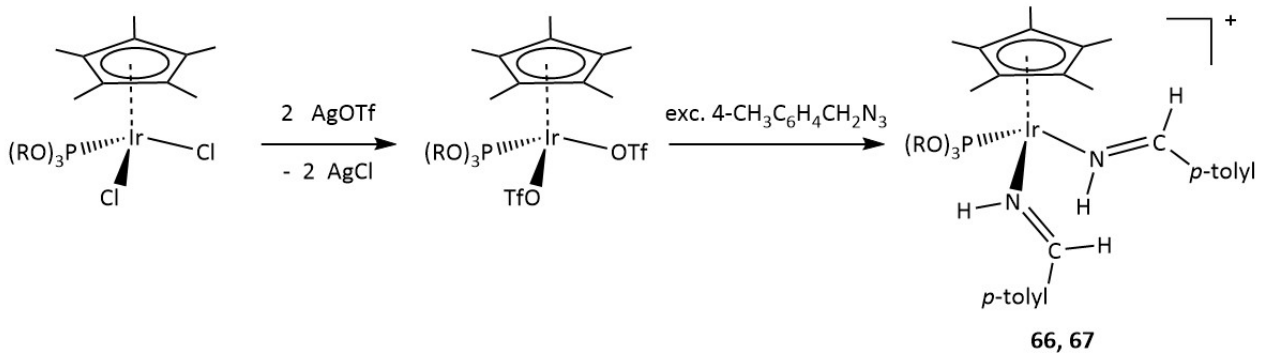

Scheme 7.44 R = Me (66), Et (67).

The bis imino derivatives $[Ir(\eta^5\text{-}C_5Me_5)(\kappa^1\text{-}NH{=}C(H)p\text{-tolyl})_2\{P(OR)_3\}](BPh_4)_2$ (**66, 67**) were precipitated from ethanol, as tetraphenylborate salt and were isolated as pale-yellow solids in good yield and characterized by the standard methods.

Interestingly, in the high frequency region of the proton spectra appear two doublets at 9.15 and ppm and at 8.43 ppm which are correlated in a COSY experiment with a doublet at 8.14 ppm and with a doublet of doublets at 8.00 ppm. These signals may be interpreted on the basis of the presence of a mixture of these complexes containing both cis and trans isomers of the imine ligand (Figure 7.20).

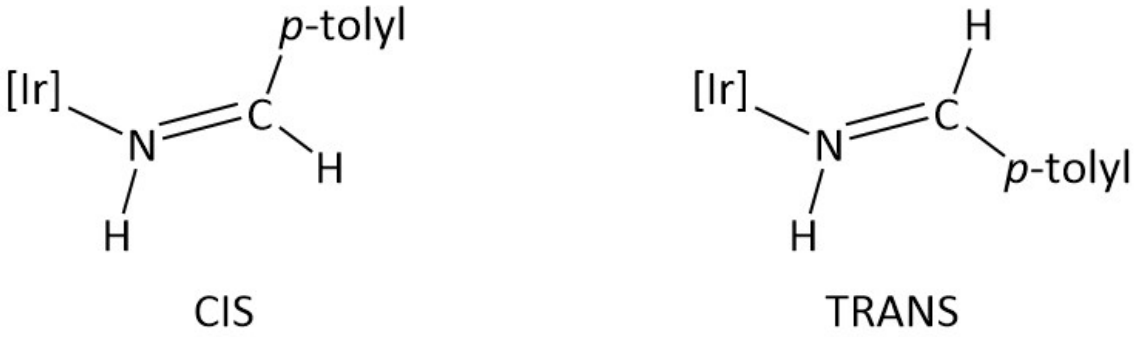

Figure 7.20 Possible configurations of the complexes 66,67

This hypothesis is confirmed by the appearance of two set of signals for the ancillary ligands $P(OR)_3$ and $\eta^5\text{-}C_5Me_5$ and two singlets for the methyl substituent of the *p*-tolyl group. Two singlets at 70.50 ppm and at 68.77 ppm also appear in the ^{31}P spectra fitting the proposed formulation for the complexes.

CONCLUSIONS

In PhD thesis work we have described the preparation of azine, diazoalkane and organic azide complexes from the appropriate metal fragments of Ru, Os, Rh and Ir. Moreover, we have studied their reactivity with the perspective of highlighting novel chemical poperties so deepen the coordination chemistry of these ligands. In particular, we have reported that both half-sandwich fragments $[RuCl(\eta^6\text{-}p\text{-cymene})L]^+$ and $[Ru(\eta^5\text{-}C_5H_5)(PPh_3)\{P(OMe)_3\}]^+$ (L=phosphite) can κ^1-coordinate azine molecules R1(H)C=N–N=C(H)R1 producing stable and isolable complexes. However, whereas aldazine gives stable compounds, ketazine is activated towards hydrolysis, affording hydrazone derivatives. The asymmetric azine $Ph(CH_3)C=N–N=C(H)Ph$ complexes $[RuCl(\eta^6\text{-}p\text{-cymene})\{\kappa^1\text{-}[N=C(CH_3)Ph]–N=C(H)Ph\}L]BPh_4$ were also prepared. Oxidation of the coordinated hydrazone with HgO, yielded the dimethyldiazoalkane derivative $[Ru(\eta^5\text{-}C_5H_5)\text{-}\{N_2=C(CH_3)_2\}(PPh_3)\{P(OMe)_3\}]BPh_4$.

The *p*-cymene fragment $[OsCl(\eta^6\text{-}p\text{-cymene})\{P(OR)_3\}]^+$ can κ^1-coordinate both aldazine $(R1C_6H_4)C(H)=N–N=C(H)(R1C_6H_4)$ and ketazine $(CH_3)_2C=N–N=C(CH_3)_2$ molecules. Among the properties shown by these azine derivatives, we can highlight the metalation reaction of arylaldazine which leads to the formation of the κ^2-chelate complexes $[Os\{\kappa^2\text{-}R1C_6H_3C(H)=N\text{-}N=C(H)C_6H_4R1\}(\eta^6\text{-}p\text{-cymene})\text{-}\{P(OR)_3\}]BPh_4$. Finally, the $[OsCl(\eta^6\text{-}p\text{-cymene})\{P(OR)_3\}]^+$ fragment, like the ruthenium homologous, can activate the κ^1-ketazine towards hydrolysis, producing hydrazone derivatives.

Azine complexes of rhodium $[RhCl(\eta^5\text{-}C_5Me_5)\{\kappa^1\text{-}[N=C(H)Ph]–N=C(H)Ph\}L]BPh_4$ and $[Rh\{\kappa^2\text{-}R1C_6H_3C(H)=N\text{-}N=C(H)C_6H_4R1\}(\eta^5\text{-}C_5Me_5)\{P(OR)_3\}]BPh_4$ were also prepared using the dichloro derivatives as precursors.

Aldazine $(R1C_6H_4)C(H)=N–N=C(H)(R1C_6H_4)$ and ketazine $(CH_3)_2C=N–N=C(CH_3)_2$ molecules react with iridium complexes $[IrCl_2(\eta^5\text{-}C_5Me_5)P(OR)_3]$, producing both κ^1- and κ^2-azine derivatives. κ^2-Chelate species are formed through metalation of the κ^1-coordinated azine. The promising photophysical features exhibited by some of the novel κ^2-arylazine derivatives open up the possibility of using aromatic azine ligands to prepare new luminescent Ir(III) complexes.

The pentamethylcyclopentadienyl fragment $[Os(\eta^5\text{-}C_5Me_5)(PPh_3)\{P(OR)_3\}]^+$ can stabilise diazoalkane complexes giving a rare example of this class of compounds for osmium. Among the properties shown by these complexes, the dipolar (3+2) cycloaddition with acetylene HC≡CH is paticularly interesting because it allows to obtain 3-H pyrazole derivatives in mild conditions (1 atm, R. T.). The substitution of the diazoalkane ligand also occurs with dioxygen yielding novel $\kappa^2\text{-}O_2$ derivatives. Conversely, with terminal alkynes R1C≡CH, the formation of vinylidene derivatives $[Os(\eta^5\text{-}C_5Me_5)\{=C=C(H)R1\}(PPh_3)\{P(OMe)_3\}]BPh_4$ is observed. In addition, reactions with propargylic alcohols HC≡CC(OH)R1R2 allowed allenylidene and hydroxyvinylidene complexes, stabilised by the pentamethylcyclopentadienyl osmium fragment, to be prepared.

In this thesis we also reported that the half-sandwich fragment $[Os(\eta^5\text{-}C_5H_5)(PPh_3)\{P(OR)_3\}]^+$ can stabilise organic azide complexes $[Os(\eta^5\text{-}C_5H_5)(\kappa^1\text{-}N_3R)(PPh_3)\{P(OR1)_3\}]BPh_4$. Spectroscopic data suggest a κ^1-diazoamino coordination mode of the azide ligand. Imine derivatives $[Os(\eta^5\text{-}C_5H_5)\{\kappa^1\text{-}NH=C(R1)Ar\}(PPh_3)\{P(OR)_3\}]BPh_4$ (R1 = H, CH_3) were obtained from benzylazide complexes. Instead, the binuclear dinitrogen derivative $[Os(\eta^5\text{-}C_5H_5)(PPh_3)\{P(OMe)_3\}_2(\mu\text{-}N_2)](BPh_4)_2$ was prepared from phenylazide PhN_3 complexes.

Finally, we found that the reaction between azides and half-sandwich fragment of the type $[IrCl(\eta^5\text{-}C_5Me_5)\{P(OR1)_3\}]^+$ leads to the formation of imino $[IrCl(\eta^5\text{-}C_5Me_5)\{\kappa^1\text{-}NH=C(R1)Ar\}(PPh_3)\text{-}\{P(OR)_3\}]BPh_4$ (R1= H, CH_3; Ar=C_6H_5, *p*-tolyl) and amino $[IrCl(\eta^5\text{-}C_5Me_5)(NH_2Ph)\{P(OR)_3\}]BPh_4$ derivatives. Moreover, changing the reaction condition, the reaction between azides and the dimeric compound $[IrCl(\mu\text{-}Cl)(\eta^5\text{-}C_5Me_5)]_2$ leads to the formation of both mono- $[IrCl_2(\eta^5\text{-}C_5Me_5)(\kappa^1\text{-}NH=C(R1)Ar)]$ and bis-imine complexes $[IrCl(\eta^5\text{-}C_5Me_5)(\kappa^1\text{-}NH=C(R1)Ar)_2]BPh_4$ (R1= H, CH_3; Ar=C_6H_5, *p*-tolyl). The treatment of the fragment $[Ir(\kappa^1\text{-}Otf)_2(\eta^5\text{-}C_5Me_5)\{P(OR1)_3\}]^+$ with azides yield the bis-imine derivatives $[Ir(\eta^5\text{-}C_5Me_5)(\kappa^1\text{-}NH=C(R1)Ar)_2\{P(OR)_3\}](BPh_4)_2$.

BIBLIOGRAPHY

1 G. Wagner and R. Herrmann, *Ferrocenes Homogenous Catalysis, Organic Synthesis, Material Science*, VCH, 1995.

2 A. Togni and R. L. Halterman, Eds., *Metallocenes*, Wiley-VCH Verlag GmbH, 1998.

3 T. J. Kealy and P. L. Pauson, *Nature*, 1951, **168**, 1039–1040.

4 G. Wilkinson, M. Rosenblum, M. C. Whiting and R. B. Woodward, *J. Am. Chem. Soc.*, 1952, **74**, 2125–2126.

5 E. O. Fischer and W. Pfab, *Z. Naturforsch*, 1952, **76**, 377–392.

6 G. Wilkinson, *J. Am. Chem. Soc.*, 1952, **74**, 6146–6147.

7 A. Bennett, M. Bruce and T. W. Matheson, *Comprehensive Organometallic Chemistry*, Pergamon Press, 1982.

8 C. Elschenbroich, *Organometallics*, Wiley-VCH, 3rd Ed., 2006.

9 R. Noyori and S. Hashiguchi, *Acc. Chem. Res.*, 1997, **30**, 97–102.

10 W. Hoffmüller, M. Maurus, K. Severin and W. Beck, *Eur. J. Inorg. Chem.*, 1998, 729–731.

11 F. Simal, A. Demonceau and A. F. Noels, *Tetrahedron Lett.*, 1998, **39**, 3493–3496.

12 H. Brunner and M. Prommesberger, *Tetrahedron Asymmetry*, 1998, **9**, 3231–3239.

13 D. Carmona, F. J. Lahoz, S. Elipe, L. A. Oro, M. P. Lamata, F. Viguri, C. Mir, C. Cativiela and M. P. López-Ram De Víu, *Organometallics*, 1998, **17**, 2986–2995.

14 D. S. Gill, C. White and P. M. Maitlis, *J. C. S. Dalt.*, 1978, 617–626.

15 J. Safari and S. Gandomi-Ravandi, *RSC Adv.*, 2014, **4**, 46224–46249.

16 M. Lewis and R. Glaser, *J. Org. Chem.*, 2002, **67**, 1441–1447.

17 R. Glaser, L. R. Dendi, N. Knotts and C. L. Barnes, *Cryst. Growth Des.*, 2003, **3**, 291–300.

18 M. Lewis, C. L. Barnes and R. Glaser, *Can. J. Chem.*, 1998, **76**, 1371–1378.

19 R. Glaser and G. S. Chen, *J. Comput. Chem.*, 1998, **19**, 1130–1140.

20 N. P. Neureiter, *J. Am. Chem. Soc.*, 1959, **81**, 2910–2910.

21 J. Safari and S. Gandomi-Ravandi, *Synth. Commun.*, 2011, **41**, 645–651.

22 H. D. Hartzler, *J. Org. Chem.*, 1971, **36**, 3629–3630.

23 J. Barluenga, S. Fustero, N. Gomez and V. Gotor, *Synthesis (Stuttg).*, 1982, 966–967.

24 V. M. Kolb, A. C. Kuffe, H. O. Sniwek and T. E. Janota, *J. Org. Chem.*, 1989, **54**, 2771–2775.

25 C. J. Abelt and J. M. Pleier, *J. Am. Chem. Soc.*, 1989, **111**, 1795–1799.

26 R. Karmakar, C. R. Choudhury, S. R. Batten and S. Mitra, *J. Mol. Struct.*, 2007, **826**, 75–81.

27 Q. Wei, L. Shi, H. Cao, L. Wang, H. Yang and Y. Wang, *Liq. Cryst.*, 2008, **35**, 581–585.

28 S. N. Shah and N. K. Chudgar, *Molecules*, 2000, **5**, 657–664.

29 M. Kodaka, S. N. Shah, T. Tomohiro and N. K. Chudgar, *J. Phys. Chem. B*, 1998, **102**, 1219–1223.

30 R. Centore, B. Panunzi, A. Roviello, A. Sirigu and P. Villano, *Mol. Cryst. Liq. Cryst.*, 1996, **275**, 107–120.

31 S. C. Bennur, J. D. Gault, T. Kroin, G. R. Ouriques and T. R. Taylor, *Mol. Cryst. Liq. Cryst.*, 1988, **154**, 267–275.

32 H. S. Nalwa and J. Mukai, *J. Phys. Chem.*, 1995, **99**, 10766–10774.

33 V. A. Sauro and M. S. Workentin, *J. Org. Chem.*, 2001, **66**, 831–838.

34 T. W. Bell and A. T. Papoulie, *Angew. Chemie - Int. Ed.*, 1992, **31**, 749–751.

35 H. Zachová, S. Man, J. Taraba and M. Potáček, *Tetrahedron*, 2009, **65**, 792–797.

36 R. Cohen, B. Rybtchinski, M. Gandelman, L. J. W. Shimon, J. M. L. Martin and D. Milstein, *Angew. Chemie - Int. Ed.*, 2003, **42**, 1949–1952.

37 D. Dragancea, V. B. Arion, S. Shova, E. Rentschler and N. V. Gerbeleu, *Angew. Chemie - Int. Ed.*, 2005, **44**, 7938–7942.

38 I. Picón-Ferrer, F. Hueso-Ureña, N. A. Illán-Cabeza, S. B. Jiménez-Pulido, J. M. Martínez-Martos, M. J. Ramírez-Expósito and M. N. Moreno-Carretero, *J. Inorg. Biochem.*, 2009, **103**, 94–100.

39 J. Risse, R. Scopelliti and K. Severin, *Organometallics*, 2011, **30**, 3412–3418.

40 J. Jayabharathi, V. Thanikachalam, A. Thangamani and M. Padmavathy, *Med. Chem. Res.*, 2007, **16**, 266–279.

41 A. Garg and J. P. Tandon, *Transit. Met. Chem.*, 1988, **13**, 395–397.

42 J. Easmon, G. Pürstinger, G. Heinisch, T. Roth, H. H. Fiebig, W. Holzer, W. Jäger, M. Jenny and J. Hofmann, *J. Med. Chem.*, 2001, **44**, 2164–2171.

43 K. C. Murdock, R. G. Child, Y. I. Lin, J. D. Warren, P. F. Fabio, V. J. Lee, P. T. Izzo, S. A. Lang, R. B. Angier, R. V. Citarella, R. E. Wallace and F. E. Durr, *J. Med. Chem.*, 1982, **25**, 505–518.

44 B. T. Gillis and M. P. LaMontagne, *J. Org. Chem.*, 1967, **32**, 3318–3320.

45 F. M. T. Almeida, M. F. N. N. Carvalho, A. M. Galvao, J. Cermak, V. Blechta, A. J. L. Pombeiro and B. L. Shaw, *Inorganica Chim. Acta*, 2002, **338**, 201–209.

46 S. Satsumabayashi, S. Motoki and H. Nakano, *J. Org. Chem.*, 1976, **41**, 156–157.

47 J. Gorse and R. W. Binkley, *J. Org. Chem.*, 1972, **37**, 575–578.

48 A. Hashidzume, J. Shiota, Y. Ueno, T. Noda, Y. Takashima, A. Harada and M. Kamachi, *Polym. Commun.*, 2006, **47**, 501–505.

49 F. Muller, G. van Koten, L. H. Polm, K. Vrieze, M. C. Zoutberg, D. Heijdenrijk, E. Kragten and C. H. Stam, *Organometallics*, 1989, **8**, 1340–1349.

50 A. Albini and H. Kisch, *J. Organomet. Chem.*, 1975, 94, 75–85.

51 L. S. Hegedus and A. Kramer, *Organometallics*, 1984, **3**, 1263–1267.

52 F. A. Cotton, S. A. Duraj and W. J. Roth, *J. Am. Chem. Soc.*, 1984, **106**, 4749–4751.

53 A. Zimniak and J. Zachara, *J. Org. Chem.*, 1997, **533**, 45–50.

54 C. H. Stapfer and R. W. D'Andrea, *Inorg. Chem.*, 1971, **10**, 1224–1227.

55 D. Dönnecke, K. Halbauer and W. Imhof, *J. Organomet. Chem.*, 2004, **689**, 2707–2719.

56 C. Y. Wu, C. S. Lee, S. Pal and W. S. Hwang, *Polyhedron*, 2008, **27**, 2681–2687.

57 W. von E. Doering and A. K. Hoffmann, *J. Am. Chem. Soc.*, 1954, **76**, 6162–6165.

58 P. S. Skell and R. C. Woodworth, *J. Am. Chem. Soc.*, 1956, **78**, 4496–4497.

59 G. Herzberg and J. Shoosmith, *Nature*, 1959, **183**, 1801–1802.

60 G. W. Robinson and M. McCarty, *J. Am. Chem. Soc.*, 1960, **82**, 1859–1864.

61 G. W. Cowell and A. Ledwith, *Q. Rev. Chem. Soc.*, 1970, **24**, 119–167.

62 A. P. Cox, L. F. Thomas and J. Sheridan, *Nature*, 1958, **181**, 1000–1001.

63 A. J. Owen, *Tetrahedron*, 1969, **25**, 3693–3699.

64 C. B. Moore and G. C. Pimentel, *J. Chem. Phys.*, 1964, 3504–3509.

65 R. A. M. O' Ferrall, in *Advances in Physical Organic Chemistry Vol. 5*, Academic Press Inc. London Ldt., 1967.

66 D. Bethell, D. Whittaker and J. . D. Callister, *J. Chem. Soc.*, 1965, 2466–2476.

67 D. Bethell, A. R. Newall, G. Stevens and D. Whittaker, *J. Chem. Soc.*, 1969, 749–754.

68 C. D. Gutsche, in *Organic Reactions*, John Wiley and Sons, Inc., 1954.

69 R. Huisgen, *Angew. Chemie - Int. Ed.*, 1963, 565–632.

70 A. Ledwith and D. Parry, *J. Chem. Soc.*, 1966, 1408–1410.

71 M. Dartiguenave, M. Joëlle Menu, E. Deydier, Y. Dartiguenave and H. Siebald, *Coord. Chem. Rev.*, 1998, **178**–**180**, 623–663.

72 W. A. Herrmann, G. Kriechbaum, M. L. Ziegler and P. Wüknitz, *Chem. Ber.*, 1981, **114**, 276–284.

73 K. D. Schramm and J. A. Ibers, *J. Am. Chem. Soc.*, 1978, **100**, 2932–2933.

74 K. D. Schramm and J. A. Ibers, *Inorg. Chem.*, 1980, **19**, 2435–2440.

75 K. D. Schramm and J. A. Ibers, *Inorg. Chem.*, 1980, **19**, 1231–1236.

76 L. Brandt, J. Wolf and H. Werner, *J. Org. Chem.*, 1993, **444**, 235–244.

77 Y. Mizobe, Y. Ishii and M. Hidai, *Coord. Chem. Rev.*, 1995, **139**, 281–311.

78 L. Messerle and M. D. Curtis, *J. Am. Chem. Soc.*, 1980, **102**, 7789–7791.

79 V. M. Iluc and G. L. Hillhouse, *J. Am. Chem. Soc.*, 2014, **136**, 6479–6488.

80 J. Zhang, M. Gandelman, L. J. W. Shimon and D. Milstein, *Organometallics*, 2008, **27**, 3526–3533.

81 J. Egloff, M. Ranocchiari, A. Schira, C. Schotes and A. Mezzetti, *Organometallics*, 2013, **32**, 4690–4701.

82 M. Nomura, A. Kusui and M. Kajitani, *Organometallics*, 2005, **24**, 2811–2818.

83 D. J. Mindiola and G. L. Hillhouse, *J. Am. Chem. Soc.*, 2002, **124**, 9976–9977.

84 G. Albertin, S. Antoniutti, A. Botter and J. Castro, *Inorg. Chem.*, 2015, **54**, 2091–2093.

85 G. Albertin, S. Antoniutti, M. Bortoluzzi, A. Botter, J. Castro and F. Sibilla, *RSC Adv.*, 2016, **6**, 97650–97658.

86 S. K. Russell, E. Lobkovsky and P. J. Chirik, *J. Am. Chem. Soc.*, 2009, **131**, 36–37.

87 S. C. Bart, A. C. Bowman, E. Lobkovsky and P. J. Chirik, *J. Am. Chem. Soc.*, 2007, **129**, 7212–7213.

88 G. Albertin, S. Antoniutti, D. Baldan, J. Castro and G. Comparin, *Organometallics*, 2013, **32**, 3157–3160.

89 G. Albertin, S. Antoniutti, M. Bortoluzzi, A. Botter and J. Castro, *J. Organomet. Chem.*, 2016, **822**, 259–268.

90 G. Albertin, S. Antoniutti, A. Botter, J. Castro and M. Giacomello, *Organometallics*, 2014, **33**, 3570–3582.

91 T. Urbanskl, Ed., *Chemistry and technology of explosives (Vol. 3)*, Pergamon Press, 1967.

92 K. A. Frederick and J. G. Babish, *Regul. Toxicol. Pharmacol.*, 1982, **2**, 308–322.

93 A. Kleinhofs, W. M. Owais and R. A. Nilan, *Mutat. Res.*, 1978, **55**, 165–95.

94 R. J. Griffin, *Prog. Med. Chem.*, 1994, **31**, 121–232.

95 K. Banert, *Organic Azides Syntheses and Applications*, John Wiley & Sons Ltd., 2010.

96 M. E. C. Biffin, J. Miller and D. B. Paul, *Introduction of the azido group*, John Wiley & Sons Ltd., 1971.

97 H. D. Fair and R. F. Walker, Eds., *Energetic Materials*, Plenum Press, 1977.

98 G. L'abbé, *Chem. Rev.*, 1969, **69**, 345–363.

99 A. Hassner, in *Introduction of Azide Functions*, 1971.

100 S. Patai and Z. Rapport, Eds., *The chemistry of Halides, pseudo-halides and azines*, John Wiley & Sons Ltd., 1983.

101 E. F. V. Scriven, *Azides and Nitrenes*, 1984.

102 E. F. V. Scriven and K. Turnbull, *Chem. Rev.*, 1988, **88**, 297–368.

103 S. Bräse, C. Gil, K. Knepper and V. Zimmermann, *Angew. Chemie - Int. Ed.*, 2005, **44**, 5188–5240.

104 M. Köhn and R. Breinbauer, *Angew. Chemie - Int. Ed.*, 2004, **43**, 3106–3116.

105 P. A. S. Smith, *Org. React.*, 1946, 337–449.

106 J. H. Boyer and F. C. Canter, *Chem. Rev.*, 1954, **54**, 1–57.

107 N. N. Greenwood and A. Earnshaw, in *Chemistry of the Elements*, Reed Educational and Professional Publishing Ltd., 1997.

108 K. Banert, Y. H. Joo, T. Rüffer, B. Walfort and H. Lang, *Tetrahedron Lett.*, 2010, **51**, 2880–2882.

109 W. Binder and C. Kluger, *Curr. Org. Chem.*, 2006, **10**, 1791–1815.

110 F. Palacios, D. Aparicio, G. Rubiales, C. Alonso and J. de los Santos, *Curr. Org. Chem.*, 2006, **10**, 2371–2392.

111 S. G. Alvarez and M. T. Alvarez, *Synthesis (Stuttg).*, 1997, 413–414.

112 H. Bock and R. Dammel, *Angew. Chemie - Int. Ed.*, 1987, **26**, 504–526.

113 R. O. Lindsay and C. F. H. Allen, *Org. Synth.*, 1955, **3**, 710.

114 G. Smolinsky and G. A. Pryde, in *Chemistry of the Azido Group*, ed. S. Patai, John Wiley & Sons Ltd., 1971.

115 J. D. Roberts and M. C. Caserio, Eds., *Basic Principles Of Organic Chmistry*, W. A. Benjamin Inc., Second Edi., 1977.

116 J. March, Ed., *Advanced Organic Chemistry*, John Wiley & Sons Ltd., forth Edit., 1992.

117 G. Wilkinson, *Comprehensive Coordination Chemistry*, Pergamon Press, 1987.

118 M. G. Fickes, W. M. Davis and C. C. Cummins, *J. Am. Chem. Soc.*, 1995, **117**, 6384–6385.

119 G. Guillemot, E. Solari and C. Floriani, *Organometallics*, 2001, **20**, 607–615.

120 G. Proulx and R. G. Bergman, *J. Am. Chem. Soc.*, 1995, **117**, 6382–6383.

121 G. Proulx and R. G. Bergman, *Organometallics*, 1996, **15**, 684–692.

122 M. Barz, E. Herdtweck and W. R. Thiel, *Angew. Chemie - Int. Ed.*, 1998, **37**, 2262–2265.

123 M. Mitani, M. Takayama and K. Koyama, *J. Org. Chem.*, 1981, **46**, 2226–2227.

124 Y. Naruta, N. Nagai, Y. Arita and K. Maruyama, *J. Org. Chem.*, 1987, **52**, 3956–3967.

125 T. Sheradsky, in *Chemistry of Functional Groups: Chemistry of the Azido Group*, ed. S. Patai, John Wiley & Sons Ltd., 1971, pp. 331–395.

126 L. I. Smith, *Chem. Rev.*, 1938, **23**, 193–285.

127 C. I. Schilling and S. Bräse, *Org. Biomol. Chem.*, 2007, **5**, 3586–3588.

128 M. Meldal and C. W. Tornoee, *Chem. Rev.*, 2008, **108**, 2952–3015.

129 C. T. Zhang, X. Zhang and F. L. Qing, *Tetrahedron Lett.*, 2008, **49**, 3927–3930.

130 B. C. Boren, S. Narayan, L. K. Rasmussen, L. Zhang, H. Zhao, Z. Lin, G. Jia and V. V. Fokin, *J. Am. Chem. Soc.*, 2008, **130**, 8923–8930.

131 L. Zhang, X. Chen, P. Xue, H. H. Y. Sun, I. D. Williams, K. B. Sharpless, V. V. Fokin and G. Jia, *J. Am. Chem. Soc.*, 2005, **127**, 15998–15999.

132 M. M. Majireck and S. M. Weinreb, *J. Org. Chem.*, 2006, **71**, 8680–8683.

133 R. Rabinowitz and J. Pellon, *J. Org. Chem.*, 1961, **26**, 4623–4626.

134 H. Loghmani-Khouzani, M. M. M. Sadeghi, J. Safari, M. S. Abdorrezaie and M. Jafarpisheh, *J. Chem. Res.*, 2001, 80–81.

135 J. Safari, S. Gandomi-Ravandi and M. Monemi, *Monatshefte fur Chemie*, 2013, **144**, 1375–1380.

136 A. C. Day and M. C. Whiting, *Org. Synth.*, 1970, **50**, 3–4.

137 A. I. Vogel, *Textbook of Practical Organic Chemistry*, 4th Ed., 1987.

138 J. B. Miller, *J. Org. Chem.*, 1959, **24**, 560–561.

139 R. Baltzly, N. B. Mehta, E. M. Grivsky, P. B. Russell, R. E. Brooks and A. M. Steinberg, *J. Org. Chem.*, 1961, **26**, 3669–3676.

140 H. Aneetha, M. Jiménez-Tenorio, M. C. Puerta, P. Valerga and K. Mereiter, *Organometallics*, 2002, **21**, 628–635.

141 K. Suzuki, A. Kobayashi, S. Kaneko, K. Takehira, T. Yoshihara, H. Ishida, Y. Shiina, S. Oishi and S. Tobita, *Phys. Chem. Chem. Phys.*, 2009, **11**, 9850.

142 P. McArdle, K. Gilligan, D. Cunningham, R. Dark and M. Mahon, *Cryst. Eng. Comm.*, 2004, **6**, 303–309.

143 G. M. Sheldrick, *Acta Crystallogr. Sect. A Found. Crystallogr.*, 2015, **71**, 3–8.

144 G. M. Sheldrick, *Acta Crystallogr. Sect. C Struct. Chem.*, 2015, **71**, 3–8.

145 G. Albertin, S. Antoniutti, J. Castro and S. Paganelli, *J. Organomet. Chem.*, 2010, **695**, 2142–2152.

146 M. A. Bennett, T. N. Huang, T. W. Matheson and A. K. Smith, *Inorg. Synth.*, 1982, **XXI**, 74–78.

147 G. Albertin, S. Antoniutti, A. Bacchi, G. Pelizzi and G. Zanardo, *Organometallics*, 2008, **27**, 4407–4418.

148 G. Albertin, S. Antoniutti and J. Castro, *Eur. J. Inorg. Chem.*, 2009, 5352–5357.

149 J. A. Cabeza and P. M. Maitlis, *J. Chem. Soc. Dalt. Trans.*, 1985, 573–578.

150 G. Albertin, S. Antoniutti, M. Bortoluzzi and J. Castro, *Inorganica Chim. Acta*, 2018, **470**, 139–148.

151 C. White, A. Yates, P. M. Maitlis and D. M. Heinekey, *Inorg. Synth.*, 1992, **29**, 228–234.

152 R. G. Ball, W. A. G. Graham, J. K. Hoyano, A. D. McMaster, B. M. Mattson, D. M. Heinekey, B. M. Mattson and S. T. Michel, *Inorg. Chem.*, 1990, **29**, 2023–2025.

153 C. L. Gross and G. S. Girolami, *Organometallics*, 1996, **15**, 5359–5367.

154 C. L. Gross, J. L. Brumaghim, J. M. Jefferis, P. W. Dickinson and G. S. Girolami, *Angew. Chemie - Int. Ed.*, 2004, **33**, 241.

155 P. W. Wanandi and T. D. Tilley, *Organometallics*, 1997, **16**, 4299–4313.

156 S. Patai, Ed., *The chemistry of diazonium and diazo groups*, Wiley & Sons, Chichester, UK, 1978.

157 G. Albertin, S. Antoniutti, J. Castro and F. Sibilla, *ChemistrySelect*, 2016, **1**, 6188–6195.

158 S. K. Singh, M. Chandra, D. S. Pandey, M. C. Puerta and P. Valerga, *J. Organomet. Chem.*, 2004, **689**, 3612–3620.

159 K. S. Singh, Y. A. Mozharivskyj, C. Thöne and M. R. Kollipara, *J. Organomet. Chem.*, 2005, **690**, 3720–3729.

160 P. Cai, M. Li, C. Duan, F. Lu, D. Guo and Q. Meng, *New J. Chem.*, 2005, **29**, 1011–1016.

161 S. D. Dwivedi, A. K. Singh, S. K. Singh, S. Sharma, M. Chandra and D. S. Pandey, *Eur. J. Inorg. Chem.*, 2008, 5666–5673.

162 L. K. Filak, G. Mühlgassner, F. Bacher, A. Roller, M. Galanski, M. A. Jakupec, B. K. Keppler and V. B. Arion, *Organometallics*, 2011, **30**, 273–283.

163 W. J. Geary, *Coord. Chem. Rev.*, 1971, **7**, 81–122.

164 L. J. Farrugia, *J. Appl. Crystallogr.*, 1997, **30**, 565.

165 G. Albertin, S. Antoniutti, J. Castro and S. García-Fontán, *Eur. J. Inorg. Chem.*, 2011, **4**, 510–520.

166 G. Albertin, S. Antoniutti and J. Castro, *J. Organomet. Chem.*, 2010, **695**, 574–579.

167 R. M. Ceder, J. Sales, X. Solans and M. Font-altaba, *J. Chem. Soc., Dalt. Trans.*, 1986, 1351–1358.

168 Y. Chen, H. Sun, U. Flörke and X. Li, *Organometallics*, 2008, **27**, 270–275.

169 J. Li, X. Li and H. Sun, *J. Organomet. Chem.*, 2013, **743**, 114–122.

170 R. Lalrempuia, H. P. Yennawar and M. R. Kollipara, *J. Coord. Chem.*, 2009, **62**, 3661–3678.

171 M. Burke-Laing and M. Laing, *Acta Crystallogr. Sect. B Struct. Crystallogr. Cryst. Chem.*, 1976, **32**, 3216–3224.

172 V. Mom and G. de With, *Acta Cryst.*, 1978, **B34**, 2785–2789.

173 V. R. Vangala, A. Nangia and V. M. Lynch, *Chem. Commun.*, 2002, 1304–1305.

174 C. F. Chang, C. H. Cheng, C. C. Wang and S. L. Wang, *Acta Crystallogr. Sect. C Cryst. Struct. Commun.*, 1989, **45**, 1705–1707.

175 C. Woitha, U. Behrens, V. Vergopoulos and D. Rehder, *J. Organomet. Chem.*, 1990, **393**, 97–109.

176 Q. H. Wang, W. Weng, J. M. Liu, L. Z. Cai and G. C. Guo, *J. Coord. Chem.*, 2006, **59**, 485–492.

177 M. J. Nolte and E. Singleton, *J. C. S. Dalt.*, 1974, 2406–2410.

178 M. Abrahamsson, L. Hammarström, D. A. Tocher, S. Nag and D. Datta, *Inorg. Chem.*, 2006, **45**, 9580–9586.

179 V. W. Day, T. A. Eberspacher, W. G. Klemperer, R. P. Planalp, P. W. Schiller, A. Yagasaki and B. Zhong, *Inorg. Chem.*, 1993, **32**, 1629–1637.

180 S. O. Owalude, E. O. Odebunmi, U. B. Eke, R. Meijboom, V. N. Nesterov, E. Singleton and N. J. Coville, *Bull. Chem. Soc. Ethiop.*, 2013, **27**, 405–411.

181 M. J. Nolte and R. H. Reimann, *J. C. S. Dalt.*, 1978, 932–937.

182 L. I. Smith and K. L. Howard, *Organic Syntheses Vol. 3*, Wiley, New York, USA, 1955.

183 M. Trivedi, M. Chandra, D. S. Pandey, M. C. Puerta and P. Valerga, *J. Organomet. Chem.*, 2004, **689**, 879–882.

184 G. Albertin, A. Albinati, S. Antoniutti, M. Bortoluzzi and S. Rizzato, *J. Organomet. Chem.*, 2012, **702**, 45–51.

185 M. Baya, M. A. Esteruelas, A. I. González, A. M. López and E. Oñate, *Organometallics*, 2005, **24**, 1225–1232.

186 H. Werner, *Organometallics*, 1999, **18**, 1185–1195.

187 L. K. Filak, S. Göschl, S. Hackl, M. A. Jakupec and V. B. Arion, *Inorganica Chim. Acta*, 2012, **393**, 252–260.

188 W. F. Schmid, R. O. John, V. B. Arion, M. A. Jakupec and B. K. Keppler, *Organometallics*, 2007, **26**, 6643–6652.

189 C. R. Ojala, W. H. Ojala and D. Britton, *J. Chem. Crystallogr.*, 2011, **41**, 464–469.

190 W. N. A. Al-Mehana, R. M. Shakir, R. Yahya, S. N. Abd Halim and E. R. T. Tiekink, *Acta Crystallogr. Sect. E Struct. Reports Online*, 2011, **67**, 1659.

191 W. N. A. Al-Mehana, R. Yahya, F. Sonsudin, I. N. A. Al-Mehana and K. M. Lo, *Acta Crystallogr. Sect. E Struct. Reports Online*, 2012, **68**, 2990–2990.

192 B. Schmitt, T. I. A. Gerber, E. C. Hosten and R. Betz, *Zeitschrift fur Krist. - New Cryst. Struct.*, 2014, **229**, 470–472.

193 M. Talavera, S. Bolaño, J. Bravo, J. Castro and S. García-Fontán, *J. Organomet. Chem.*, 2012, **715**, 113–118.

194 M. Talavera, S. Bolaño, J. Bravo, J. Castro and S. García-Fontán, *Organometallics*, 2013, **32**, 7241–7244.

195 M. Talavera, S. Bolaño, J. Bravo, J. Castro, S. García-Fontán and J. M. Hermida-Ramón, *Organometallics*, 2013, **32**, 4402–4408.

196 X. Li, H. Sun, F. Yu, U. Flörke and H. F. Klein, *Organometallics*, 2006, **25**, 4695–4697.

197 Y. Park, J. Heo, M. H. Baik and S. Chang, *J. Am. Chem. Soc.*, 2016, **138**, 14020–14029.

198 D. L. Davies, O. Al-Duaij, J. Fawcett, M. Giardiello, S. T. Hilton and D. R. Russell, *Dalt. Trans.*,

2003, **2**, 4132–4138.

199 Y.-F. Han and G.-X. Jin, *Chem. Soc. Rev.*, 2014, **43**, 2799–2823.

200 A. J. Millett, A. Habtemariam, I. Romero-Canelón, G. J. Clarkson and P. J. Sadler, *Organometallics*, 2015, **34**, 2683–2694.

201 L. C. Sudding, P. Chellan, P. Govender and G. S. Smith, *J. Inorg. Organomet. Polym. Mater.*, 2015, **25**, 457–465.

202 H. Xu, R. Chen, Q. Sun, W. Lai, Q. Su, W. Huang and X. Liu, *Chem. Soc. Rev.*, 2014, **43**, 3259–3302.

203 K. Hasan, A. K. Bansal, I. D. W. Samuel, C. Roldán-Carmona, H. J. Bolink and E. Zysman-Colman, *Sci. Rep.*, 2015, 1–16.

204 Y. Lu, N. McGoldrick, F. Murphy, B. Twamley, X. Cui, C. Delaney, G. M. Ó. Máille, J. Wang, J. Zhao and S. M. Draper, *Chem. - A Eur. J.*, 2016, **22**, 11349–11356.

205 P. H. Lanoë, J. Chan, G. Gontard, F. Monti, N. Armaroli, A. Barbieri and H. Amouri, *Eur. J. Inorg. Chem.*, 2016, 1631–1634.

206 T. Giridhar, T. H. Han, W. Cho, C. Saravanan, T. W. Lee and S. H. Jin, *Chem. - A Eur. J.*, 2014, **20**, 8260–8264.

207 E. C. Constable, C. E. Housecroft, G. E. Schneider, J. A. Zampese, H. J. Bolink, A. Pertegás and C. Roldán-Carmona, *Dalt. Trans.*, 2014, **43**, 4653–4667.

208 T. Yu, Y. Niu, S. Yu, Z. Xu, Y. Zhao and H. Zhang, *J. Organomet. Chem.*, 2017, **830**, 85–92.

209 A. M. Bünzli, H. J. Bolink, E. C. Constable, C. E. Housecroft, J. M. Junquera-Hernández, M. Neuburger, E. Ortí, A. Pertegás, J. J. Serrano-Pérez, D. Tordera and J. A. Zampese, *Dalt. Trans.*, 2014, **43**, 738–750.

210 D. Maggioni, M. Galli, L. D'Alfonso, D. Inverso, M. V. Dozzi, L. Sironi, M. Iannacone, M. Collini, P. Ferruti, E. Ranucci and G. D'Alfonso, *Inorg. Chem.*, 2015, **54**, 544–553.

211 L. Flamigni, A. Barbieri, C. Sabatini, B. Ventura and F. Barigelletti, *Top. Curr. Chem.*, 2007, **281**, 143.

212 G. A. Carlson, P. I. Djurovich and R. J. Watts, *Inorg. Chem.*, 1993, **32**, 4483–4484.

213 F. Neve, A. Crispini, S. Campagna and S. Serroni, *Inorg. Chem.*, 1999, **38**, 2250–2258.

214 T. Bolaño, M. A. Esteruelas, M. P. Gay, E. Oñate, I. M. Pastor and M. Yus, *Organometallics*, 2015, **34**, 3902–3908.

215 P. Barthazy, M. Wörle, H. Rüegger and A. Mezzetti, *Inorg. Chem.*, 2000, **39**, 4903–4912.

216 T. Y. Bartucz, A. Galombek, A. J. Lough, P. A. Maltby, R. H. Morris, R. Ramachandran and M. Schlaf, *Inorg. Chem.*, 1998, **37**, 1555–1562.

217 S. M. Maddock, C. E. F. Richard, W. R. Roper and L. J. Wright, *Organomet. Chem.*, 1996, **510**, 267–279.

218 A. Mezzetti, E. Zangrando, A. Del Zotto and P. Rigo, *J. Chem. Soc., Chem. Commun.*, 1994, 1597.

219 A. E. Reed, L. a Curtiss and F. Weinhold, *Chem. Rev.*, 1988, **88**, 899–926.

220 L. A. Curtiss, K. Raghavachari, G. W. Trucks and J. A. Pople, *J. Chem. Phys.*, 1991, **94**, 7221–7230.

221 H. V. R. Dias, S. Polach, S. Goh, E. F. Archibong and D. S. Marynick, *Inorg. Chem.*, 2000, **39**, 3894–3901.

222 W. S. Brotherton, P. M. Guha, H. Phan, R. J. Clark, M. Shatruk and L. Zhu, *Dalt. Trans.*, 2011, **40**, 3655–3665.

223 G. Albertin, S. Antoniutti, D. Baldan, J. Castro and S. García-Fontän, *Inorg. Chem.*, 2008, **47**, 742–748.

224 M. G. Fickes, W. M. Davis and C. C. Cummins, *J. Am. Chem. Soc.*, 1995, **117**, 6384–6385.

225 G. Proulx and R. G. Bergman, *Organometallics*, 1996, **15**, 684–692.

226 G. Guillemot, E. Solari, C. Floriani and C. Rizzoli, *Organometallics*, 2001, **20**, 607–6015.

227 N. P. Mankad, P. Müller and J. C. Peters, *J. Am. Chem. Soc.*, 2010, **132**, 4083–4085.

228 W. H. Harman, M. F. Lichterman, N. A. Piro and C. J. Chang, *Inorg. Chem.*, 2012, **51**, 10037–10042.

229 M. Barz, E. Herdtweck and W. R. Thiel, *Angew. Chemie - Int. Ed.*, 1998, **37**, 2262–2265.

230 W. S. Brotherton, P. M. Guha, M. Phan, R. J. Clark, M. Shatruk and L. Zhu, *Dalt. Trans.*, 2011, **40**, 3655–3665.

231 G. Albertin, S. Antoniutti, L. Bonaldo, A. Botter and J. Castro, *Inorg. Chem.*, 2013, **52**, 2870–2879.

232 W. H. Harman, M. F. Lichterman, N. A. Piro and C. J. Chang, *Inorg. Chem.*, 2012, **51**, 10037–10042.

233 C. M. Che, H. W. Lam, W. F. Tong, T. F. Lai and T. C. Lau, *J. Chem. Soc., Chem. Commun.*, 1989, 1883–1884.

234 K. D. Demadis, T. J. Meyer and P. S. White, *Inorg. Chem.*, 1997, **36**, 5678–5679.

235 W. L. Man, G. Chen, S. M. Yiu, L. Shek, W. Y. Wong, W. T. Wong and T. C. Lau, *Dalt. Trans.*, 2010, **39**, 11163–11170.

236 E. P. Kyba and R. A. Abramovitch, in *Chemistry of Functional Groups: Chemistry of the Azido Group*, ed. S. Patai, John Wiley & Sons Ltd, 1971.

237 G. Albertin, S. Antoniutti, M. Bortoluzzi and J. Castro, *Inorganica Chim. Acta*, 2018, **470**, 139–148.

238 Y.-H. Lo, T.-H. Wang, C.-Y. Lee and Y.-H. Feng, *Organometallics*, 2012, **31**, 6887–6899.

239 X. Tu, H. Truong, E. Alster, A. Muñoz-Castro, R. Arratia-Pérez, G. S. Nichol and Z. Zheng, *Chem. - A Eur. J.*, 2011, 580–587.

240 T. B. Gunnoe, P. S. White and J. L. Templeton, *J. Am. Chem. Soc.*, 1996, **118**, 6916–6923.

PUBLICATIONS AND PRESENTATIONS

- G. Albertin, S. Antoniutti, J. Castro, V. Ganz, F. Sibilla, "*Preparation and reactivity of half-sandwich organic azide complexes of osmium", Dalton Transactions*, 2018, **47**, 11658-11668
- G. Albertin, S. Antoniutti, J. Castro, F. Sibilla, "*Preparation of Half-Sandwich Azine Complexes of Osmium", Polyhedron,* 2017, **138**, 133-139
- G. Albertin, S. Antoniutti, M. Bortoluzzi, J. Castro, F. Sibilla, E. Trave, "Preparation of metalated azine complexes of iridium(III)", *New Journal Of Chemistry*, 2017, **41**, 12976-12988
- G. Albertin, S. Antoniutti, J. Castro, F. Sibilla, "*Preparation of Azine Complexes of Ruthenium(II)*", *Chemistryselect*, 2016, **1**, 6188-6195
- G. Albertin, S. Antoniutti, M. Bortoluzzi, A. Botter, J. Castro, F. Sibilla, "*Preparation of Diazoalkane Complexes of Iron(II)*", *Rsc Advances*, 2016, **6**, 97650-97658
- G. Albertin, S. Antoniutti, J. Castro, and F. Sibilla "Osmium Diazoalkane Derivatives with Pentamethylcyclopentadienyl Ligand: Preparation and Reactivity" Manuscript in preparation
- G. Albertin, S. Antoniutti, J. Castro, and F. Sibilla "Reactions of Organic Azides with Half-Sandwich Complexes of Iridium: Preparation of Imine and Amine Derivatives" Manuscript in preparation

- F. Sibilla, S. Antoniutti, J. Castro, G. Albertin, "*Osmium Diazoalkane Derivatives with Pentamethylcyclopentadienyl Ligand: Synthesis and Reactivity*", presentazione poster al XLVI Congresso Nazionale di Chimica Inorganica organizzato dalla Società Chimica Italiana, 10-13 settembre 2018
- G. Abertin, S. Antoniutti, M. Bortoluzzi, J. Castro, F. Sibilla "*Half-Sandwich Dioxygen Complexes of Ruthenium: Preparation and Reactivity*", presentazione poster al XLVI Congresso Nazionale di Chimica Inorganica organizzato dalla Società Chimica Italiana, 10-13 settembre 2018
- F. Sibilla, S. Antoniutti, J. Castro, G. Albertin, "*Reactions of Azines with Half-sandwich Osmium Complexes: Preparation of Metalated Derivatives*" presentazione orale al XXVI International Conference on Coordination and Bioinorganic Chemistry, 4-9 giugno 2017
- F. Sibilla, S. Antoniutti, J. Castro, G. Albertin, "*Diazoalkane Complexes of Iron*", presentazione poster al XLIV Congresso Nazionale di Chimica Inorganica, 14-17 settembre 2016
- F. Sibilla, S. Antoniutti, J. Castro, G. Albertin, "*Reactions of Azines with Half-sandwich Iridium Complexes: C-H Activation to Metalated Derivatives*" presentazione poster al XLIV Congresso Nazionale di Chimica Inorganica, 14-17 settembre 2016 (Vincitore del premio miglior poster)

APPENDIX FIGURES

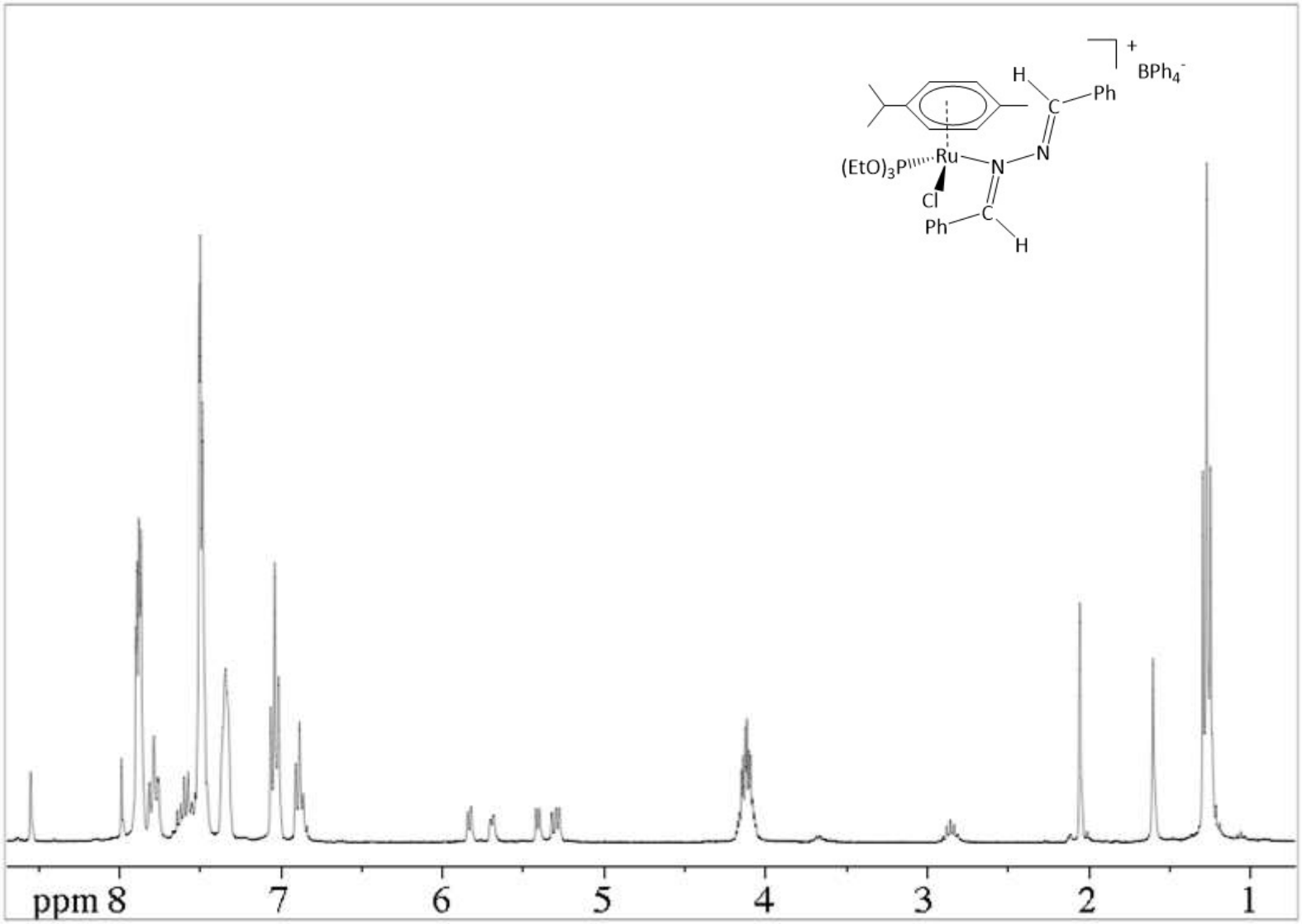

Appendix 11.1 ^{1}H NMR spectra in CD_2Cl_2 at room temperature of complex 2a.

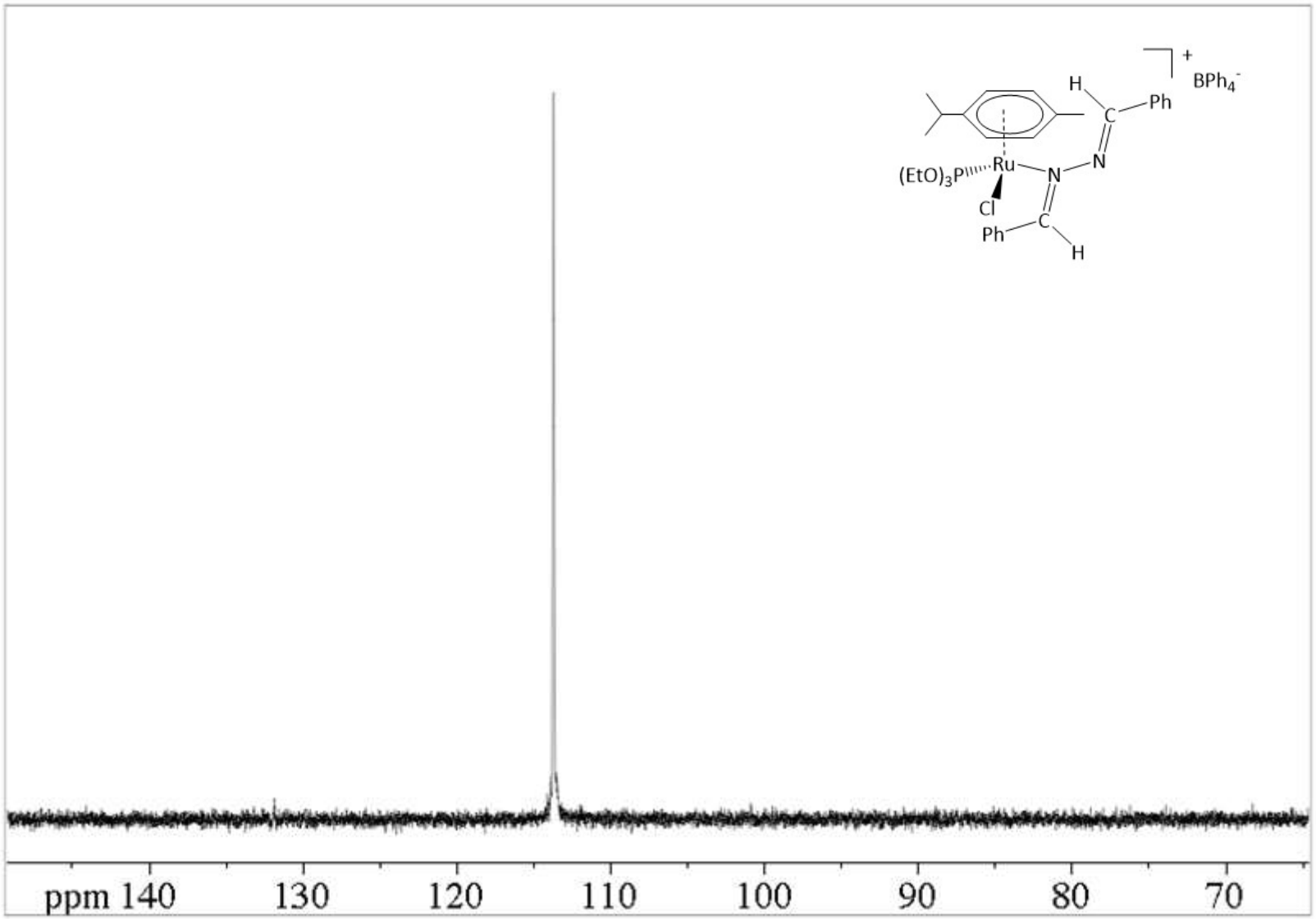

Appendix 11.2 $^{31}P\{^{1}H\}$ NMR spectra in CD_2Cl_2 at room temperature of complex 2a.

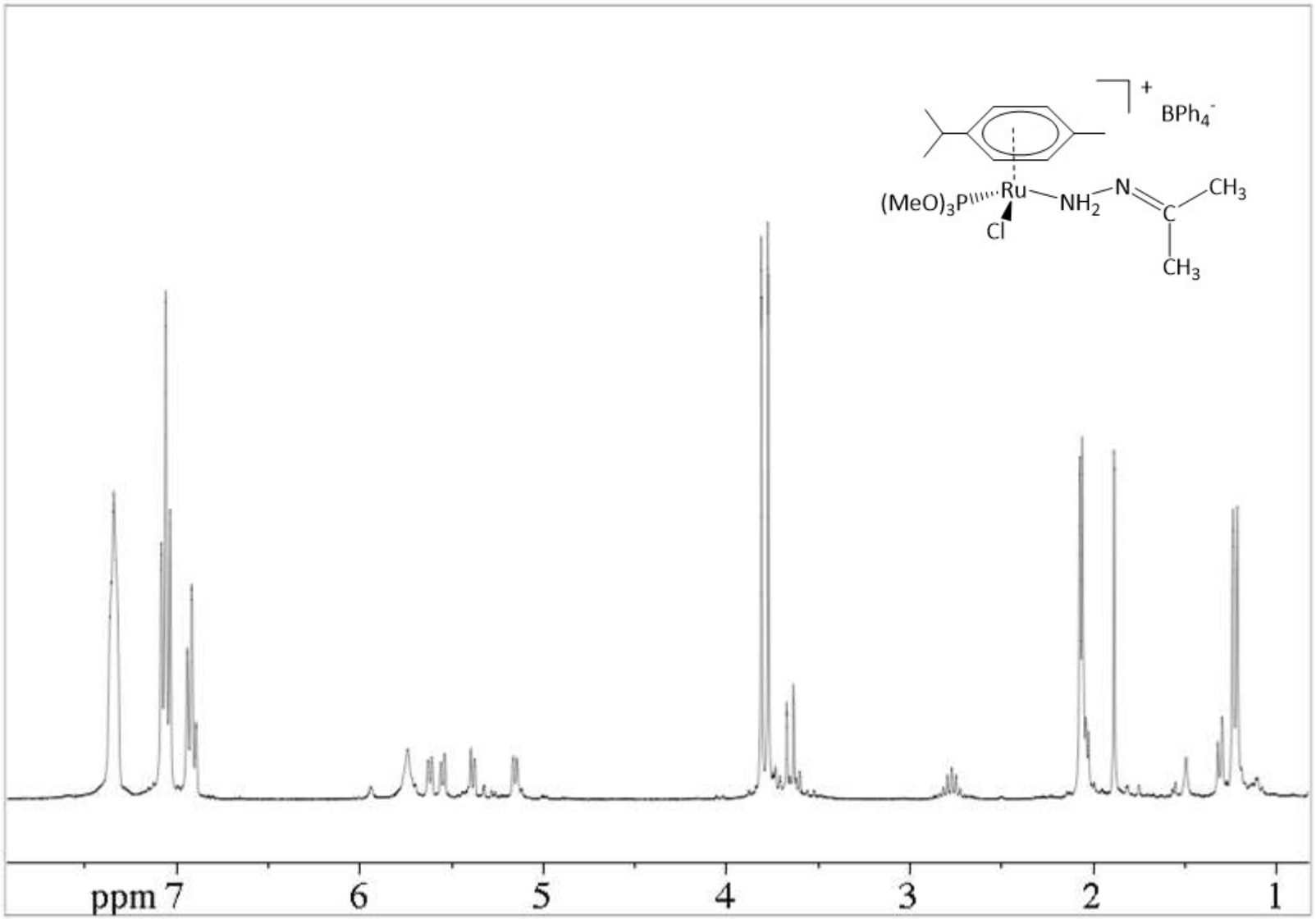

Appendix 11.3 ^{1}H NMR spectra in CD_2Cl_2 at room temperature of complex 5.

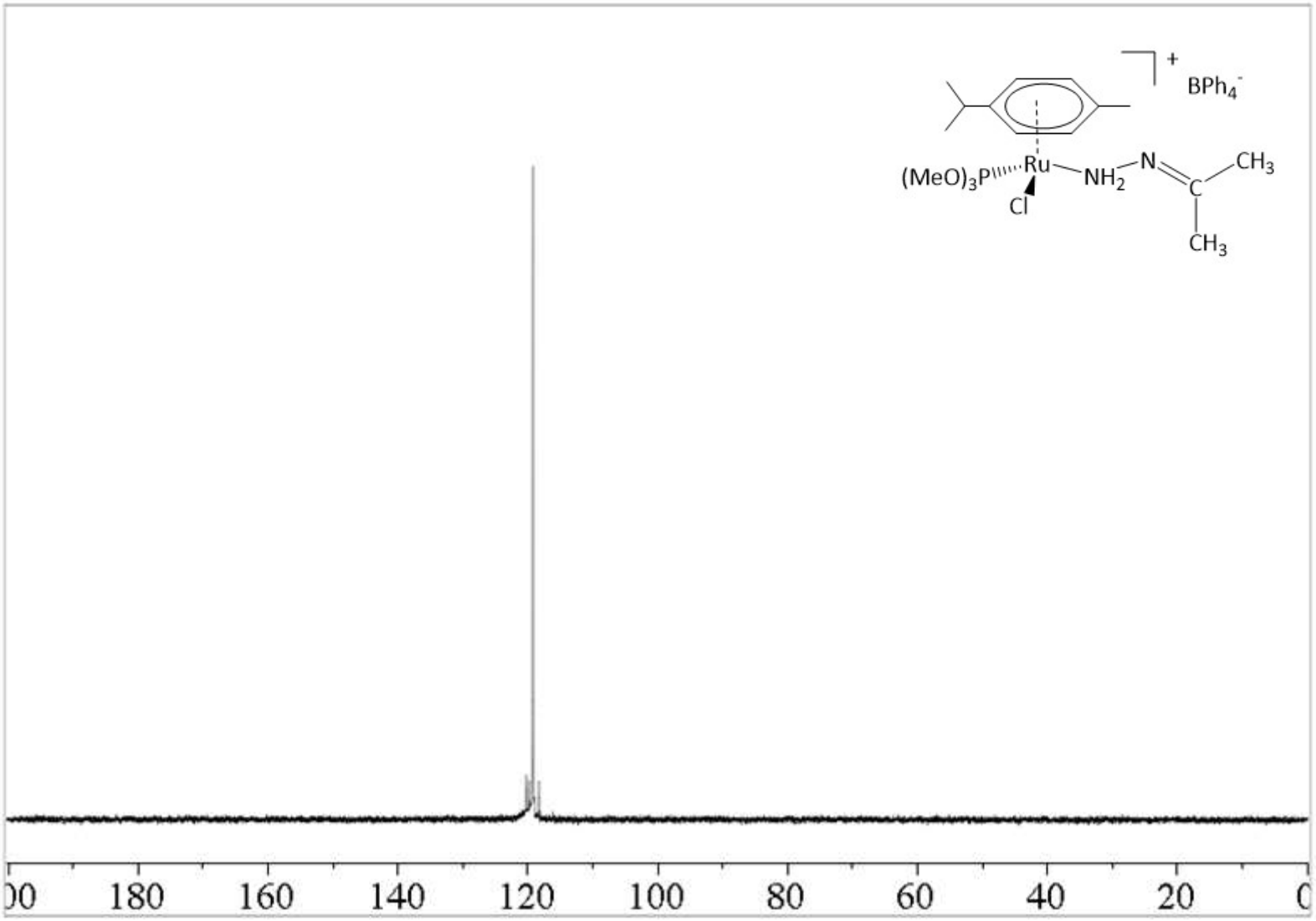

Appendix 11.4 $^{31}P\{^{1}H\}$ NMR spectra in CD_2Cl_2 at room temperature of complex 5.

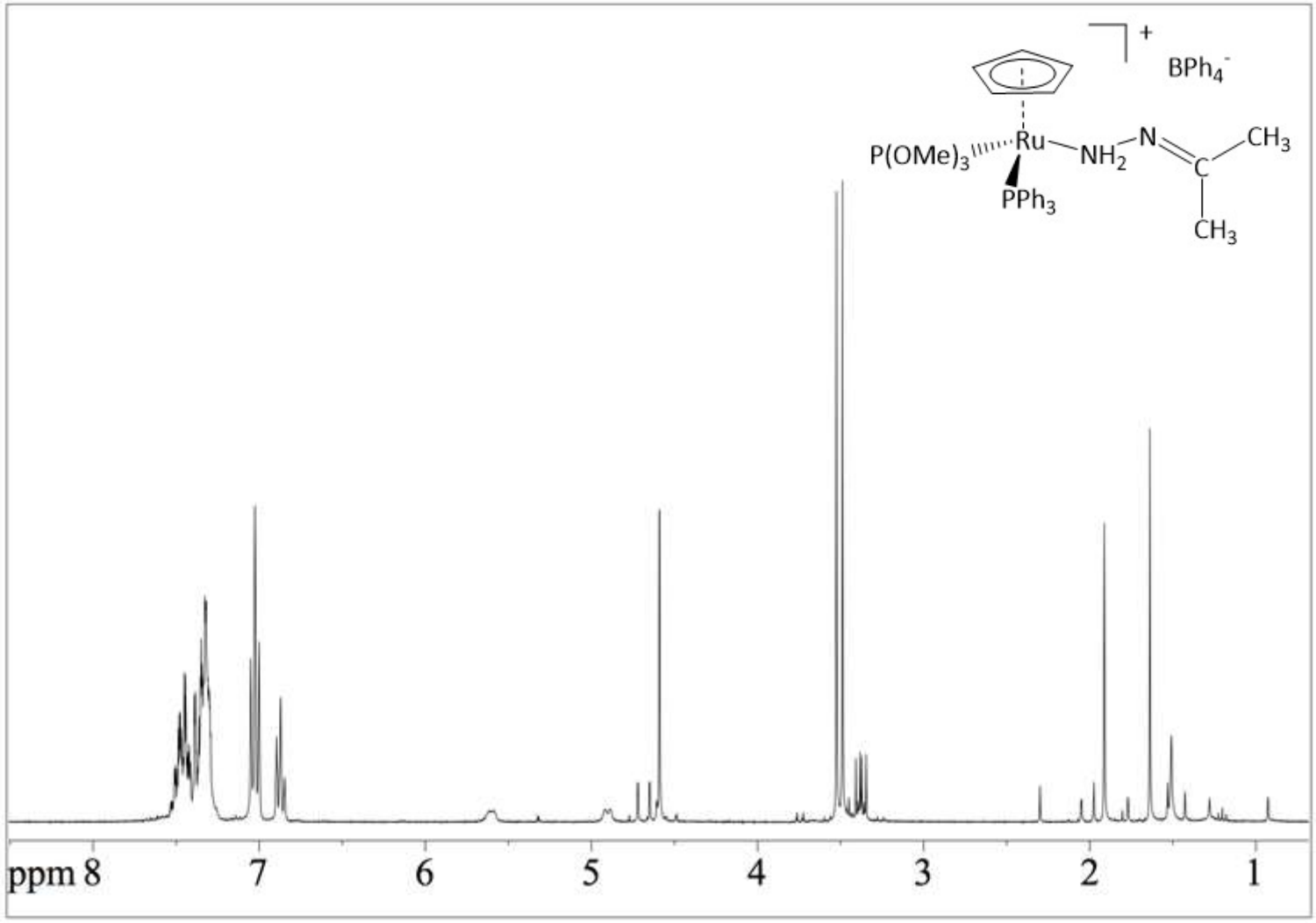

Appendix 11.5 ^{1}H NMR spectra in CD_2Cl_2 at room temperature of complex 11.

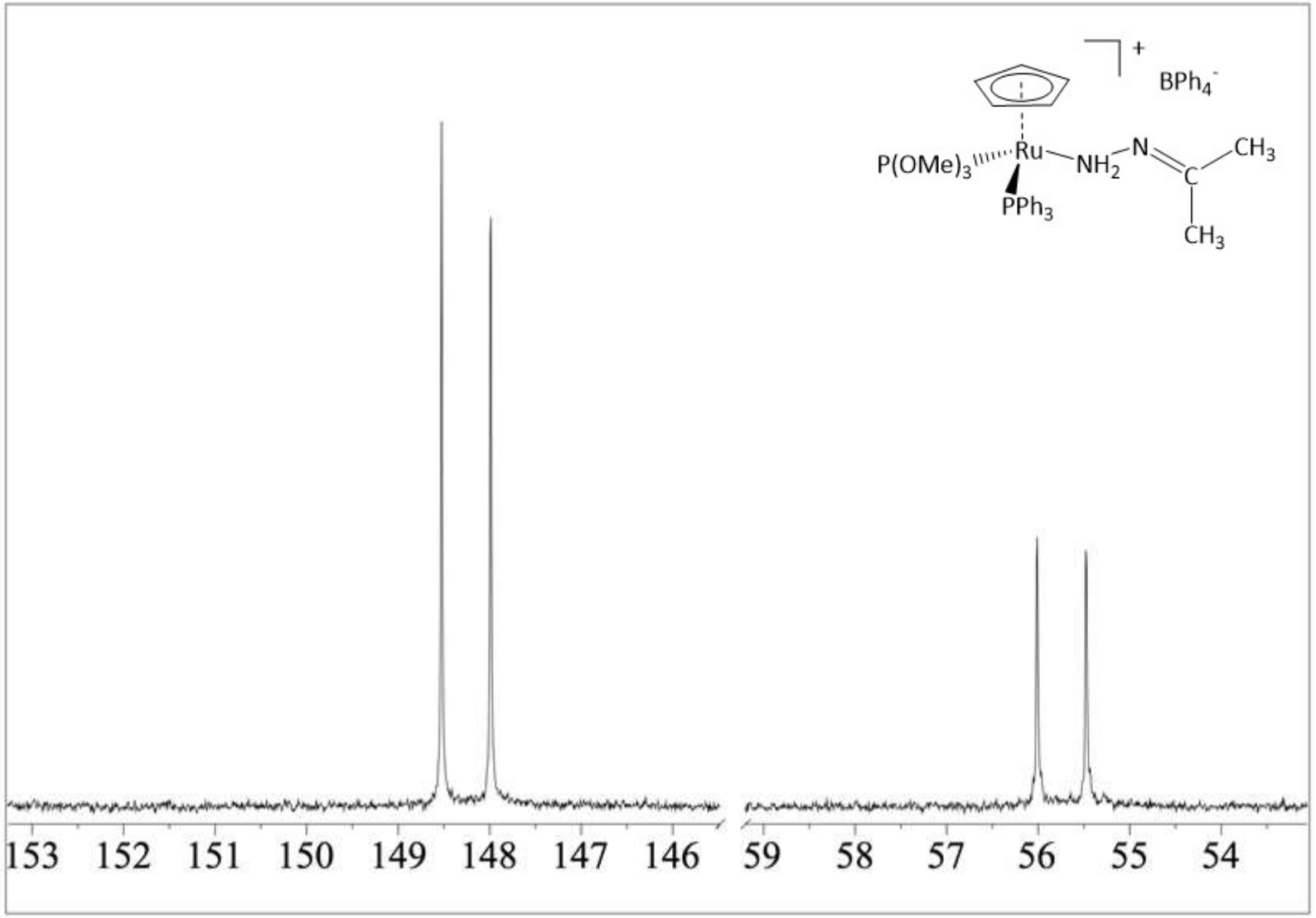

Appendix 11.6 $^{31}P\{^{1}H\}$ NMR spectra in CD_2Cl_2 at room temperature of complex 11.

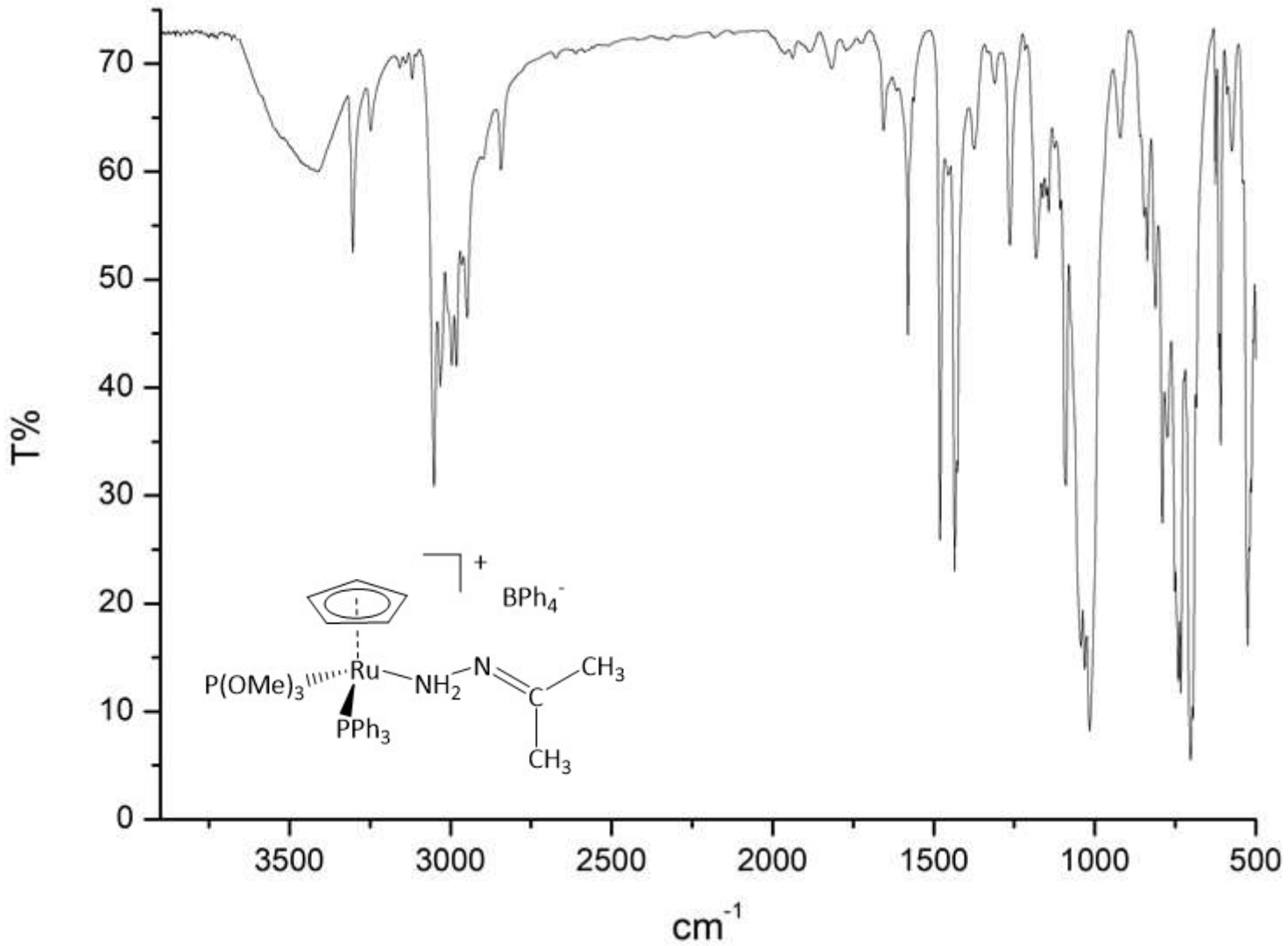

Appendix 11.7 IR spectra in KBr pallets at room temperature of complex 11.

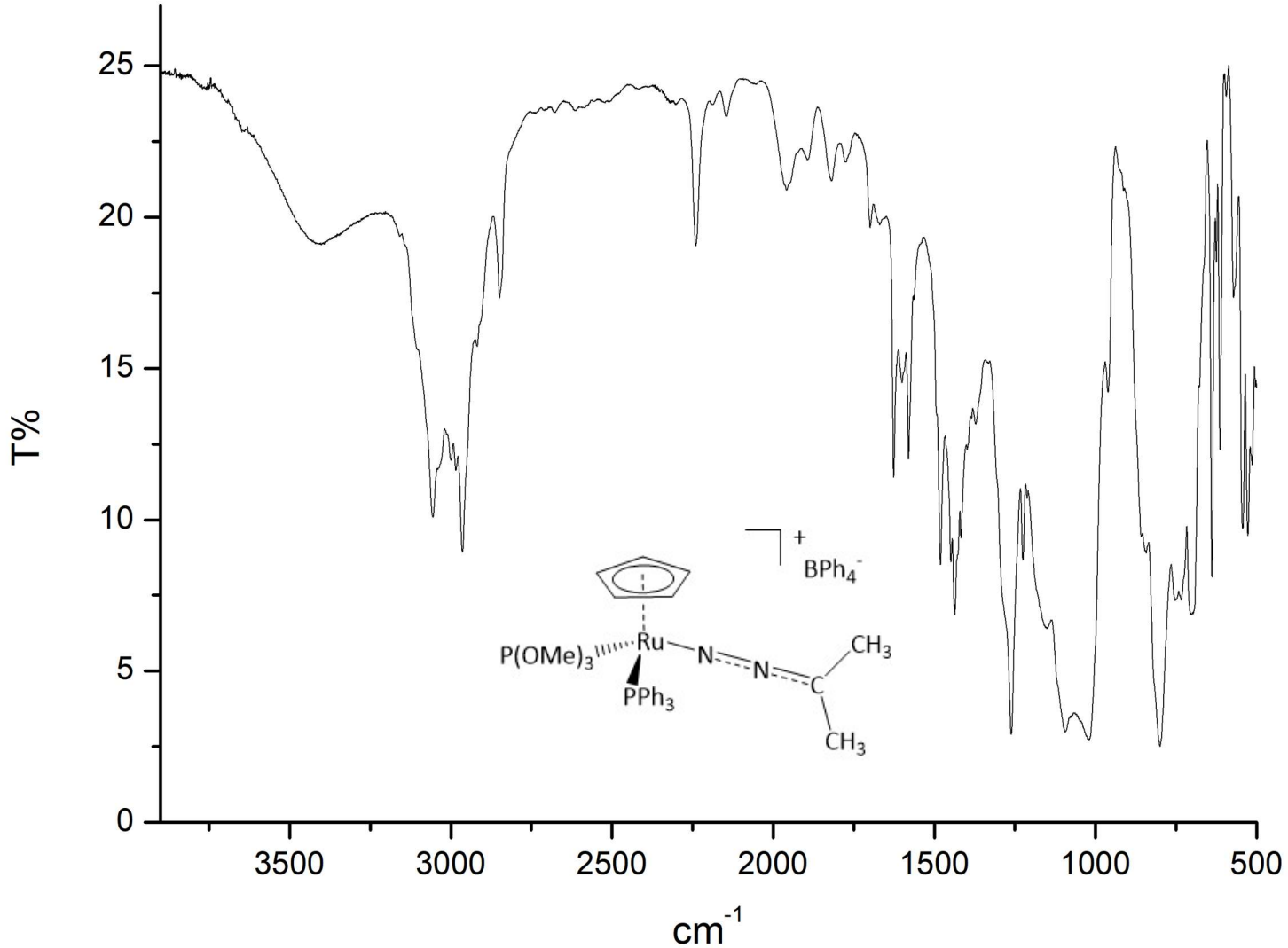

Appendix 11.8 IR spectra in KBr pallets at room temperature of complex 13

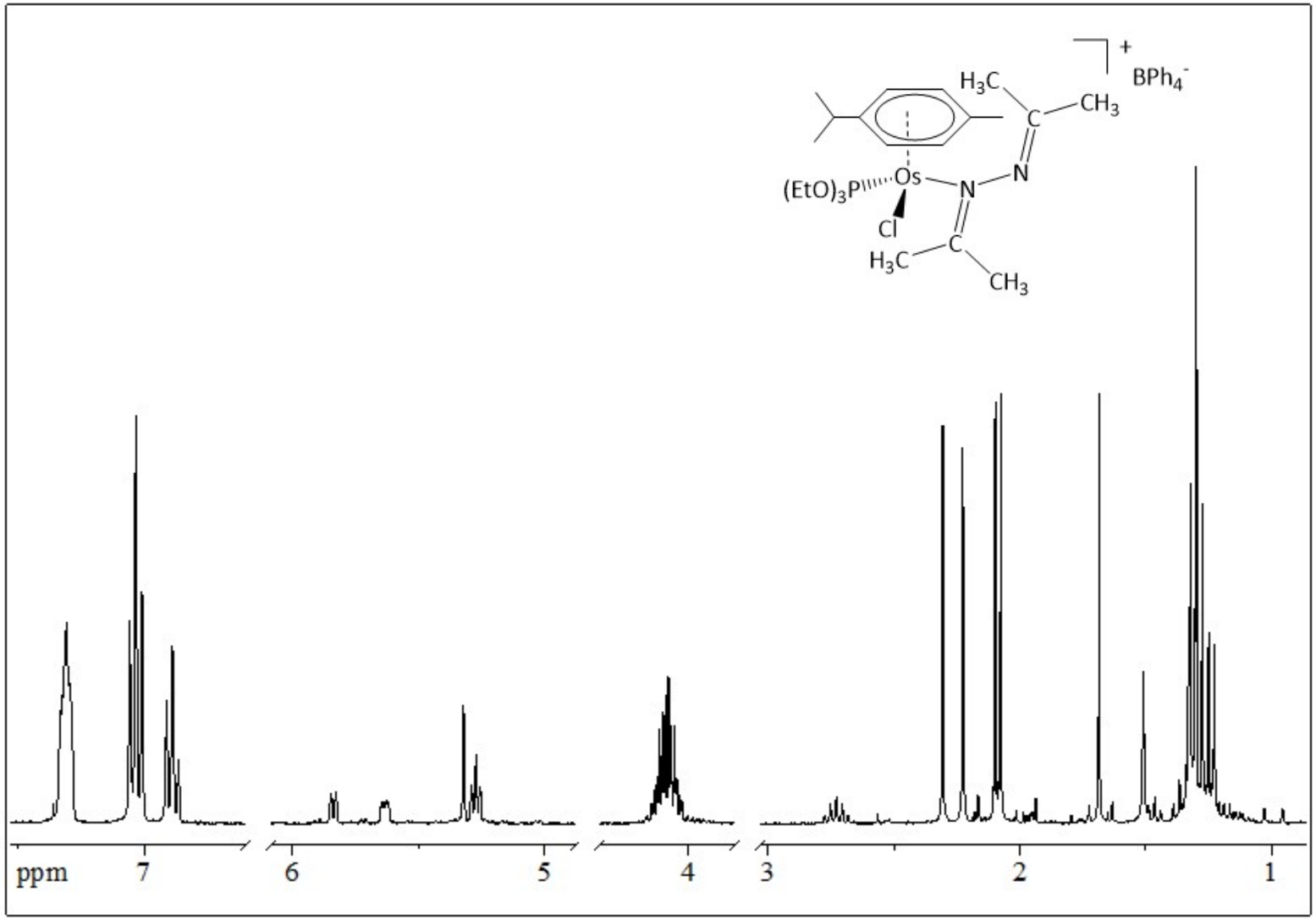

Appendix 11.9 ^{1}H NMR spectra in CD_2Cl_2 at room temperature of complex 17.

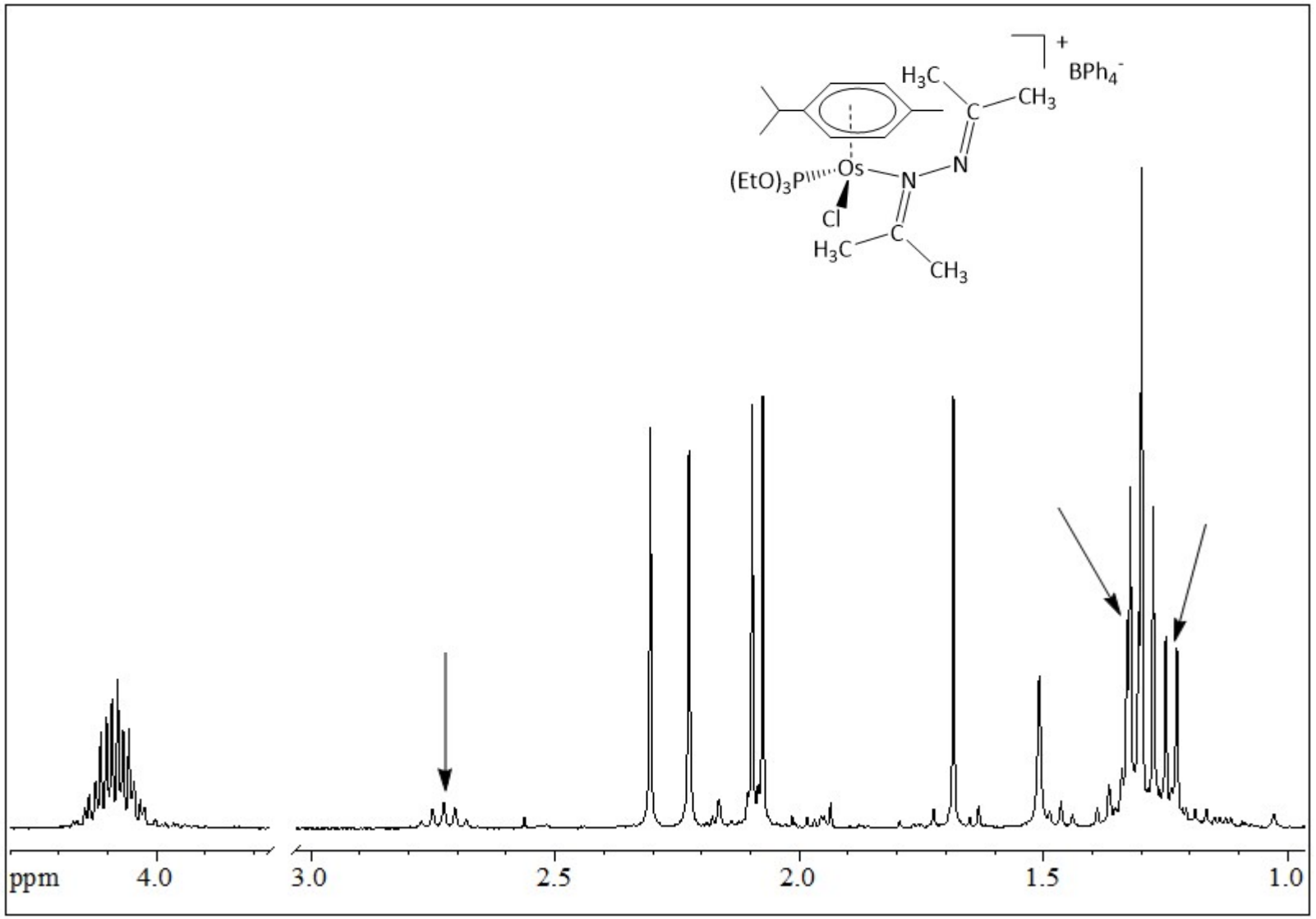

Appendix 11.10 Magnification of ^{1}H NMR spectra in CD_2Cl_2 at room temperature of complex 17.

.

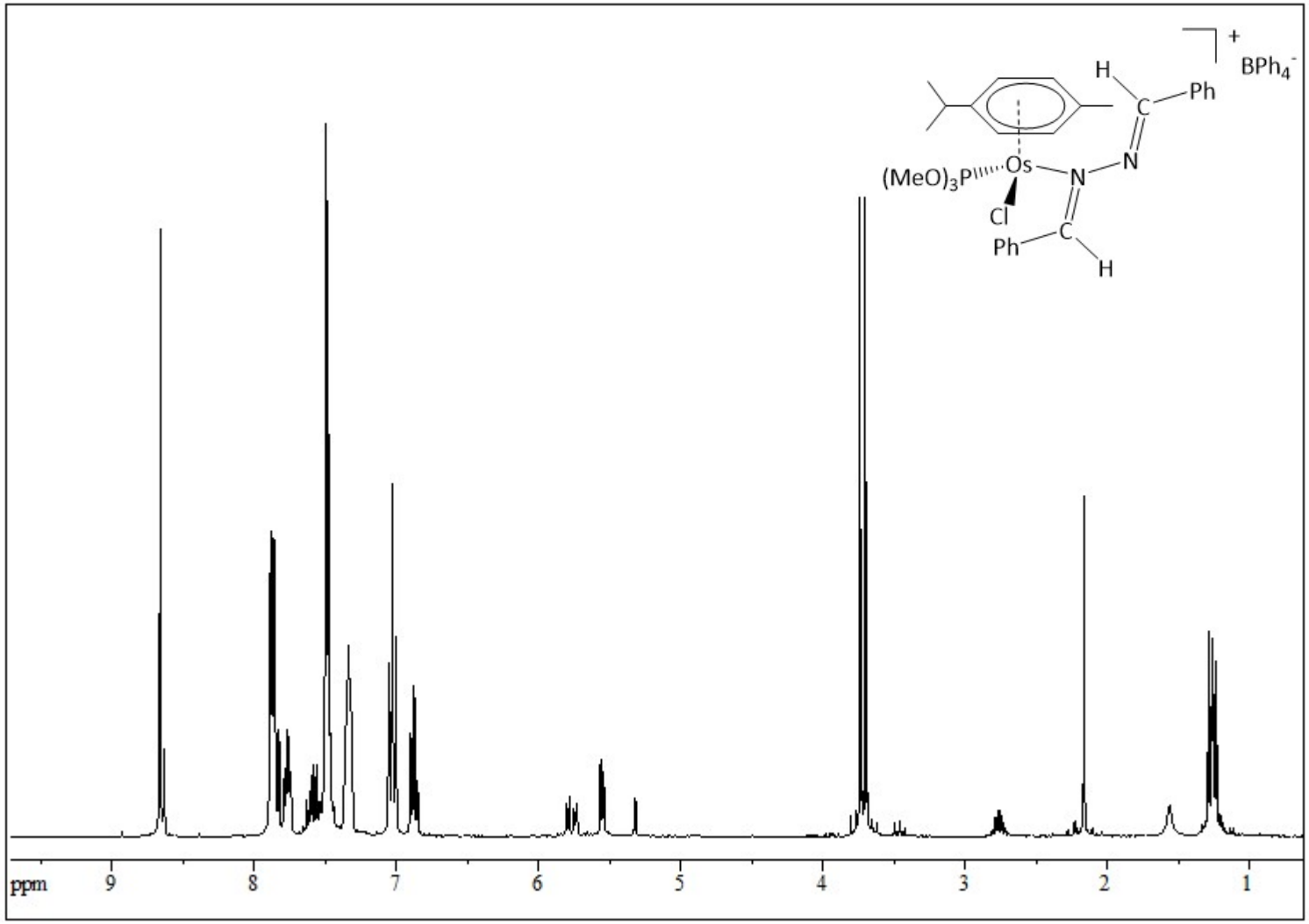

Appendix 11.11 ^{31}H NMR spectra in CD_2Cl_2 at room temperature of complex 14a.

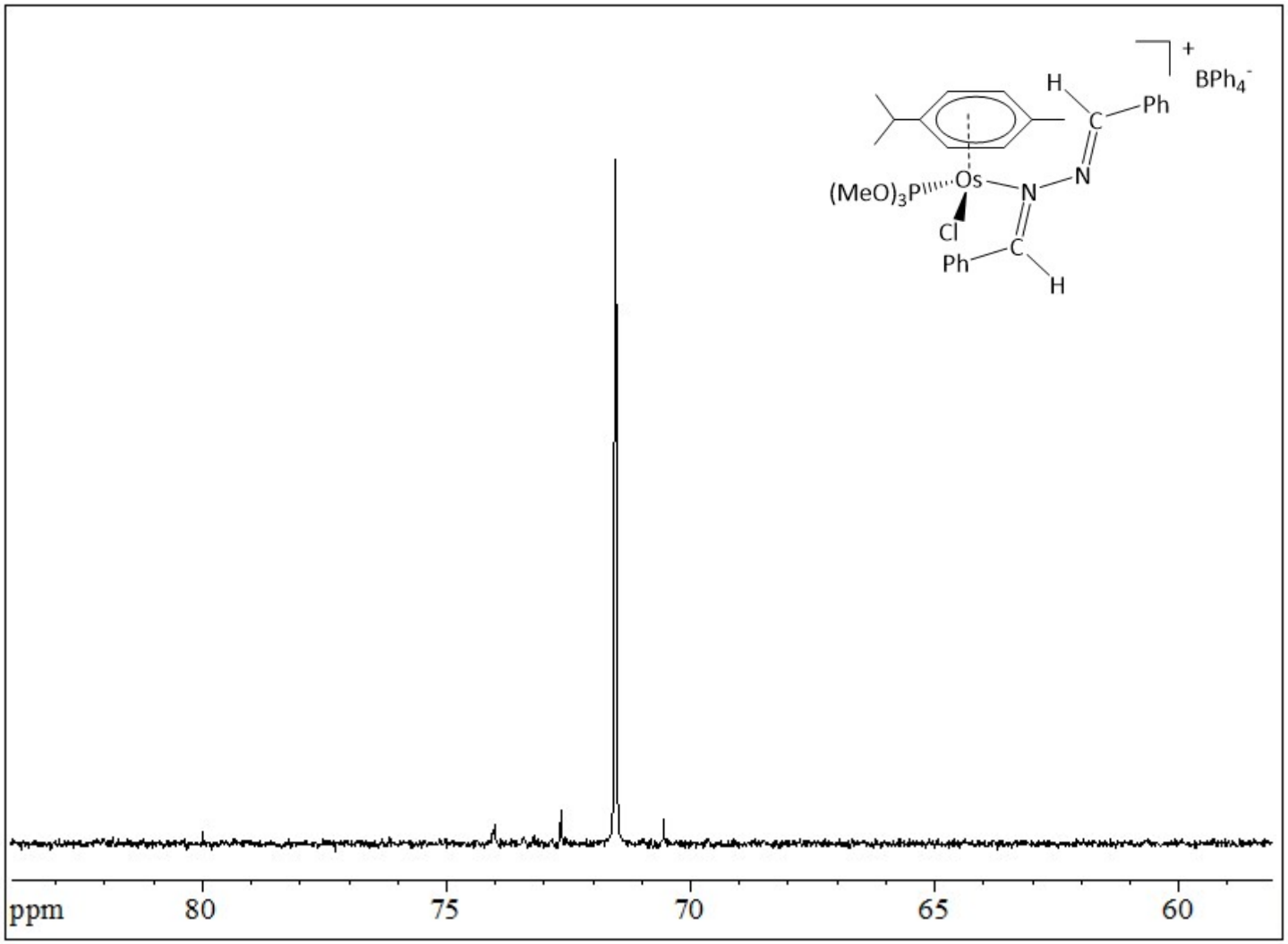

Appendix 11.12 $^{31}P\{^{1}H\}$ NMR spectra in CD_2Cl_2 at room temperature of complex 14a.

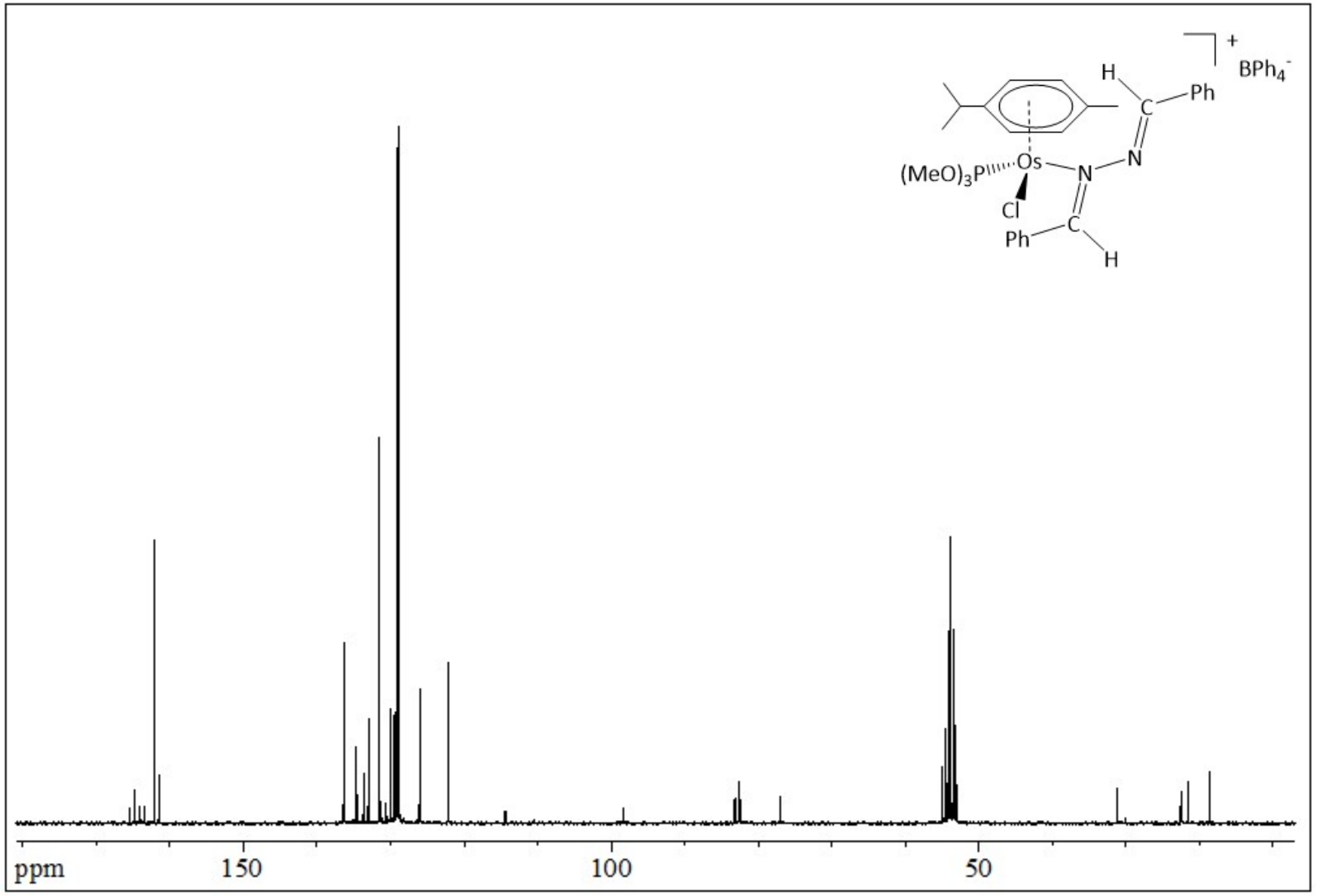

Appendix 11.13 $^{13}C\{^{1}H\}$ NMR spectra in CD_2Cl_2 at room temperature of complex 14a.

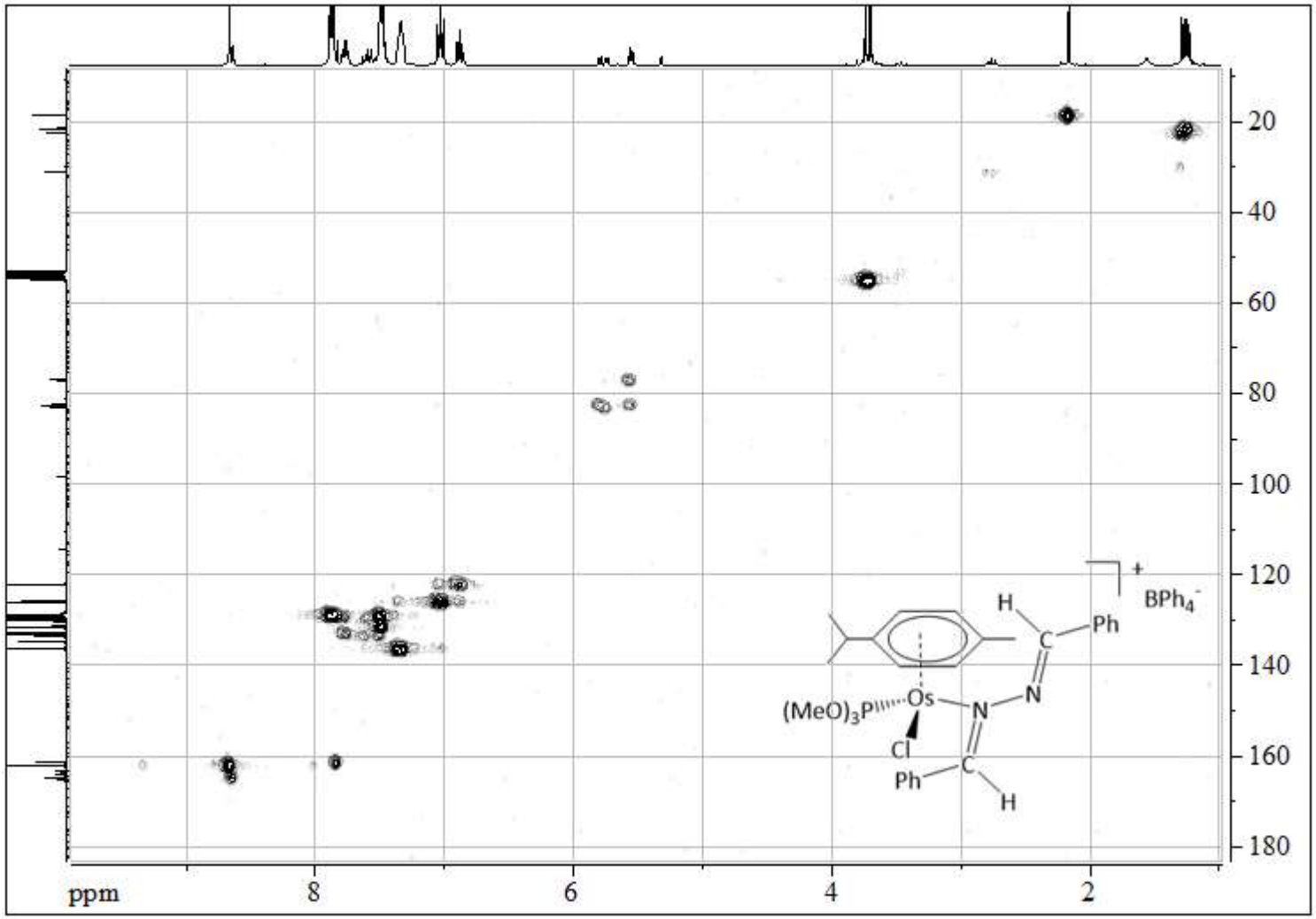

Appendix 11.14 $^{1}H/^{13}C$ HMQC spectra in CD_2Cl_2 at room temperature of complex 14a.

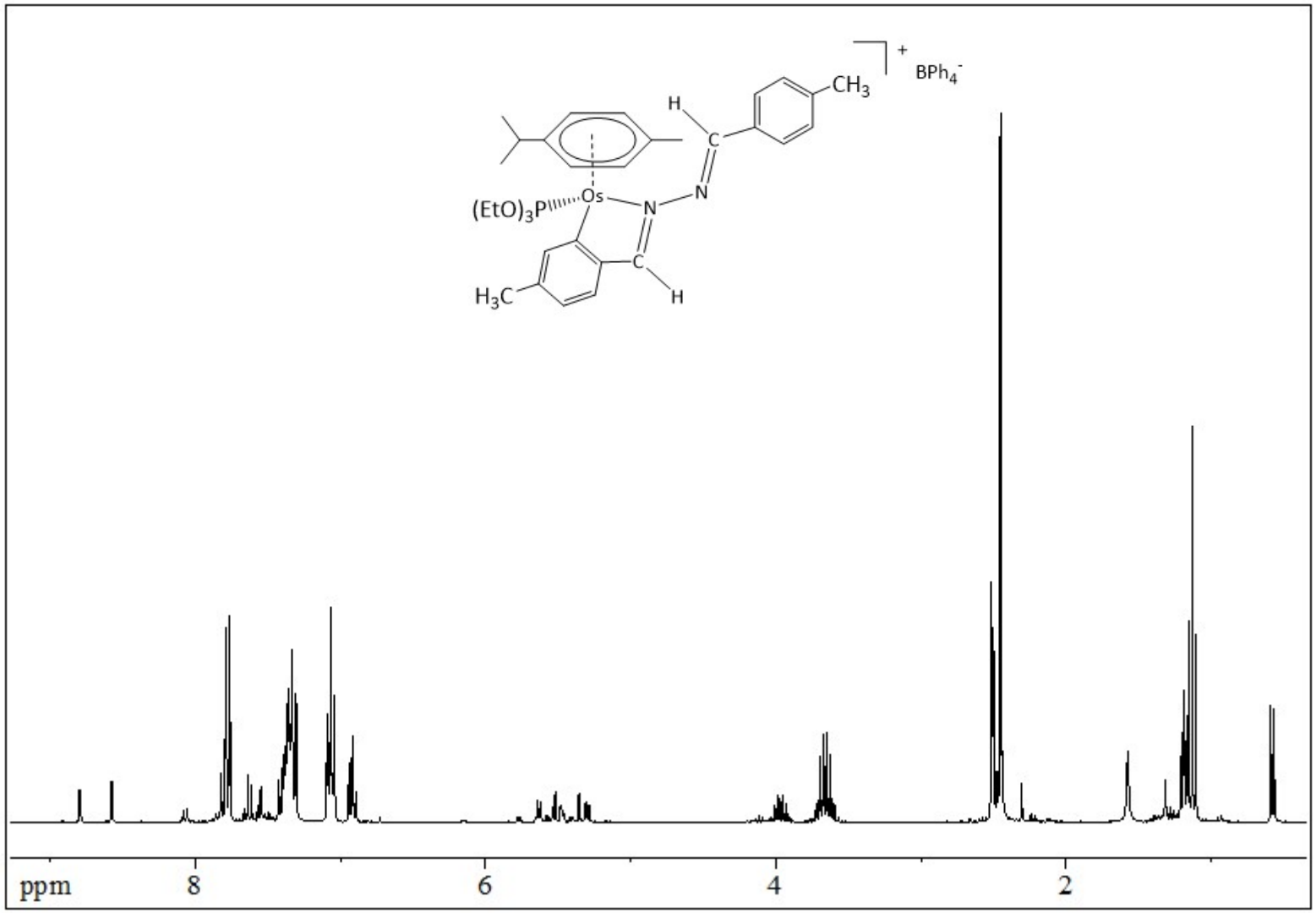

Appendix 11.15 ^{1}H NMR spectra in CD_2Cl_2 at room temperature of complex 21b

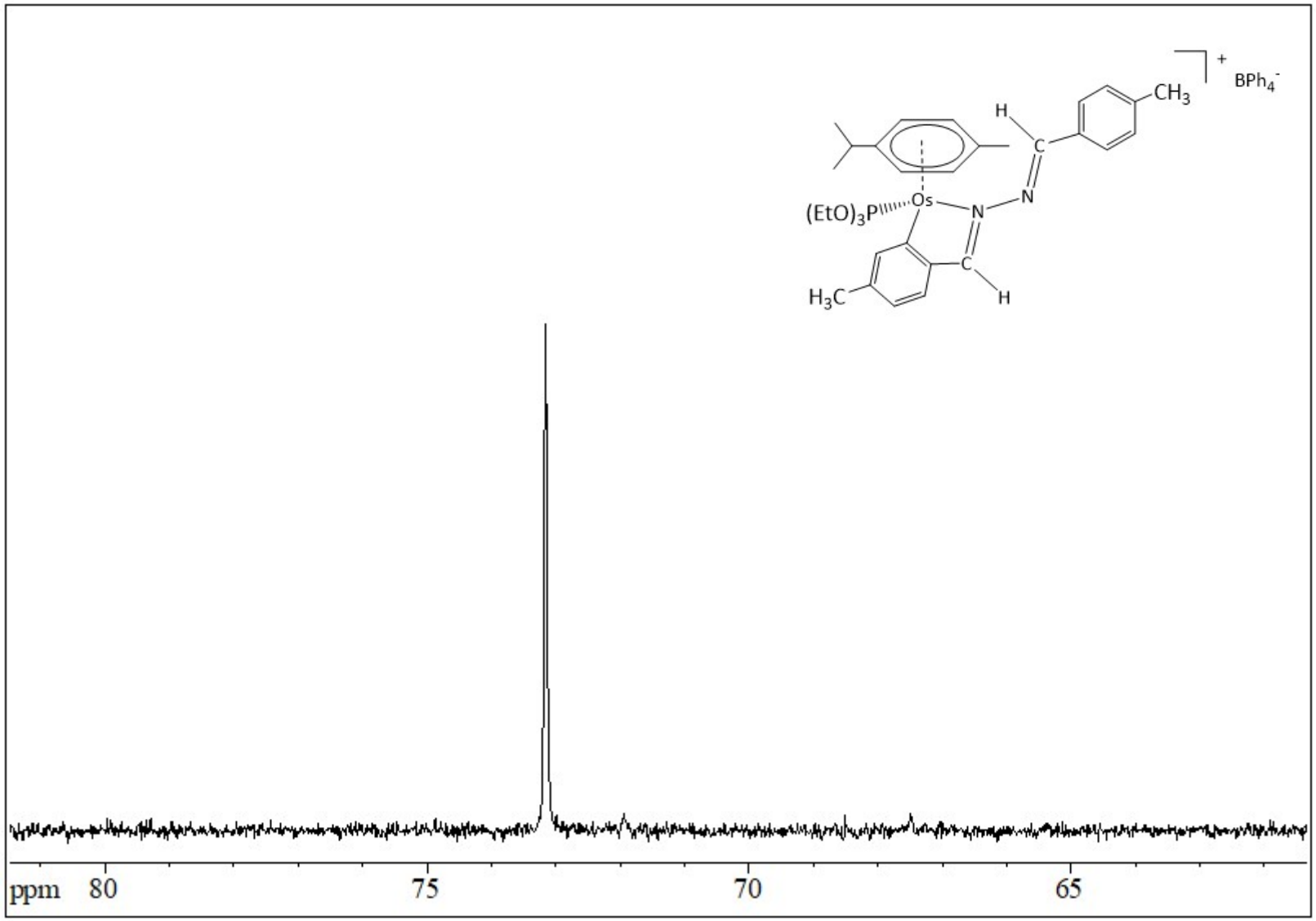

Appendix 11.16 $^{31}P\{^{1}H\}$ NMR spectra in CD_2Cl_2 at room temperature of complex 21b

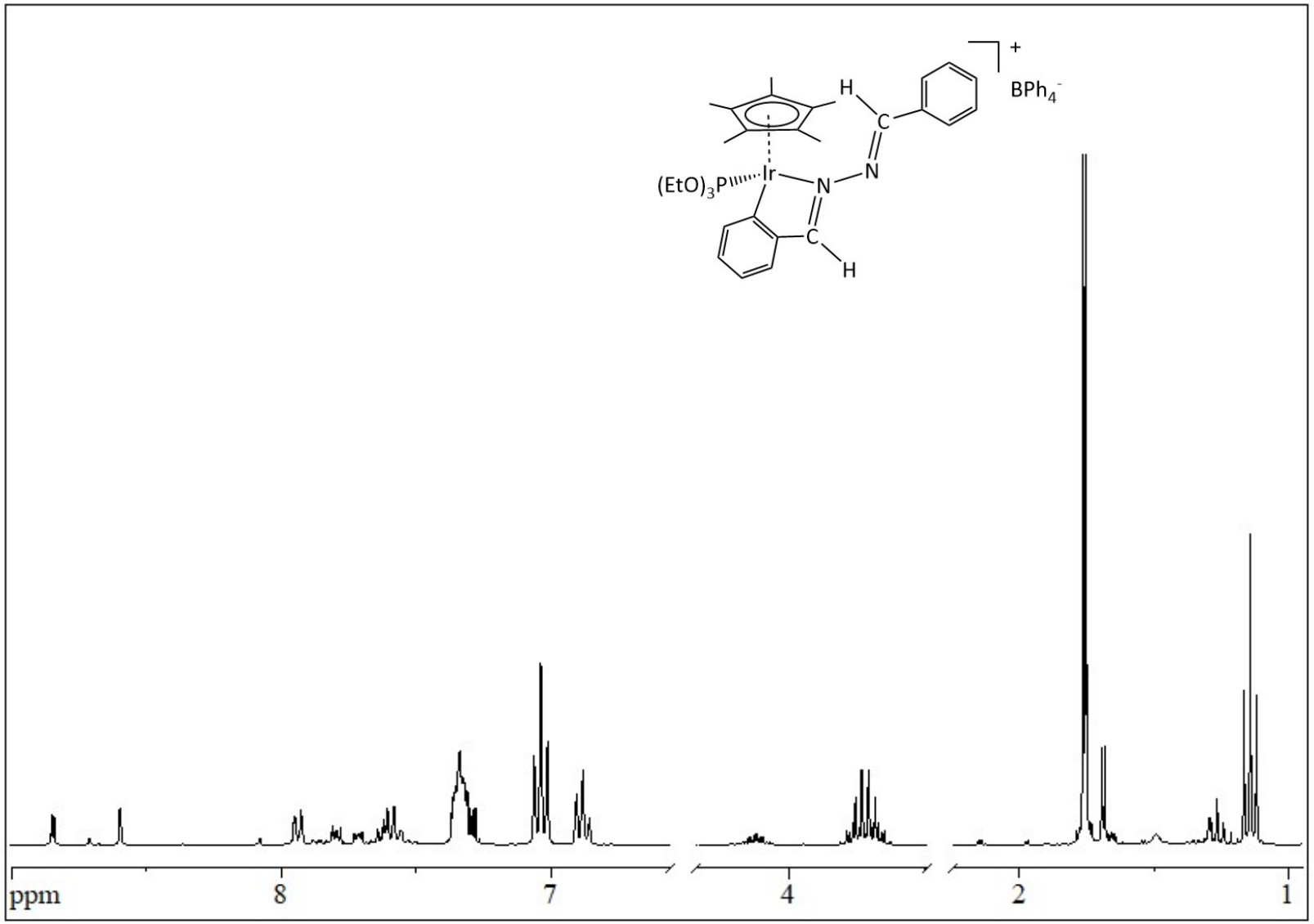

Appendix 11.17 ^{1}H NMR spectra in CD_2Cl_2 at room temperature of complex 30a.

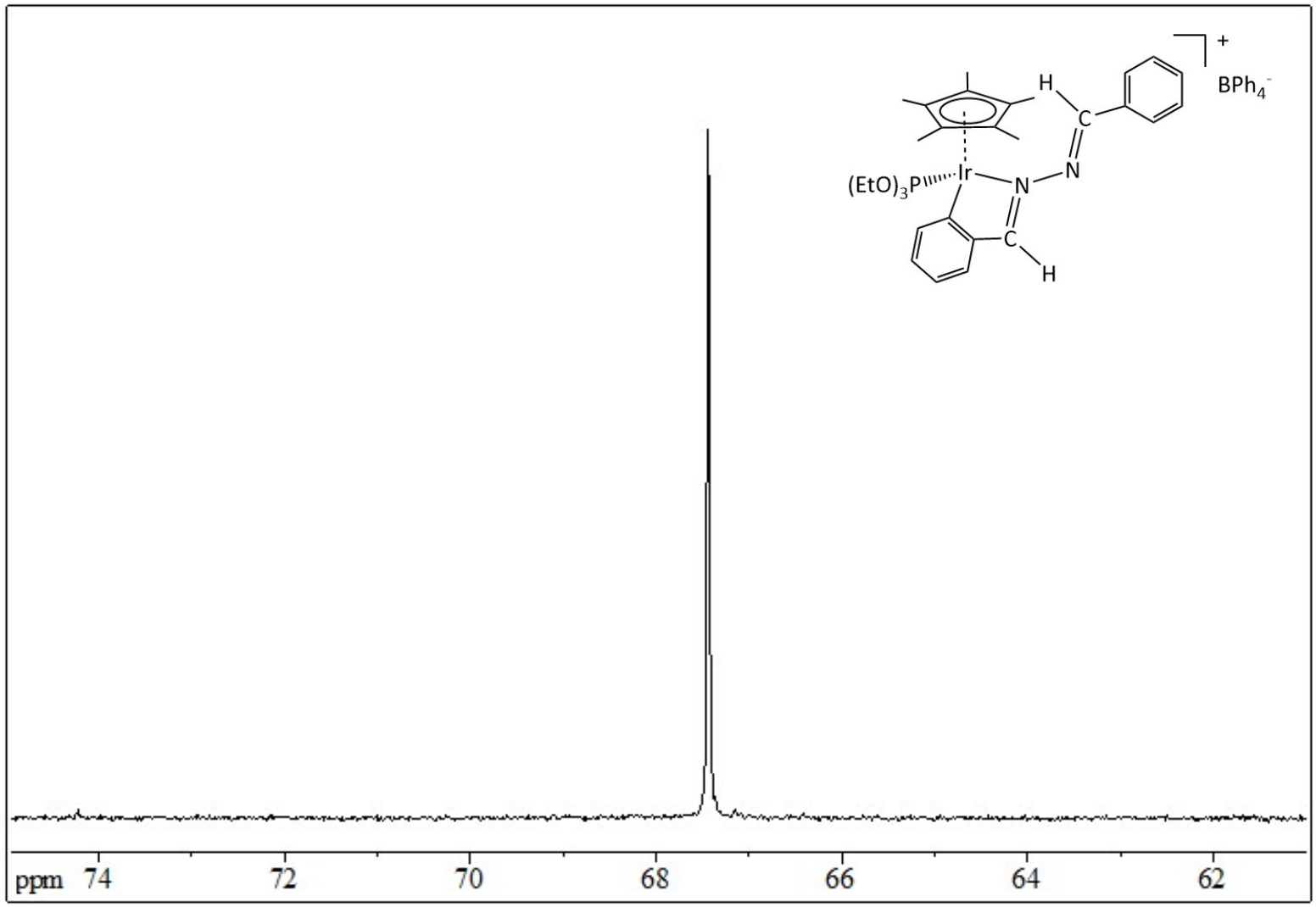

Appendix 11.18 $^{31}P\{^{1}H\}$ NMR spectra in CD_2Cl_2 at room temperature of complex 30a.

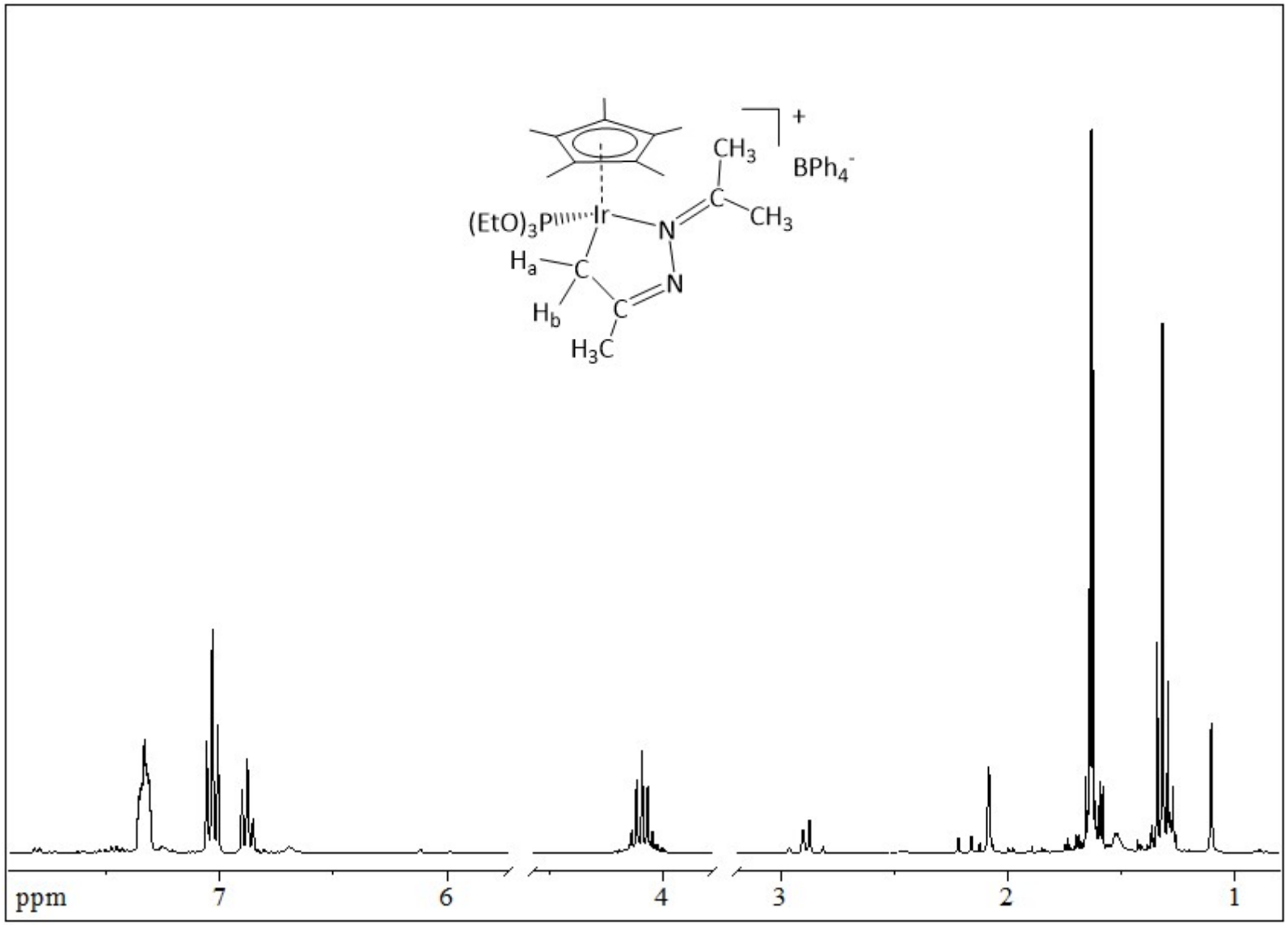

Appendix 11.19 ^{1}H NMR spectra in CD_2Cl_2 at room temperature of complex 32.

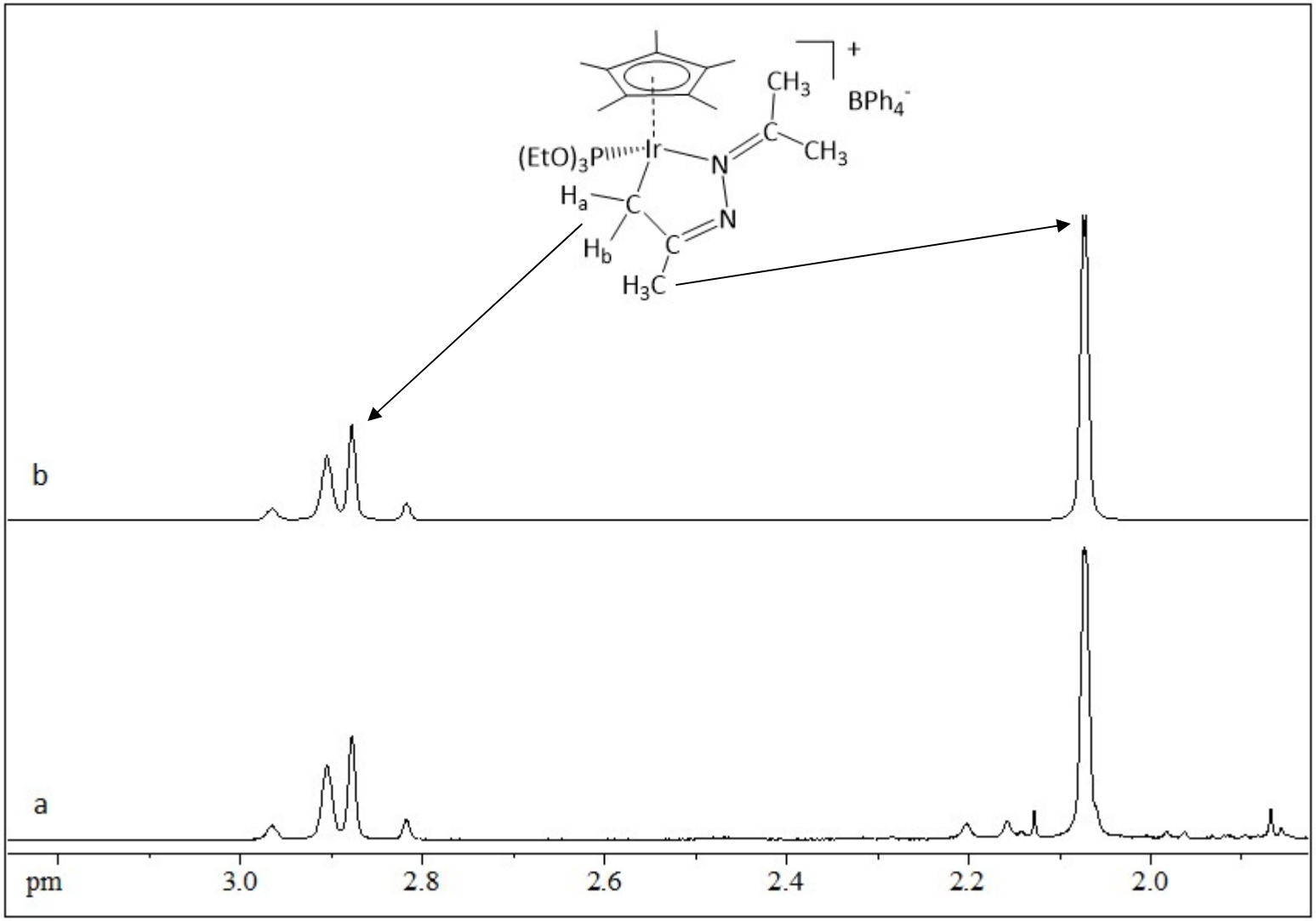

Appendix 11.20 Magnification of ^1H NMR spectra in CD_2Cl_2 at room temperature of complex 32: higher spectra is simulated, lower spectra is the real one.

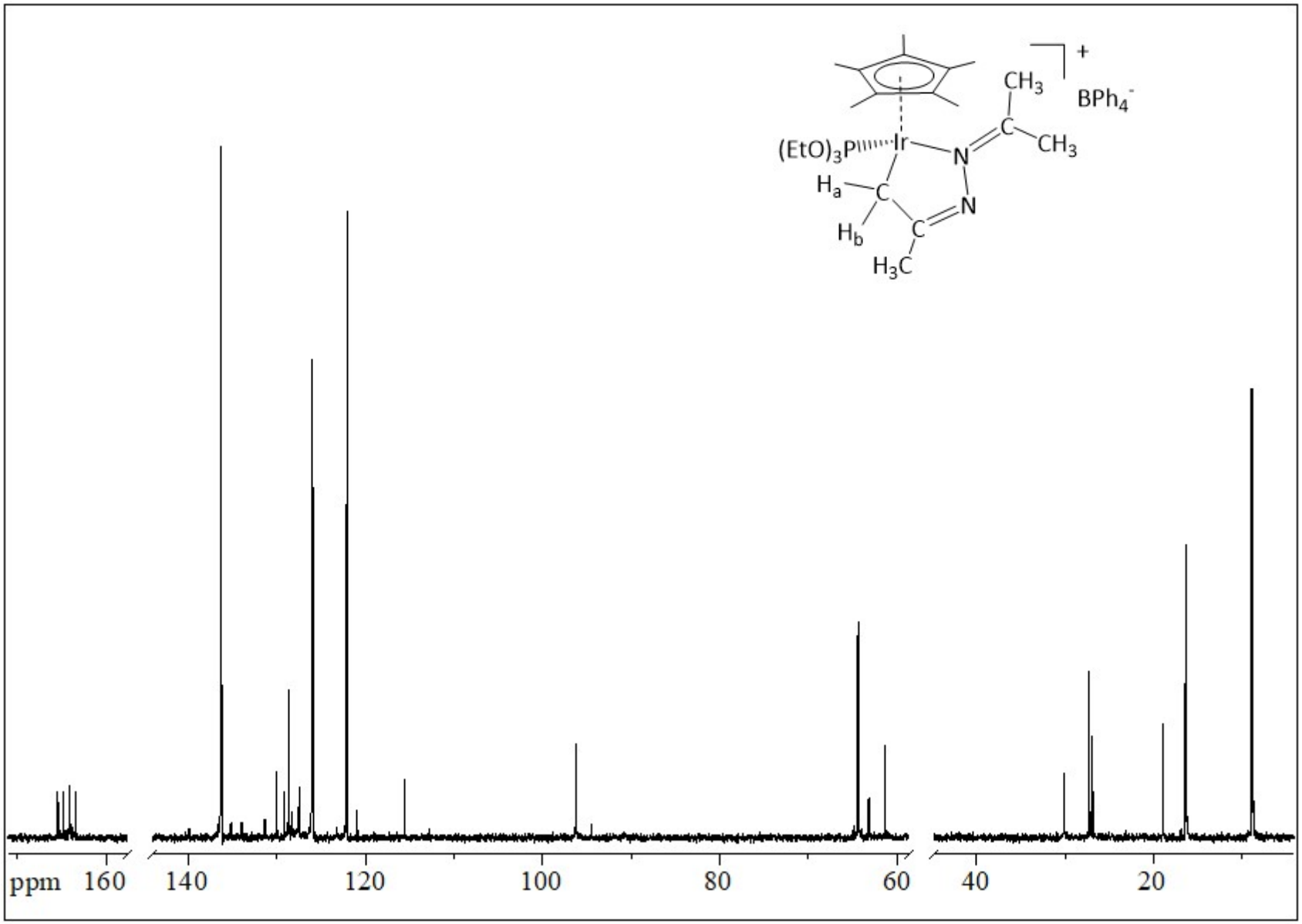

Appendix 11.21 $^{13}C\{^{1}H\}$ NMR spectra in CD_2Cl_2 at room temperature of complex 32.

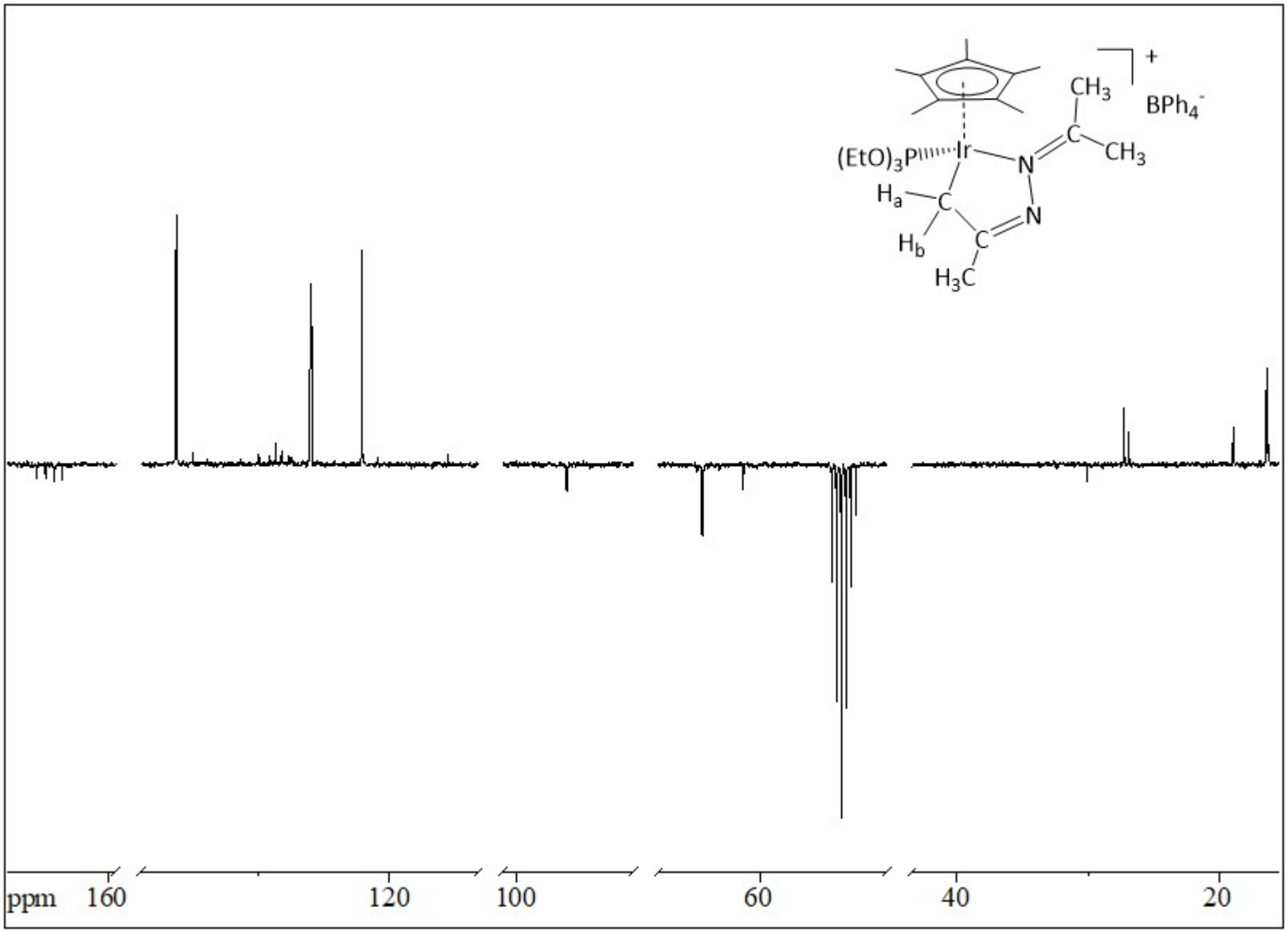

Appendix 11.22 ^{13}C APT spectra in CD_2Cl_2 at room temperature of complex 32.

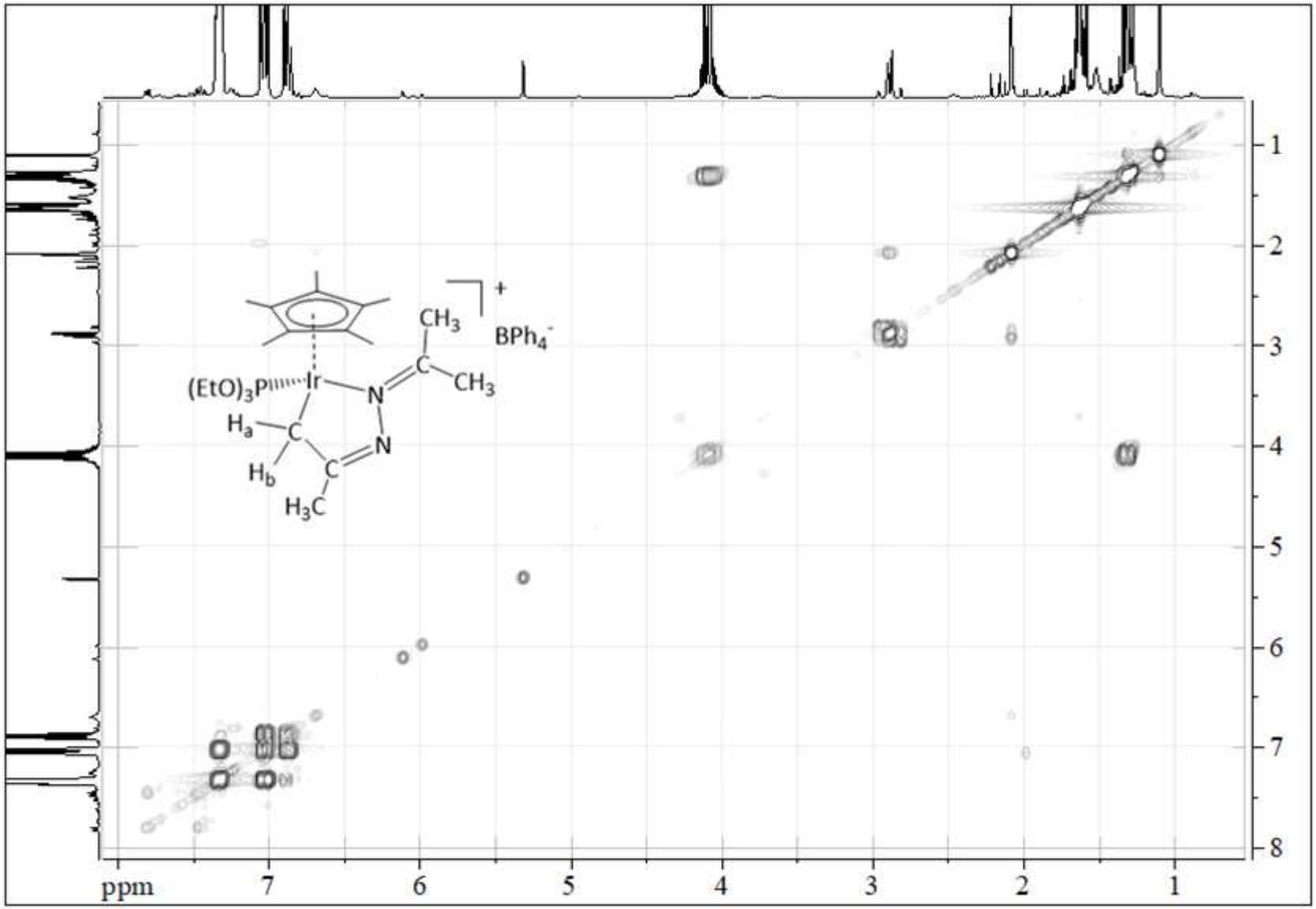

Appendix 11.23 ^{1}H COSY spectra in CD_2Cl_2 at room temperature of complex 32.

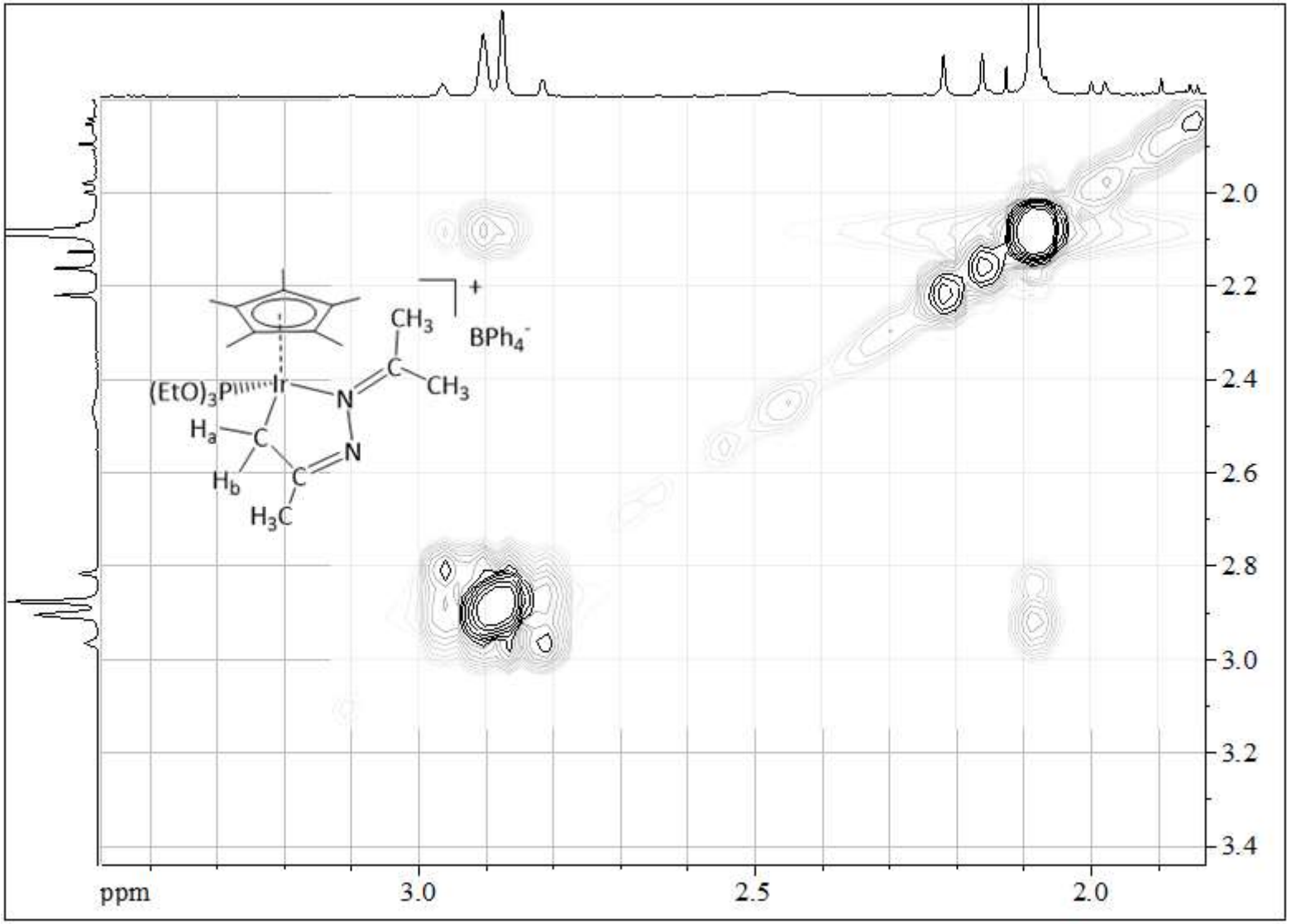

Appendix 11.24 Magnification of ^{1}H COSY spectra in CD_2Cl_2 at room temperature of complex 32.

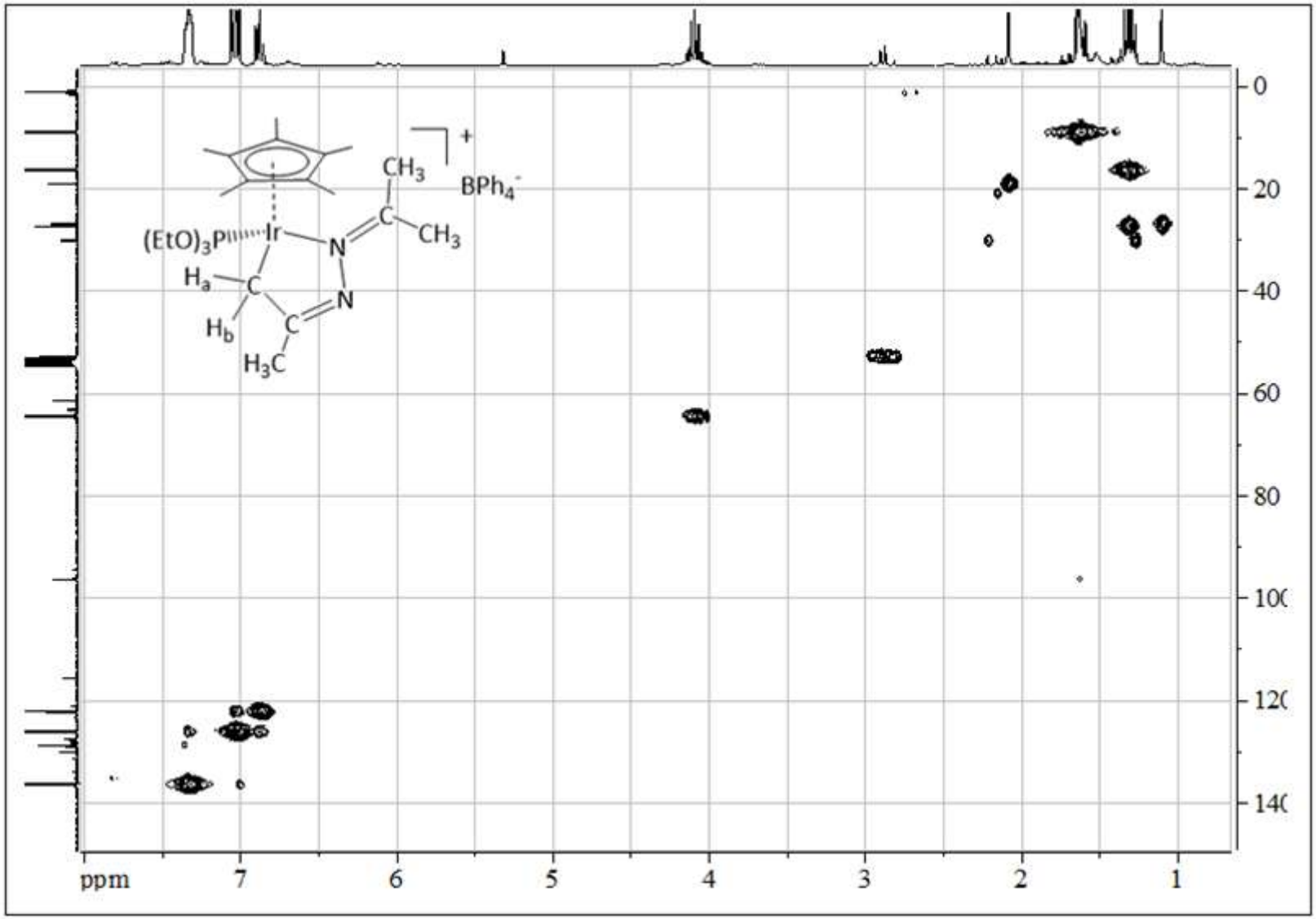

Appendix 11.25 $^{13}C/^{1}H$ HMQC spectra in CD_2Cl_2 at room temperature of complex 32.

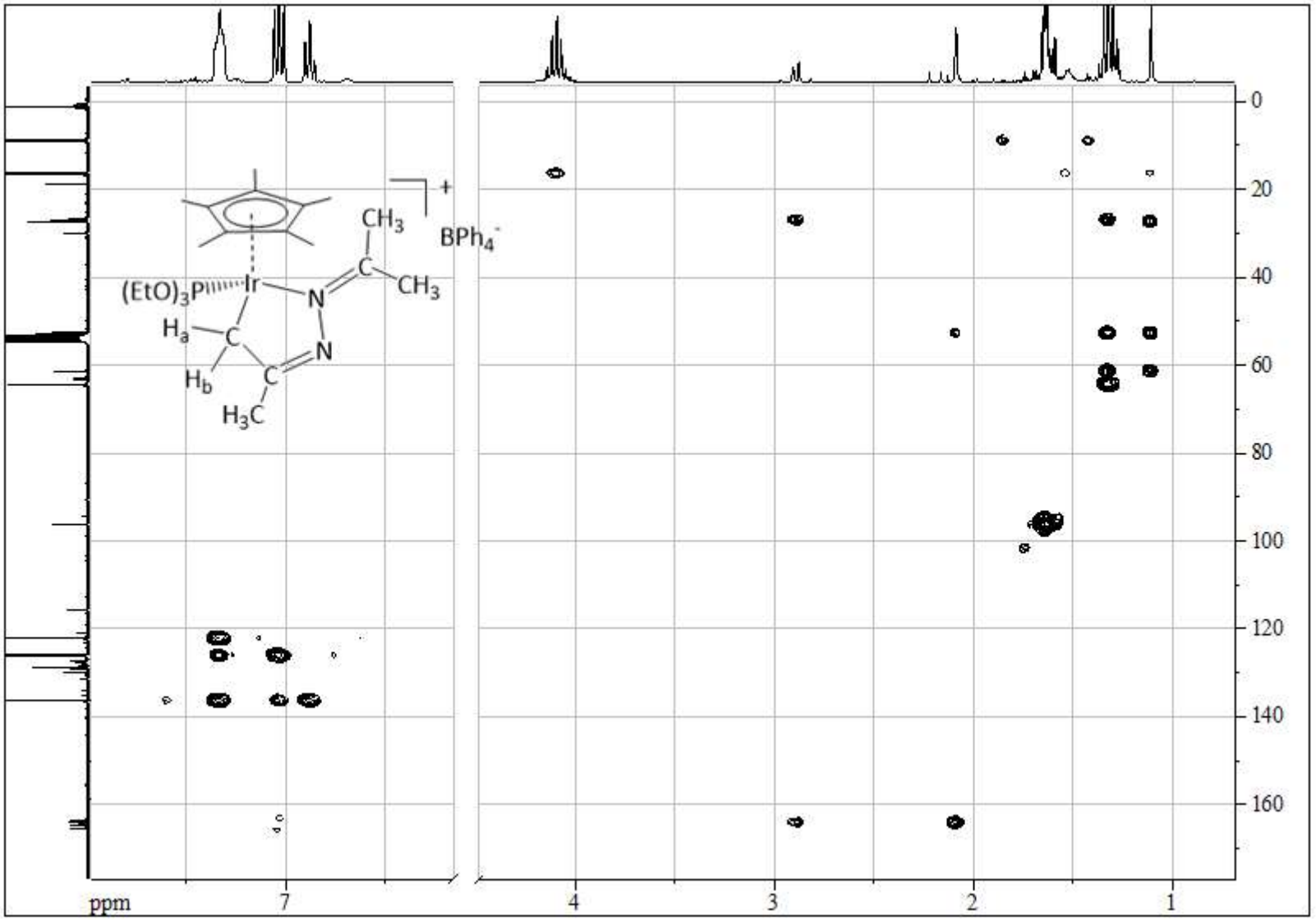

Appendix 11.26 $^{13}C/^{1}H$ HMBC spectra in CD_2Cl_2 at room temperature of complex 32.

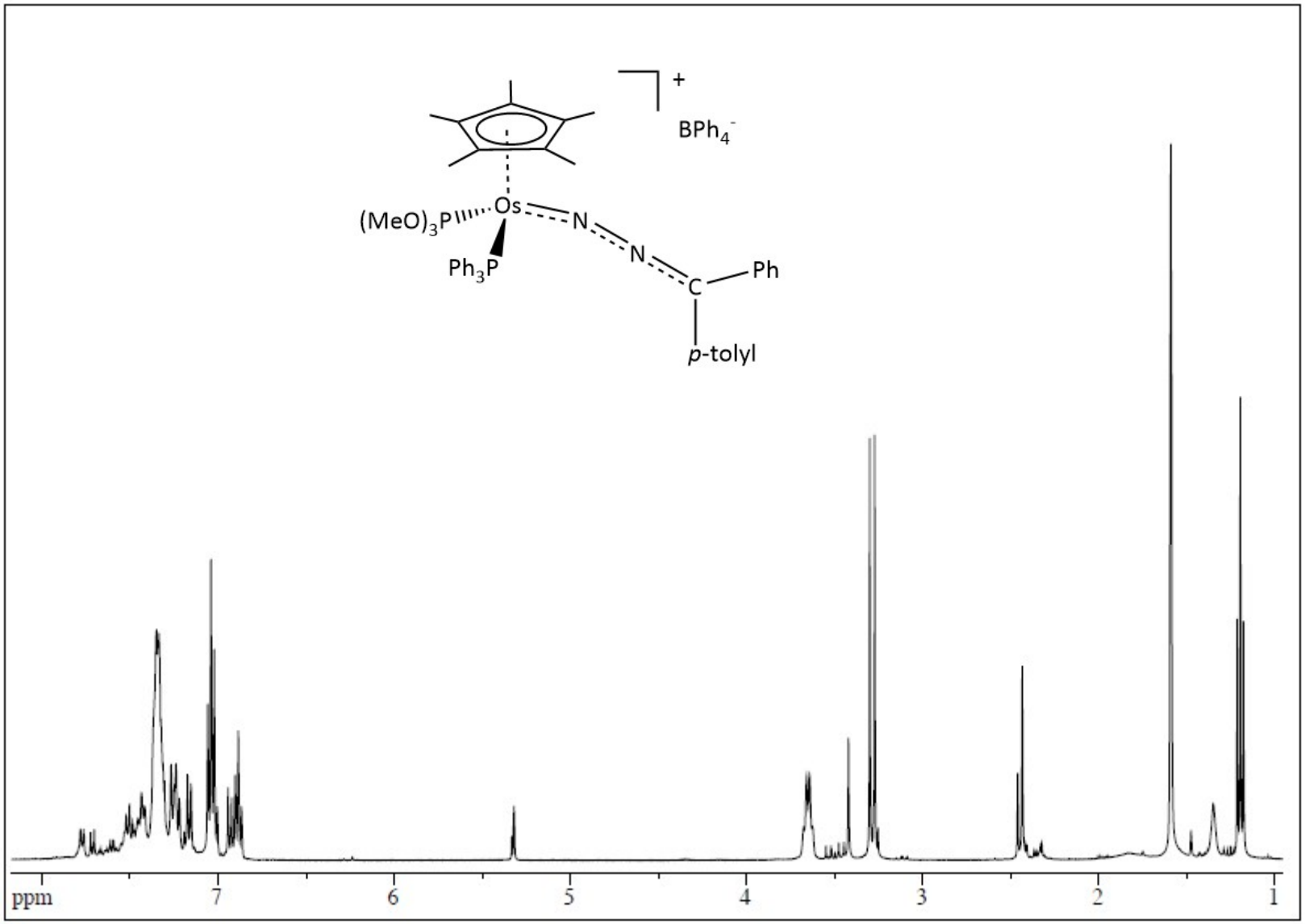

Appendix 11.27 ^{1}H NMR spectra in CD_2Cl_2 at room temperature of complex 33b.

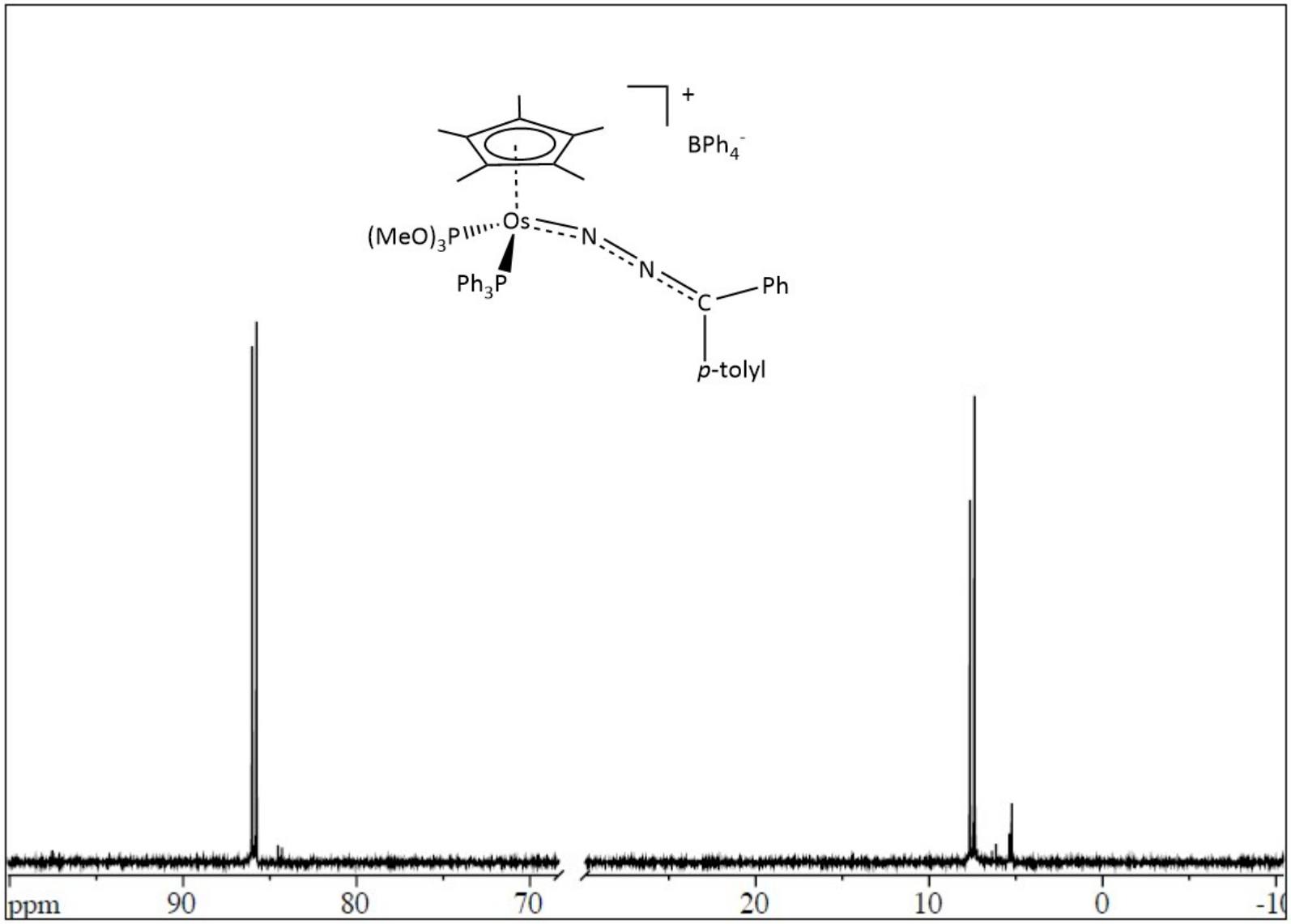

Appendix 11.28 $^{31}P\{^{1}H\}$ NMR spectra in CD_2Cl_2 at room temperature of complex 33b.

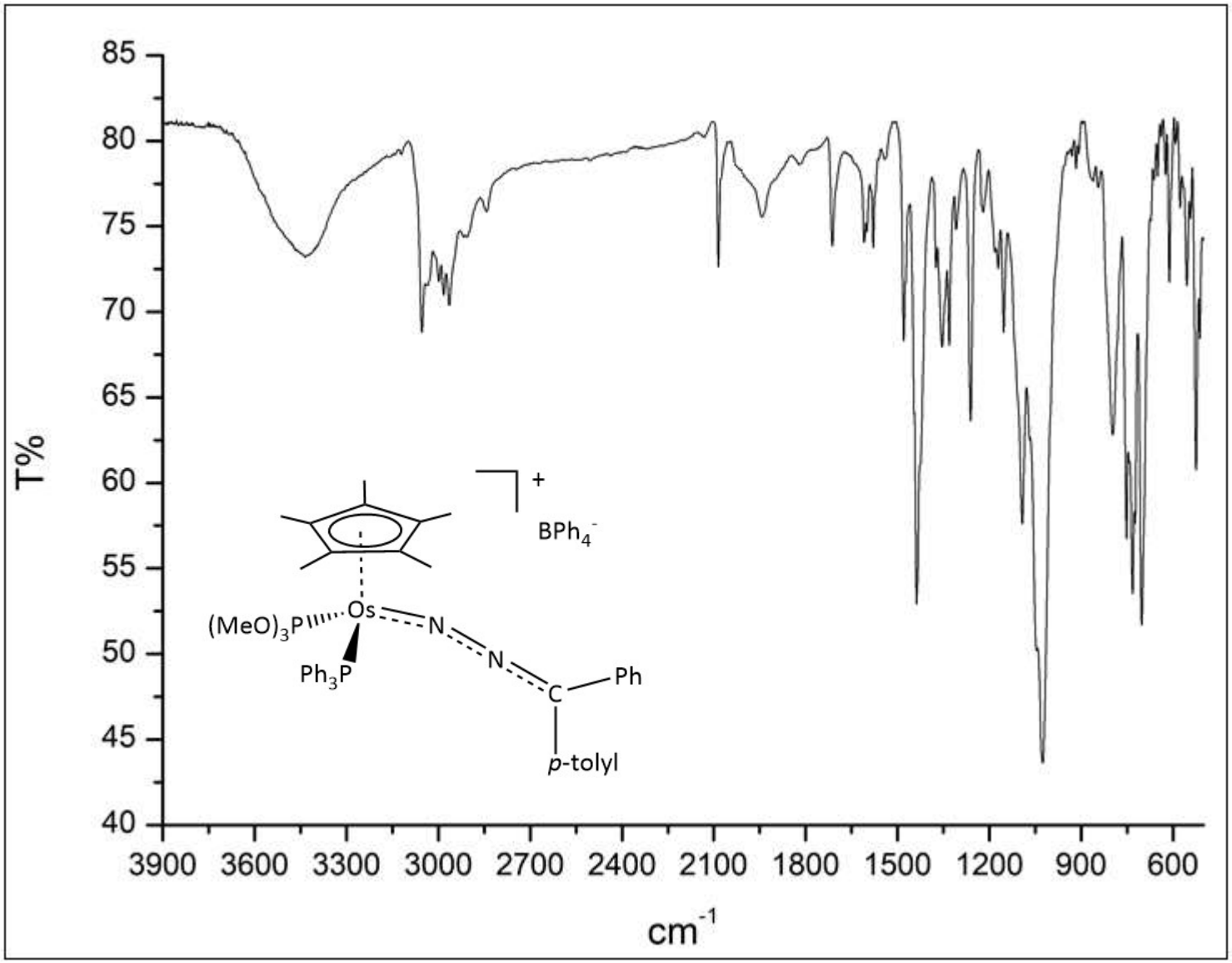

Appendix 11.29 IR spectra in KBr pallets at room temperature of complex 33b.

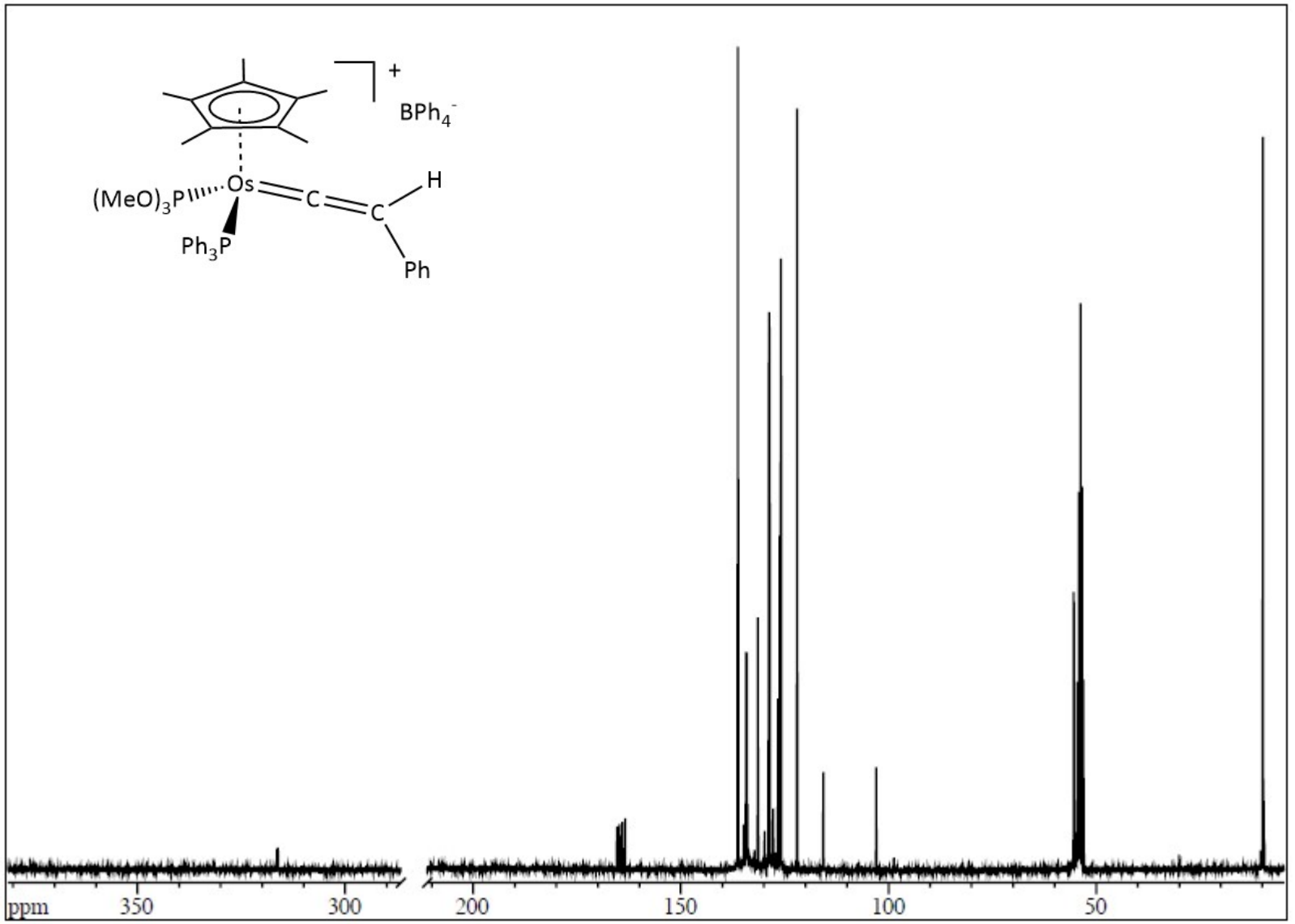

Appendix 11.30 $^{13}C\{^{1}H\}$ NMR spectra in CD_2Cl_2 at room temperature of complex 40b.

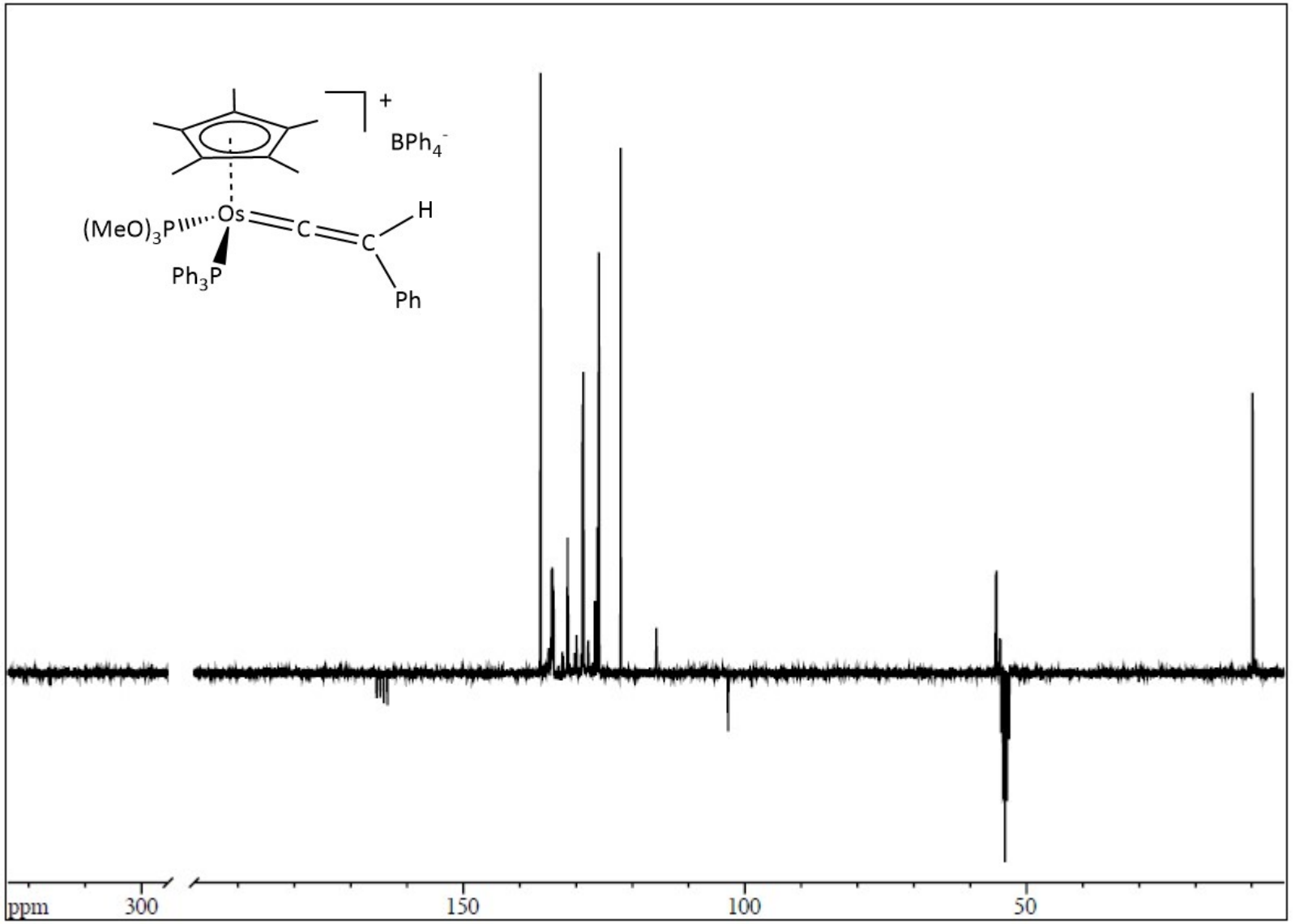

Appendix 11.31 ^{13}C APT spectra in CD_2Cl_2 at room temperature of complex 40b.

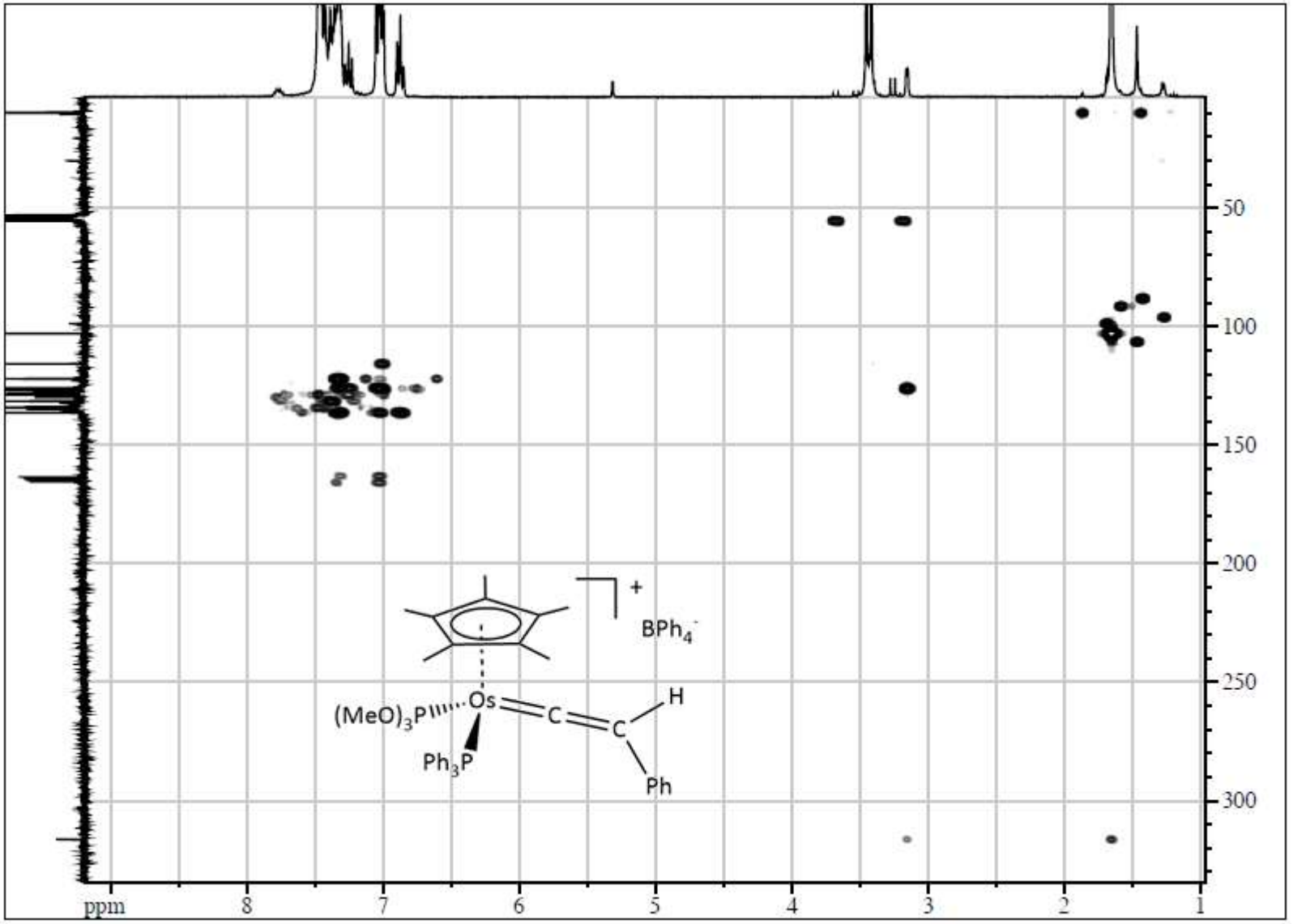

Appendix 11.32 $^{13}C/^{1}H$ HMBC spectra in CD_2Cl_2 at room temperature of complex 40b.

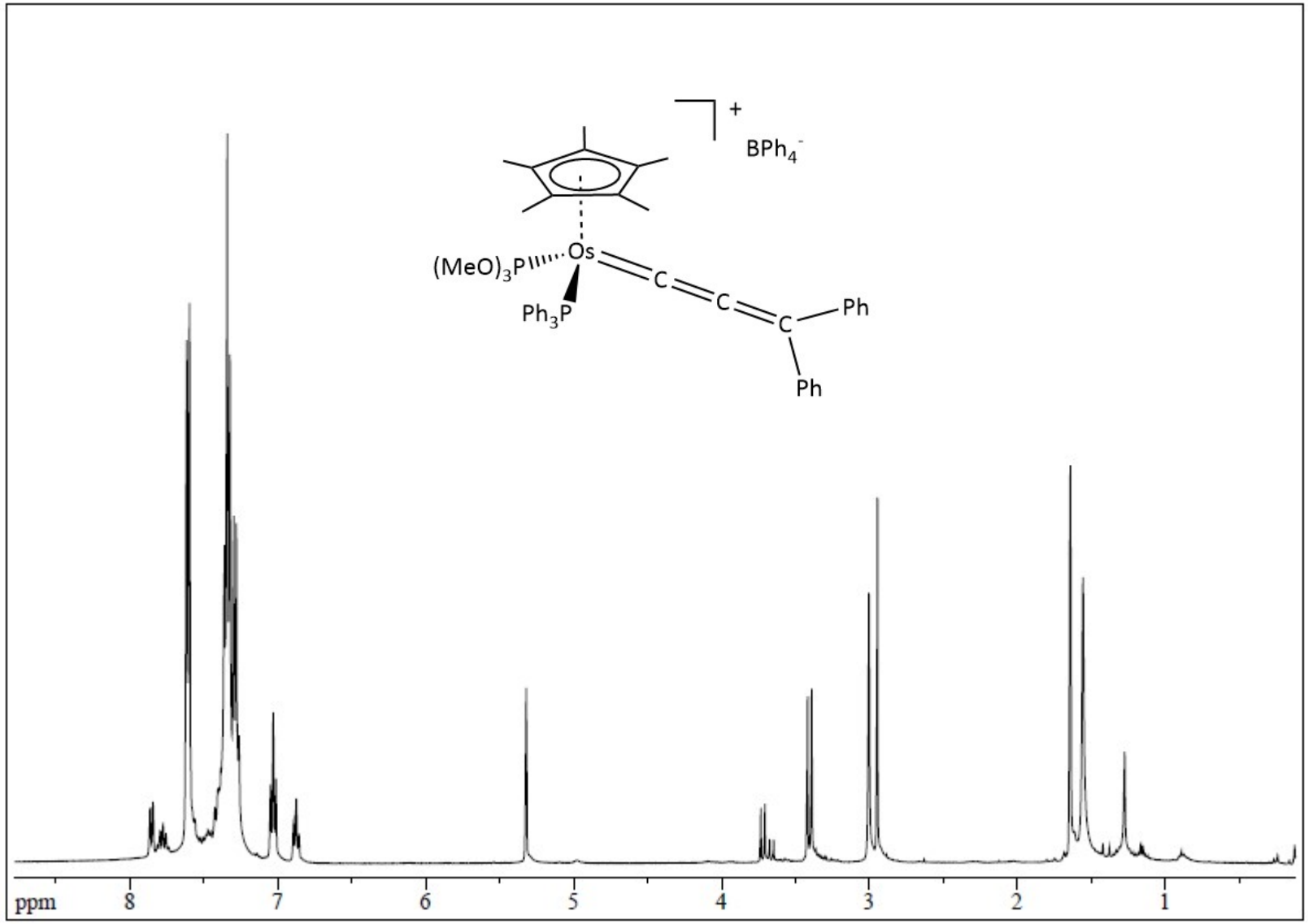

Appendix 11.33 ^{1}H NMR spectra in CD_2Cl_2 at room temperature of complex 44.

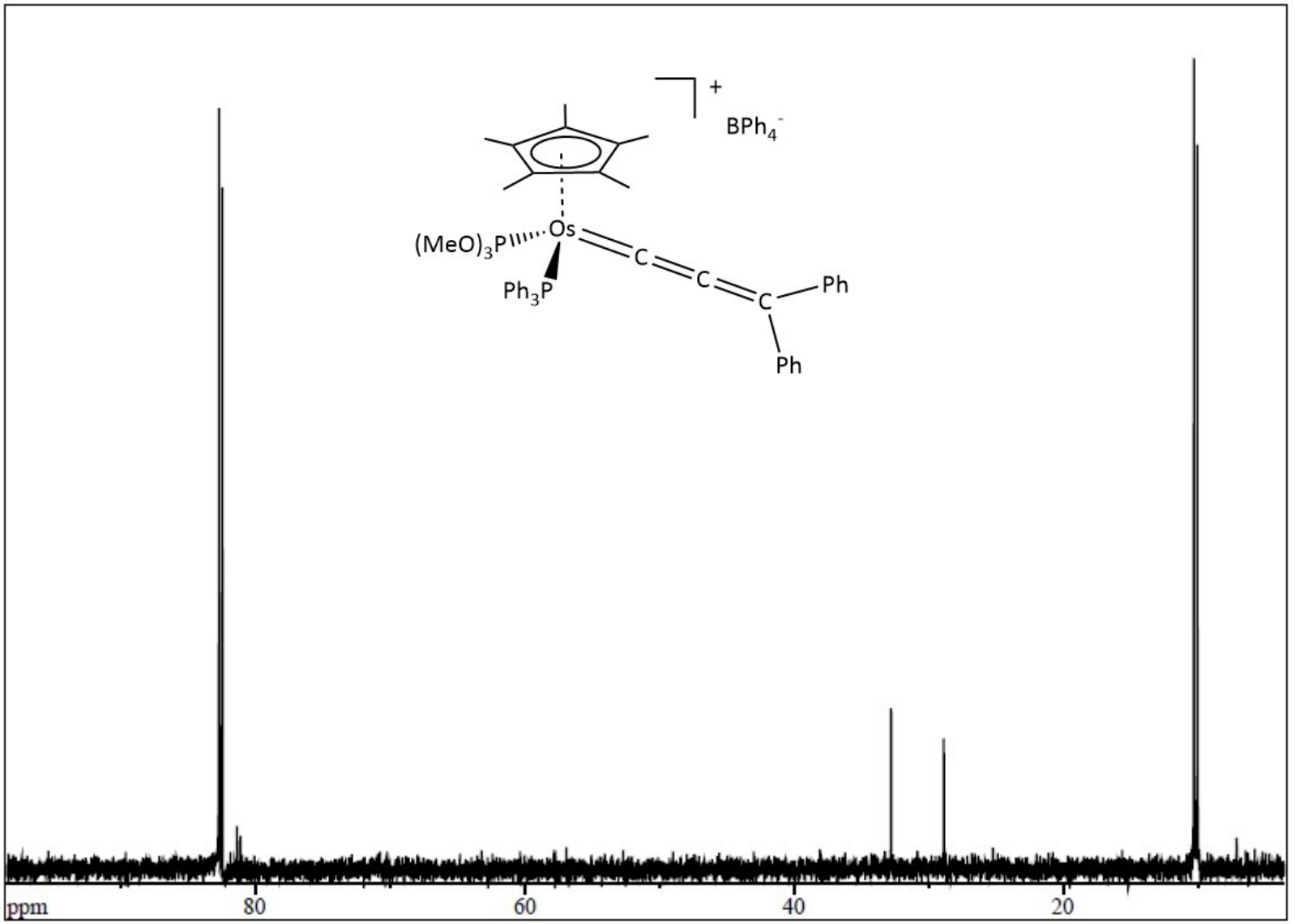

Appendix 11.34 $^{31}P\{^{1}H\}$ NMR spectra in CD_2Cl_2 at room temperature of complex 44.

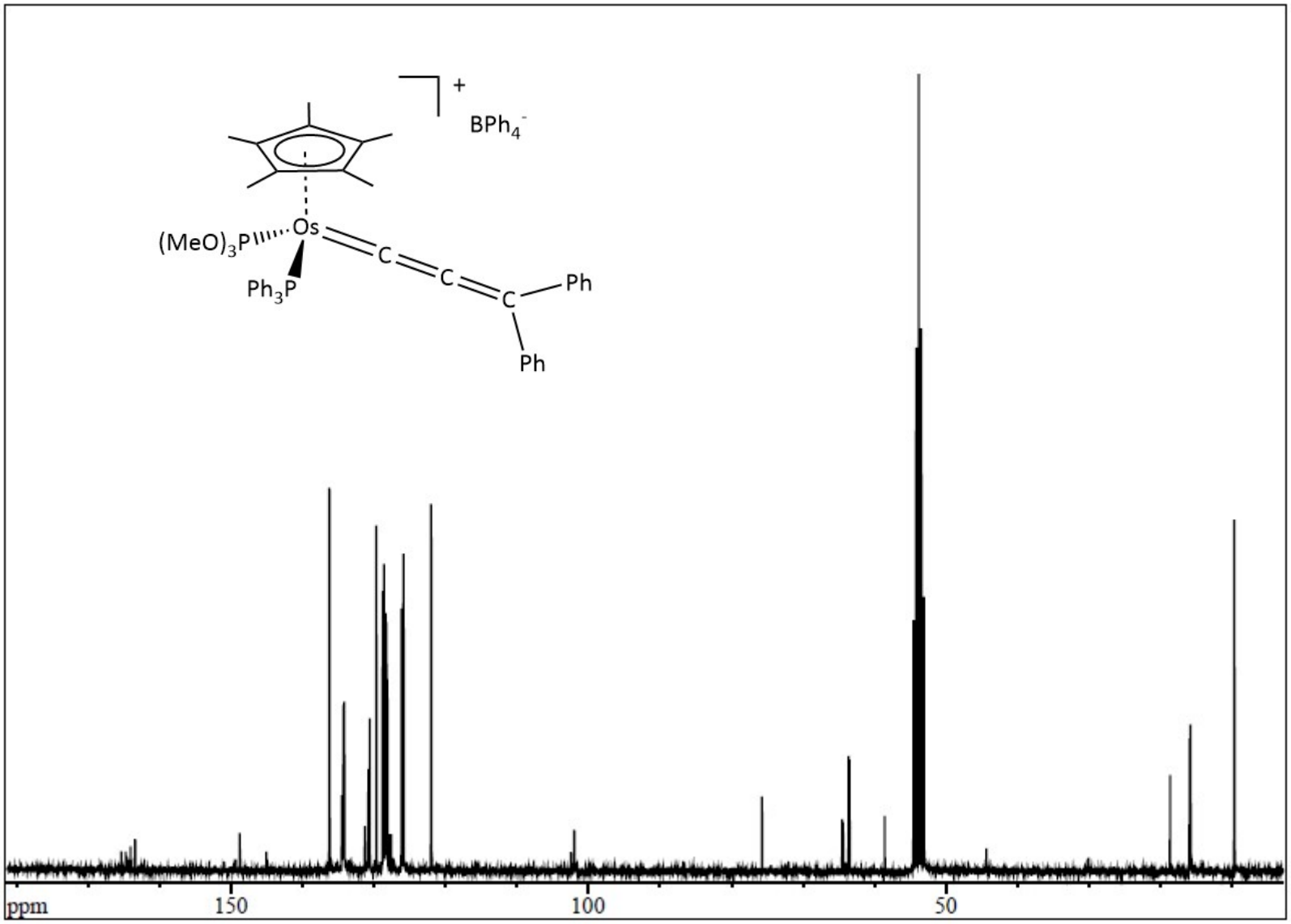

Appendix 11.35 $^{13}C\{^{1}H\}$ NMR spectra in CD_2Cl_2 at room temperature of complex 44.

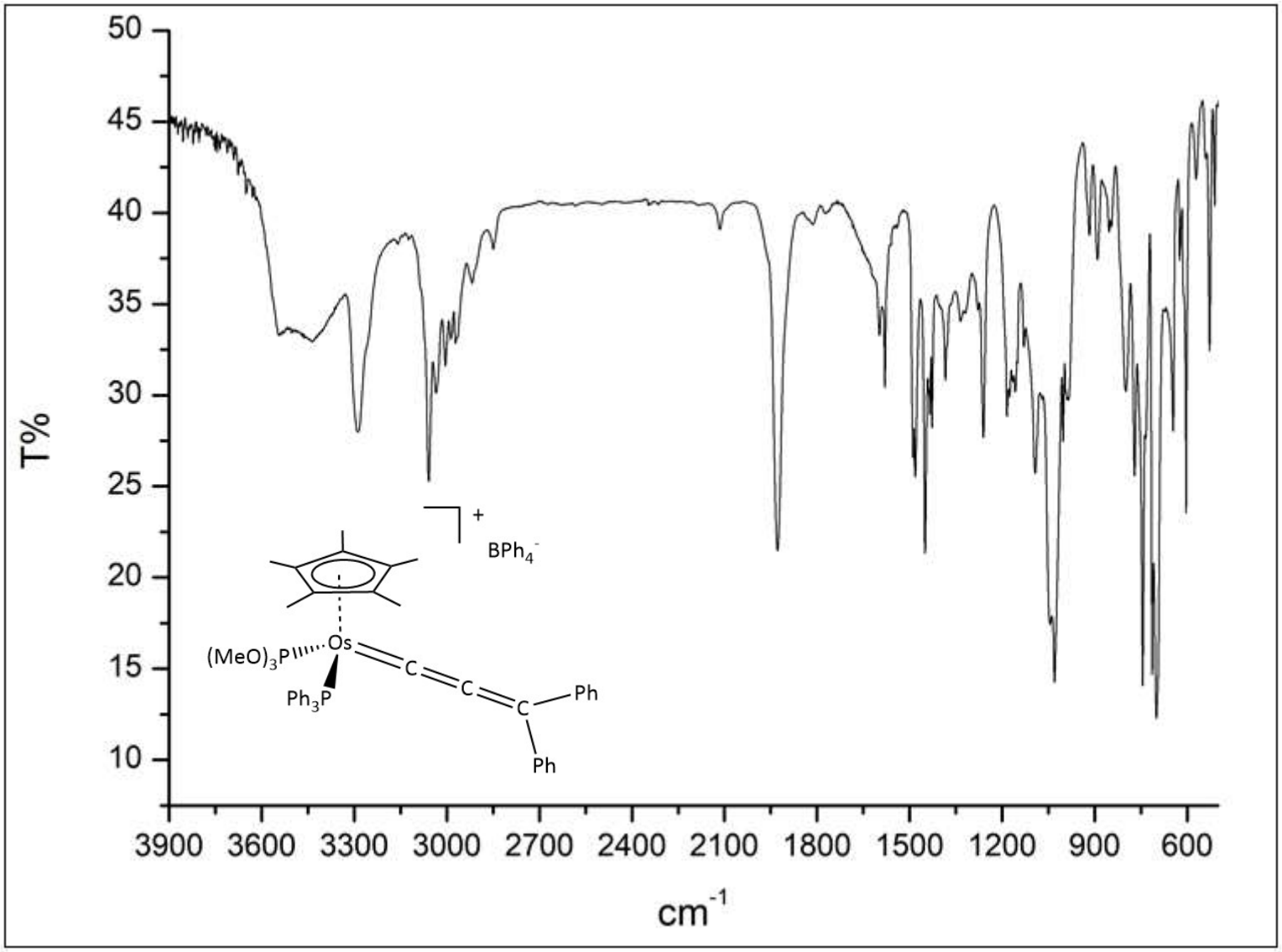

Appendix 11.36 IR spectra in KBr pallets at room temperature of complex 44.

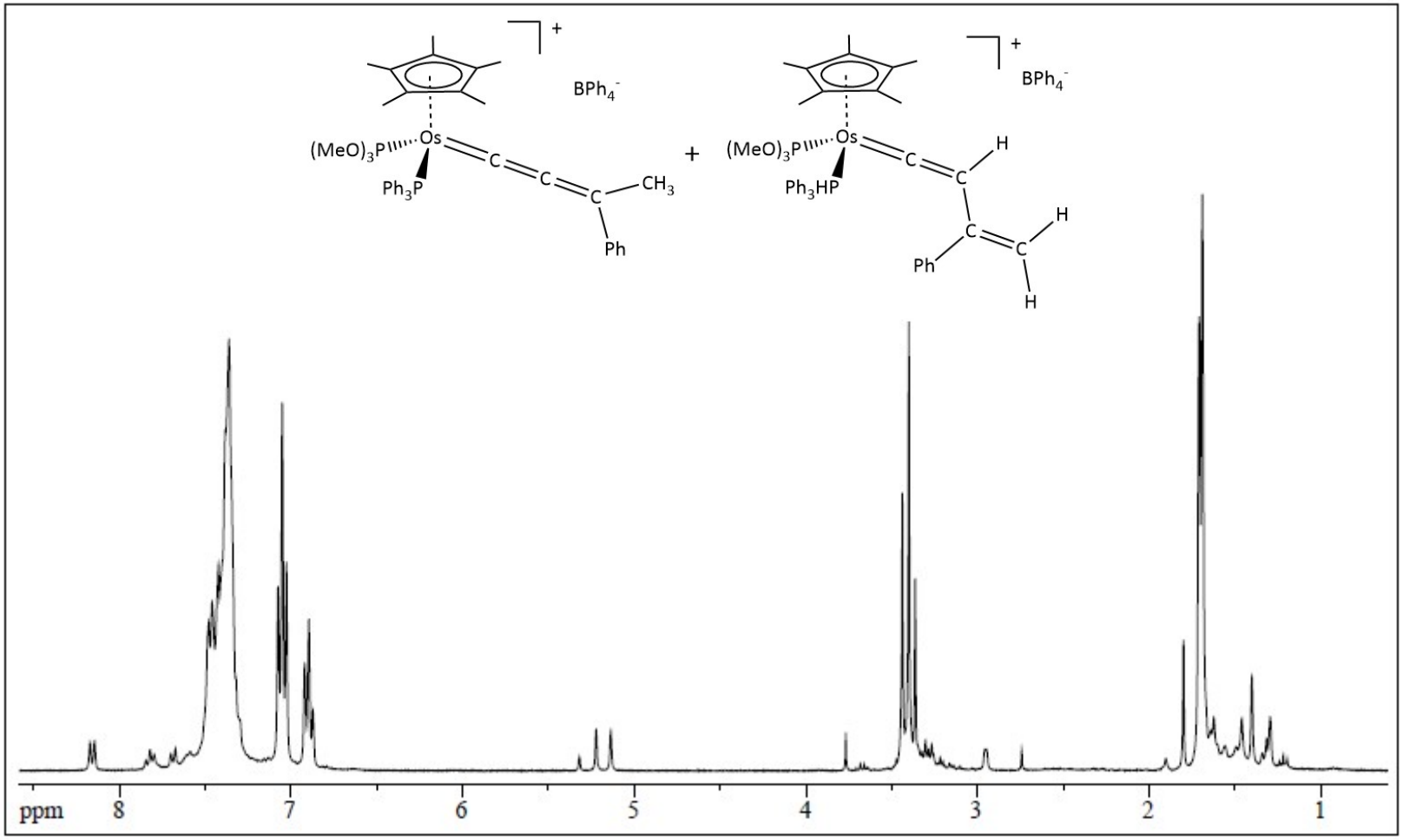

Appendix 11.37 ^{1}H NMR spectra in CD_2Cl_2 at room temperature of complexes 46 and 47.

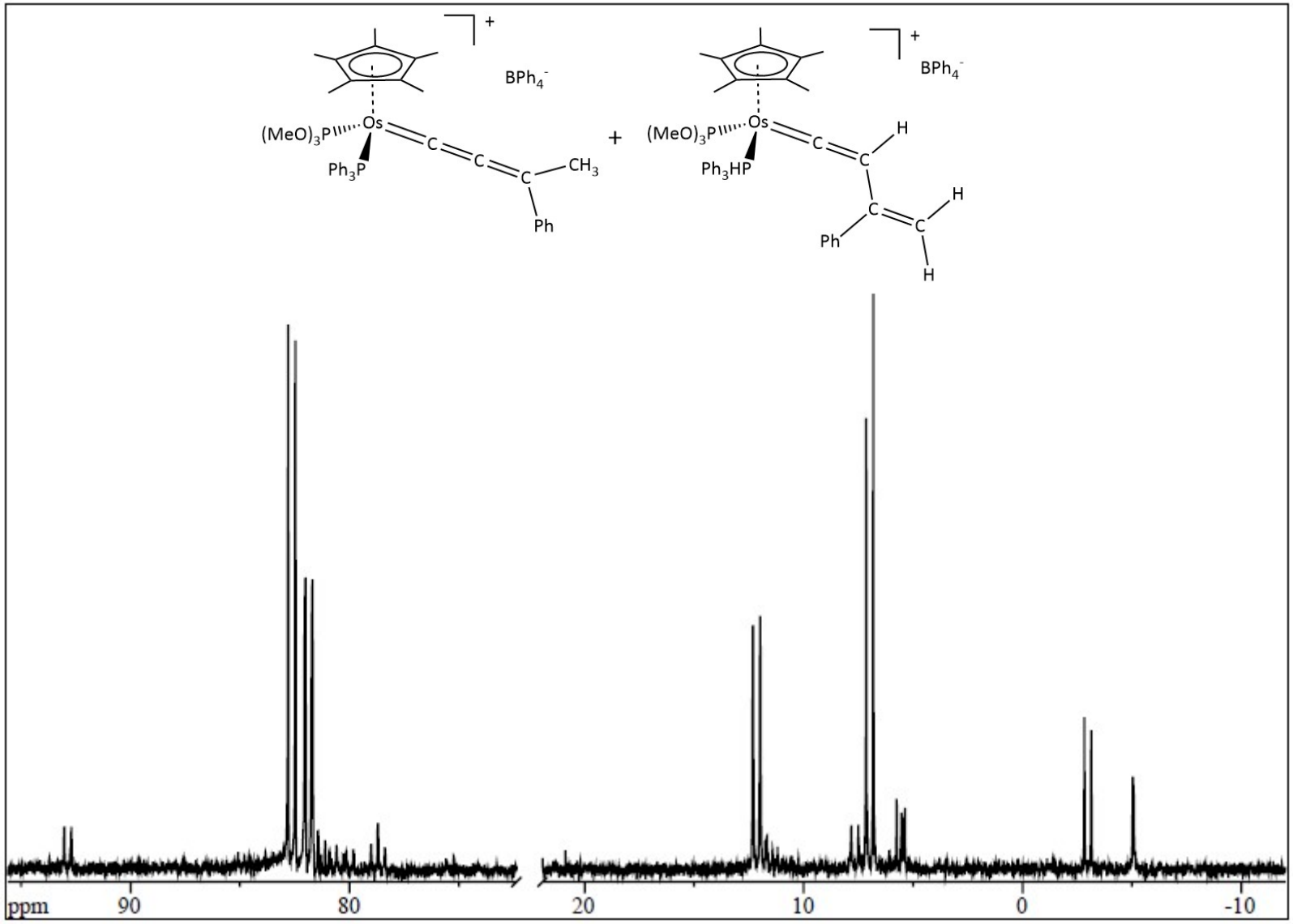

Appendix 11.38 $^{31}P\{^{1}H\}$ NMR spectra in CD_2Cl_2 at room temperature of complexes 46 and 47.

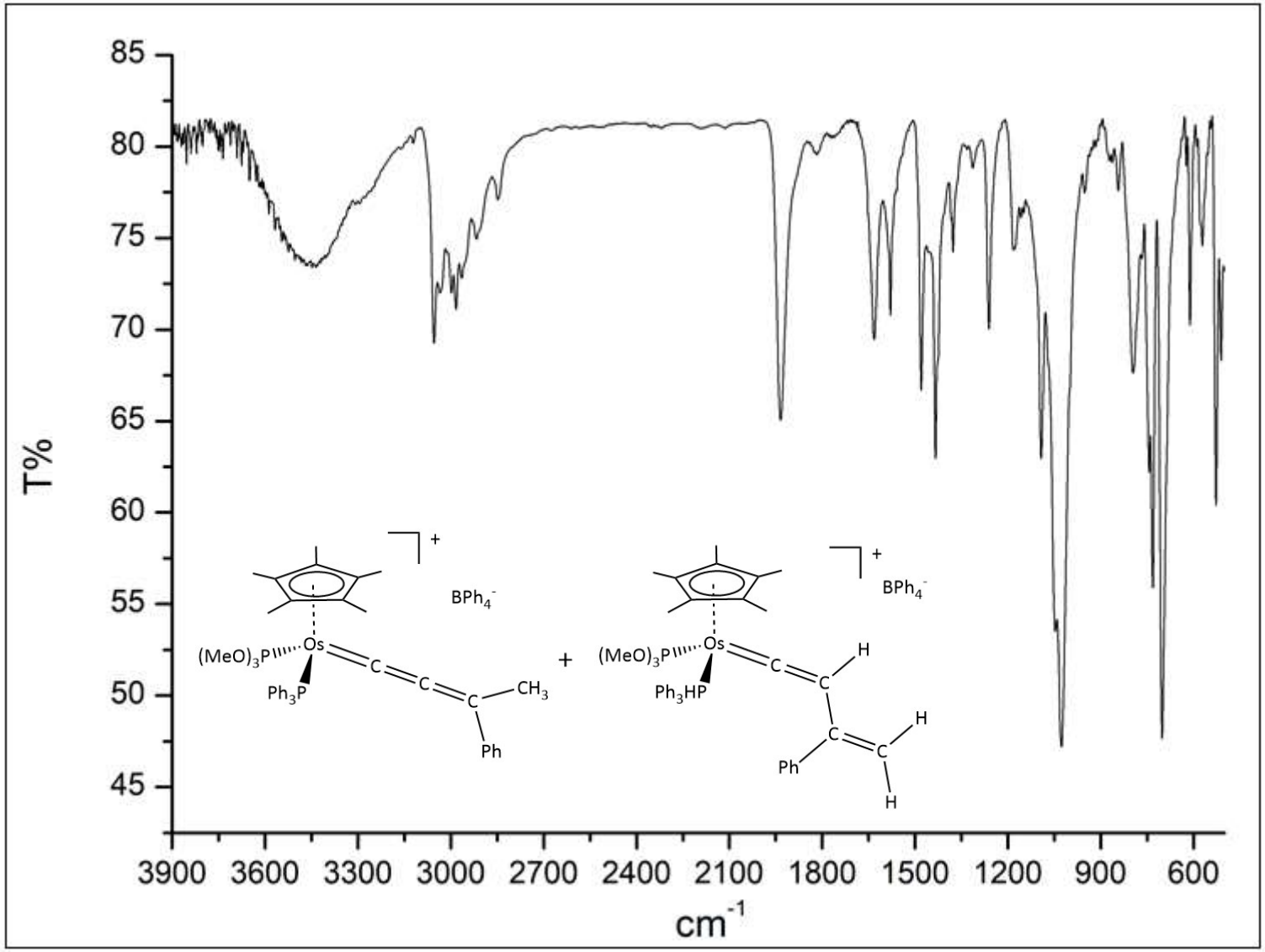

Appendix 11.39 IR spectra in KBr pallets at room temperature of complexes 46 and 47.

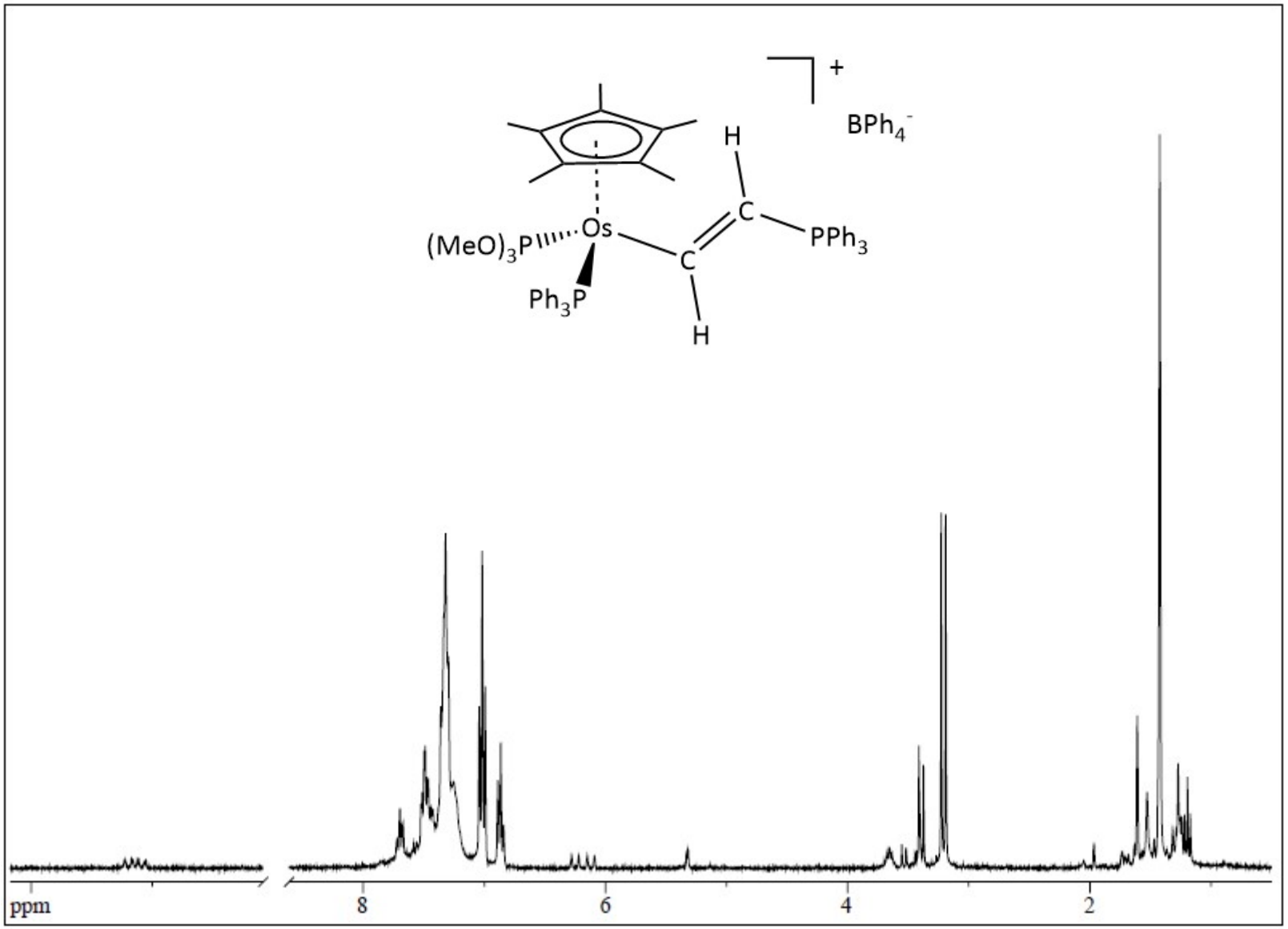

Appendix 11.40 ^{1}H NMR spectra in CD_2Cl_2 at room temperature of complex 50.

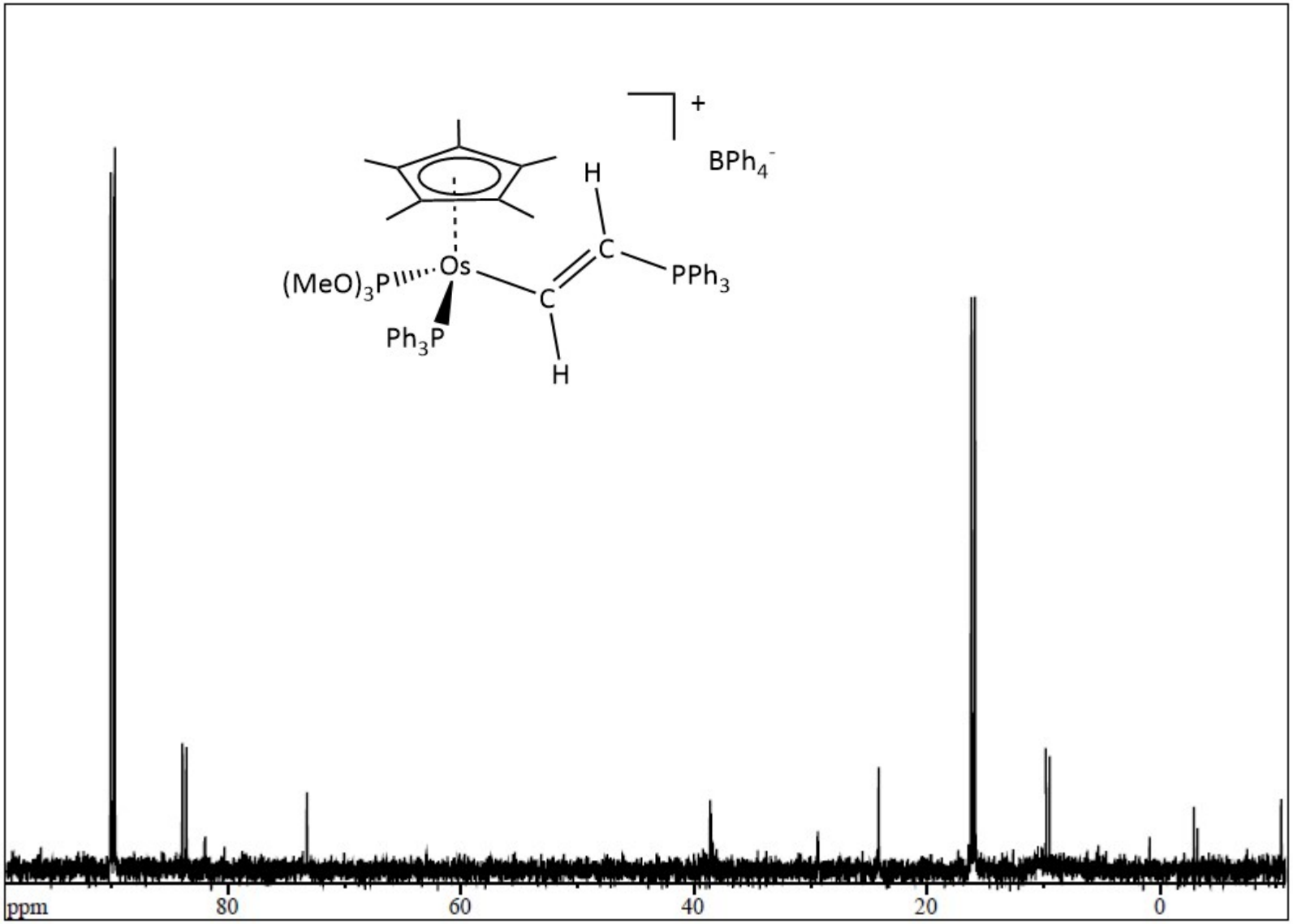

Appendix 11.41 $^{31}P\{^{1}H\}$ NMR spectra in CD_2Cl_2 at room temperature of complex 50.

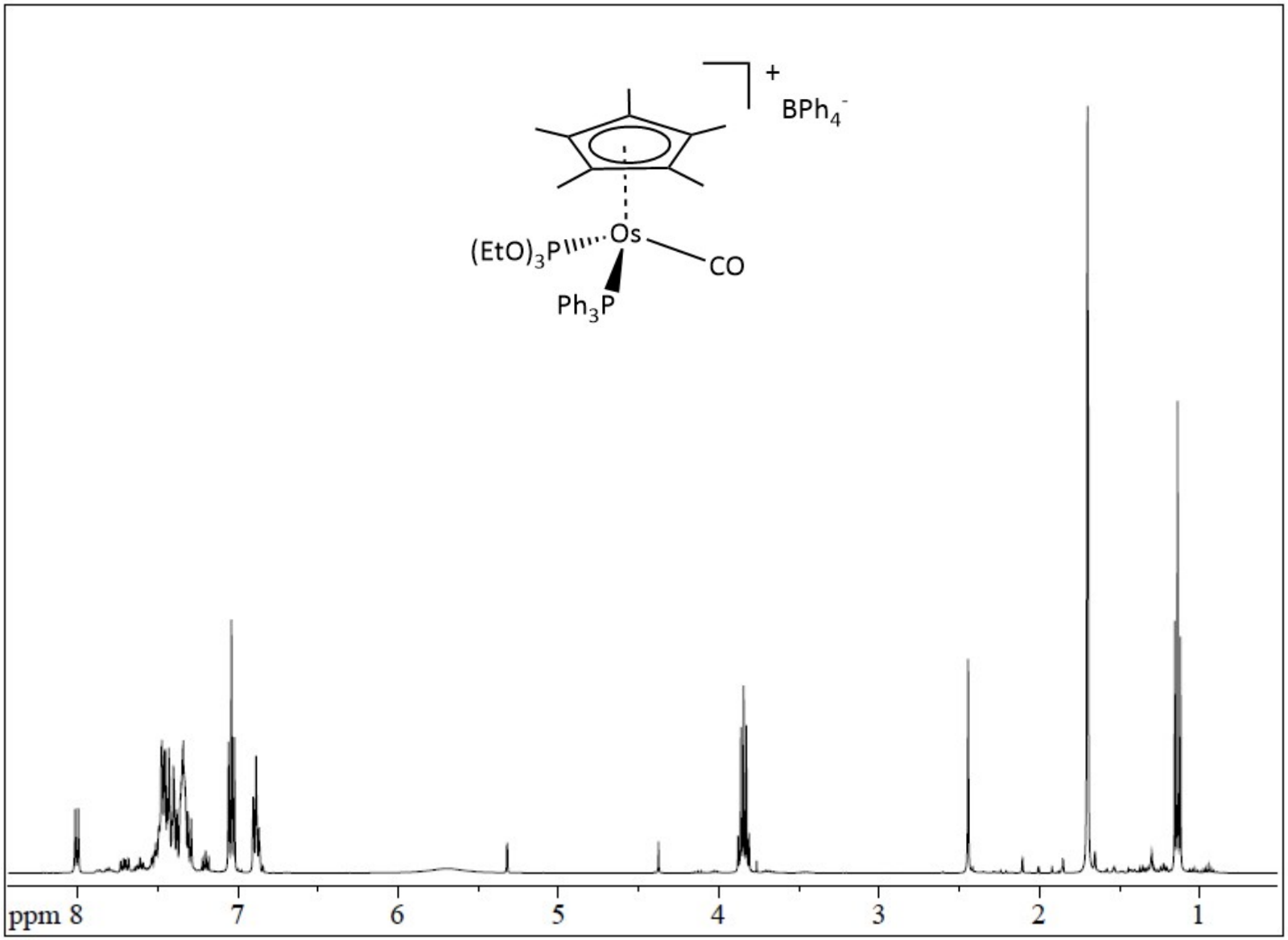

Appendix 11.42 ^{1}H NMR spectra in CD_2Cl_2 at room temperature of complex 52.

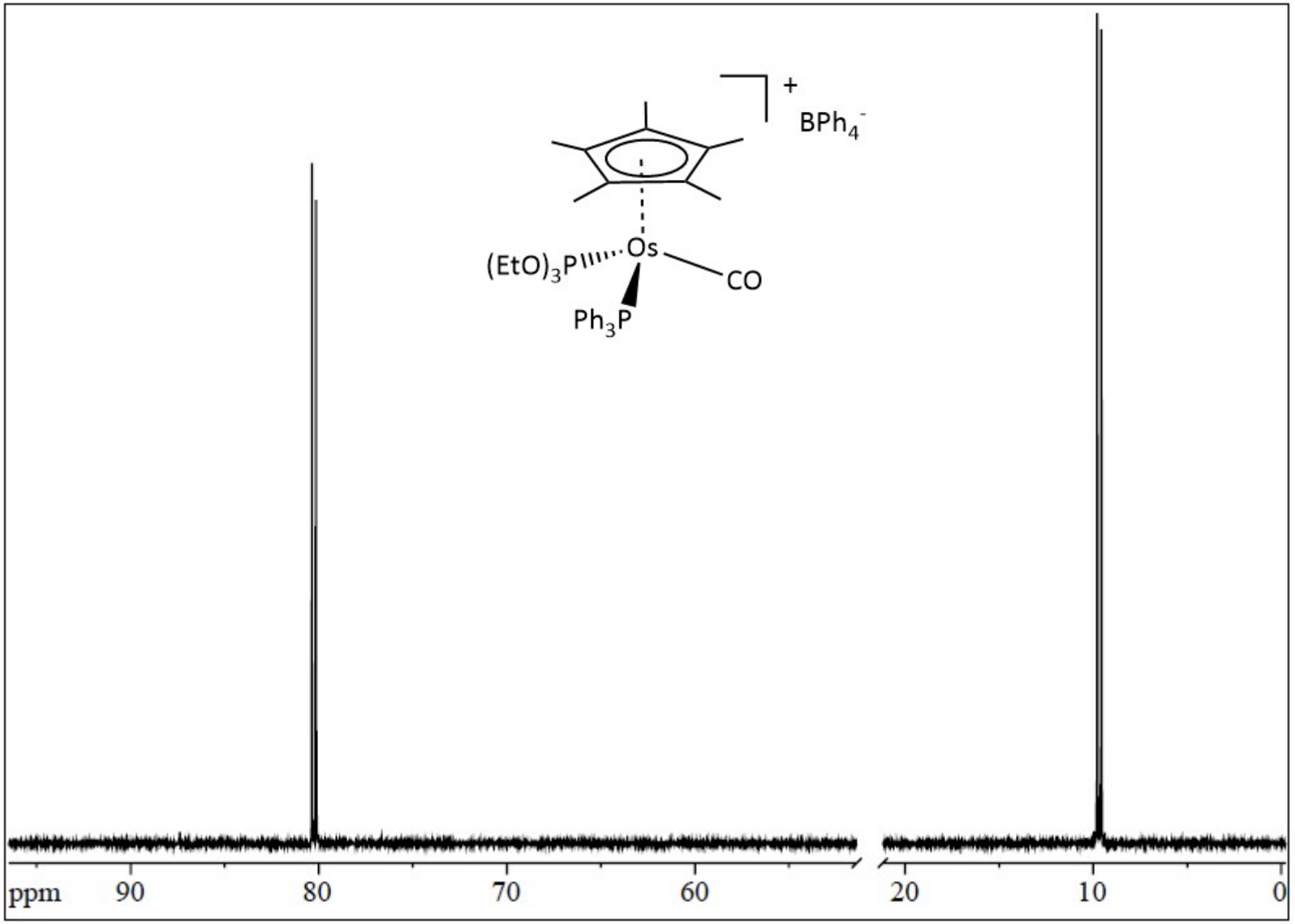

Appendix 11.43 $^{31}P\{^{1}H\}$ NMR spectra in CD_2Cl_2 at room temperature of complex 52.

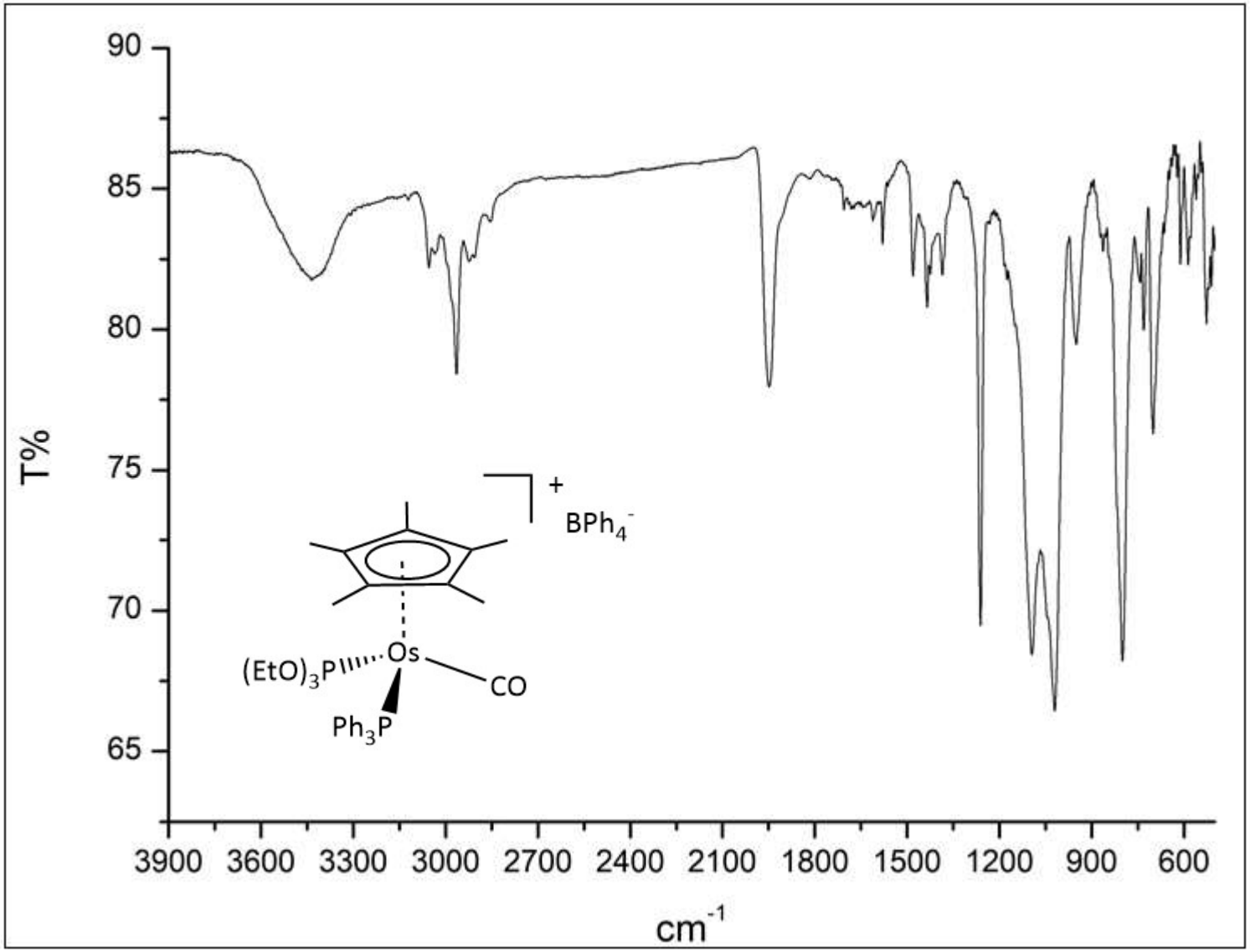

Appendix 11.44 IR spectra in KBr pallets at room temperature of complex 52.

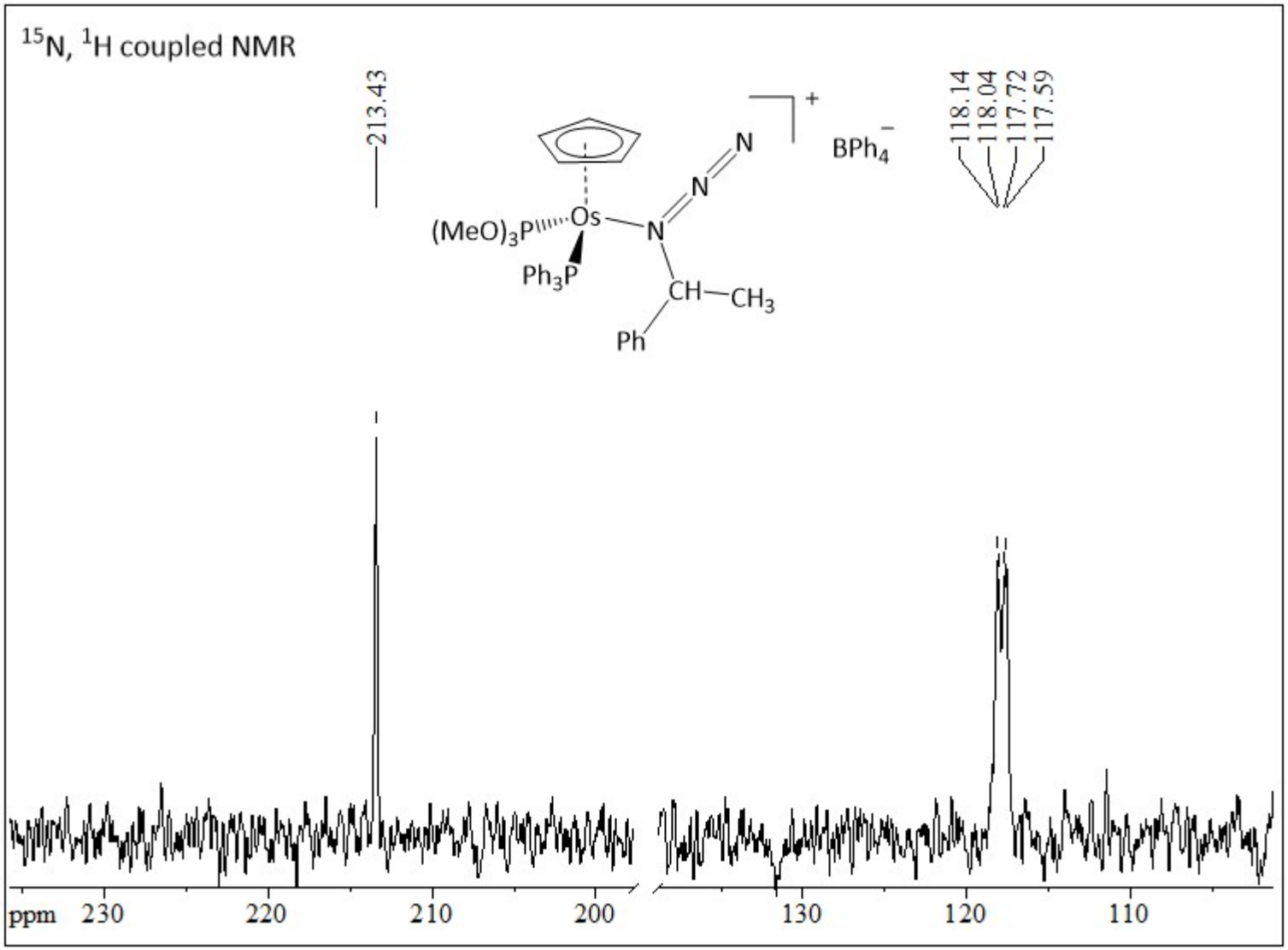

Appendix 11.45 ^{15}N NMR spectra in CD_2Cl_2 at room temperature of complex $53c_1$: higher spectra is simulated, lower spectra is the real one.

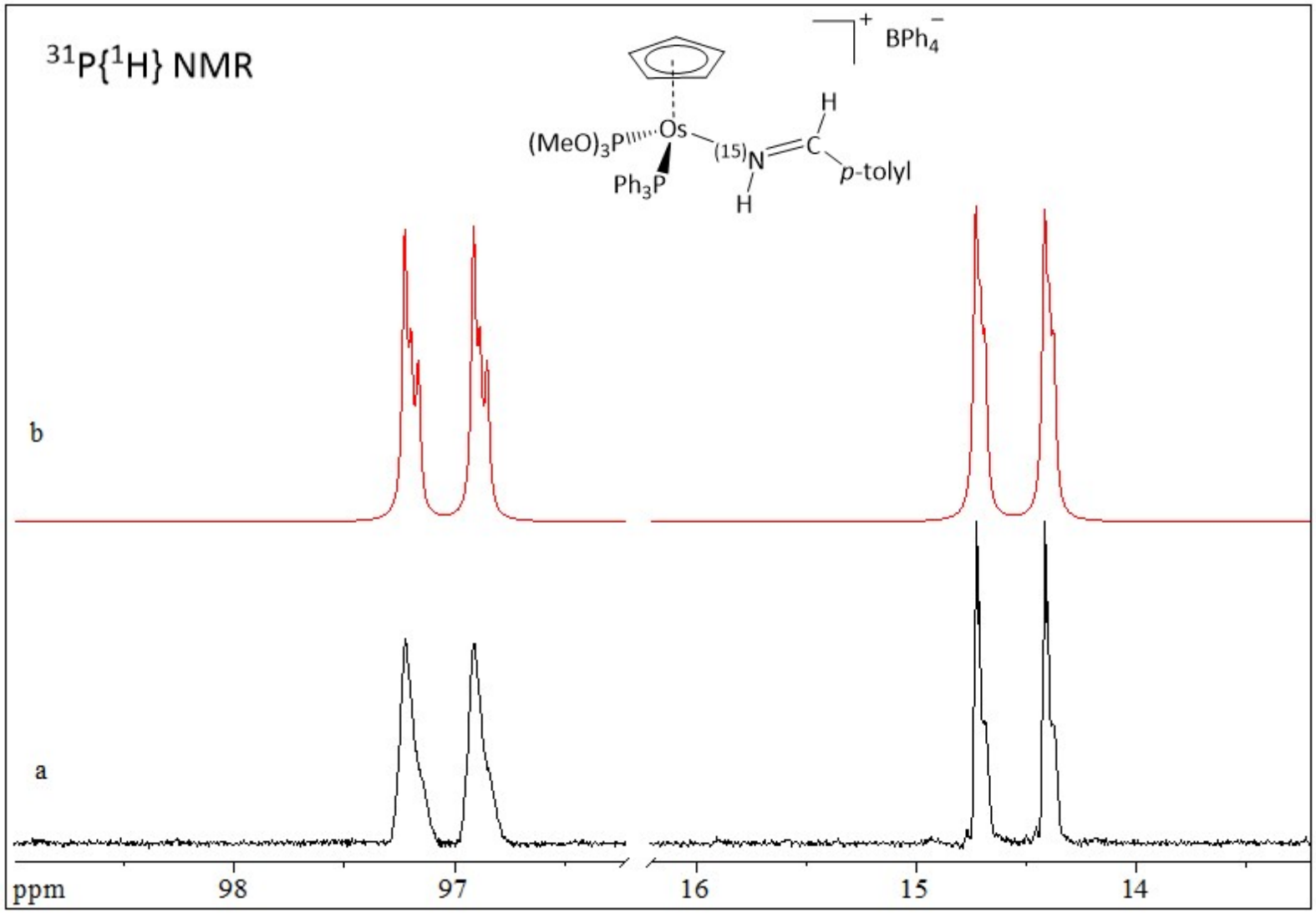

Appendix 11.46 Magnification of $^{31}P\{^{1}H\}$ NMR spectra in CD_2Cl_2 at room temperature of complex $55b_1$: higher spectra is simulated, lower spectra is the real one.

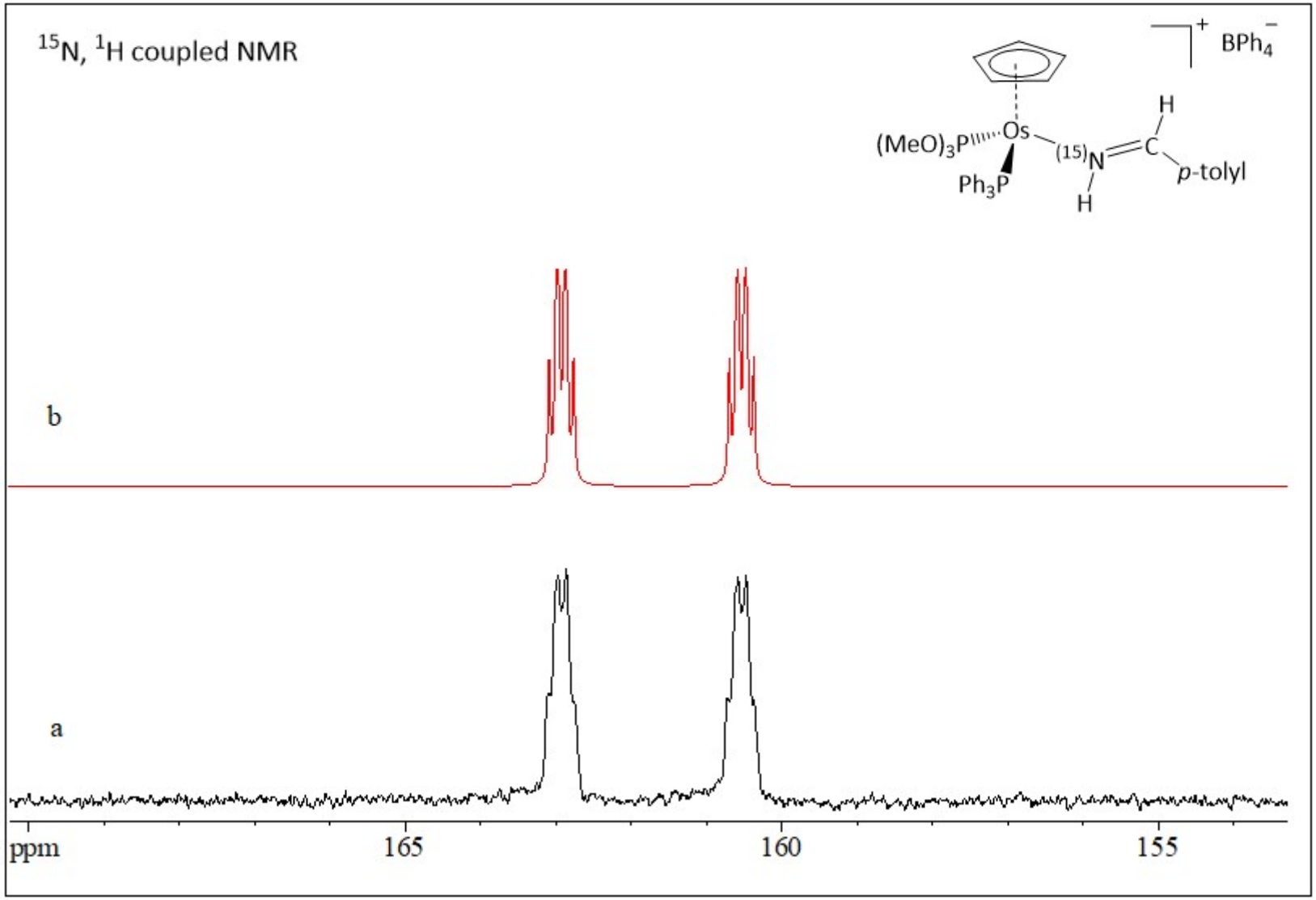

Appendix 11.47 ^{15}N NMR spectra in CD_2Cl_2 at room temperature of complex $55b_1$: higher spectra is simulated, lower spectra is the real one.

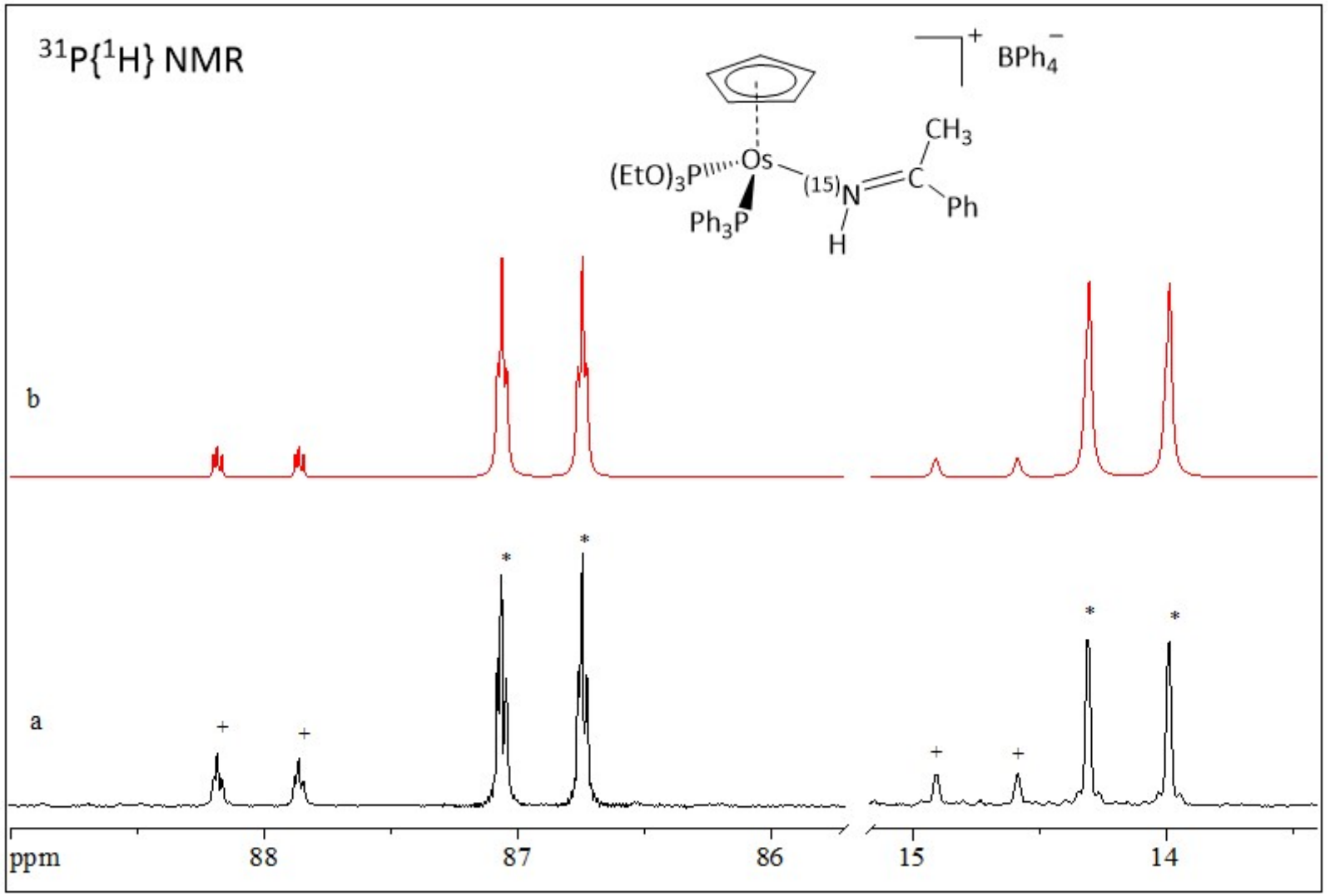

Appendix 11.48 $^{31}P\{^{1}H\}$ NMR spectra in CD_2Cl_2 at room temperature of complex $56c_1$: higher spectra is simulated, lower spectra is the real one.

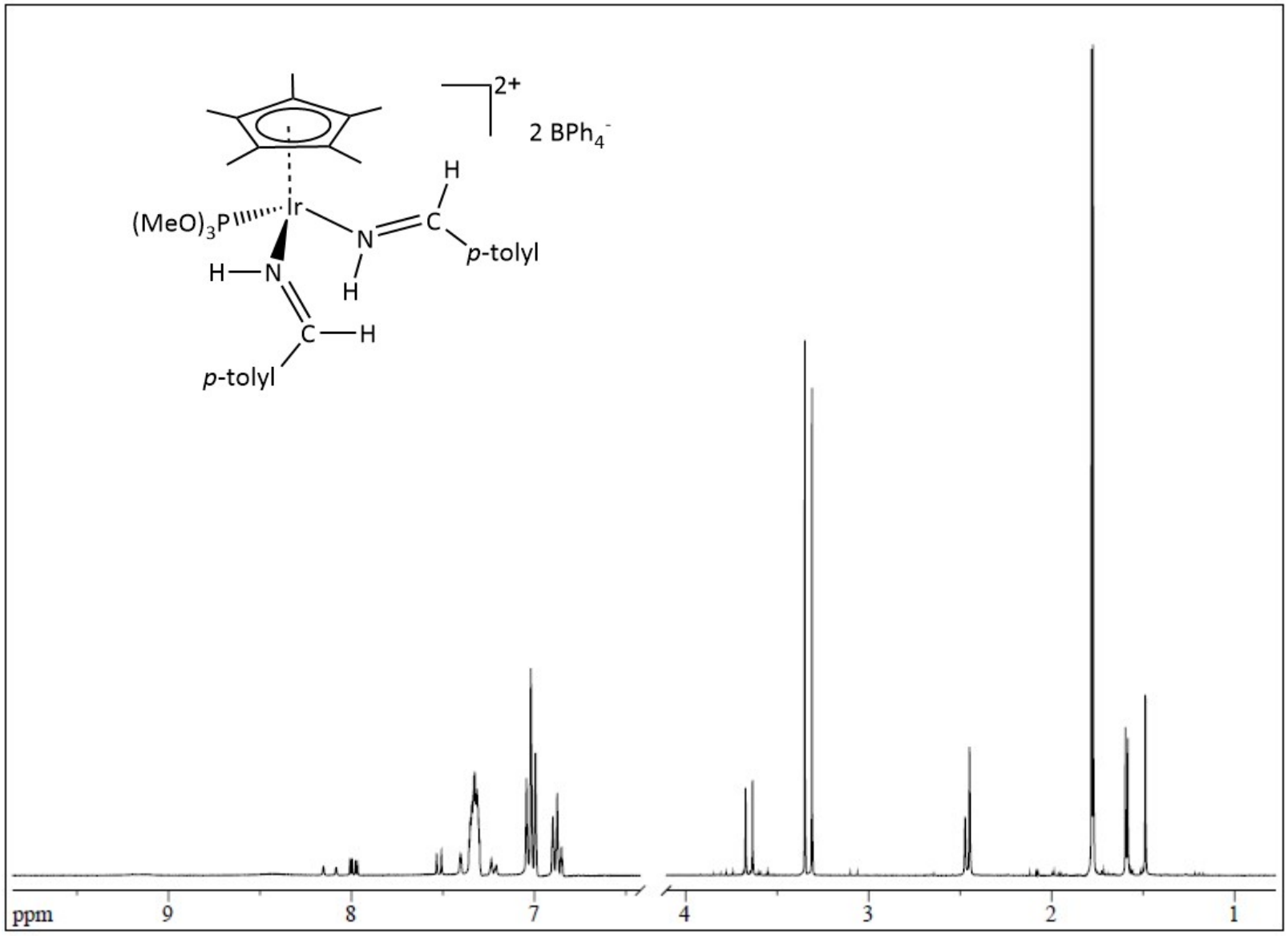

Appendix 11.49 ^{1}H NMR spectra in CD_2Cl_2 at room temperature of complex 66.

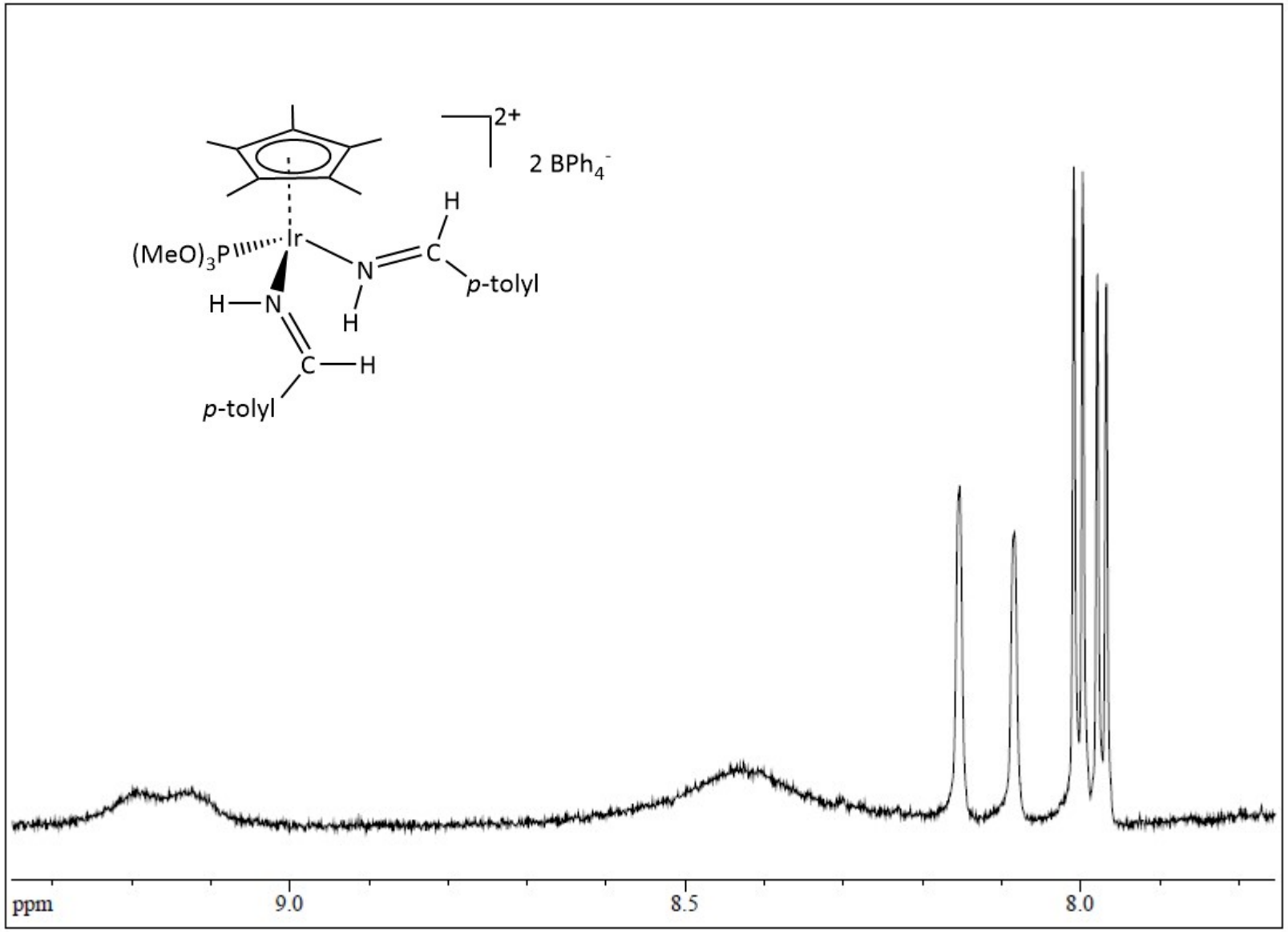

Appendix 11.50 Magnification of $^{1}H\}$ NMR spectra in CD_2Cl_2 at room temperature of complex 66.

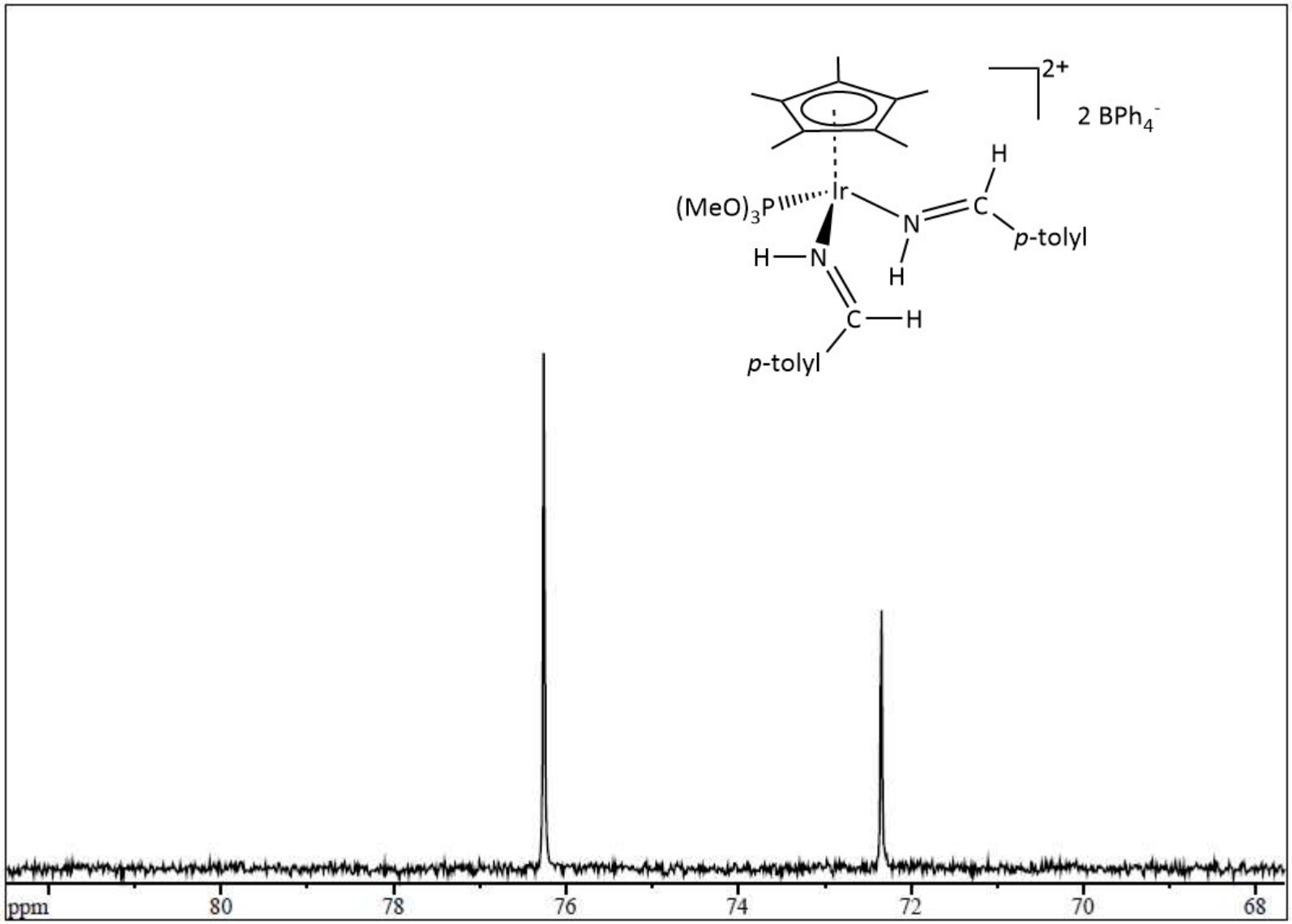

Appendix 11.51 $^{31}P\{^{1}H\}$ NMR spectra in CD_2Cl_2 at room temperature of complex 66.